INTRA- AND INTER-MOLECULAR ELECTRON TRANSFER IN FLAVOCYTOCHROME *b*$_2$

PATRICIA WHITE

THESIS PRESENTED FOR THE DEGREE OF DOCTOR OF PHILOSOPHY

UNIVERSITY OF EDINBURGH

1993

FOR MUM AND DAD,

AS EVERYTHING ALWAYS HAS BEEN.

ACKNOWLEDGEMENTS

First and foremost, I would like to thank my excellent supervisor, Dr. Stephen.K.Chapman, for all the help and advice he has given me throughout my research.

My thanks also go to my second supervisor, Dr. Graeme A.Reid, and to the entire flavocytochromes group, especially Simon Daff, Eryl Sharp, Duncan Short, Sara Pealing and Dr. Forbes Manson. The first three of whom helped enormously with proof-reading, and Forbes who constructed nearly all of my mutants.

I am grateful to those involved with the NMR spectroscopy, both in Edinburgh and at the University of East Anglia, namely Drs. John Parkinson and Geoff.R.Moore, Mark Cox and Andy Thurgood.

I would also like to acknowledge Dr. Graham Pettigrew for his help in determining redox potentials, as well as Dr. Mariella Tegoni for kindly providing me with photographs of the flavocytochrome *b*$_2$/cytochrome *c* model.

I would like to thank the SERC for my postgraduate award, and the University of Edinburgh for use of facilities.

Finally, I would like to acknowledge the three most important people in my life, Mum, Dad and Alister, for all their love and support (not only the financial kind!).

ABSTRACT

Flavocytochrome *b*2 from *Saccharomyces cerevisiae* is located in the mitochondrial intermembrane space where it catalyses the oxidation of L-lactate to pyruvate with concomitant electron transfer to cytochrome *c*. The enzyme is a homotetramer, each protomer having two distinct domains; one of which binds flavin mononucleotide (FMN) and the other protohaem IX. The domains are connected by a region of polypeptide which constitutes the interdomain hinge. The pathway of electron transfer is from L-lactate to FMN to haem to cytochrome *c*. The work described in this thesis focuses on the latter two steps in the catalytic cycle, namely intramolecular electron transfer from FMN to haem and intermolecular electron transfer from flavocytochrome *b*2 to cytochrome *c*.

Intramolecular electron transfer has been investigated by the generation of interspecies hybrid enzymes. These include hinge-swap-*b*2, in which the hinge region of the *S.cerevisiae* enzyme has been replaced with that from *Hansenula anomala*; and domain-swap-*b*2 which comprises the flavodehydrogenase domain of *H.anomala* with the hinge region and haem domain from *S.cerevisiae*. For both hinge-swap and domain-swap enzymes, the most significant effect was a dramatic decrease in the rate of haem reduction. The rate constant for this decreases from $445s^{-1}$ to $1.61s^{-1}$ for the hinge-swap enzyme and to $0.99s^{-1}$ for domain-swap-*b*2. This indicates that flavin to haem

electron transfer is severely affected in both hybrids, to such an extent that this step is now rate-limiting, rather than C2-H abstraction as in the *S.cerevisiae* wild-type enzyme. Other kinetic parameters including deuterium kinetic isotope effects also support this. We can therefore conclude that the interdomain hinge, and more generally, the structural integrity of this region are crucial in ensuring recognition and efficient electron transfer between the domains.

Intermolecular electron transfer has been investigated with a view to identification of association sites for cytochrome *c* on flavocytochrome b_2. Initial kinetic characterisation of C-terminal tail mutants, including point mutations and deletions, have indicated that this region is involved in formation of a catalytically-competent complex between the two proteins. The participation of the tail and hinge regions in electron transfer to cytochrome *c* has been investigated by stopped-flow kinetics; and the nature and strength of association between the two proteins by 600MHz proton NMR spectroscopy. Analysis of second-order rate constants derived from stopped-flow data revealed that the efficiency of electron transfer decreased in the order: wild-type > Glu-509→Lys (a point charge-change close to the end of the C-terminal tail) > hinge-swap-b_2. The strength of association between flavocytochrome b_2 and cytochrome *c* was estimated by the extent of linewidth broadening in the NMR signals corresponding to haem

methyl-3 and -8 of cytochrome *c*. Linewidths for these resonances were broader with the wild-type enzyme than with both mutants, inferring that cytochrome *c* binding is much stronger in wild-type than in either of the mutants. Thus the C-terminal tail, and in particular the final three residues, influences cytochrome *c* binding, whereas structural integrity within the hinge region appears to be important for both cytochrome *c* binding and electron transfer.

The effects of pH upon electron transfer in flavocytochrome b_2 were investigated using wild-type and active site point mutants; Tyr-143 to Phe and Tyr-254 to Phe. Two pK_as were identified by steady-state analysis of the wild-type enzyme, with values of 5.40 ± 0.12 and 10.92 ± 0.11. The former value was categorically assigned to protonation of haem propionate-7 by means of an NMR-monitored pH titration. Protonation of this group causes disruption of the hydrogen-bonding to Tyr-143 with the result that the rate of flavin to haem electron transfer is drastically lowered. The pK_a value of 10.92 ± 0.11 is postulated to be due, in part, to deprotonation of a tyrosine residue, such as Tyr-254.

ABBREVIATIONS AND UNITS

Amino acids have been denoted by both the single and three letter codes:-

AMINO ACID	THREE LETTER ABBREVIATION	ONE LETTER SYMBOL
Alanine	Ala	A
Arginine	Arg	R
Asparagine	Asn	N
Aspartic acid	Asp	D
Cysteine	Cys	C
Glutamic acid	Glu	E
Glutamine	Gln	Q
Glycine	Gly	G
Histidine	His	H
Isoleucine	Ile	I
Leucine	Leu	L
Lysine	Lys	K
Methionine	Met	M
Phenylalanine	Phe	F
Proline	Pro	P
Serine	Ser	S
Threonine	Thr	T
Tryptophan	Trp	W
Tyrosine	Tyr	Y
Valine	Val	V

When referring to oligonucleotides, the following abbreviations are used:-

A, adenine; T, thymine; C, cytosine; G, guanine.

The following nomenclature has been adopted in referring to flavocytochrome *b*2 (*b*2):-

Wild-type-*b*2 is abbreviated to either WT-*b*2 or just WT.

S.cerevisiae-*b*2 and *H.anomala*-*b*2 denote flavocytochrome *b*2 from *Saccharomyces cerevisiae* and *Hansenula anomala* respectively.

Point mutations are referred to as, for example, E509K or E509K-*b*2. This denotes an enzyme in which the glutamic acid at position 509 in the amino acid sequence has been substituted with lysine, using site-directed mutagenesis.

TD-*b2* and E509* represent the enzymes with 23 and 3 residue deletions of the C-terminal tail, respectively.

The hybrid enzymes are referred to as hinge-swap-*b2* and domain-swap-*b2*, and also by the codes pFM303 and pFM306 respectively.

Kinetic parameters:-

K_M	Michaelis constant
k_{cat}	enzyme turnover number
V_{max}	limiting value for reaction rate
K_I	inhibition constant
K_d	dissociation constant
K_S	dissociation constant of the enzyme-substrate complex
S_{opt}	substrate concentration at which turnover is maximal

Other abbreviations include:-

ATP	adenosine-5'-triphosphate
CD	circular dichroism
DNA	deoxyribonucleic acid
E.coli	*Escherichia coli*
EDTA	ethylenediaminetetraacetic acid
EPR	electron paramagnetic resonance
FAD	flavin adenine dinucleotide
FMN	flavin mononucleotide
H.anomala	*Hansenula anomala*
I	ionic strength
KIE	kinetic isotope effect
lactate	L-[2-^{1}H]-lactate (unless otherwise stated)
LB	Luria Broth
M_R	relative molecular weight
NAD	nicotinamide adenine dinucleotide
NMR	nuclear magnetic resonance
PMSF	phenylmethylsulphonylfluoride
S.cerevisiae	*Saccharomyces cerevisiae*
SDS-PAGE	Sodium Dodecyl Sulphate-Polyacrylamide Gel Electrophoresis
UV	ultra-violet

Abbreviations of units are of standard form:-

Da	dalton units	V	volt (s)
Å	angstrom (s)	Ω	ohm (s)
Hz	hertz	°C	degrees Centigrade
K	kelvin (s)	g	gram (s)
l	litre (s)	s	second (s)
M	molar		

Other unit abbreviations include:-

s^{-1}	first order rate constant
$M^{-1}s^{-1}$	second order rate constant
$M^{-1}cm^{-1}$	molar extinction coefficient
ppm	parts per million
p.s.i.	pounds per square inch
rpm	revolutions per minute

INDEX

CHAPTER 7 (CONTINUED)

7.5 (CONTINUED)

FIGURE INDEX

CHAPTER 2 : INTRAMOLECULAR COMMUNICATION

THE ROLE OF THE INTERDOMAIN HINGE

PAGE NUMBER

CHAPTER 5 : INTERMOLECULAR COMMUNICATION

INVESTIGATION OF CYTOCHROME *c*

BINDING SITE BY KINETIC AND

SPECTROSCOPIC METHODS

PAGE NUMBER

CHAPTER 6 : EFFECT OF pH ON ELECTRON TRANSFER IN FLAVOCYTOCHROME *b*2

TABLE INDEX

CHAPTER 1

INTRODUCTION

1.1 INTRODUCTION

Flavocytochrome *b*2 (L-lactate:cytochrome *c* oxidoreductase, EC.1.1.2.3) is a soluble respiratory enzyme found in the intermembrane space of yeast mitochondria (1). It catalyses the two-electron oxidation of L-lactate to pyruvate with concomitant electron transfer to cytochrome *c* (2).

The enzyme is a homotetramer (3) with each subunit containing both flavin mononucleotide (FMN) and protohaem IX prosthetic groups (2) (see Figure 1.1), bound in two functionally distinct domains. Consequently it has been postulated that flavocytochrome *b*2 evolved as a result of fusion between a gene coding for a *b*-type cytochrome another encoding an FMN-binding dehydrogenase (4).

Flavoproteins often act as electron-carrier enzymes in reactions where electrons flow from two-electron donors to one-electron acceptors, or vice versa. The electron carrier component is a riboflavin (vitamin B_2) derivative bound to the protein as a cofactor. Riboflavin is composed of a substituted isoalloxazine ring linked to D-ribitol as illustrated in Figure 1.2. Although the more common riboflavin derivative is flavin adenine dinucleotide (FAD), riboflavin 5'-phosphate (also called flavin adenine mononucleotide (FMN)) also acts as an electron carrier in certain enzymes, one of which is flavocytochrome *b*2. The isoalloxazine ring is the only part of the flavin molecule which is involved in the

FIGURE 1.1

THE PROSTHETIC GROUPS OF FLAVOCYTOCHROME *b*2

(a) FLAVIN MONONUCLEOTIDE (FMN)

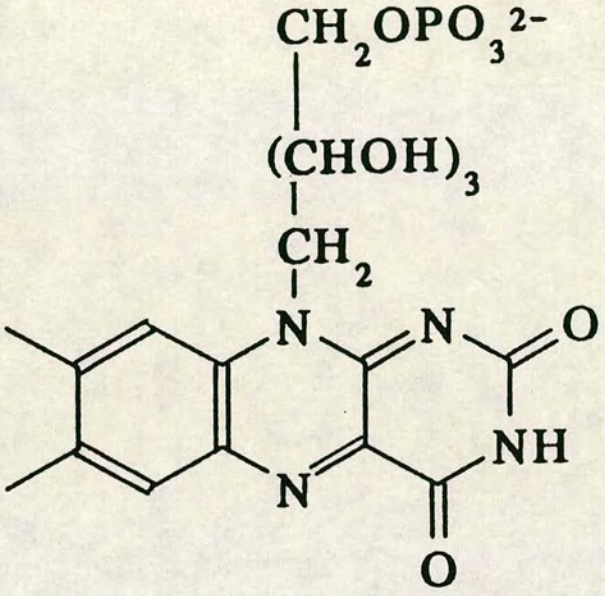

(b) PROTOHAEM IX

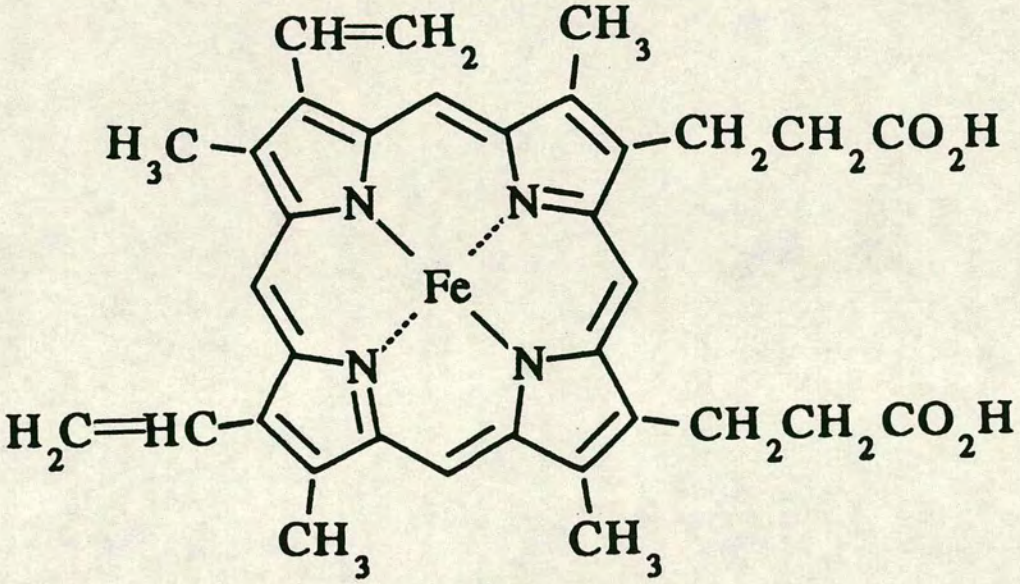

FIGURE 1.2

RIBOFLAVIN (VITAMIN B_2)

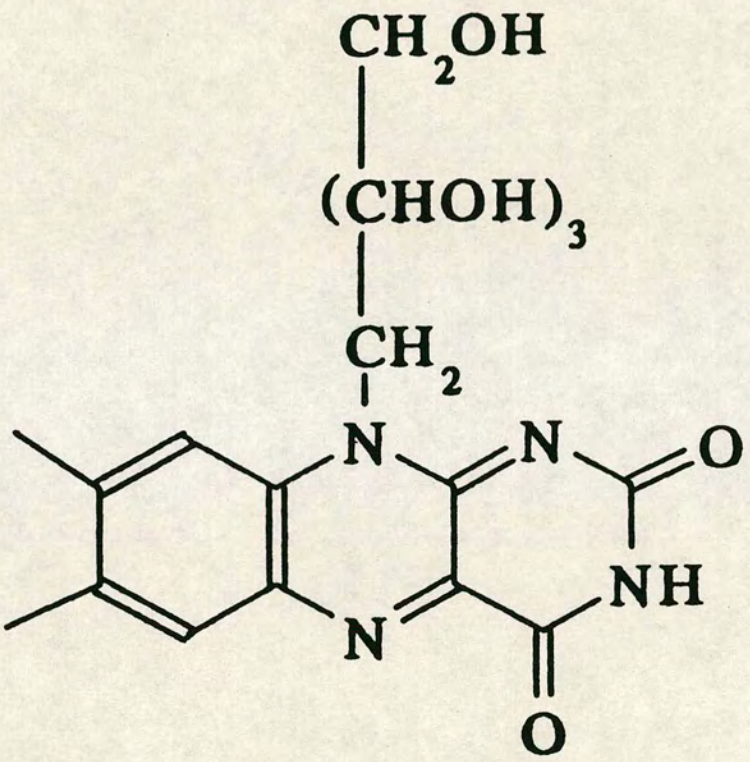

redox reaction; the side chains merely acting as anchors to hold the cofactor in place within the protein.

Flavoproteins can catalyse a wide range of redox reactions as a result of their ability to exist as a semiquinone (one electron reduced form) as well as either fully oxidised or fully reduced. It is this ability which enables them to act as biological electron transformers - linking a two-electron carrier to a one-electron carrier within an electron transport chain.

The three oxidation states of flavins are spectrally distinguishable. The oxidised and reduced forms are yellow and colourless respectively, whereas the semiquinone form is either blue or red depending on whether the unpaired electron exists on N1 or N5 of the isoalloxazine ring.

The cytochromes are a class of redox enzymes that are principally concerned with the sequential transfer of electrons from flavoproteins to molecular oxygen in the respiratory chain of aerobic cells. They employ protohaem IX, or one of its derivatives, as the cofactor and it is the iron atom within this moiety which undergoes cyclic one-electron oxidation and reduction during the course of catalysis.

Numerous cytochromes from various sources have been described, and are classified into groups *a*, *b*, *c* and *d* according to the position of the α-band in their very distinctive absorption spectra (5). These four families of cytochromes differ from one another by virtue of the

degree and nature of substitution of the porphyrin ring.

1.2 HISTORICAL PERSPECTIVE

In 1915 Harden and Norris observed that when dried yeast was mixed with lactic acid, methylene blue was reduced and pyruvate was formed (6). Meyerhof demonstrated that this process occurred in the absence of any coenzyme (7). Thirteen years later in 1928 Bernheim reported a partial purification of a baker's yeast extract which had lactate dehydrogenase activity (8). Bach and coworkers discovered that this activity was associated with a *b*-type cytochrome which they named cytochrome b_2 (9).

Appleby and Morton succeeded in co-crystallising a protein which incorporated both lactate dehydrogenase activity and cytochrome b_2 (2), going on to identify FMN as the enzyme's second prosthetic group, present in a stoicheometric ratio with protohaem IX. They proposed that the dehydrogenase activity was dependent on the flavin cofactor and the electron transfer ability on cytochrome b_2.

Crystallisation of flavocytochrome b_2 facilitated the preparation of purified enzyme and opened up the way to further structural and functional studies. More recently, the three-dimensional crystal structure has been resolved to 2.4Å (10); this has allowed identification of residues which may be important structurally and/or functionally. This, along with cloning of the gene and high level expression in *E.coli*

(11), has facilitated site-directed mutagenesis, which in turn has allowed investigation into the functions of specific amino-acid residues. A wealth of information has been generated in the last few years some of which is summarised in this chapter and some of which constitutes this thesis.

1.3 ISOLATION AND PURIFICATION

In 1928, as already mentioned, Bernheim reported the partial purification of a lactate dehydrogenase extract from baker's yeast (*Saccharomyces cerevisiae*) (8). The first significant development in purification was achieved by Appleby and Morton who, after treatment of yeast with n-butanol and separation of lipid material (probably of mitochondrial origin), succeeded in crystallising the protein (2). These crystals of flavocytochrome b_2, termed type I, were found to contain DNA. This could be removed by either dialysis at high ionic strength (12) or by chromatography on DEAE-cellulose (13). The resulting DNA-free crystals were termed type II. The enzyme after crystallisation was found to be unstable and inconsistent activities were recorded by different research groups (12-14).

Nichols and coworkers observed that there were changes in the enzyme during crystallisation, specifically that both the K_M for lactate and the electrophoretic mobility had increased (15). Simultaneously Somlo and Slonimski

reported that a "modification" was required within the enzyme in order for crystallisation to occur (16). Analysis of the crystallised enzyme by SDS-polyacrylamide gel electrophoresis showed that it consisted of two fragments of uneven chain length, 36 and 21kDa, corresponding to the haem-binding domain and to part of the flavin-binding domain respectively. Thus the reported "modification" could be ascribed to selective cleavage by yeast proteases. This was confirmed in 1972 by Lederer and Simon (17).

Jacq and Lederer purified the enzyme in the presence of phenylmethylsulphonyl fluoride (PMSF, a known protease inhibitor) and, although crystallisation did not take place, they succeeded in obtaining an "intact" form of the enzyme. Denaturing gel electrophoresis (SDS-PAGE) showed that this "intact" form of flavocytochrome b_2 had a chain length of 57kDa. This was identical to that obtained for the enzyme from *Hansenula anomala* which is not subject to proteolytic cleavage. Purification of flavocytochrome b_2 from *H.anomala* can therefore be carried out in the absence of PMSF. A comparison of the purification procedures of the enzyme from the different sources is reported by Labeyrie *et al.* (18).

Following Jacq and Lederer's discovery, new purification techniques for the *S.cerevisiae* enzyme utilising PMSF were introduced. The enzyme produced by crystallisation was termed "cleaved", whereas that produced in the presence of PMSF was termed "intact". The cleaved enzyme

could be stored at 4°C under nitrogen for up to four months without appreciable activity loss. The best yields from *S.cerevisiae* gave ~50mg of flavocytochrome b_2 per kg of dry yeast.

A major advance in the isolation and purification of flavocytochrome b_2 from *S.cerevisiae* has been the high level expression (~5%) of the gene encoding the enzyme in *E.coli*. This achievement has led to significant increases in yield of enzyme and has facilitated purification. The yield of flavocytochrome b_2 from *E.coli* is estimated to be between 500- and 1000-fold greater than from a similar wet weight of yeast (11).

1.4 LOCATION AND FUNCTION

Flavocytochrome b_2 is coded in the nucleus and is synthesised in the cytoplasm of yeast cells. It is transported to the intermembrane space by way of an eighty amino-acid N-terminal extension. Once in the mitochondria this precursor is converted to the soluble, mature flavocytochrome b_2 by a two-step process.

The first step involves transport of the soluble precursor across the outer mitochondrial membrane to penetrate the inner membrane, resulting in part of the precursor protruding into the protein matrix. It is here that proteolysis takes place to yield a smaller intermediate which is exposed to the intermembrane space. The second step results in conversion of this

intermediate to the mature protein (1,19,20).

Flavocytochrome *b*2, residing in the intermembrane space, transfers electrons from L-lactate to cytochrome *c*. This is part of a short electron transport chain involving cytochrome *c* oxidase (20,21,3) (Figure 1.3).

Pajot and Claisse (3, also 21,22) demonstrated that flavocytochrome *b*2 enables yeast to respire on L-lactate when the main respiratory pathway is blocked. This is illustrated in Figure 1.4. Path B is the usual NADP-dependent respiratory pathway which results in the production of 11 moles of adenosine triphosphate (ATP), together with 1 mole of ATP from pathway A. When the oxidative phosphorylation pathway (B) is blocked, in this example by Antimycin A (a *Streptomyces* antibiotic which inhibits respiratory electron transfer by preventing oxidation of cytochrome *b*), path A involving flavocytochrome *b*2 can still function, generating its 1 mole of ATP which is sufficient energy to maintain cell life, growth and protein biosynthesis.

1.5 STRUCTURE

1.5.1 OVERVIEW

Flavocytochrome *b*2 is a multifunctional protein consisting of a single polypeptide chain, with multiple catalytic or binding functions created by folding of contiguous stretches into domains. These domains can be identified by "nicking" of the enzyme by proteases, which

FIGURE 1.3

REPRESENTATION OF THE SHORT ELECTRON TRANSPORT CHAIN INVOLVING FLAVOCYTOCHROME *b*2 IN YEAST MITOCHONDRIA (102)

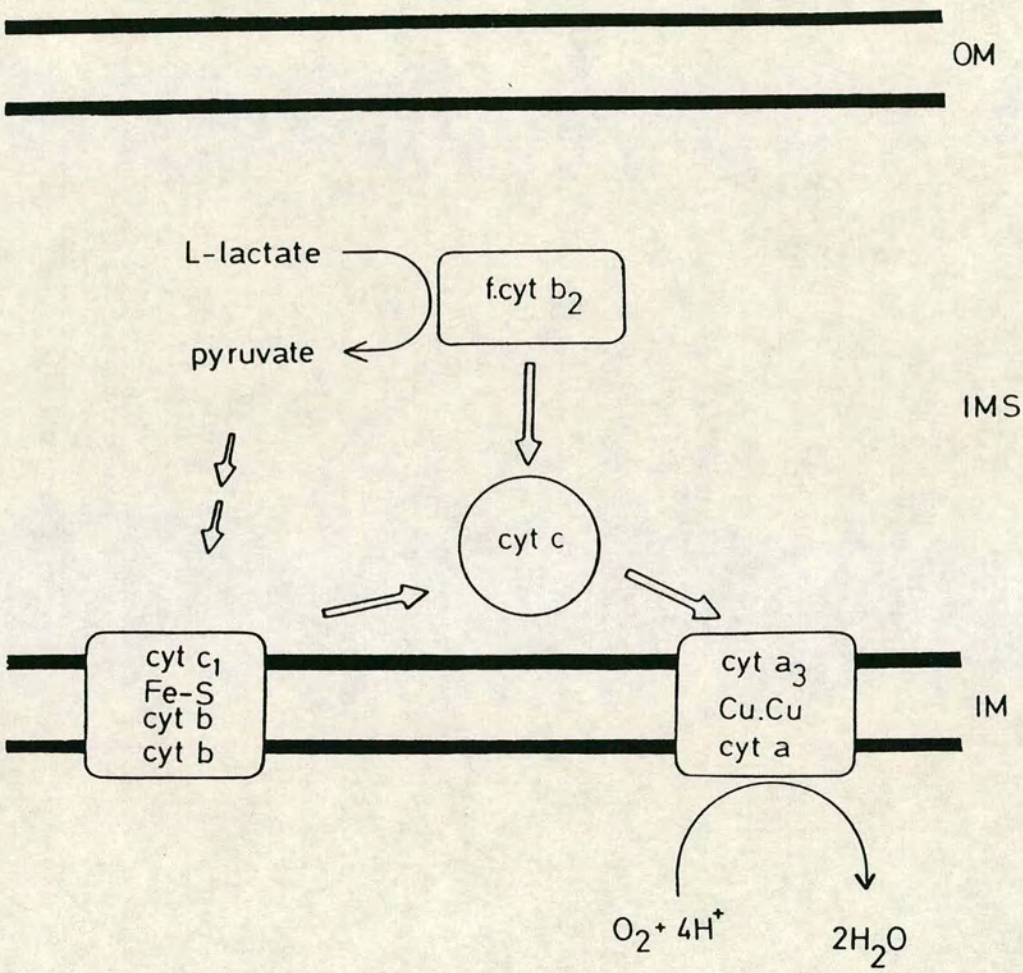

Abbreviations : **OM, outer membrane; IMS, intermembrane space; IM, inner membrane; cyt , cytochrome; f.cyt *b*2 , flavocytochrome *b*2 .**

FIGURE 1.4

THE RESPIRATORY CHAIN OF YEAST MITOCHONDRIA

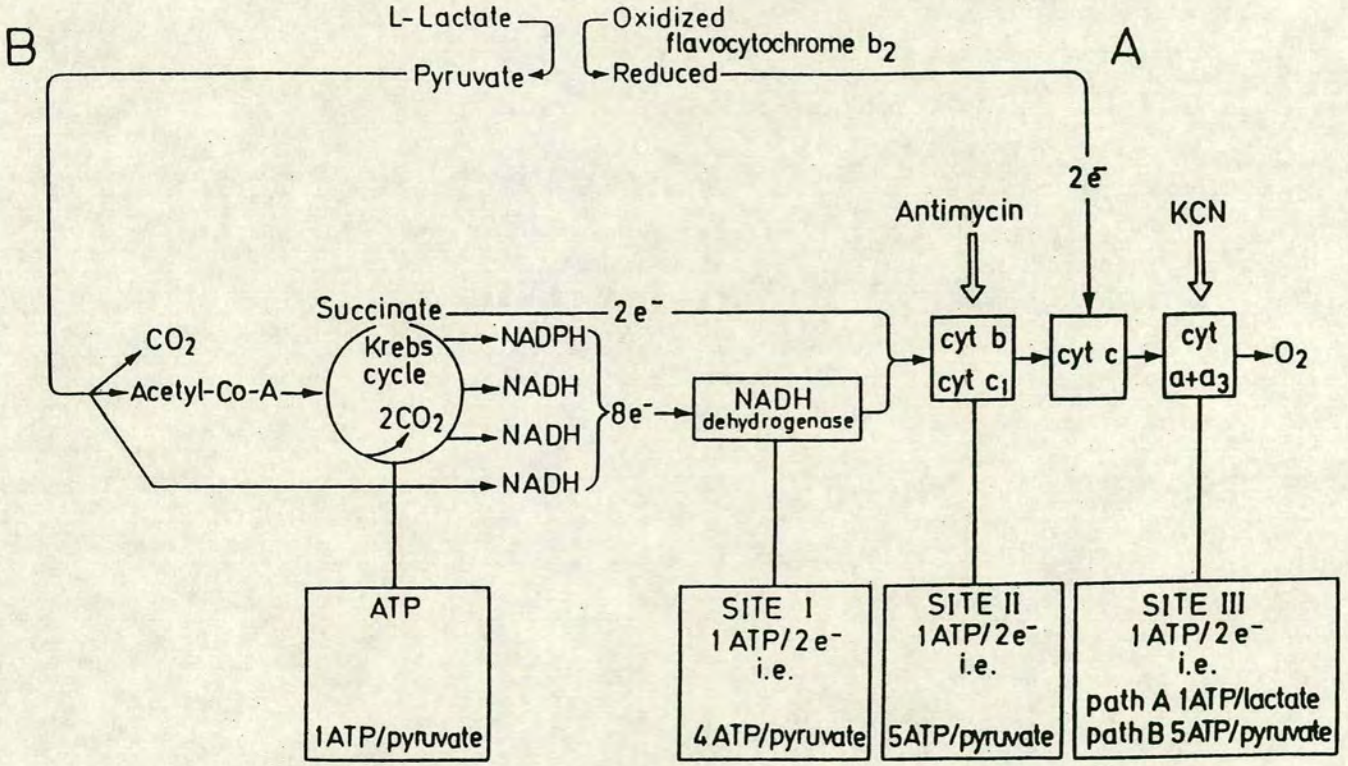

The figure shows the oxidation pathways of L(+)lactate in yeast mitochondria as determined by Pajot and Claisse (3). Pathway A is the direct route of electron transfer from flavocytochrome *b*2 to cytochrome *c* which allows the yeast to respire should pathway B become blocked , for example, by antimycin. Pathway A produces 1 mole of ATP per mole of L-lactate and pathway B 11 moles of ATP per mole of L-lactate.

can lead to generation of non-interacting enzymes without drastic property changes. Such domain folding may therefore be more highly conserved than the amino acid sequence (23).

The molecular weight of the single polypeptide chain (511 residues) of flavocytochrome b_2, determined by SDS-PAGE, is 57,500Da for the *Saccharomyces cerevisiae* enzyme (24) and 58,000Da for the analogous enzyme from *Hansenula anomala* (25). However the native enzyme exists as a tetramer of molecular weight 230kDa (25, 26). That the *S.cerevisiae* enzyme is a homotetramer with pseudo-four-fold symmetry has been confirmed by X-ray crystallography (10) (Figure 1.5).

Within each protomer the polypeptide chain is folded into two crystallographically distinguishable domains, a flavin mononucleotide (FMN) -binding domain and a cytochrome (or haem) -binding domain. Three-dimensional X-ray crystallography has shown that the cytochrome domains in two of the four subunits are positionally disordered, that is to say the structure cannot be resolved due to a degree of mobility, this is further supported by NMR studies as discussed in 1.6.3.4. The mobility is centred upon the length of polypeptide chain which links the two domains, which can therefore be regarded as a hinge. The b_2 subunit is illustrated in Figure 1.6. All intersubunit contacts within the tetramer are provided by the flavin domains which pack around the four-fold axis forming an ellipsoid disc,

FIGURE 1.5

THE FLAVOCYTOCHROME *b*$_2$ TETRAMER (*S.cerevisiae*)

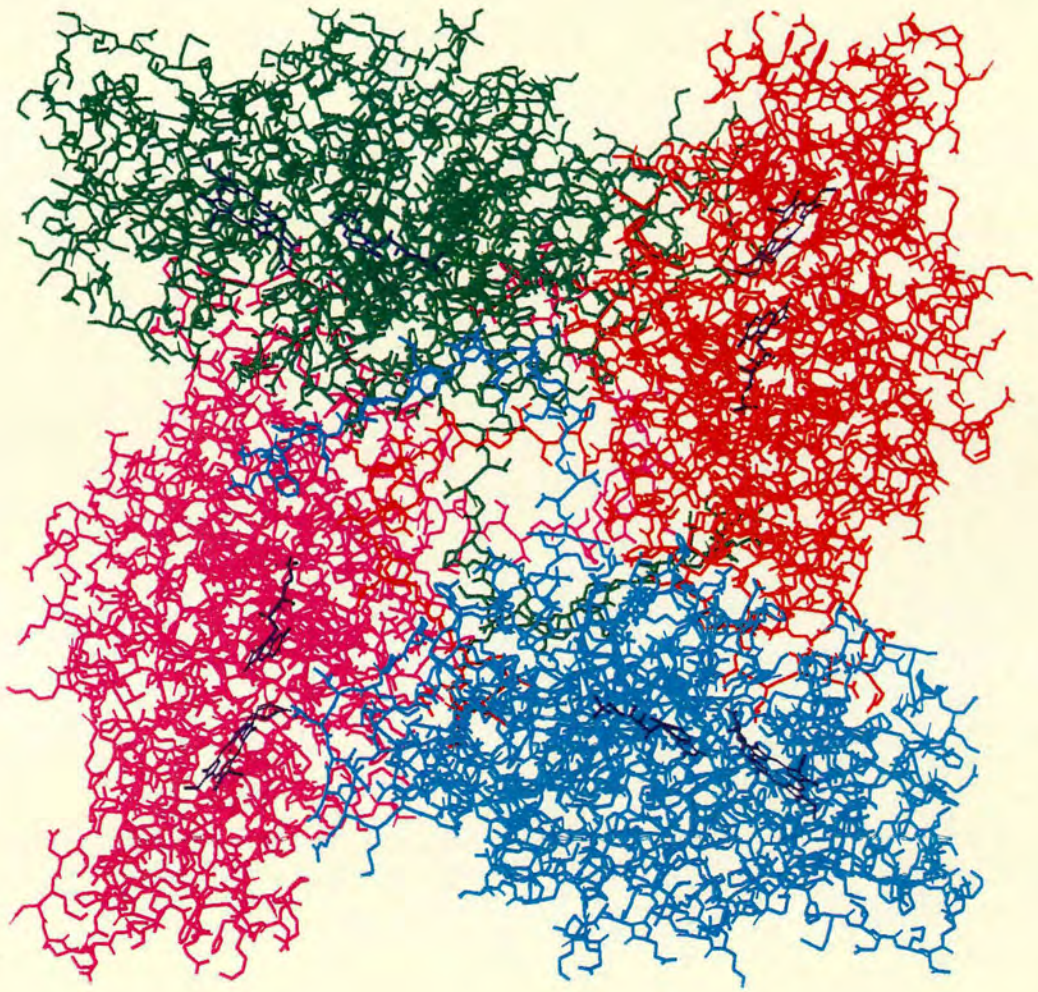

Each subunit is shown in a different colour, with the prosthetic groups in dark blue.

FIGURE 1.6
THE Cα-BACKBONE STRUCTURE OF THE FLAVOCYTOCHROME b_2 SUBUNIT

The cytochrome domain is shown in red, with the flavin domain in green

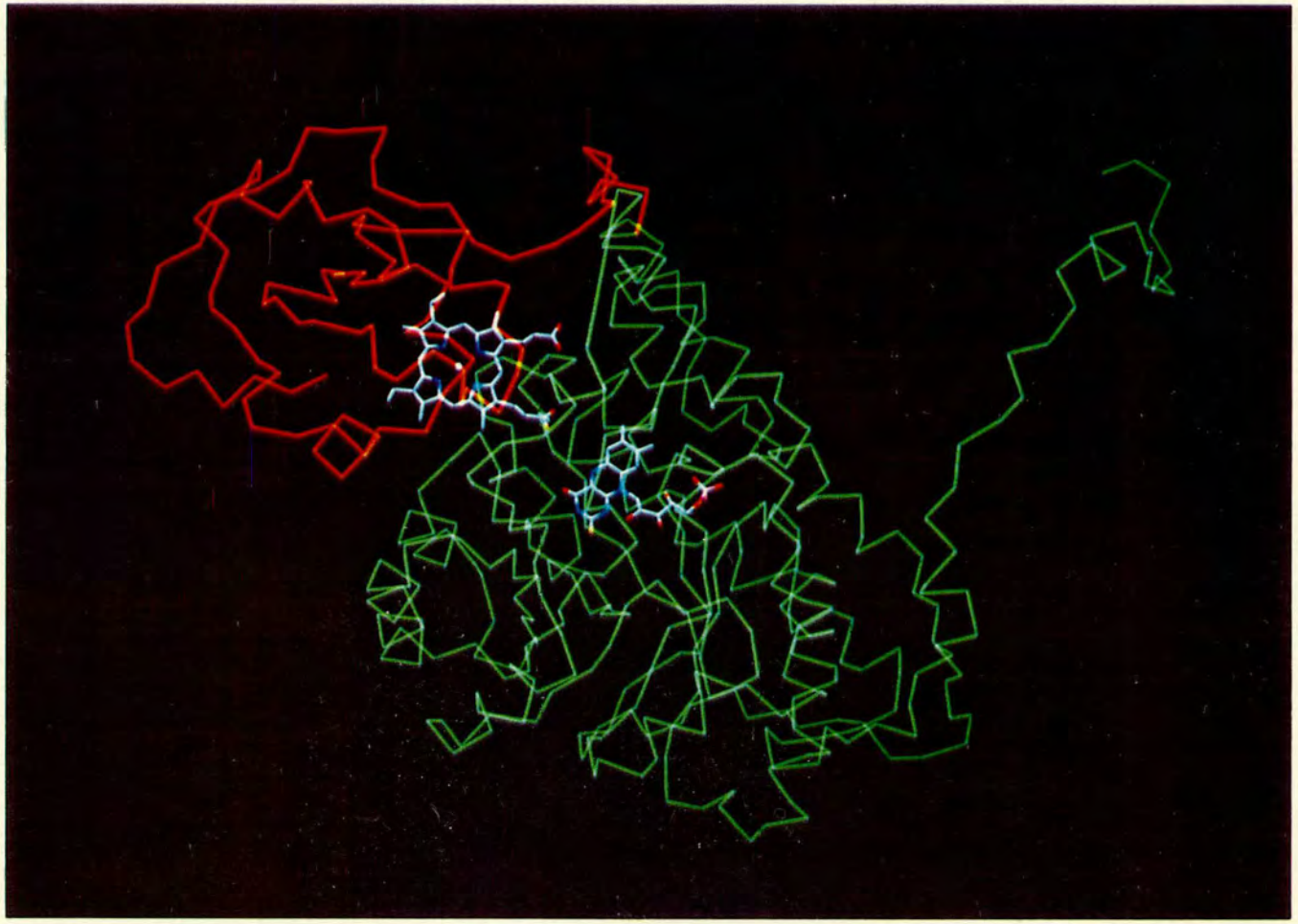

approximately 60Å thick and 100Å in diameter. The cytochrome domains protrude from the edge of the ellipsoid above the mid-plane,as illustrated in Figure 1.7.

1.5.2 THE CYTOCHROME-BINDING DOMAIN

The cytochrome-binding domain is formed by residues 1-100 and can be isolated by tryptic digestion to form the cytochrome b_2 core which is stable to further proteolysis. The cytochrome b_2 core, which is structurally homologous to liver microsomal cytochrome b_5 (27), has been expressed in *E.coli* (28).

The polypeptide chain forming the cytochrome-binding domain is folded into a 6-stranded mixed ß-sheet which is surrounded by a helix on one side and two pairs of anti-parallel helices on the other (10) (Figure 1.8). Protohaem IX is harboured within a hydrophobic crevice close to the domain interface. The propionate groups extend towards the flavin domain and are hydrogen-bonded to Tyr-143 and Tyr-97 respectively. Although the haem is bound non-covalently, two histidine ligands (His-43 and 66) coordinate axially to the low spin iron forming a stable complex.

1.5.3 THE FLAVIN-BINDING DOMAIN

The flavin-binding domain, illustrated in Figure 1.9, is comprised of residues 101-511. The main secondary

FIGURE 1.7

THE THREE-DIMENSIONAL CRYSTAL STRUCTURE OF *S.cerevisiae* FLAVOCYTOCHROME *b*2 (103)

(a) View of the tetramer down the pseudo-four-fold symmetry axis. The dashed lines in subunits 2 and 4 represent the disordered cytochrome domains.

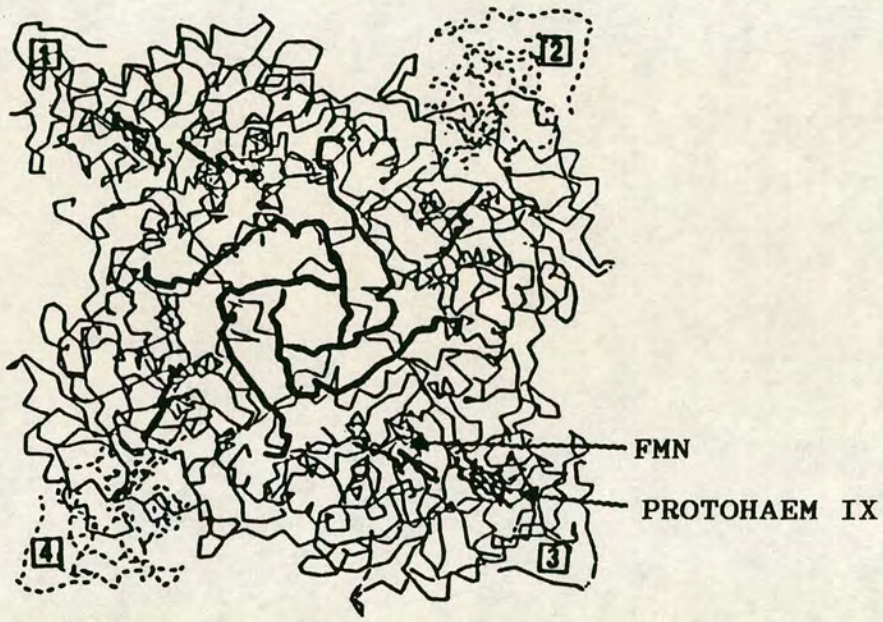

(b) Side view of Figure 1.7a, perpendicular to the above, omitting the disordered cytochrome domains.

FIGURE 1.8

STRUCTURAL REPRESENTATION OF THE CYTOCHROME *b*2 DOMAIN

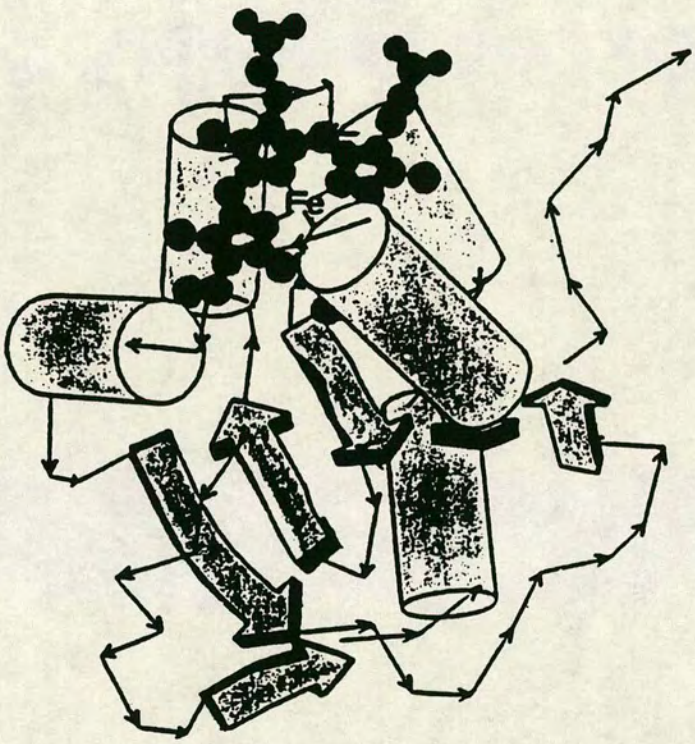

The cylinders and arrows represent helices and ß-strands respectively.

Information taken from reference 99.

FIGURE 1.9

TOPOLOGICAL REPRESENTATION OF THE FOLDING OF THE FLAVIN DOMAIN OF FLAVOCYTOCHROME *b*2

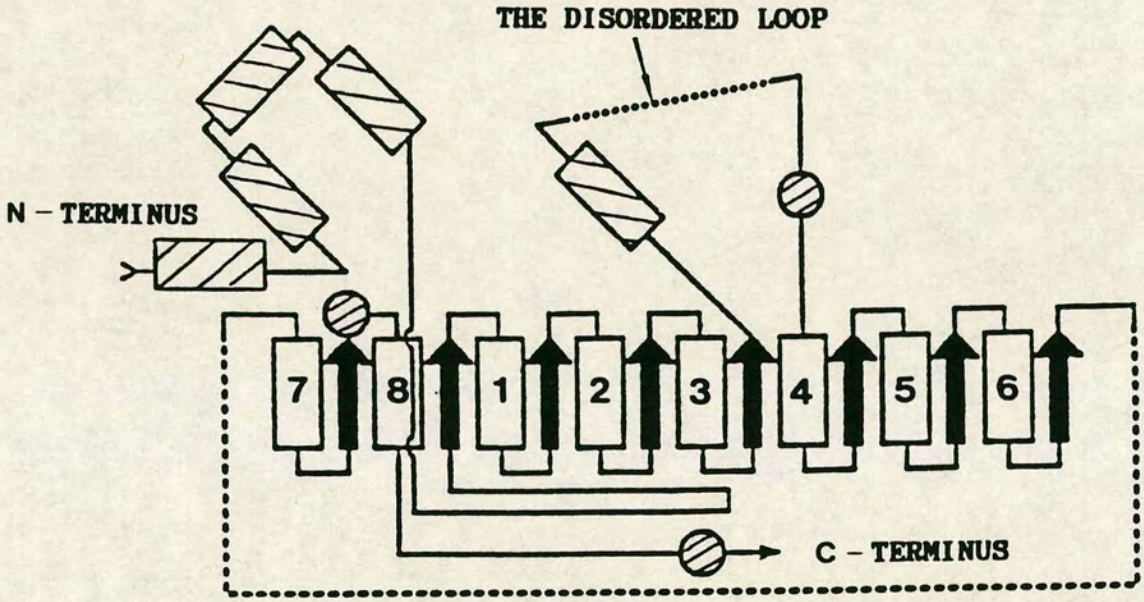

Rectangles represent helices; those numbered 1 to 8, along with the arrows (ß-sheet), represent the $ß_8$ α_8 structure. The shaded areas represent helices outwith the barrel structure.

structure within this domain is a ß8α8-barrel consisting of residues 192 to 465. The segment of polypeptide chain prior to this (residues 101-191), which includes four helices and three short ß-strands, runs parallel to the barrel structure and is part of the region which forms intersubunit contacts. This role is in part shared with the C-terminal extension (residues 487 to 511) which forms a tail which wraps around the central four-fold axis of the tetramer. There is a 40 residue interruption to the ß8α8-barrel between segments ß8 and α8; this section of polypeptide chain forms the protease-sensitive disordered loop, which is evident in the crystal structure (10), and which encompasses two short helices.

The FMN cofactor is bound non-covalently at the end of the ß-barrel corresponding to the C-terminus of the ß-strands and the N-terminus of the helices. The plane of the flavin ring is inclined at approximately 45° to the barrel and is positioned just above the ß1-strand. The flavin is slightly bent with an angle of 172° between the planes. It is slightly exposed to solvent at ring positions C4a, N5 and C5a, and also at one of the phosphate oxygen atoms.

The haem and flavin groups are almost coplanar and the shortest distance between the two is that between N5 of flavin and the edge of the haem ring, which is 9.7Å. Unlike the cytochrome domain, it has not been possible to isolate the flavin domain by selective proteolysis, however it has recently been expressed in and isolated

from *E.coli* (29).

1.6 BIOPHYSICAL AND BIOCHEMICAL PROPERTIES

1.6.1 REDUCTION POTENTIALS

Reduction potentials for the haem and FMN prosthetic groups in various forms of flavocytochrome b_2 are listed in Table 1.1. The values for haem reduction are similar to reduction potentials for b_5-type cytochromes (30). These values do not vary significantly within different forms of the enzyme, in other words the haem redox potential appears to be independent from the rest of the molecule, since removal of the flavin domain barely affects the value. Reduction potentials for flavin are only slightly higher than for haem; this is consistent with reversible electron transfer between the prosthetic groups (4).

1.6.2 SUBSTRATE SPECIFICITY

Flavocytochrome b_2 is capable of oxidising a wide range of α-hydroxy-acids. Dikstein established that the three basic requirements for a substrate were that it should be a carboxylate with an α-hydrogen and a α-hydroxyl group (39). Whilst L-lactate is the most efficient substrate, flavocytochrome b_2 can oxidise many long-chain α-hydroxy-acids, such as 2-hydroxycaproate and 2-hydroxyoctanoate. Steric factors also play an important role in substrate specificity, for example, acids with bulky substituents

TABLE 1.1

REDUCTION POTENTIALS (mV) FOR THE FLAVIN AND HAEM GROUPS IN DIFFERENT FORMS OF FLAVOCYTOCHROME *b2*

ENZYME	H_{OX}/H_{RED}	F_{OX}/F_{SQ}	F_{SQ}/F_{RED}	F_{OX}/F_{RED}	REF.
S_I	10	-94	-34	-64	(31)
S_I	-19	-	-	-	(29)
S_I *b2* CORE	-31	-	-	-	(28)
S_X	0 ± 3	-	-	-	(32)
S_X	6	-50	-	-	(33)
S_X	6 ± 2	-44 ± 8	-57 ± 9	-51 ± 16	(34)
S_X *b2* CORE	-28	-	-	-	(19)
H_I	-19 ± 5	-23 ± 10	-45 ± 12	-34 ± 10	(34)
H_I	-16 ± 5	-16	-60	-54 ± 10	(35)
H_I *b2* CORE	-10 ± 5	-	-	-	(36)

Other potentials : Lactate/Pyruvate = -190 mV (37)

Ferri/Ferrocytochrome *c* = +273 mV (38)

Abbreviations used above : S_I, intact *b2* from *S.cerevisiae*; S_X, cleaved *b2* from *S.cerevisiae*; H_I, intact *b2* from *H.anomala*; *b2* core, the isolated haem domain; H, haem; F, FMN; SQ, semiquinone; REF., reference.

such as mandelate (39,40) are sterically hindered to such an extent that they are unable to act as substrates but may still inhibit the enzyme.

1.6.3 SPECTROSCOPIC PROPERTIES

1.6.3.1 ELECTRONIC ABSORPTION SPECTROSCOPY

The UV/visible spectra for for both oxidised and reduced forms of *S.cerevisiae* flavocytochrome b_2 are shown in Figure 1.10. The sharp peaks apparent in the reduced spectrum at 557, 528 and 423nm are typical of a *b*-type cytochrome. Although the flavin absorbances are masked at these wavelengths, one broad peak is evident in the oxidised spectrum at 362nm. The far-UV absorbance (~270nm) is due to aromatic residues on the polypeptide chain and the absorbance ratio of this peak to the Soret band at 423nm provides a useful indication of protein purity (18). The molar extinction coefficients have been determined (12) and are given in Table 1.2.

1.6.3.2 ELECTRON PARAMAGNETIC RESONANCE STUDIES

Flavin semiquinone formation occurring upon the enzymic oxidation of L-lactate has been observed at 123K in the form of an EPR signal. This signal has a g value of 2.0039 ± 0.002 and a bandwidth of approximately 15G; such results are very similar to those of an anionic, or red, semiquinone (33).

FIGURE 1.10

THE ELECTRONIC ABSORPTION SPECTRUM OF *S.cerevisiae* FLAVOCYTOCHROME *b*2

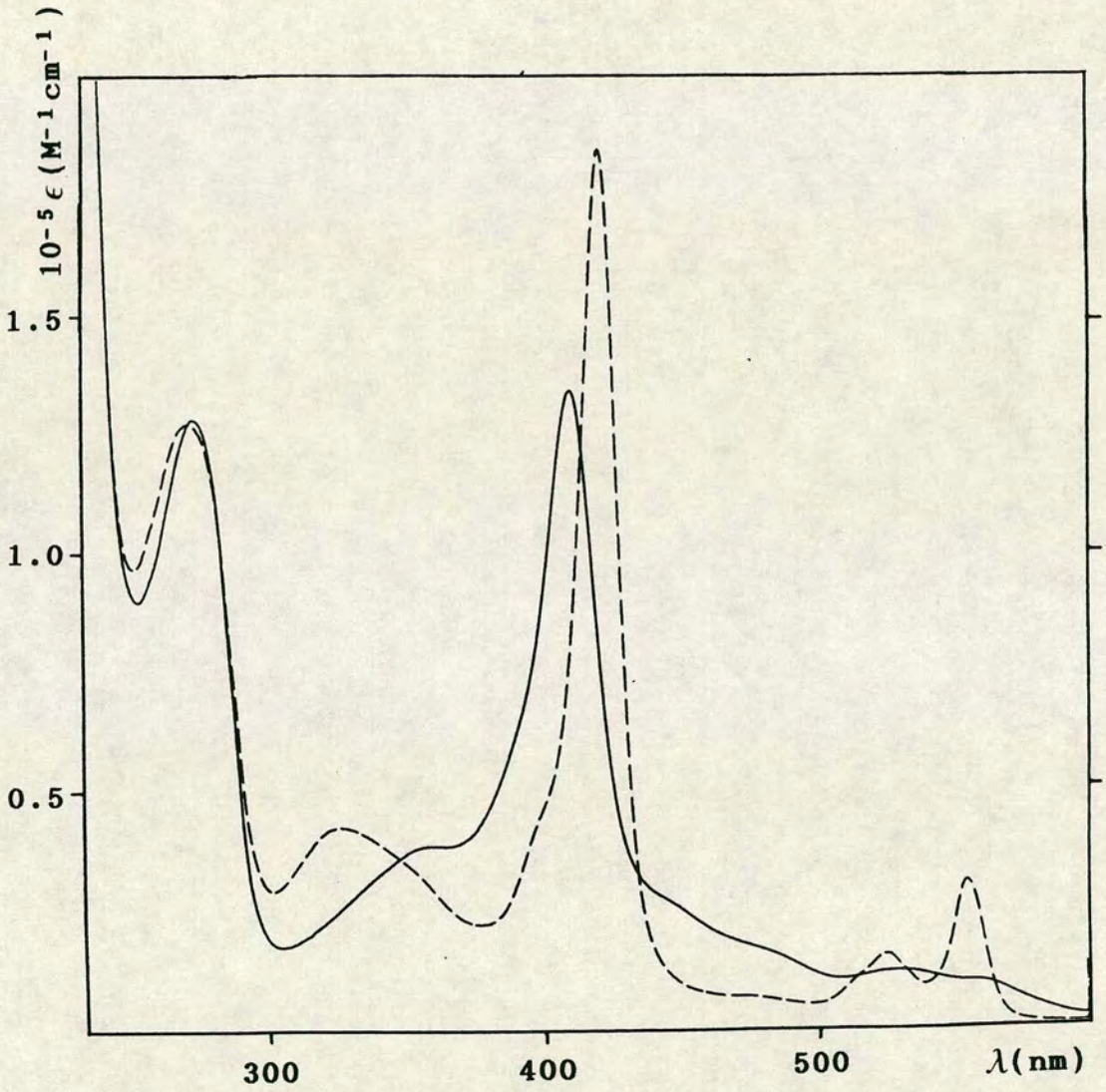

The oxidised and reduced states are represented by solid and dashed lines respectively. The relevant extinction coefficients are listed in Table 1.2.

TABLE 1.2

PEAK POSITIONS AND MOLAR EXTINCTION COEFFICIENTS OF OXIDISED AND REDUCED FLAVOCYTOCHROME *b*$_2$[a]

	OXIDISED FORM[b]		REDUCED FORM	
BAND	λ_{max} (nm)	ϵ ($mM^{-1}cm^{-1}$)	λ_{max} (nm)	ϵ ($mM^{-1}cm^{-1}$)
α	560	9.2	557	30.9
ß	530	11.3	528	15.6
γ	413	129.5	423	183.0
δ	362	34.4	328	39.0
UV	275	89.0	269	88.0

Notes : [a]Data from reference (12); [b]oxidised *b*$_2$ core: λ_{max} = 413nm, ϵ = 121.5 $mM^{-1}cm^{-1}$.

EPR signals have also been reported for the low spin ferric haem at 28K, although they are to some extent masked by those of the semiquinone. The g values for the haem signal are 2.99, 2.22 and 1.47 which are very like those reported for cytochrome b_5 (41).

EPR rapid-freezing studies have been used to monitor the reactive intermediates enabling detailed mechanistic studies (34).

1.6.3.3 CIRCULAR DICHROISM AND MAGNETIC CIRCULAR DICHROISM

Circular dichroism spectroscopy (CD) is a technique which relies on the differential absorption of circularly polarised radiation by an optically active chromophore. It is used as an aid to the determination of secondary protein structure, being especially useful in the detection of conformational change.

Ever since the first reported CD study of the cleaved enzyme (42), CD and its magnetically induced equivalent, MCD, have been extensively used to study various forms of flavocytochrome b_2. These studies showed that bands in the CD and MCD spectra corresponding to haem were affected by the removal of the FMN group, proving the existence of a direct interaction between the two prosthetic groups. A later CD experiment comparing intact and cleaved *S.cerevisiae* flavocytochromes b_2 led to the conclusion that the haems in each of these two forms were

bound in different environments (43).

1.6.3.4 NUCLEAR MAGNETIC RESONANCE SPECTROSCOPY

NMR experiments have been performed at 220 (44), 400 (28,45,46) and 600 MHz (28,46) on both the holoenzyme and the isolated *b*2 core. Initial experiments were restricted since protein was extracted in low yield directly from yeast. The advent of over-expression of flavocytochrome *b*2 in *E.coli* (11) enabled rapid generation of large quantities of pure protein and facilitated its study by NMR, a technique which requires both highly concentrated and highly purified protein.

The 600MHz NMR spectrum of the oxidised cytochrome *b*2 core is shown in Figure 1.11. It is typical for a paramagnetic protein of this molecular weight (10.5kDa), having peaks corresponding to haem resonances shifted to regions upfield of 10ppm and downfield of 0ppm. The large shifts are a result of both the paramagnetic nature of the ferric iron and the ring current shift induced by the aromaticity of the porphyrin ring. Further NMR experiments including 2D-NMR have enabled the assignment of most of the haem resonances (Figures 6.9 and 6.10).

The 1-D NMR spectrum of cytochrome *b*2 core comprises sharp peaks. These narrow linewidths are consistent with the fast molecular tumbling rate which would be expected for this relatively low molecular weight species, since linewidths are dependent upon the proton/proton dipolar

FIGURE 1.11

1D NMR SPECTRUM OF OXIDISED CYTOCHROME b_z CORE (29)

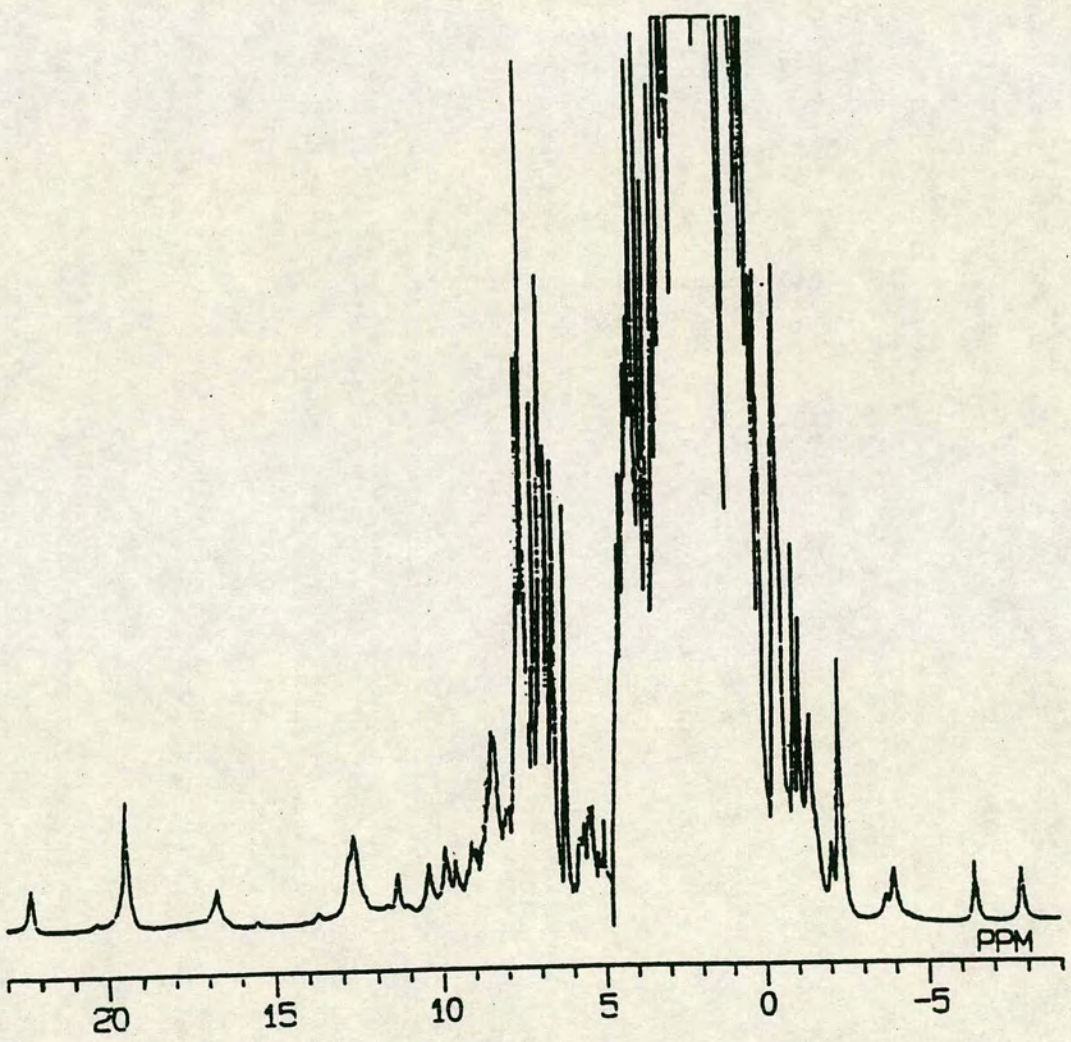

This 400MHz spectrum was taken at 25°C in 50mM phosphate/D_2O buffer, pH 7.0.

relaxations which are caused by such tumbling.

Comparison of the proton NMR spectra for the cytochrome *b*2 core and the holoenzyme (Figure 1.12), shows that the chemical shifts are identical for the shifted haem resonances in both spectra, although the linewidths are markedly broader for the holoenzyme. However the peaks are surprisingly sharp for a molecule of molecular weight equal to 230kDa, indicating that the cytochrome domain has a degree of flexibility with respect to the flavodehydrogenase domain.

Cytochrome *b*2 core is homologous to microsomal cytochrome *b*5 in both primary and tertiary structure. The 1D-NMR spectra support this, since the assignments of the haem resonances are very similar. NMR pH titrations of both proteins have enabled assignment of pK_a values to the haem propionates, which has illuminated some structural differences. The values obtained were consistent with both propionates being exposed to solvent in cytochrome *b*2 but only one is exposed in cytochrome *b*5, the other being folded back into the protein (28,44) (see Section 6.3.3).

Since both proteins interact with cytochrome *c*, NMR was used in an attempt to study the resultant complexes, in the hope of elucidating which region of flavocytochrome *b*2 acts as a cytochrome *c* binding site. It was postulated that this electron acceptor would bind to the cytochrome *b*2 core since it can only accept electrons from this domain (47), hence proton NMR spectra were monitored for

FIGURE 1.12

COMPARISON OF THE HIGHLY SHIFTED REGIONS OF THE 1D NMR SPECTRA OF FLAVOCYTOCHROME *b*2 AND THE CYTOCHROME *b*2 CORE

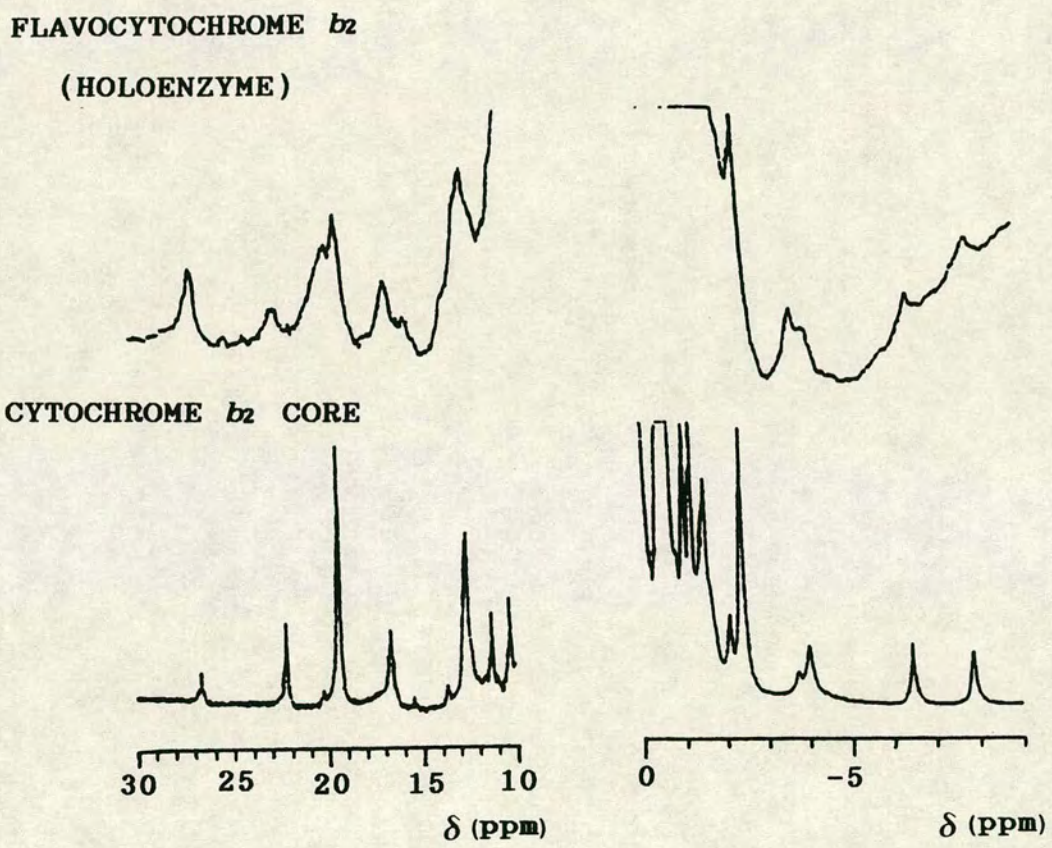

Both 400MHz spectra were recorded at 25°C in 5mM phosphate/D_2O buffer, pH 7.0 (28).

a cytochrome *c* titration for both the isolated cytochrome b_2 core and the holoenzyme. The linewidth broadening and resonance shifts of peaks corresponding to cytochrome *c* haem-methyls were used to assess the degree of binding since on complexation a larger molecule is formed which has a slower tumbling rate and hence broader linewidths. The study led to the conclusion that although cytochrome *c* binds strongly to the holoenzyme, it binds very weakly to the cytochrome b_2 domain (46). Further research aimed at locating the binding site flavocytochrome b_2's physiological electron acceptor is described in Chapter 5.

1.7 MECHANISM OF ACTION

1.7.1 THE ELECTRON PATHWAY

It is generally accepted that the physiological pathway of electron flow through flavocytochrome b_2 is as shown below:-

BOUND LACTATE ----> FLAVIN ----> HAEM ----> CYTOCHROME *c*

The catalytic cycle of flavocytochrome b_2 is represented in Figure 1.13. Flavin is fully reduced by the two electrons gained from lactate, it then passes one of these electrons to the haem resulting in formation of fully reduced haem and flavin semiquinone. The haem is then able to reduce a molecule of cytochrome *c*. The flavin semiquinone passes its electron to haem allowing

FIGURE 1.13

THE PHYSIOLOGICAL PATHWAY OF ELECTRON TRANSFER IN FLAVOCYTOCHROME *b*2

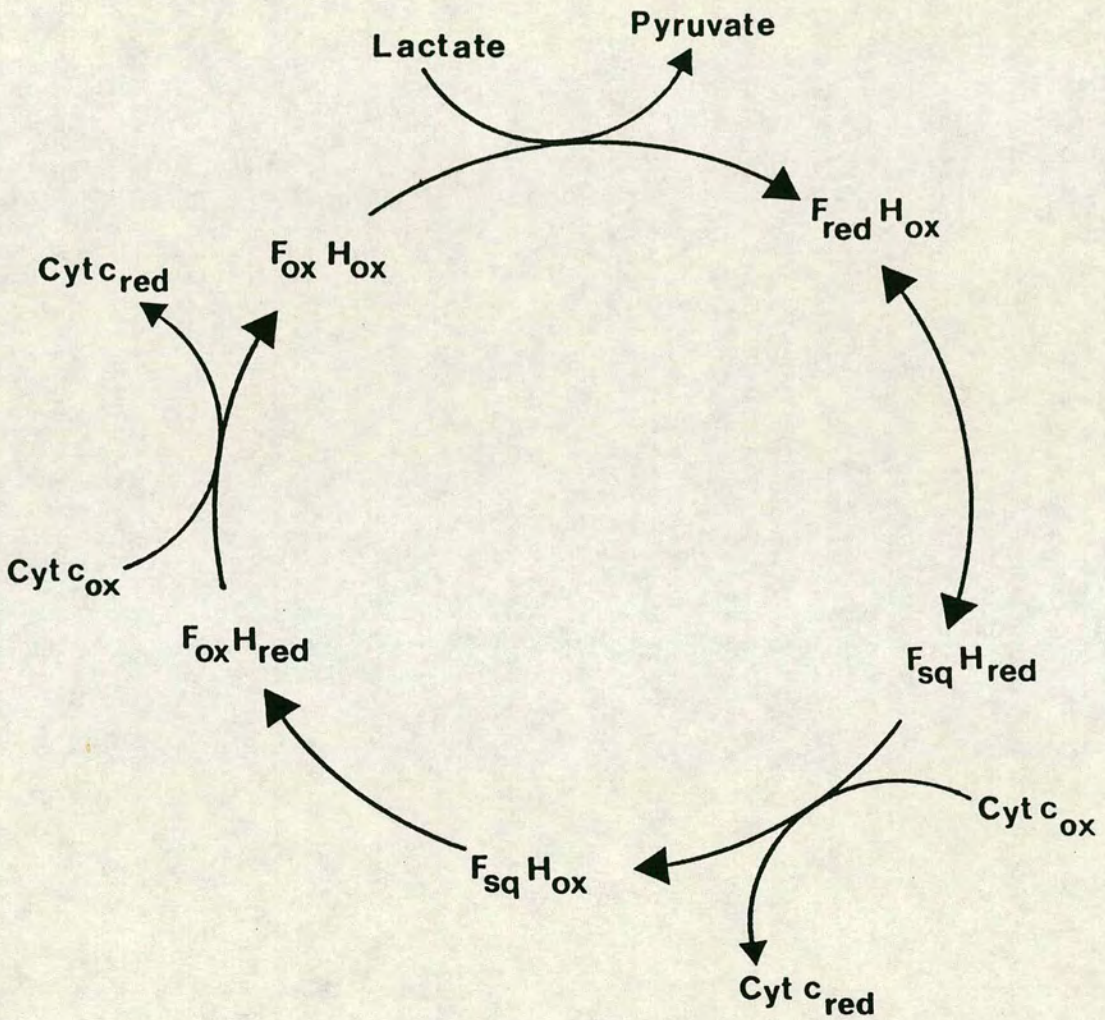

Abbreviations : F_{ox}, oxidised FMN; F_{sq}, flavosemiquinone; F_{red}, reduced FMN; H_{ox}, oxidised haem; H_{red}, reduced haem; Cyt c, cytochrome c.

reduction of a second molecule of cytochrome *c*.

The kinetic isotope effect, obtained using DL-lactate which had been deuterated at the C2 position, has been evaluated as 5.0 for the *S.cerevisiae* enzyme in the steady-state (48). This result is consistent with abstraction of the C2-hydrogen (as a proton) being the major rate-limiting step in the catalytic cycle. Pre-steady-state kinetic analyses have shown that flavin and haem reduction have isotope effects of 8 and 6 respectively (49), which indicates that C2-hydrogen abstraction is not totally rate-limiting.

Appleby and Morton first suggested that flavin was the entry point for lactate reducing equivalents; they noticed a parallel between loss of FMN and reduction of haem-b_2 by lactate (2,14). Baudras went on to demonstrate a direct correlation between lactate dehydrogenase activity and FMN content by means of enzyme resolution and FMN reconstitution (32). Further evidence came from Hasegawa who found that the redox potential of the flavin group was lower than that of the haem group (50). Flavin to haem electron transfer is intramolecular (51), however since the difference in redox potentials is small (~50mV) this process is most probably reversible.

It is the b_2-haem which is responsible for transfer of electrons to the physiological acceptor. This was first suggested by Forestier and Baudras who found that there was a linear relationship between enzyme activity and haem content; extrapolation of their data to zero haem

revealed that there was no cytochrome *c* reduction, however there was residual ferricyanide reductase activity. This is consistent with the b_2-haem being essential for cytochrome *c* reductase activity but not for the dehydrogenase function (52).

1.7.2 ELECTRON TRANSFER FROM LACTATE TO FLAVIN

1.7.2.1 LACTATE OXIDATION: CARBANION OR HYDRIDE MECHANISM?

Since flavins have the ability to transfer either pairs of electrons or single electrons, there are several possible mechanisms available for a dehydrogenation reaction such as the oxidation of L-lactate to pyruvate:-

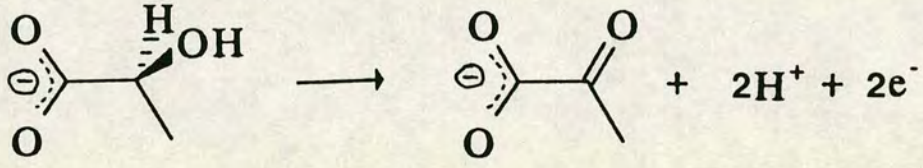

The possibilities are (i) homolytic cleavage of the C2-H bond which would give rise to a radical mechanism; (ii) heterolytic cleavage which would lead to a hydride mechanism if H^- was the leaving group: or (iii) a carbanion mechanism as a result of heterolytic cleavage with a proton as the leaving group. The latter two possibilities are illustrated in Figure 1.14.

The first of the above three mechanisms can be disregarded since the formation of free radicals from simple organic compounds under physiological conditions

FIGURE 1.14

POSSIBLE MECHANISMS FOR THE OXIDATION OF LACTATE BY FLAVOCYTOCHROME *b*$_2$

(a) HYDRIDE TRANSFER

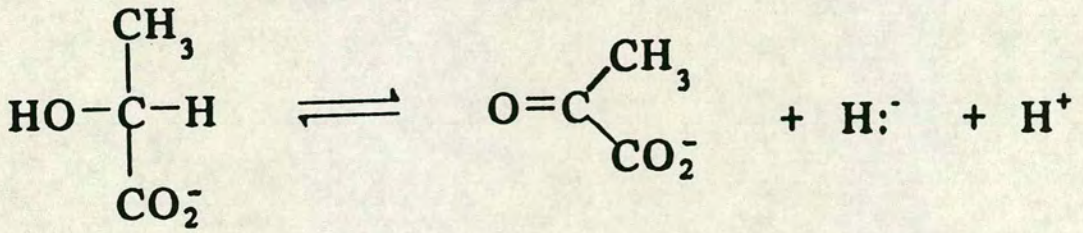

(b) CARBANION MECHANISM

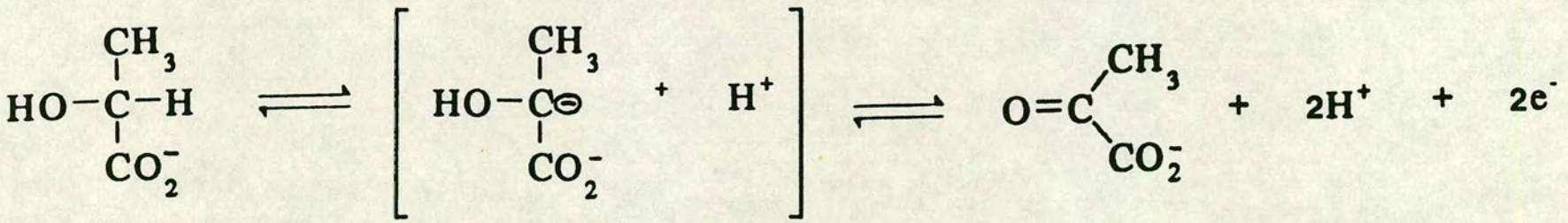

is not chemically realistic. The main body of evidence is in favour of a carbanion mechanism although a hydride mechanism has not been conclusively disproven.

In the case of flavocytochrome *b*$_2$, this evidence has come from parallel experiments to those previously carried out on a number of flavooxidases, namely through the use of various substrates and substrate analogues, such as halohydroxy-acids, hydroxybutynoate and ethane nitronate. Several flavooxidases have been found to catalyse halide ion elimination from ß-halosubstrates, for example D- and L-aminoacid oxidases catalyse the non-oxidative transformation of 3-chloroaniline and 2-amino-3-chlorobutyrate to pyruvate and 2-ketobutyrate respectively (53,54). Similarly lactate oxidase from *Mycobacterium smegmatis* catalyses the non-oxidative transformation of 3-chlorolactate to pyruvate (55). On the basis of this evidence it was suggested that a proton had to be abstracted from a C-H bond early in catalysis with the result that an α-carbanion would be an intermediate common to pathways of both the normal oxidative reaction and the non-oxidative halide ion elimination (53,55). However flavocytochrome *b*$_2$ does not dehydrohalogenate 3-chlorolactate even though this substrate can be oxidised by the enzyme. It was proposed that in this case carbanion processing might be much faster than chloride ion elimination. To overcome this, the transhydrogenation between halogenopyruvates (with the halogen on C-3) and reduced flavocytochrome *b*$_2$ was

studied (56). The hypothesis behind this was that since the reverse reaction is slower and protonation of the carbanion is the slowest step, then halide ion elimination might be in a position to compete. This was indeed the case for bromo- and chloropyruvate, but not for fluoropyruvate. Evaluation of partition ratios for the reaction with bromopyruvate resulted in a value of 500 for carbanion oxidation versus elimination (the forward reaction) and 2 for carbanion reduction versus elimination (the reverse reaction). The fact that elimination occurs in both directions implies that the reaction must take place via an intermediate lying on the redox pathway. This intermediate is most likely to be a carbanion although this has not been conclusively proven. The proposed mechanism for halosubstrate oxidation or elimination via a carbanion intermediate is illustrated in Figure 1.15.

In α-hydroxy-acid oxidation, if C_α-H bond breakage is rate limiting, then by the principle of microreversibility, C_α-H bond formation in the α-keto-acid will be the slowest step in the reverse reaction. The deuterium kinetic isotope of the reverse reaction (reduction of bromopyruvate by flavocytochrome *b*$_2$ in the presence of L-[2-^{2}H]-lactate) was found to be 4.4 which is consistent with the rate-limitation proposal above (56). An apparent inverse isotope effect was observed for bromide ion elimination (pyruvate formation). This supports the idea that the carbanion can undergo the two

FIGURE 1.15

THE MECHANISM FOR HALOSUBSTRATE OXIDATION (ROUTE a) OR ELIMINATION (ROUTE b) VIA A CARBANION INTERMEDIATE

(E, enzyme; S, substrate; B, active site base; Hal, halogen; ox, oxidised; red, reduced)

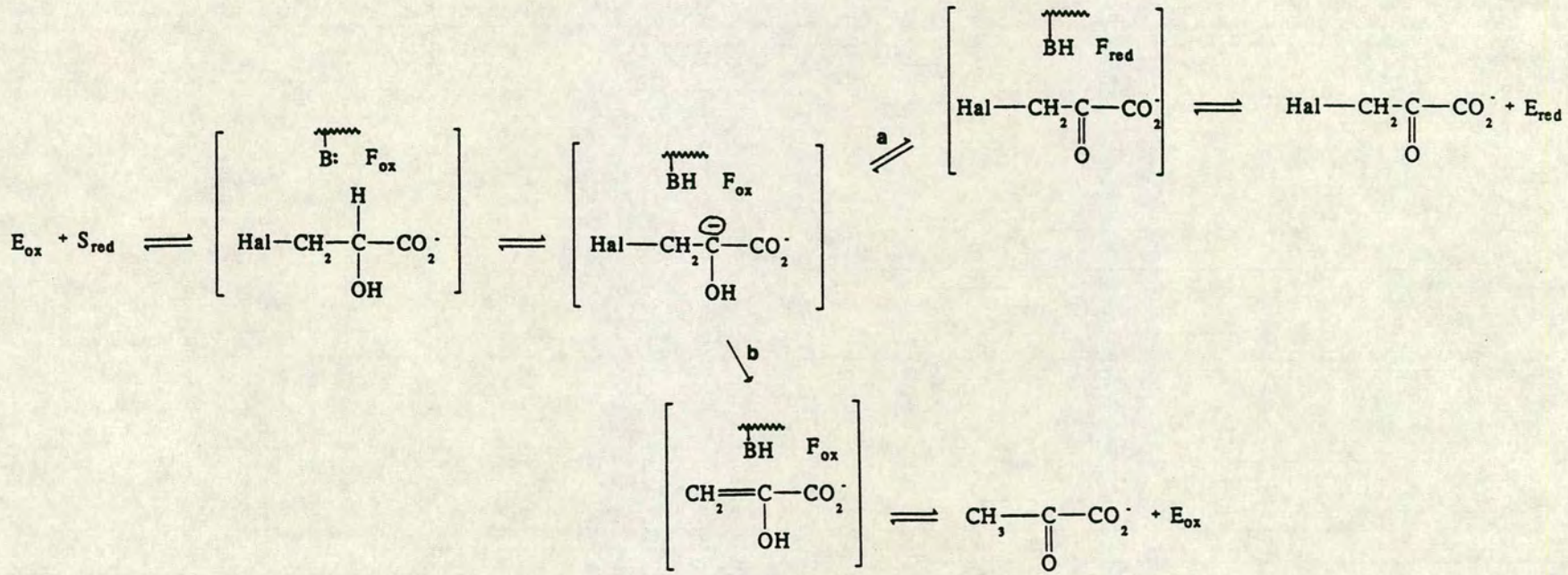

competing reactions of protonation and elimination, the former being subject to a strong isotope effect and the latter being independent of isotopic substitution. If bromide elimination were occurring via a hydride mechanism then an isotope effect would be expected for this step as well as for carbanion protonation.

When *S.cerevisiae* flavocytochrome *b*$_2$ is incubated with bromopyruvate in the presence of excess lactate, a transhydrogenation reaction takes place. In this reaction the haem is completely bypassed and the reaction products are bromolactate and pyruvate (57). This intermolecular hydrogen transfer provides strong evidence for a carbanion mechanism. When flavocytochrome *b*$_2$ functions in transhydrogenation mode in the presence of 2-^{3}H-lactate and bromopyruvate, intermolecular tritium transfer occurs from C2 of the tritiated hydroxysubstrate to C2 of the ketosubstrate, with tritium also being released into the solvent water. When bromopyruvate undergoes halide ion elimination, tritium is also found at C3 of the resulting pyruvate (56) (Figure 1.16). Incorporation of tritium into this pyruvate was significantly higher than into water, and significantly lower than into bromolactate. These results were explained as arising from ketonisation of an intermediate enol pyruvate partially on the enzyme and partially in the solvent (58). Such a scenario cannot be justified by a hydride mechanism and thus provides strong evidence in favour of a carbanion mechanism.

Further evidence for a such a mechanism comes from

FIGURE 1.16

THE MECHANISM FOR THE INTERMOLECULAR HYDROGEN TRANSFER CATALYSED BY FLAVOCYTOCHROME *b*2

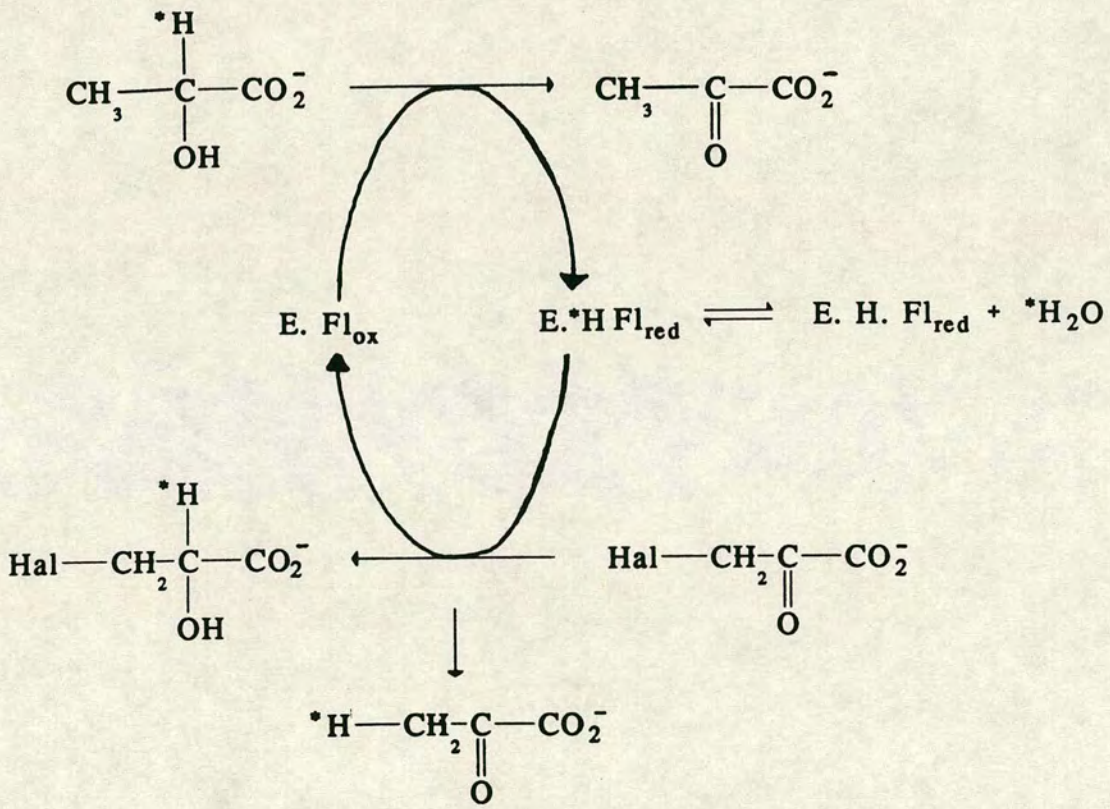

Key: Hal, halogen; *H, tritium; E, enzyme; Fl, flavin, ox, oxidised; red, reduced.

studies of the inactivation of flavocytochrome *b*2 by acetylenic substrates (48,59). It has previously been shown that 2-hydroxy-3-butynoic acid inhibits lactate oxidase by formation of a covalent adduct with the flavin cofactor (60,61). This "substrate" is a suicide inhibitor for flavocytochrome *b*2 although, contrary to the observations with lactate oxidase, no inactivation occurs under anaerobic conditions (59). This is due to the acetylenic carbanion, formed by C2-H abstraction, being rapidly processed to the ketoacid, which dissociates immediately. In the presence of electron acceptor the partition ratio between carbanion oxidation and inactivation is 3200, implying that competition between these reactions is not efficient. In the reverse reaction carbanion protonation is very slow due to negative charge delocalisation (62), hence inactivation can compete and the partition ratio is only 5. These results are compatible with a reaction scheme in which inactivation occurs through attack of the resulting allenic carbanion on the flavin. The chemical nature of this adduct was investigated (59) and it was predicted to be a C4a (flavin)- C4 (carbanion) adduct. The postulated mechanism of action of 2-hydroxy-3-butynoic acid on flavocytochrome *b*2 is shown in Figure 1.17.

The first piece of evidence in favour of a catalytically competent covalent intermediate between N5 of flavin and C2 of substrate was that reported between nitroethane carbanion and flavin N5 in a reaction catalysed by

FIGURE 1.17

THE MECHANISM FOR ENZYME INHIBITION BY 2-HYDROXY-3-BUTYNOATE (58,59)

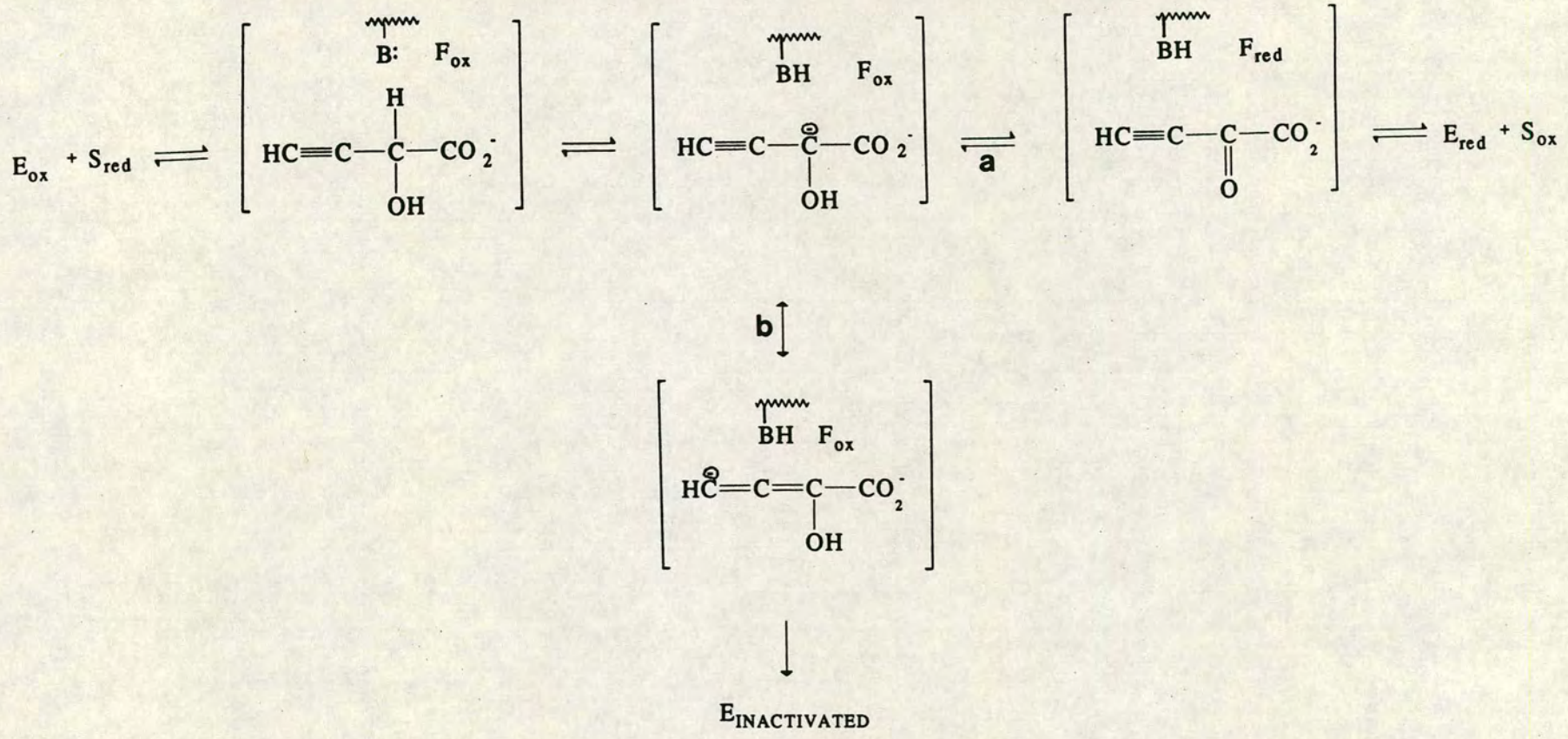

Inactivation occurs through nucleophilic attack by the allenic carbanion on C4a of flavin, resulting in formation of a covalent adduct (route b). Route a shows oxidation of the substrate.
(E, enzyme; S, substrate; B, active site base; F, flavin; ox, oxidised; red, reduced).

D-aminoacid oxidase (63). This inspired a study of the interaction between nitroethane and flavocytochrome *b*2 in the hope of finding conclusive evidence for this type of covalent intermediate. Unfortunately nitroethane turned out to be a competitive inhibitor of the enzyme (64). Several other enzymes, which are postulated to operate via a carbanion mechanism, such as L-amino-acid oxidase and lactate oxidase, also fail to react with ethane nitronate (4), hence this reaction is a poor means of verification of a carbanion mechanism.

All the studies described above provide evidence for a carbanion intermediate, however no information has been obtained to substantiate the existence of a transient covalent adduct between carbanion and flavin. In order to investigate this further, flavin-free cytochrome *b*2 was reconstituted with 5-deaza-5-carbaflavin (5-deazaFMN) (65). Deazaflavins behave as good isosteres of FMN and function efficiently as transhydrogenation catalysts, although they do not allow normal oxidative functions of oxidases. The resulting 5-deazaFMN-*b*2 was reducible by lactate and reoxidised by pyruvate although electrons were not transferred to the haem and no ferricyanide reductase activity was observed (65). Tritium transfer experiments indicate that 5-deazaFMN reduction and reoxidation occurs via a hydride mechanism. However, a carbanion mechanism in which a solvent-shielded active site base (His-373) could transfer the substrate proton directly to N5 of the reduced flavin anion cannot be

ruled out. This led to the postulation that a "mechanistic switch" occurs from a carbanion mechanism to a hydride transfer mechanism upon FMN substitution by 5-deazaFMN. This switch being dependent upon the different chemical reactivity of 5-deazaFMN which is generally considered to be a "flavin-shaped nicotinamide" (66).

1.7.2.2 NATURE OF ELECTRON TRANSFER FROM CARBANION TO FLAVIN

Assuming that lactate is oxidised via a carbanion mechanism there are three possible modes of electron transfer to the oxidised flavin: (i) nucleophilic attack at N5 of FMN by the substrate carbanion, or (ii) one electron transfer followed by collapse of the radical pair to give the covalent intermediate, or (iii) two consecutive one-electron transfers to give the fully reduced flavin (67,68) (Figure 1.18).

In practice, differentiation between nucleophilic attack and a radical mechanism could prove difficult, if collapse of the radical pair was fast. Experimental evidence does in fact favour the existence of covalent intermediates. The first case being the cyanide trapping of a catalytically competent covalent intermediate between ethane nitronate and D-aminoacid oxidase (see 1.7.2.1) and the second being the characterisation of two glycol-flavin adducts formed between glycolate and lactate oxidase (68). From analysis of the *S.cerevisiae*

FIGURE 1.18

POSSIBLE MODES OF ELECTRON TRANSFER FROM THE SUBSTRATE CARBANION TO THE FLAVIN (FMN)

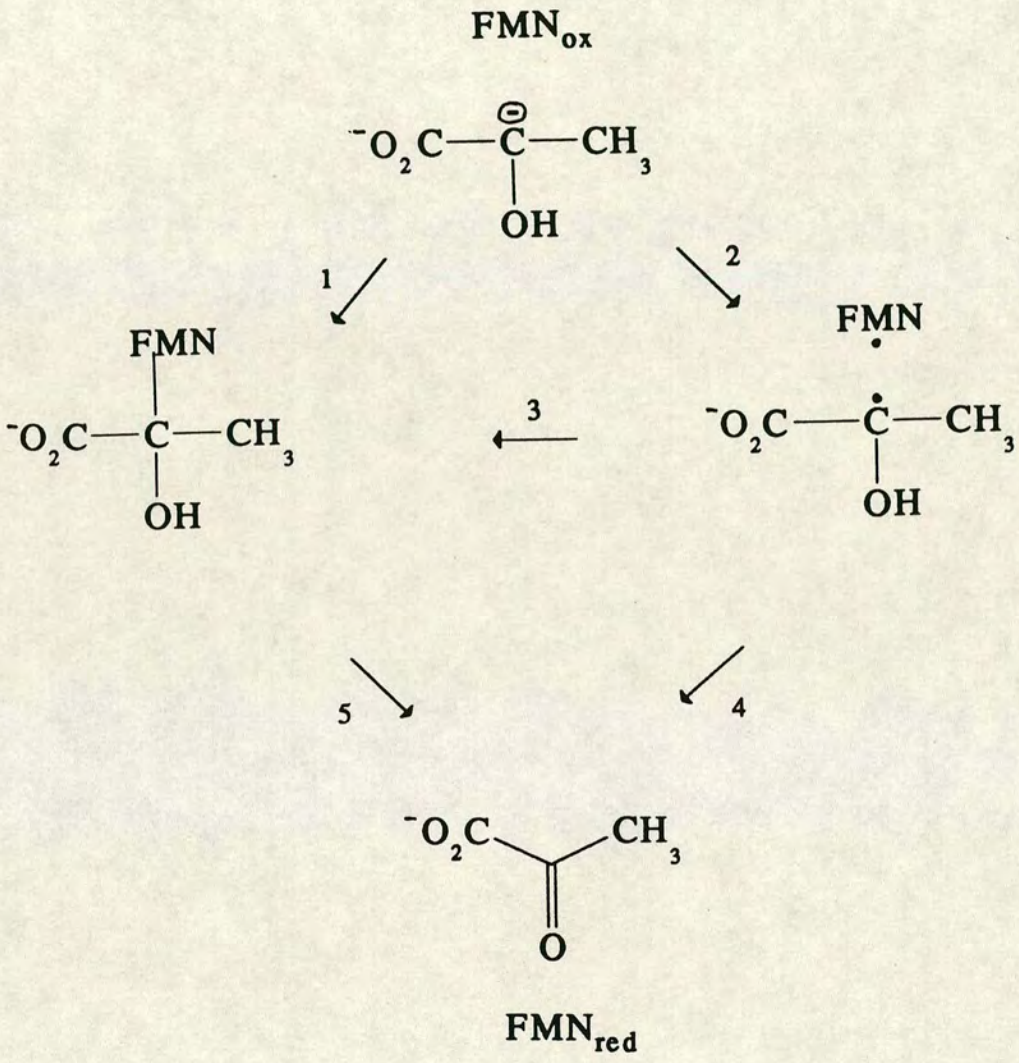

Route 1 involves formation of a covalent intermediate by nucleophilic attack at N-5 of flavin. Routes 2 and 3 show formation of the same covalent intermediate but via the formation and the subsequent collapse of a radical pair. The covalent intermediate is fragmented resulting in reduced flavin and pyruvate (route 5). These products can also be formed by generation of a radical pair followed by a second one electron transfer.

flavocytochrome b_2 crystal structure (10) it was considered that C2 of pyruvate was too close to N5 for there not to be a covalent adduct (69) and the formation of the lactate oxidase/glycolate adduct was put forward as verification.

With a defined chemical mechanism (carbanion) and substantial knowledge of the crystal structure of the active site in subunit 2 (10), Lederer and Mathews were able to ascribe catalytic roles to the various side-chains and were hence able to propose the sequence of events as shown in Figure 1.19 (58).

The substrate has two points of attachment through hydrogen bonding and ionic interactions. The carboxylate is both hydrogen-bonded and has an ionic interaction with the guanido group of Arg-376. The other oxygen atom is hydrogen-bonded to the phenolic group of Tyr-143.

The C2-H of lactate is abstracted by the active site base, His-373 (the rate-limiting step (49)), and the resulting imidazolium ion is stabilised by Asp-282. The carbanion formed collapses to the putative covalent intermediate. This places a negative charge on N1 of FMN, which is stabilised by Lys-349. Tyr-254 was originally assumed to be responsible for removal of the hydroxyl hydrogen, but has recently been shown to play a role in transition state stabilisation (4). Thus the flavin is fully reduced to the hydroquinone which then passes its two electrons to the haem in two one-electron steps via formation of a semiquinone intermediate. In

FIGURE 1.19

THE PROPOSED MECHANISM OF L(+)LACTATE OXIDATION BY FLAVOCYTOCHROME *b*$_2$

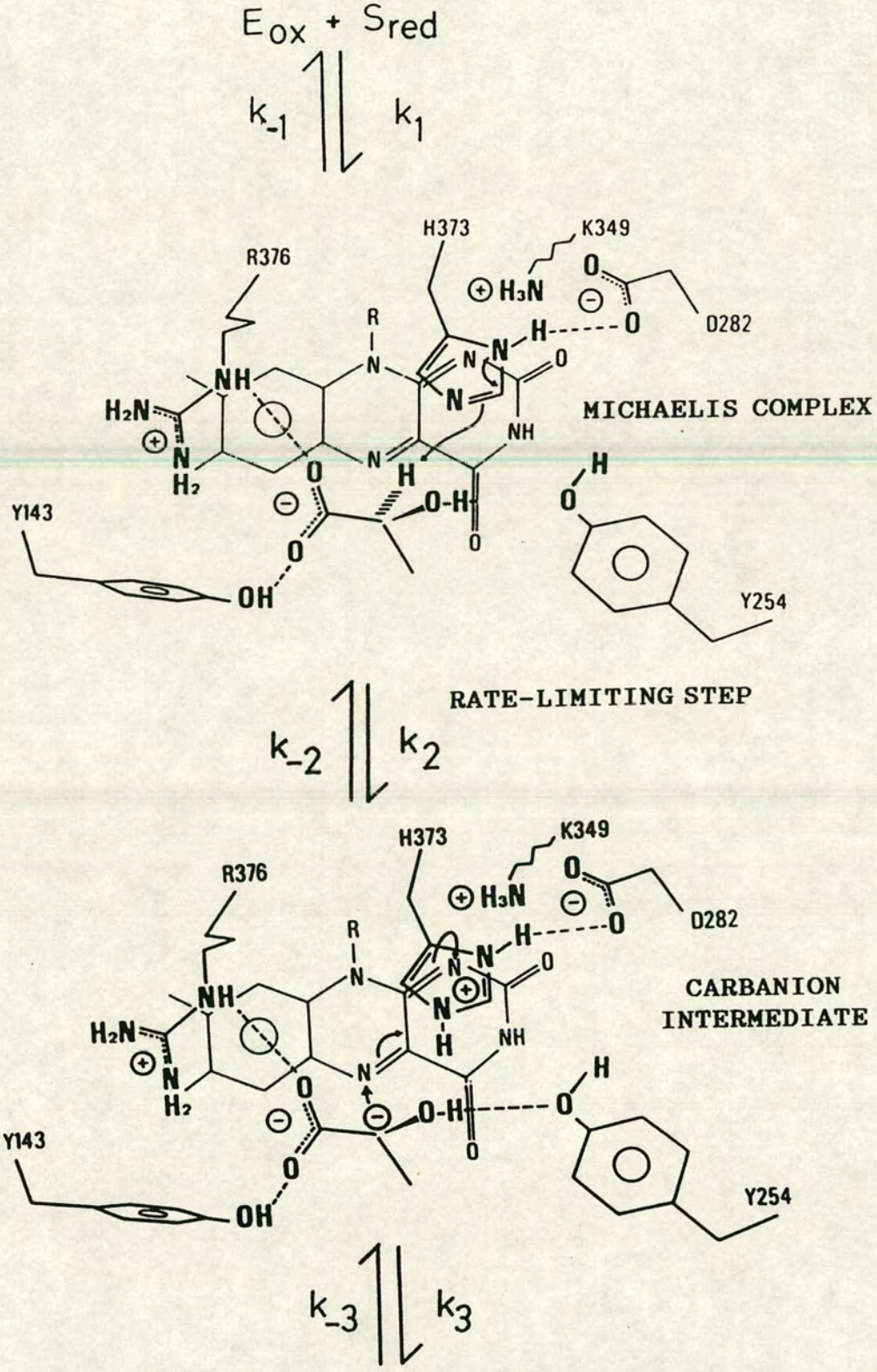

This mechanism is based on the original proposal by Lederer and Mathews (57) and shows the reaction proceeding via a carbanion intermediate. Presence of the covalent adduct is at present conjecture.
(E, enzyme; S, substrate)

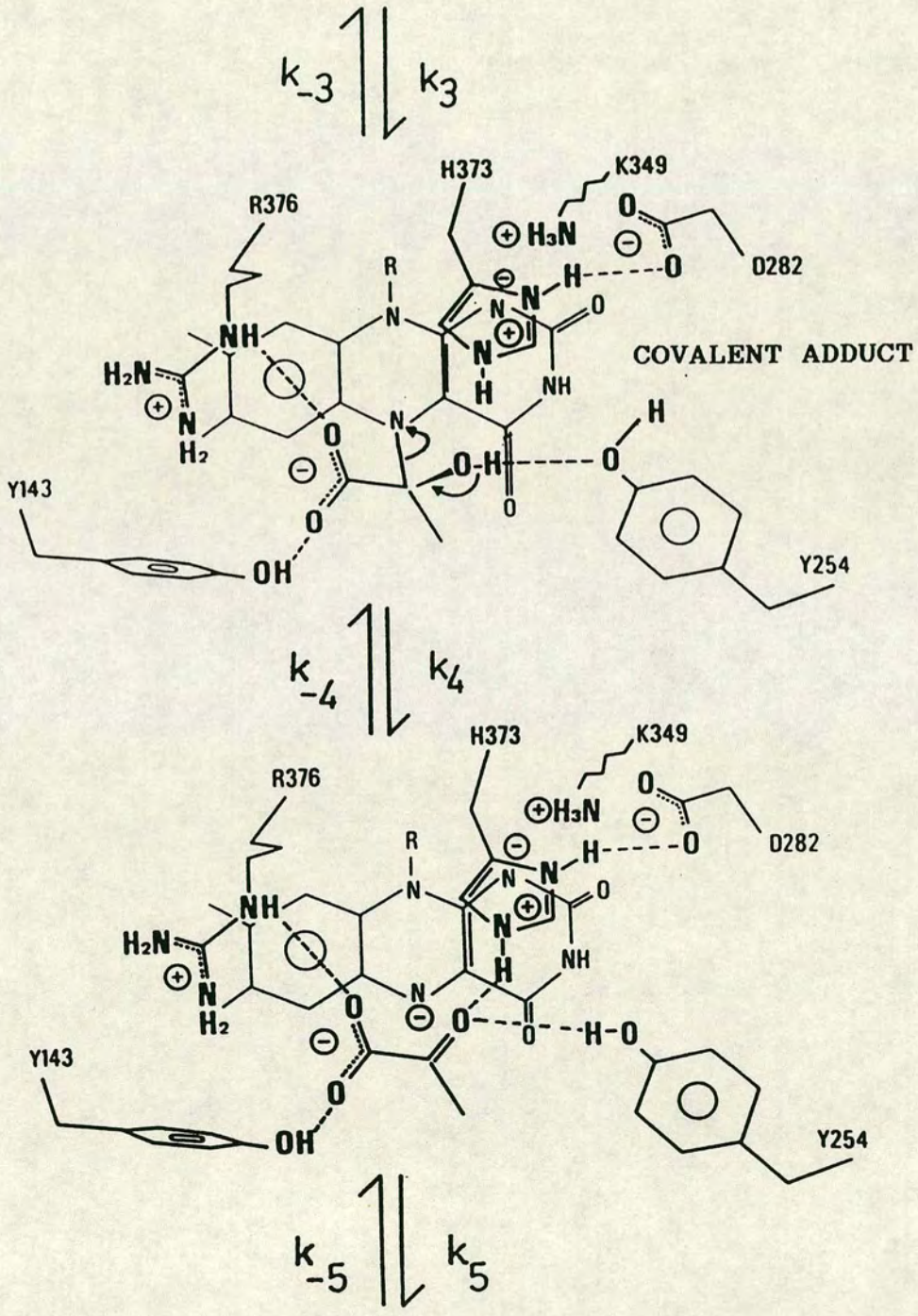

$E_{red} + S_{ox}$

this semiquinone state, Tyr-254 and His-373 are positioned so as to stabilise pyruvate binding, each providing one hydrogen bond to the keto-group.

1.7.3 FLAVIN TO HAEM ELECTRON TRANSFER

Flavin to haem electron transfer was first shown to be an intramolecular process by Morton and Sturtevant (51). They performed stopped-flow kinetics on the cleaved enzyme and observed that the rate of haem reduction was independent of protein concentration in the range 0.4 to 10.5 μM. This intramolecular electron transfer has to be studied by rapid-kinetics techniques, since the rate-limiting step occurs before flavin reduction (see 1.7.1). There were problems regarding the choice of observation wavelength in the initial studies. Haem reduction can easily be measured by monitoring the absorbance increase at 557nm or 423nm (see Figure 1.10), but choice of observation wavelength for flavin reduction is not so simple. Several researchers monitored flavin reduction at 470nm (70-72) but they encountered difficulties since it was found that haem reduction contributed to 50% of the absorbance change at this wavelength (70). Iwatsubo proposed to monitor flavin reduction at 438.5nm which he calculated to be the haem isosbestic point from oxidised and reduced spectra of the flavin-free enzyme (73). Capeillère-Blandin and coworkers reinvestigated intramolecular electron transfer in the cleaved enzyme by

means of stopped-flow (at 24°C) and rapid-freezing EPR spectroscopy experiments (33). They monitored flavin reduction at 438.3nm which is a redetermination of the isosbestic point. It was demonstrated that the flavin semiquinone also absorbs at this wavelength, with an absorbance similar to that of the hydroquinone therefore absorbance decrease at 438.3nm only correlates to disappearance of the oxidised flavin. The parallel EPR experiment allowed direct observation of the semiquinone species, hence enabling complete description of the time courses of the various redox states of the prosthetic groups.

It was confirmed that each protomer required three electrons in order to become fully reduced; two for flavin and one for haem. Biphasic time courses were observed for both flavin and haem reduction. An initial burst of fully reduced flavin was detected in the first 6ms of phase I. After 6ms up to the end of the first phase (35ms) the redox forms which accumulated were the reduced haem (up to 80%), the flavin semiquinone (up to 50%) and the fully reduced flavin (from 25% up to 35%). The authors proposed that phase I corresponded to the entry of two electrons into the protomer and was followed by the much slower phase II which corresponds to entry of the third electron, which therefore cannot be involved in turnover. A previous stopped-flow study had observed this second phase but had dismissed it as a contribution from inactive enzyme (73).

The Capeillère-Blandin results were interpreted with the aid of computer simulation and were presented schematically as shown in Figure 1.20. After the initial flavin reduction (two electrons), one electron is rapidly passed to the haem, interprotomer electron transfer between flavin-semiquinone couples then occurs, which results in regeneration of two oxidised flavins per tetramer. Entry of the third electron follows. It was suggested that this slow phase was due to a slow conformational change at the active site after acceptance of the first two electrons per protomer. Such a conformational change could affect the affinity for lactate and/or the electron transfer from bound lactate to enzyme.

The Capeillère-Blandin model was based on kinetic experiments carried out under saturating substrate concentrations. Pompon performed stopped-flow experiments at 5°C with both intact and cleaved forms of flavocytochrome *b*$_2$ under varying concentrations of 2-[2-^{1}H]- and 2-[2-^{2}H]-lactate (49,74). He observed an isotope effect of 8 for flavin reduction; such large effects meant that he could observe phenomena at very low rates of electron transfer. This work led to modification of the Capeillère-Blandin model.

Pompon observed biphasic reaction courses for both flavin and haem reductions although at very low substrate concentrations flavin reduction became monophasic and appeared to be slower than haem reduction. This was

FIGURE 1.20

THE CAPEILLÈRE-BLANDIN SCHEME FOR ELECTRON TRANSFER IN FLAVOCYTOCHROME b_2 (33)

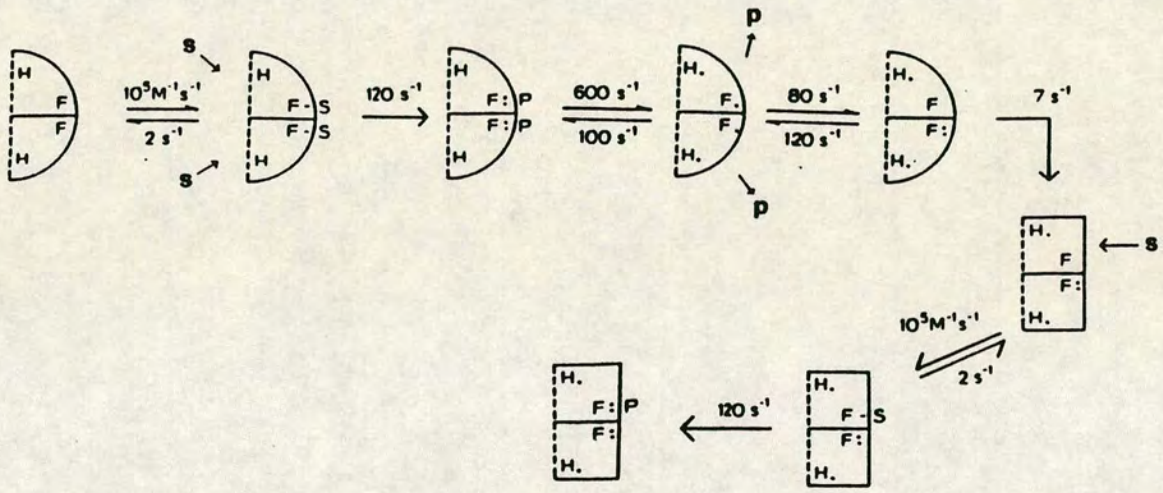

The enzyme is represented as a dimer for clarity. Two electron pairs are introduced into the enzyme which results in reduction of haem and formation of two flavin semiquinones. Interprotomer electron transfer then occurs to form one flavin hydroquinone and one oxidised flavin per dimer. Phase two, entry of the third electron, can then occur after a conformational change takes place (illustrated by the rectangles).
(F, flavin; H, haem; S, substrate; P, product)

explained by the suggestion that interprotomer electron transfer was taking place faster than the initial flavin reduction by substrate. Pompon's kinetic isotope effect values of 8 and 6 for flavin and haem reduction respectively indicated that flavin to haem electron transfer has a small contribution to rate-limitation.

The Pompon model differed from that of Capeillère-Blandin in several ways. Firstly, Pompon assumed that the electron transfer from lactate to flavin was random whereas in the Capeillère-Blandin model this process was postulated to occur simultaneously in the two subunits of the dimer. Secondly, Pompon proposed that this interprotomer electron transfer could take place between flavin and flavin, flavin and haem or haem and haem, athough study of the X-ray crystal structure shows that the latter is highly unlikely as an interhaem distance of 52.8Å is involved (10). Thirdly, Pompon suggested that a fast conformational change controlled by the redox state of the flavin or haem of one protomer could modulate electron transfer in another protomer. Taking the temperature differences into account, the intramolecular electron transfer rates estimated by the two models do not differ significantly. However, rates of interprotomer electron transfer do differ from 80-120s^{-1} at 24°C to 1-10s^{-1} at 4°C. This led to the idea of "priveleged" pairs of cofactors, with rapid electron transfer between two members of a pair and slow electron transfer from one pair to another.

The Pompon study provided an investigation of the effect of proteolysis on intramolecular electron transfer. It was found that for similar rates of electron entry, haem reduction rates did not differ for the intact and cleaved enzymes. Proteolytic cleavage must therefore affect the first steps in the mechanism, namely substrate binding and flavin reduction.

Laser flash photolysis studies on the intact enzyme showed that intramolecular electron transfer only occurred in the presence of pyruvate (31). This was interpreted in terms of conformational change induced by pyruvate binding in order to permit electron transfer between the prosthetic groups. The rate constant found in the presence of pyruvate was dependent upon ionic strength suggesting that electrostatic effects govern this conformational change.

Although the rates of intramolecular electron transfer have been thoroughly investigated, the actual pathway of electron flow between the prosthetic groups is still conjecture. Study of the three-dimensional X-ray crystal structure of *S.cerevisiae* flavocytochrome b_2 reveals that there are two crystallographically distinguishable subunits: subunit 1 in which both the flavin and cytochrome domains are ordered, and subunit 2 where pyruvate is present at the active site and the cytochrome domain is disordered (Figure 1.21).

It was noticed that Tyr-143 was present in both subunits and apparently plays a dual role. In subunit 1 Tyr-143

FIGURE 1.21

THE TWO ACTIVE SITES OF FLAVOCYTOCHROME *b*$_2$

(a) SUBUNIT ONE (PYRUVATE ABSENT)

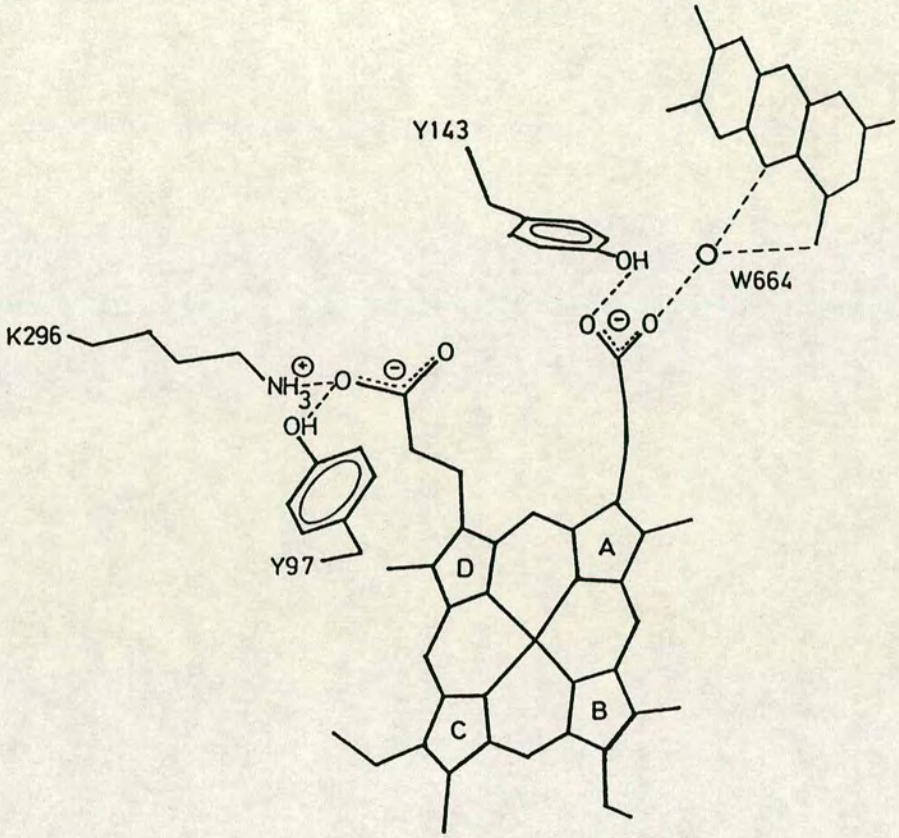

(b) SUBUNIT TWO (PYRUVATE PRESENT)

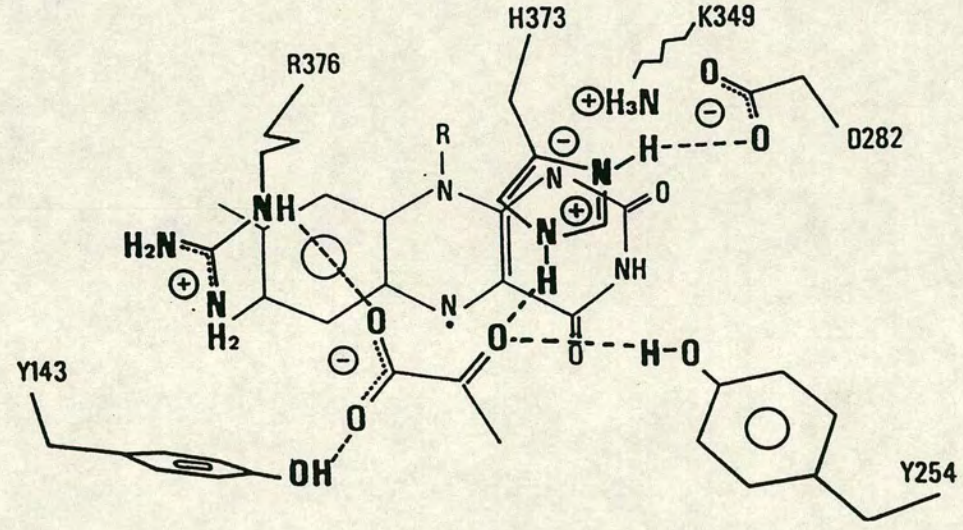

appears to be important for substrate binding (the residue is hydrogen bonded to the pyruvate carboxylate), but in subunit 2 this residue forms a hydrogen bond to haem propionate-7 suggesting that Tyr-143 could be involved in controlling the flow of electrons from flavin to haem. These suggestions were investigated by kinetic characterisation of a mutant flavocytochrome *b*2 in which site-directed mutagenesis had been used to replace Tyr-143 with Phe, thereby removing the residue's ability to form hydrogen bonds (75). It was concluded that Tyr-143 was crucial in facilitating electron transfer between the prosthetic groups.

Site-directed mutagenesis of other residues and the subsequent characterisation of these mutants may help to elucidate the exact electron pathway. Regions which may be involved include interface residues such as Tyr-97 and the interdomain hinge. Characterisation of a hinge-mutated flavocytochrome *b*2 forms part of this thesis.

1.7.4 ELECTRON ACCEPTORS

1.7.4.1 CYTOCHROME *c*

Cytochrome *c* is the physiological electron acceptor for flavocytochrome *b*2 (2) and accepts electrons exclusively from the *b*2-haem (47). Complex formation has been shown to take place in both aqueous and crystalline states (76). Interaction between the two proteins is thought to be electrostatically-dominated since complexation is

dependent upon both pH and ionic strength (76-79).

The stoicheometry of complexation and the location of cytochrome *c* binding sites on flavocytochrome *b*$_2$ have been the subject of much debate and are discussed in more detail in Chapters 4 and 5 of this thesis.

1.7.4.2 FERRICYANIDE

Ferricyanide is the most commonly used electron acceptor for steady-state experiments with flavocytochrome *b*$_2$, having the advantage that acceptor reduction is essentially independent of concentration over the range 0.2 to 3.0mM.

It was originally suggested that ferricyanide could, like cytochrome *c*, only accept electrons from the *b*$_2$-haem (80). This has been disproven by the discovery that dehaemo-flavocytochrome *b*$_2$ (81) and the independently-isolated flavodehydrogenase domain (47) can both reduce ferricyanide, albeit with decreased activity. These results implied that ferricyanide could accept electrons from both flavin hydroquinone and flavin semiquinone. It was calculated for the *S.cerevisiae* enzyme that reduction by the semiquinone was twenty-fold faster than by the hydroquinone. Thus, in the holoenzyme ferricyanide can rapidly accept electrons from two donors: flavin semiquinone and the *b*$_2$-haem.

As cytochrome *c* can only accept electrons from the latter, this possibly explains why, in general, enzyme

activity is lower with cytochrome *c* than with ferricyanide as acceptor.

1.8 FLAVOCYTOCHROME b_2 FROM *Hansenula anomala*

1.8.1 STRUCTURAL AND KINETIC COMPARISON WITH *S.cerevisiae* ENZYME

Flavocytochrome b_2 has also been isolated from the yeast *Hansenula anomala* (82). Extensive kinetic studies have been carried out on the *H.anomala* enzyme and have revealed differences in catalytic behaviour compared to the enzyme from *S.cerevisiae* (83,34). The molar activity of the *H.anomala* enzyme is several-fold higher than that of the *S.cerevisiae* enzyme and the catalytic cycles of the two enzymes possess different rate-limiting steps; the rate-limiting step for the *S.cerevisiae* enzyme is C2-H abstraction, whereas for the *H.anomala* enzyme it is flavin to haem electron transfer.

Although only the *S.cerevisiae* enzyme is of known three-dimensional structure (10), the amino-acid sequences of both enzymes are known (84,85). Comparison of these sequences (Figure 1.22) shows that there is 60% identity; all of the active site residues identified in the *S.cerevisiae* enzyme are conserved in the *H.anomala* enzyme. However, there are significant regions of sequence divergence in two surface loops of the protein; the interdomain hinge and a proteinase sensitive loop on the flavodehydrogenase domain. Both regions are shorter

FIGURE 1.22

SEQUENCE ALIGNMENT OF FLAVOCYTOCHROMES *b*$_2$ FROM *S.cerevisiae* (Sc) AND *H.anomala* (Ha) (84,85)

```
Sc  MLKYKPLLKI SKNCEAAILR ASKTRLNTIR AYGSTVPKSK SFEQDSRKRT QSWTALRVGA ILAATSSVAY LNWHNGQIDN EPKLDMNKQK ISPAEVAKHN  20
Ha  ..MFKSQLRT ATARSS..FR SLASKLNPQR FNSSKTPLLN A.TRGSNRSK NSLIALAIS. .LSAVSSSYY L.YQKDKFIS ADVPHWKDIE LTPEIVSQHN  19
    ----K--L-- ---------R -----LN--R ---S--P--- -----S---- -S--AL---- -L-A-SS--Y L--------- ---------- --P--V--HN

Sc  KPDDCWVVIN GYVYDLTRFL PNHPGGQDVI KFNAGKDVTA IFEPLHAPNV IDKYIAPEKK LGPLQGSMPP ELVCPPYAPG ETKEDIARKE QLKSLLPPLD  120
Ha  KKDDLWVVLN GQVYDLTDFL PNHPGGQKII IRYAGKDATK IFVPIHPPDT IEKFIPPEKH LGPLVGEFEQ E......EEE LSDEEIDRLE RIER.KPPLS  112
    K-DD-WVV-N G-VYDLT-FL PNHPGGQ--I ---AGKD-T- IF-P-H-P-- I-K-I-PEK- LGPL-G---- E--------- ---E-I-R-E ------PPL-

Sc  NIINLYDFEY LASQTLTKQA WAYYSSGAND EVTHRENHNA YHRIFFKPKI LVDVRKVDIS TDMLGSHVDV PFYVSATALC KLGNPLEGEK DVARGCGQGV  220
Ha  QMINLHDFET IARQILPPPA LAYYCSAADD EVTLRENHNA YHRIFFNPKI LIDVKDVDIS TEFFGEKTSA PFYISATALA KLGHP.EGEV AIAKGAGRE.  210
    --INL-DFE- -A-Q-L---A -AYY-S-A-D EVT-RENHNA YHRIFF-PKI L-DV--VDIS T---G----- PFY-SATAL- KLG-P-EGE- --A-G-G---

Sc  TKVPQMISTL ASCSPEEIIE AAPSDKQIQW YQLYVNSDRK ITDDLVKNVE KLGVKALFVT VDAPSLGQRE KDMKLKFSNT KAGPKAMKKT NVEESQGASR  320
Ha  .DVVQMISTL ASCSFDEIAD ARIPGQQ.QW YQLYVNADRS ITEKAVRHAE ERGMKGLFIT VDAPSLGRRE KDMKMKFEAD SDVQG..DDE DIDRSQGASR  306
    --V-QMISTL ASCS--EI-- A-----Q-QW YQLYVN-DR- IT---V---E --G-K-LF-T VDAPSLG-RE KDMK-KF--- ---------- ----SQGASR

Sc  ALSKFIDPSL TWKDIEELKK KTKLPIVIKG VQRTEDVIKA AEIGVSGVVL SNHGGRQLDF SRAPIEVLAE TMPILEQRNL KDKLEVFVDG GVRRGTDVLK  420
Ha  ALSSFIDPSL SWKDIAFIKS ITKMPIVIKG VQRKEDVLLA AEHGLQGVVL SNHGGRQLDY TRAPVEVLAE VMPILKERGL DQKIDIFVDG GVRRGTDVLK  406
    ALS-FIDPSL -WKDI---K- -TK-PIVIKG VQR-EDV--A AE-G--GVVL SNHGGRQLD- -RAP-EVLAE -MPIL--R-L --K---FVDG GVRRGTDVLK

Sc  ALCLGAKGVG LGRPFLYANS CYGRNGVEKA IEILRDEIEM SMRLLGVTSI AELKPDLLDL STLKARTVGV PNDVLYNEVY EGPTLTEFED A...        511
Ha  ALCLGAKGVG LGRPFLYAMS SYGDKGVTKA IQLLKDEIEM NMRLLGVNKI EELTPELLDT RSIHNRAVPV AKDYLYEQNY QRMSGAEFRP GIED       500
    ALCLGAKGVG LGRPFLYA-S -YG--GV-KA I--L-DEIEM -MRLLGV--I -EL-P-LLD- -----R-V-V --D-LY---Y ------EF-- ----
```

The sequences shown include the N-terminal presequence which directs the enzyme into the mitochondrion. Numbering starts from the first residue in the mature protein. A consensus is shown wherein both sequences are identical.

and more acidic in the enzyme from *H.anomala*.

It was proposed that these structural and chemical differences were, at least in part, responsible for the catalytic differences between the flavocytochromes *b*2 from the two species, particularly in intramolecular electron transfer between the two domains and in the interaction with cytochrome *c* (85). Whether or not this is the case has been investigated by using protein engineering to generate the interspecies hybrid enzymes discussed in Chapters 2 and 3. A drawback to such investigations is the lack of a suitable expression system for the *H.anomala* holoenzyme; the individual domains have successfully been expressed in *E.coli* (86) but attempts on the holoenzyme have as yet been unsuccessful (87).

1.8.2 PROTEOLYSIS

Tryptic cleavage of the loop and hinge regions of flavocytochrome *b*2 (termed aa' and cd respectively) ultimately generates three fragments: N, ϵ and ß (88). These are illustrated in Figure 1.23. Cleavage primarily takes place in aa' and results in major activity loss although the molecule remains a stable tetramer with unchanged molecular weight. This corresponds to the "cleaved" form of the *S.cerevisiae* enzyme which is apparent during purification of the enzyme in the absence of PMSF (see 1.3). The second and third cleavages (at

FIGURE 1.23

STRUCTURAL REPRESENTATION OF THE FRAGMENTS OBTAINED BY PROTEOLYSIS OF FLAVOCYTOCHROME *b*2

Each scheme is representative of a subunit of flavocytochrome *b*2 .

(a) EFFECT OF YEAST PROTEASES ON *S.cerevisiae-b*2

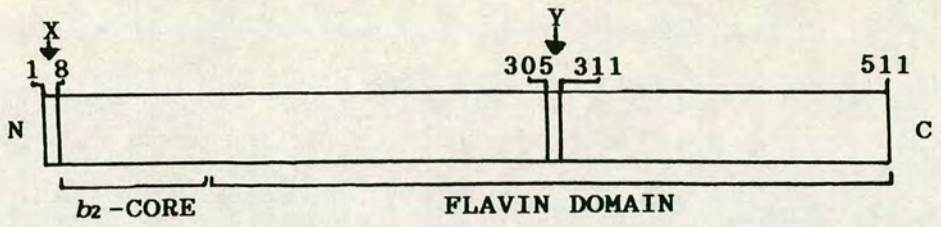

Yeast proteases cleave the polypeptide chain at the points marked by the arrows, resulting in loss of the first 8 residues from the N-terminus as well as residues 306-310. The cleaved form of the enzyme is obtained (90). *H.anomala-b*2 is more resistant to attack of this nature (18).

(b) PROTEOLYTIC DIGEST OF *H.anomala-* AND *S.cerevisiae-b*2

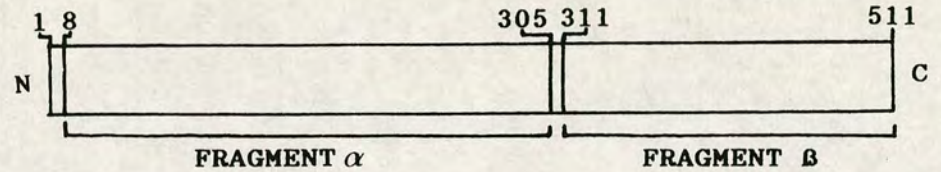

Limited proteolytic digest of the enzyme from both sources results in cleavage in the regions marked on Figure (a) for the *S.cerevisiae* enzyme, yielding two fragments, and ß of M_R 35kDa and 21kDa respectively (91)

(c) FURTHER PROTEOLYTIC ATTACK

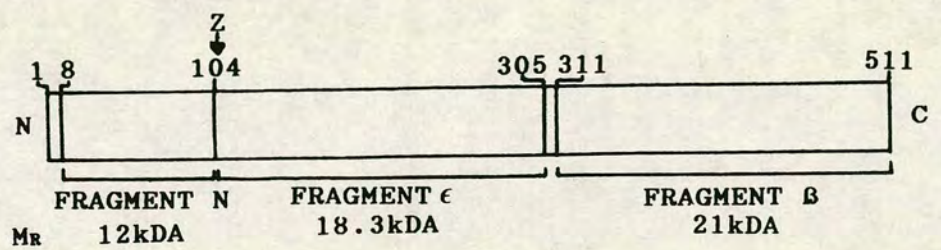

Further proteolytic attack of both enzymes results in cleavage near to residue 100 and yields two fragments, one consisting of a haem-binding peptide (N) and the other being a tetrameric flavoprotein, each subunit of which is composed of two discrete chains (88).
This cleavage is also represented in Figure 1.24.

each end of cd) take place more slowly and two trypsin-stable fragments are formed, N (M_R 12-14kDa) and ß (M_R 18.3kDa). After two-zone cleavage the four cytochrome *b*2 fragments and the tetrameric flavoprotein will dissociate in neutral buffer (88). A scheme of this is shown in Figure 1.24.

Tryptic cleavage was performed on the *H.anomala* enzyme in an attempt to isolate the domains. Since aa' is hypersensitive to a number of proteases it cleaves much faster than cd and generates an undesirable "nicked" flavoprotein. Use of the highly specific *Staphylococcus aureus* V8 protease I overcame this problem and resulted in an unnicked flavodehydrogenase derivative of *H.anomala* flavocytochrome *b*2 which spontaneously dissociates from the cytochrome domain. The flavoprotein retained approximately 80% of the lactate dehydrogenase capability of the holoenzyme but displayed no cytochrome *c* reductase activity (89).

Existence of these two protease-sensitive regions has led to the postulation that the homology between flavocytochromes *b*2 from *S.cerevisiae* and *H.anomala* extends to the tertiary structure which is consistent with a polyglobular structure, which in turn is evidence for gene fusion at the level of the hinge region.

FIGURE 1.24

SCHEMATIC ILLUSTRATION OF TWO ZONE PROTEOLYTIC CLEAVAGE IN FLAVOCYTOCHROME *b*$_2$

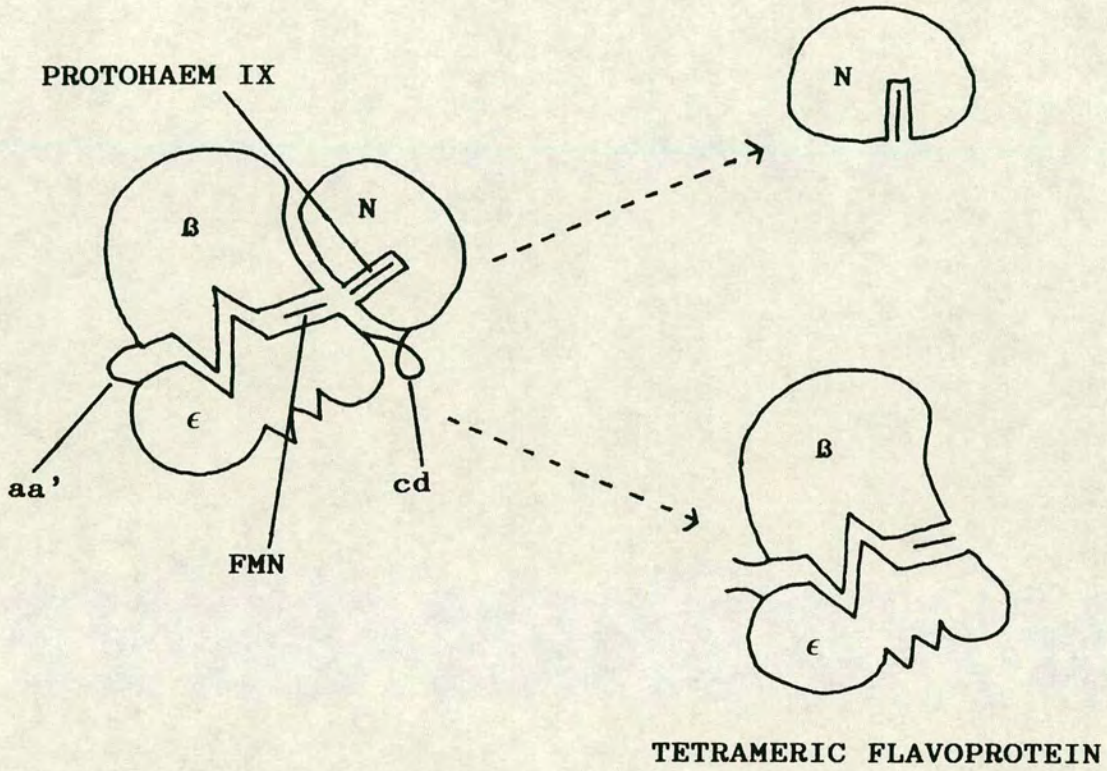

aa' and cd represent the protease-sensitive zones marked by arrows Y and Z in Figure 1.23 and correspond to the loop and hinge regions respectively. Two zone cleavage (Figure 1.23 (c)) in aa' and cd results in formation of two fragments: a haem-binding peptide (N) of M_R 12kDa and a tetrameric flavoprotein of M_R ~200kDa. These fragments dissociate in neutral buffer (88).

1.9 HOMOLOGY OF FLAVOCYTOCHROME *b*$_2$ WITH OTHER PROTEINS

1.9.1 CYTOCHROME DOMAIN ANALOGUES

The *b*$_2$-haem is a member of a group of proteins known as the cytochrome *b*$_5$ superfamily. This group includes mitochondrial and erythrocyte cytochrome *b*$_5$ (92,93) as well as the haem-binding domains of liver sulphite oxidase (a molybdohaemoprotein) (94) and assimilatory nitrate reductase (a flavomolybdohaemoprotein) (95). These proteins (and regions of proteins) all have simlar molecular weights (~11kDa) and sequence alignment shows that there are thirteen invariant residues, two of which are the histidines which ligate the haem iron.

Three-dimensional structural studies have shown that the peptide backbone folds to form a hydrophobic haem crevice. This structure essentially consists of four helices and a ß-pleated sheet and is a characteristic feature of the cytochrome *b*$_5$ superfamily (96).

1.9.2 FLAVIN DOMAIN ANALOGUES

The flavin domain of flavocytochrome *b*$_2$ is homologous to a number of FMN-dependent enzymes; all of which are α-hydroxy-acid oxidases. Such enzymes include L-lactate oxidase from *Mycobacterium smegmatis* (97), spinach glycolate oxidase (98) and long chain α-hydroxy-acid oxidase from rat kidney (99). Catalysis by these enzymes is thought to take place by a mechanism similar to that

operating in flavocytochrome *b*2. However, there are differences in electron acceptors; the flavin domain of flavocytochrome *b*2 is reoxidised by its haem domain whereas the α-hydroxy-acid oxidases are reliant upon oxygen to perform this function (4).

Sequence alignment of flavocytochrome *b*2, L-lactate oxidase and glycolate oxidase shows that there are 69 conserved residues. Some of these residues have been shown, by X-ray crystallographic studies of flavocytochrome *b*2 and glycolate oxidase, to be involved in binding of FMN and substrate, and also in catalysis.

Flavocytochrome *b*2, spinach glycolate oxidase and trimethylamine dehydrogenase from the methylotrophic bacterium W_3A_1 (100) show structural homology in that all are based on a $\beta_8\alpha_8$ barrel motif with loop and helical extensions. The amino-acid sequence of trimethylamine dehydrogenase (101) shows that, apart from the similar folding pattern, little identity with the other two enzymes exists. This is not surprising since FMN is covalently bound in trimethylamine dehydrogenase whereas in flavocytochrome *b*2 and glycolate oxidase the FMN is non-covalently bound.

1.10 REFERENCES

(1) Daum, G., Böhni, P.C. & Schatz, G.J., *J.Biol.Chem.*, **257**, 13028 (1982).

(2) Appleby,C.A. & Morton,R.K., *Nature (London)*, **173**, 749 (1954).

(3) Pajot, A.P. & Claisse, M.L., *Eur.J.Biochem.*, **49**, 275 (1974).

(4) Lederer, F.,in *"Chemistry and Biochemistry of Flavoenzymes"*, **Vol.II**, Franz, Miller (eds.), CRC Press (1991).

(5) Keilin, D., *Proc.Roy.Soc.*, **B**, 312 (1925).

(6) Harden, A. & Norris, R.V., *Biochem.J.*, **9**, 330 (1915).

(7) Meyerhof, O., *Pflug.Arch.Ges.Physiol.*, **175**, 20 (1919).

(8) Bernheim, F., *Biochem.J.*, **22**, 1178 (1928).

(9) Bach,S.J., Dixon,M. & Zerfas,L.G., *Biochem.J.*, **40**, 229 (1946).

(10) Xia, Z.-x. & Mathews, F.S., *J.Mol.Biol.*, **212**, 837 (1990).

(11) Black, M.T., White, S.A., Reid, G.A. & Chapman, S.K., *Biochem.J.*, **258**, 255 (1989).

(12) Morton, R.K. & Shepley, K., *Nature*, **192**, 638 (1961).

(13) Symons, R.H. & Burgoyne, L.A., *Methods Enzymol.*, **9**, 314 (1966).

(14) Appleby, C.A. & Morton, R.K., *Biochem.J.*, **71**, 492 (1959).

(15) Nichols, R.G., Atkinson, M.R., Burgoyne, L.A. & Symons, R.H., *Biochim.Biophys.Acta.*, **122**, 14 (1966).

(16) Somlo, M. & Slonimski, P.P., *Bull.Soc.Chim.Biol.*, **48**, 1221 (1966).

(17) Lederer, F. & Simon, A.-M., *Eur.J.Biochem.*, **20**, 469 (1971).

(18) Labeyrie, F., Baudras, A. & Lederer, F., *Methods Enzymol.*, **53**, 238 (1978).

(19) Reid, G.A., Yonetani, T. & Schatz, G., *J.Biol.Chem.*, **257**, 13068 (1982).

(20) Gasser, S.M., Ohashi, A, Daum, G., Böhni, P.C., Gibson, J., Reid, G.A., Yonetani, T. & Schatz, G., *Proc.Natl.Acad.Sci.(USA)*, **79**, 267 (1982).

(21) Ohnishi, T., Kawaguchi, K. & Hagihara, B., *J.Biol.Chem.*, **241**, 1797 (1966).

(22) Gregolin, C. & Scalella, P., *Biochim.Biophys.Acta.*, **92**, 163 (1964).

(23) Kirschner, K. & Bisswanger, H., *Annu.Rev.Biochem.*, **45**, 143 (1976).

(24) Pajot, P. & Groudinsky, O., *Eur.J.Biochem.*, **12**, 158 (1970).

(25) Labeyrie, F. & Baudras, A., *Eur.J.Biochem.*, **25**, 33 (1972).

(26) Mevel-Ninio, M., *Eur.J.Biochem.*, **25**, 254 (1972).

(27) Labeyrie,F., Groudinsky,O., Jacquot-Armand,Y. & Naslin,L., *Biochim.Biophys.Acta.*, **128**, 492 (1966).

(28) Brunt,C.E., Cox,M.C., Thurgood,A.G.P., Moore,G.R., Reid,G.A. & Chapman, S.K., *Biochem.J.*, **283**, 87 (1993).

(29) Brunt, C.E., *Ph.D. thesis*, University of Edinburgh (1993).

(30) Chapman, S.K., Davies, D.M., Vuik, C.P.J. & Sykes, A.G., *J.Am.Chem.Soc.*, **106**, 2692 (1984).

(31) Walker, M.C. & Tollin,G., *Biochemistry*, **30**, 5546 (1991).

(32) Baudras, A., *Bull.Soc.Chim.Biol.*, **47**, 1449 (1965).

(33) Capeillère-Blandin,C., Bray,R.C., Iwatsubo,M. & Labeyrie,F., *Eur.J.Biochem.*, **54**, 549 (1975).

(34) Capeillère-Blandin, C., Barber, M.J. & Bray, R.C., *Biochem.J.*, **238**, 745 (1986).

(35) Tegoni, M., Janot, J.M. & Labeyrie, F., *Eur.J.Biochem.*, **155**, 491 (1986).

(36) Silvestrini, M.C., Brunori, M., Tegoni, M., Gervais,M. & Labeyrie,F., *Eur.J.Biochem.*, **161**, 465 (1986).

(37) Labeyrie, F., Naslin, L., Curdell, A. & Wurmser, R., *Biochim. Biophys. Acta.*, **41**, 509 (1960).

(38) Augustin, M.A., Chapman,S.K., Davies, D.M., Watson, A.D. & Sykes, A.G., *J.Inorg.Biochem.*, **20** ,281 (1984).

(39) Dikstein, S., *Biochim.Biophys.Acta.*, **36**, 397 (1959).

(40) Morton,R.K., Armstrong,J.McD. & Appleby,C.A., in *"Haematin Enzymes"* (Falk, J.E., Lemberg, R. & Morton,R.K.,eds.), pp.501, Pergammon, Oxford (1961).

(41) Watari, H., Groudinsky, O. & Labeyrie, F., *Biochim.Biophys.Acta.*, **131**, 592 (1967).

(42) Sturtevant, J.M. & Tsong, T.Y.,*J.Biol.Chem.*, **244**, 4942 (1969).

(43) Jacq, C. & Lederer, F.,*Eur.J.Biochem.*, **41**, 311 (1974).

(44) Keller, R., Groudinsky, O. & Wutrich, K., *Biochim.Biophys.Acta*, **328**, 233 (1973).

(45) Labeyrie, F., Beloeil, G.C. & Thomas, M.A., *Biochim.Biophys.Acta*, **953**, 134 (1988).

(46) Cox, M.C., *Ph.D thesis*, University of East Anglia, Norwich (1993).

(47) Iwatsubo, M., Mevel-Ninio, M. & Labeyrie, F., *Biochemistry*, **16**, 3558 (1977).

(48) Lederer, F., *Eur.J.Biochem.*, **46**, 393 (1974).

(49) Pompon, D., Iwatsubo, M. & Lederer, F., *Eur.J.Biochem.*, **104**, 479 (1980).

(50) Hasegawa, H., *J.Biochem.*, **52**, 207 (1962).

(51) Morton, R.K. & Sturtevant, J.M., *J.Biol.Chem.*, **239**, 1614 (1964).

(52) Forestier, J.P. & Baudras, A., in *"Flavins and Flavoproteins"* (H.Kamin,ed.), pp.599, University Park Press, Baltimore, Maryland (1971).

(53) Walsh, C.T., Schonbrunn, A. & Abeles, R.H., *J.Biol.Chem.*, **246**, 6855 (1971).

(54) Walsh, C.T., Krodel, E., Massey,V. & Abeles,R.H., *J.Biol.Chem.*, **248**, 1946 (1973).

(55) Walsh, C.T., Lockridge, O., Massey,V. & Abeles,R.H., *J.Biol.Chem.*, **248**, 7049 (1973).

(56) Urban, P. & Lederer, F., *J.Biol.Chem.*, **260**, 11115 (1985).

(57) Urban, P., Alliel, P.M. & Lederer, F., *Eur.J.Biochem.*, **134**, 275 (1983).

(58) Lederer, F. & Mathews, F.S., in *"Flavins and Flavoproteins"*, (Edmondson, D.E. & McCormick, D.B., eds), de Gruyter, Berlin pp.133-142 (1987).

(59) Pompon, D. & Lederer, F., *Eur.J.Biochem.*, **148**, 145 (1985).

(60) Ghisla,S., Ogata,H., Massey,V., Schonbrunn,A., Abeles,R.H. & Walsh, C.T., *Biochemistry*, **15**, 1794 (1976).

(61) Schonbrunn,A., Abeles,R.H., Walsh,C.T., Ghisla,S., Ogata,H. & Massey,V., *Biochemistry*, **15**, 1798 (1976).

(62) Kresge, A.J., *Acc.Chem.Res.*, **8**, 354 (1975).

(63) Porter, D.J.T., Voet, J.G. & Bright, H.J., *J.Biol.Chem.*, **248**, 4400 (1973).

(64) Genet, R. & Lederer, F., *Biochem.J.*, **266**, 301 (1990).

(65) Pompon, D. & Lederer, F., *Eur.J.Biochem.*, **96**, 571 (1979).

(66) Balme, A. & Lederer, F., in *"Flavins and Flavoproteins"*, in press (1993).

(67) Bruice, T.C., *Acc.Chem.Res.*, **13**, 256 (1980).

(68) Ghisla, S. & Massey, V., *J.Biol.Chem.*, **255**, 5688 (1980).

(69) Ghisla, S. & Massey, V., *Eur.J.Biochem.*, **181**, 1 (1989).

(70) Hiromi, K. & Sturvetant, J.M., *J.Biol.Chem.*, **240**, 4662 (1965).

(71) Hiromi,K. & Sturtevant,J.M., in *"Flavins and Flavoproteins"*, pp.283, (Slater,E.C.,ed), Elsevier, Amsterdam (1966).

(72) Susuki, H. & Ogura, Y., *J.Biochem.*, **60**, 77 (1970).

(73) Iwatsubo,M., Baudras,A., Di Franco,A., Capeillère, C. & Labeyrie, F., in *"Flavins and Flavoproteins"*, pp.41, (Yagi, K., ed), University Park Press, Baltimore, MD (1968).

(74) Pompon, D., *Eur.J.Biochem.*, **106**, 151 (1980).

(75) Miles, C.S., Rouvière-Fourmy, N., Lederer, F., Mathews,F.S., Reid,G.A., Black,M.T. & Chapman,S.K., *Biochem.J.*, **285**, 187 (1992).

(76) Baudras,A., Krupa,M. & Labeyrie,F., *Eur.J.Biochem.*, **20**, 58 (1971).

(77) Capeillère-Blandin, C., *Eur.J.Biochem.*, **128**, 533 (1982).

(78) Tegoni, M., Mozzarelli, A., Rossi, G.L. & Labeyrie, F., *J.Biol.Chem.*, **258**, 5424 (1983).

(79) Albani,J., *Arch.Biophys.Biochem.*, **243**, 292 (1985).

(80) Ogura,Y. & Nakamura,T., *J.Biochem.(Tokyo)*, **60**, 77 (1966).

(81) Celerier, J., Risler, Y., Schwencke, J., Janot, J.-M. & Gervais,M., *Eur.J.Biochem.*, **182**, 67 (1989).

(82) Baudras, A. & Spyridakis,A., *Biochimie*, **53**, 943 (1971).

(83) Tegoni, M., Silvestrini, M.C., Labeyrie, F. & Brunori, M., *Eur.J.Biochem.*, **140**, 39 (1985).

(84) Lederer, F., Cortial, S., Becam, A.M., Haumont, P.Y. and Perez,L., *Eur.J.Biochem.*, **152**, 419 (1985).

(85) Black,M.T., Gunn,F.J., Chapman,S.K. & Reid,G.A., *Biochem.J.*, **263**, 973 (1989).

(86) Silvestrini, M.C., Tegoni, M., Celerier, J., Desbois,A. & Gervais,M., *Biochem.J.*,in press (1993).

(87) Manson, F.D.C., unpublished results (1993).

(88) Gervais,M., Groudinsky,O., Risler,Y & Labeyrie,F., *Biophys.Biochem.Res.Comm.*, **77**, 1543 (1977).

(89) Gervais,M., Risler,Y. & Corrazin,S., *Eur.J.Biochem.*, **130**, 253 (1983).

(90) Ghrir,R. & Lederer,F., *Eur.J.Biochem.*, **120**, 279 (1981).

(91) Naslin, L., Spyridakis, A. & Labeyrie, F., *Eur.J.Biochem.*, **37**, 268 (1973).

(92) Lederer, F., Ghrir, R., Guiard, B., Cortial, S. & Ito, A., *Eur.J.Biochem.*, **132**, 95 (1983).

(93) Schafer,D.A. & Hultquist,D.E., *Biochem.Biophys.Res. Comm.*, **115**, 807 (1983).

(94) Guiard, B. & Lederer, F., *Eur.J.Biochem.*, **74**, 181 (1977).

(95) Lê, K.H.D. & Lederer, F., *EMBO J.*, **2**, 1909 (1983).

(96) Guiard, B. & Lederer, F., *J.Mol.Biol.*, **135**, 639 (1979).

(97) Geigel, D.A., Williams, C.H.Jnr. & Massey, V., *J.Biol.Chem.*, **265**, 6626 (1990).

(98) Linqvuist, Y., Branden, C.-I., Mathews, F.S. & Lederer, F., *J.Biol.Chem.*, **266**, 3198 (1991).

(99) Lê, K.H.D. & Lederer, F., *J.Biol.Chem.*, **266**, 20877 (1991).

(100) Lim, L.W., Shamala, N., Mathews, F.S., Steenkamp, D.J., Hamlin, R. & Xuong, N.H., *J.Biol.Chem.*, **261**, 15140 (1986).

(101) Boyd, G., Mathews, F.S., Packman, L.C. & Scrutton, N.S., *FEBS Letters*, **308**, 271 (1992).

(102) Chapman, S.K., White, S.A. & Reid, G.A., *"Adv.Inorg.Chem."*, **36**, 257 (1991).

(103) Mathews, F.S. and Xia, Z.-x., in *"Flavins and Flavoproteins"* (McCormick, D.B. & Edmondson, D.E., eds.), pp.123-132, de Gruyter, Berlin (1987).

CHAPTER 2

INTRAMOLECULAR COMMUNICATION

THE ROLE OF THE INTERDOMAIN HINGE

2.1 INTRODUCTION

Globular proteins have rigid structures with limited internal motion. However, the folding of polypeptide chains into distinct domains allows a degree of flexibility that enables a protein to fulfill its biological role without incurring localised conformational change. Mobility occurs in different ways according to the extent of domain/domain interfaces. Citrate synthase, for example, has extensive domain/domain interactions and this enzyme responds to substrate binding by domain closure of the active site. This is brought about by the cumulative effects of small shifts and rotations of packed helices within the two domains and at their interface (1). This mechanism is quite different from the "hinge" mechanisms which allow rigid body movements of domains in proteins which have less extensive domain interfaces such as immunoglobulins (2). Combinations of both closure and hinge-bending effects do occur as seen in lactoferrin which undergoes ligand-induced conformational change (3).

Molecular hinges have been recognised in many proteins (4) and have in several cases been characterised by X-ray crystallography, for example in alcohol dehydrogenase (5) and phosphoglycerate kinase (6). Hinge-bending in most cases is triggered by ligand binding, with the notable exception of bacteriophage T4 lysozyme (7), which can undergo hinge-bending of 32° without significant

conformational alteration. Ligand-induced hinge-bending can lead to conformational changes at the active site of enzymes with the result of facilitating turnover, as for example in phosphoglycerate kinase (7). Further examples are the 2-oxoacid dehydrogenase multienzyme complexes, such as the pyruvate dehydrogenase complex, in which the hinges linking lipoyl domains to the enzyme core in E2 of the complex enables substrate to be conveyed between the three active sites (8).

Hinges typically consist of a short surface loop of the polypeptide chain comprising a high percentage of glycine, alanine and proline residues. Such residues are thought to contribute to hinge bending as a result of their short and uncharged side-chains although the specific characteristics required are as yet unconfirmed (9).

Flavocytochrome *b*2 is folded into two functionally distinct domains; a flavin-binding, or flavodehydrogenase domain and a haem-binding, or cytochrome-, domain (10). After catalysing the oxidation of L-lactate to pyruvate the flavin domain must transfer the two electrons it has gained to the haem domain. It does this by two one-electron transfers. In order for this to occur there must be recognition between the two domains.

The flavin and haem domains are covalently linked via residues 89 to 103 which constitute a hinge region. At the interface there are several important interactions: a salt bridge which is formed between Lys-296 in the flavin

domain and one of the haem propionates; hydrogen bonding interactions involving Tyr-143 and Tyr-97; and a hydrophobic interaction entailing Phe-325. Site-directed mutagenesis of one of these residues, Tyr-143, has shown this residue to be of crucial importance in maintaining the integrity of the domain interface (11). The role of Tyr-143 is further discussed in Chapter 6.

That the short section of polypeptide chain linking the two domains in flavocytochrome *b*2 functions as a hinge is supported by both crystallographic (10) and NMR spectroscopic data (12). The three-dimensional structure of flavocytochrome *b*2 from *Saccharomyces cerevisiae* has been resolved to 2.4Å and shows two crystallographically distinguishable subunits in each tetramer (13). In one of these subunits, where pyruvate is absent, the cytochrome domain is well resolved but in the second subunit where pyruvate is present, no electron density is observed for the cytochrome domain *i.e.* it is disordered. This implies a degree of mobility of the cytochrome domain with respect to the flavin domain. This mobility is confirmed by NMR spectroscopy, as discussed in Section 1.6.3.4, where sharper resonances are observed in the proton spectrum than would be expected for the tetrameric flavocytochrome *b*2 which has a molecular weight of nearly a quarter of a million (12). The sharper lines are accounted for by mobility between the domains causing a faster molecular tumbling rate.

The genes encoding flavocytochrome *b*2 from both

Saccharomyces cerevisiae and *Hansenula anomala* have been cloned and sequenced (14,15). The amino-acid sequences show 60% identity, with many important residues being especially well-conserved (see Figure 1.22). There are two regions in which the sequences differ markedly, they are the hinge region and a proteolytically-sensitive surface loop which is disordered in the crystal structure. It was postulated that these structural differences could account for the kinetic differences between the enzymes from the two sources, as summarised in Table 2.1 (16).

To probe the role of the interdomain hinge a hybrid enzyme has been constructed which consists of the bulk of the *S.cerevisiae* enzyme but with the hinge replaced by the much shorter and more acidic hinge region from *H.anomala*. The two hinge regions are compared in Figure 2.1 and the wild-type and hybrid enzymes are schematically represented in Figure 2.2. It was proposed that the hybrid enzyme, hereafter referred to as "hinge-swap-b_2", would have restricted domain mobility due to the shorter hinge region. The enzyme has been fully characterised to discern whether this mutation has had any effect on the electron transfer properties of flavocytochrome b_2.

TABLE 2.1

ENZYME MOLAR ACTIVITY AND K_M VALUES FOR L-LACTATE WITH VARIOUS FORMS OF FLAVOCYTOCHROME *b2*

ENZYME	MOLAR ACTIVITY (s^{-1})	K_M (mM)
S_X	210 ± 10	1.6
S_I	550	0.4
H_I	1000 ± 100	1.3

Abbreviations : S_X = cleaved form from *S.cerevisiae*

S_I = intact form from *S.cerevisiae*

H_I = intact form from *H.anomala*

Experimental Conditions : Determinations are the best estimates under steady-state conditions at 30°C in 0.1M phosphate buffer, pH 7.0, with 1mM ferricyanide as the electron acceptor (9). The molar activity, which corresponds to k_{cat}, is expressed as the number of mole electron equivalents transferred per mole of enzyme per second.

FIGURE 2.1

CONSTRUCTION OF THE HINGE-SWAP FLAVOCYTOCHROME *b2*

a

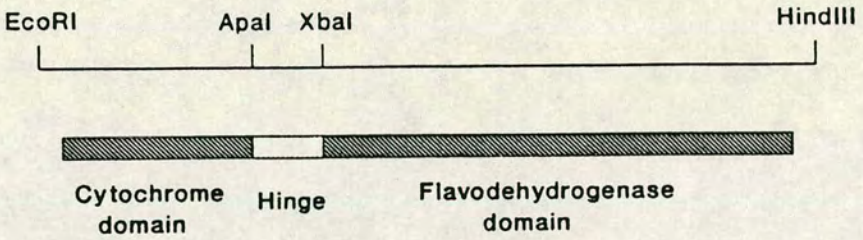

b

S. cerevisiae flavocytochrome b_2

K K L G P L Q G SMPPELVCPPYAPGETKEDIARKEQLKSLLP P L D N I

AAATTGGGTCCCCTTCAAGG — TCTAGA

G

G C

TC GA

CATCTTGGTCCATTAGTTGG — GAAAACCACCATTATCCCAAATGAT

K H L G P L V G E F EQEEEELSDEEIDRLERIE R K P P L S Q M

D

H. anomala flavocytochrome b_2

(a) DNA sequences encoding flavocytochrome *b2* from *S.cerevisiae* and *H.anomala* were modified to have the same general structure as represented by the restriction map above and the corresponding structure below (N-terminus at left).

(b) The entire amino acid sequence of the hinge region is shown. Arrows indicate the site-directed modifications at either end of the hinge-coding sequence and underlined regions show the restriction sites used for construction of the hinge-swap enzyme.

FIGURE 2.2

SCHEMATIC REPRESENTATION OF FLAVOCYTOCHROME *b*2 SUBUNIT

(a) WILD-TYPE ENZYME

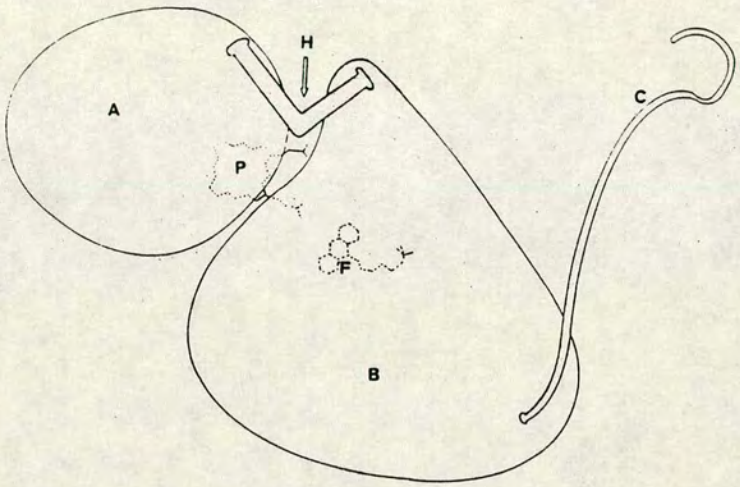

(b) HINGE-SWAP ENZYME

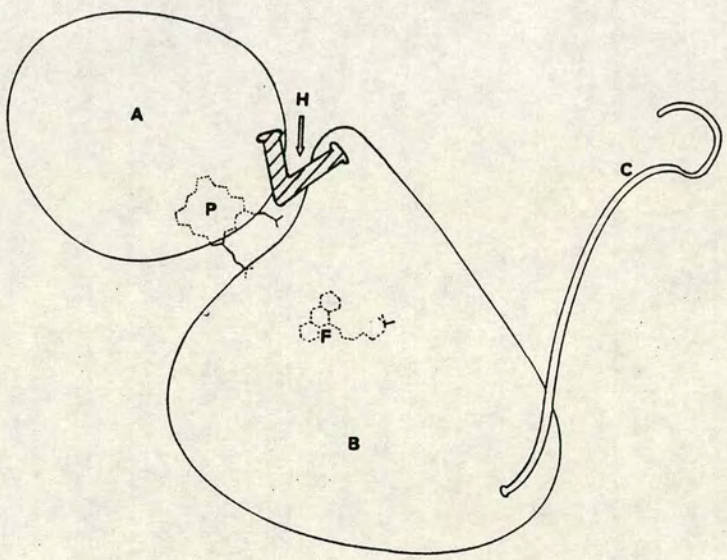

The mutant enzyme is shown with a shorter interdomain hinge (hatched) which is postulated to restrict mobility and to, possibly, alter the position of the haem domain. The schematic representation of the wild-type subunit is based on the known three-dimensional structure.

A,haem domain; B,flavin domain; C,C-terminal tail; F,FMN; P,protohaem IX; H,interdomain hinge.

2.2 EXPERIMENTAL

2.2.1 CONSTRUCTION OF THE HINGE-SWAP HYBRID ENZYME (DR.F.D.C.MANSON)

Standard methods for DNA manipulation were performed as described in Sambrook *et al.* (17). Plasmid pGR401 contains the whole of the *S.cerevisiae* flavocytochrome b_2-coding sequence on a 1.8kb *Eco*RI-*Hin*dIII fragment (18). The *H.anomala* flavocytochrome b_2 gene was subcloned from FG1 (15) as a 5.7kb *Bam*HI fragment into plasmid pTZ19r (19). The resulting recombinant plasmid, pMB3, was used for site-directed mutagenesis by the method of Kunkel *et al.* (20) to introduce *Eco*RI and *Hin*dIII cleavage sites at the beginning and the end, respectively, of the *H.anomala*-b_2 sequence encoding the mature protein. All oligonucleotides used were synthesised by the OSWEL DNA service at the University of Edinburgh. The genes encoding flavocytochrome b_2 from both *S.cerevisiae* and *H.anomala* were modified to incorporate restriction enzyme cleavage sites at equivalent positions at both ends of the interdomain hinge coding region (Figure 2.1). By use of restriction enzymes ApaI and XbaI, the large fragment was isolated from the *S.cerevisiae* sequence and the fragment encoding the hinge region was isolated from the *H.anomala* sequence. The two fragments were ligated and the structure of the recombinant verified by restriction enzyme analysis (21).

2.2.2 ENZYME PREPARATION AND PURIFICATION

Wild-type and hinge-swap flavocytochromes b_2 were expressed in *E.coli* (strain TG1) (22) and were isolated from cells which had been stored at -20°C as described in Section 7.4. The TG1 *E.coli* expressing the hinge-swap enzyme were consistently poor at producing large yields of protein. As a result, at a later date, the plasmid containing the hinge-swap enzyme was transformed into the protease-deficient *E.coli* strain AR120.

The wild-type and hinge-swap enzymes were purified as described in Section 7.4.4. Purity and structural integrity were confirmed by SDS-PAGE (Section 7.5).

2.2.3 KINETIC ANALYSIS

All experiments were carried out at 25$\pm$0.1°C in tris-HCl at pH 7.5. The buffer concentration was 0.01M in HCl with the ionic strength adjusted to 0.10M by addition of NaCl. Steady-state kinetic measurements involving the enzymatic oxidation of L-lactate were carried out using either Beckmann DU-62 or Pye-Unicam SP8-400 UV/visible spectrophotometers with either cytochrome *c* or ferricyanide acting as the external electron acceptor as described in Section 7.8.

Pre-steady-state kinetics were performed as described in Section 7.9 using an Applied Photophysics SF.17MV stopped-flow spectrofluorimeter. Flavin reduction was monitored at 438.3nm (a haem isosbestic point) and haem

reduction at either 557nm or 423nm, results at both wavelengths being identical. The SF.17MV software package was used to collect and analyse data on an Archimedes 420/1 computer. Traces for flavin reduction were fitted to single exponentials and those for haem reduction to double exponentials. For both steady-state and stopped-flow data, K_M and k_{cat} parameters were determined using non-linear regression analysis.

Kinetic isotope effects (KIEs) were measured using L-[2-^{1}H]- and L-[2-^{2}H]-lactate, the latter being synthesised and purified as described in Section 7.7.2.

2.2.4 REDOX POTENTIAL DETERMINATION

The mid-point potentials of the haem groups in the wild-type and hinge-swap enzymes were determined spectrophotometrically as described in Section 7.11. The reaction was carried out under anaerobic conditions using platinum and Ag/AgCl working and reference electrodes respectively. Enzyme was reduced by titration with sodium dithionite and oxidised by titration with potassium ferricyanide. The mediators used are listed in 7.11.2.5.

2.3 RESULTS AND DISCUSSION

2.3.1 STEADY-STATE KINETIC ANALYSIS

Results from steady-state kinetic measurements on the hinge-swap enzyme, with L-[2-^{1}H]- and L-[2-^{2}H]- lactate

as substrates and using ferricyanide and cytochrome *c* as electron acceptors, are presented in Table 2.2, where they are compared with previously reported results from the *S.cerevisiae* wild-type enzyme (23). Both enzymes exhibited typical saturation kinetics, examples for the hinge-swap enzyme are illustrated in Figures 2.3 and 2.4. Comparison of the rates obtained with ferricyanide as electron acceptor shows that there is only a 3-fold drop in the k_{cat} value from $400s^{-1}$ for wild-type to $126s^{-1}$ for hinge-swap-b_2, indicating that the hinge-swap enzyme is still a good lactate dehydrogenase. However there are other more significant differences between the kinetic properties of the two enzymes, the most obvious being the large decrease in the k_{cat} value for cytochrome *c* reduction; there is a 130-fold decrease from $207s^{-1}$ for wild-type to $1.62s^{-1}$ for the hybrid. *i.e.* hinge-swap-b_2 is a very poor cytochrome *c* reductase. Cytochrome *c* can only accept electrons from the haem group of the enzyme whereas ferricyanide is a more general electron acceptor being able to accept from either the flavin or haem moieties. This, and the fact that cytochrome *c* reduction is more severely disrupted than ferricyanide reduction, indicates that the hinge-swap mutation is having an effect on a step occurring later in the catalytic cycle than flavin reduction.

This observation is supported by another feature of the steady-state kinetics of cytochrome *c* reduction. Initially saturating kinetics are achieved (and it is the

TABLE 2.2

STEADY-STATE KINETIC PARAMETERS AND DEUTERIUM KINETIC EFFECT VALUES FOR WILD-TYPE AND HINGE-SWAP FLAVOCYTOCHROME *b*2

ENZYME	ELECTRON ACCEPTOR	k_{cat} (s^{-1})		K_M (mM)		KIE	REF.
		[^{1}H]LAC	[^{2}H]LAC	[^{1}H]LAC	[^{2}H]LAC		
WT	$Fe(CN)_6^{3-}$	400 ± 10	86 ± 5	0.49 ± 0.05	0.76 ± 0.06	4.7 ± 0.4	(23)
HINGE	$Fe(CN)_6^{3-}$	126 ± 6	61 ± 3	0.16 ± 0.02	0.60 ± 0.10	2.1 ± 0.2	This work
WT	CYT.*c*	207 ± 10	70 ± 10	0.24 ± 0.04	0.48 ± 0.10	3.0 ± 0.6	(23)
HINGE	CYT.*c*	1.62 ± 0.41	0.97 ± 0.29	0.002 ± 0.001	0.005 ± 0.003	1.7 ± 1.3	This work

Abbreviations used : WT = wild-type-*b*2 ; HINGE = hinge-swap-*b*2 ; [^{1}H]LAC = L-[2-^{1}H]-lactate; [^{2}H]LAC = L-[2-^{2}H]-lactate; CYT.*c* = cytochrome *c*.

k_{cat} is expressed in terms of number of electrons transferred per second per mole of enzyme (since L-lactate is a two-electron donor these values can be halved to express them in terms of moles of substrate reduced per second).

Experimental conditions : All experiments were carried out at 25°C in tris-HCl buffer, pH 7.5, I = 0.1M. The concentration of acceptors were as follows : $Fe(CN)_6^{3-}$ - 1mM (>90% saturating) for WT and 8mM (87% saturating) for the hinge-swap enzyme; cytochrome *c* - 50 μM (~90% saturating) for WT and 15 μM (>95% saturating) for the hinge-swap enzyme.

FIGURE 2.3

MICHAELIS-MENTEN PLOT FOR THE STEADY-STATE REDUCTION OF FERRICYANIDE BY HINGE-SWAP FLAVOCYTOCHROME *b*$_2$ WITH L-[2-^{1}H]-LACTATE

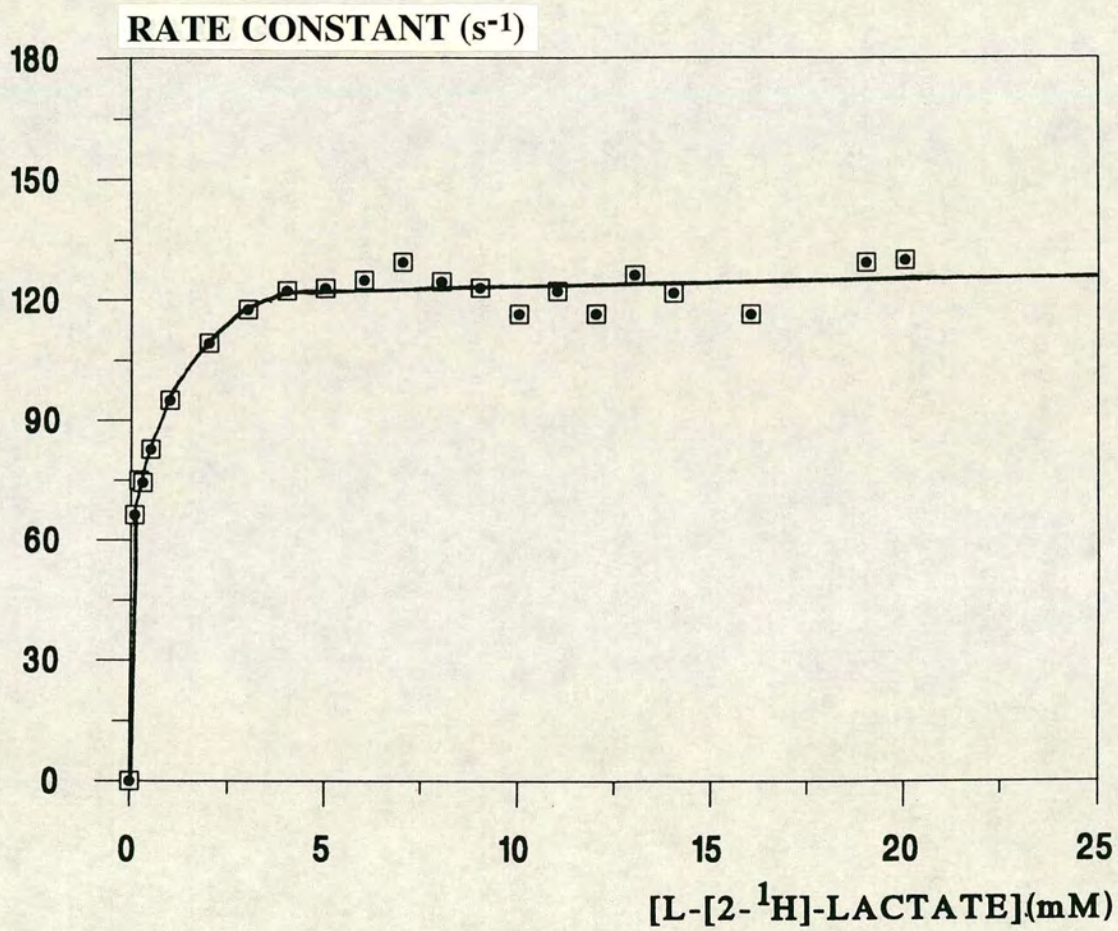

Experimental conditions are described in Section 2.2.3

FIGURE 2.4

MICHAELIS-MENTEN PLOT FOR THE STEADY-STATE REDUCTION OF CYTOCHROME *c* BY HINGE-SWAP FLAVOCYTOCHROME *b*$_2$ WITH L-[2-^{1}H]-LACTATE

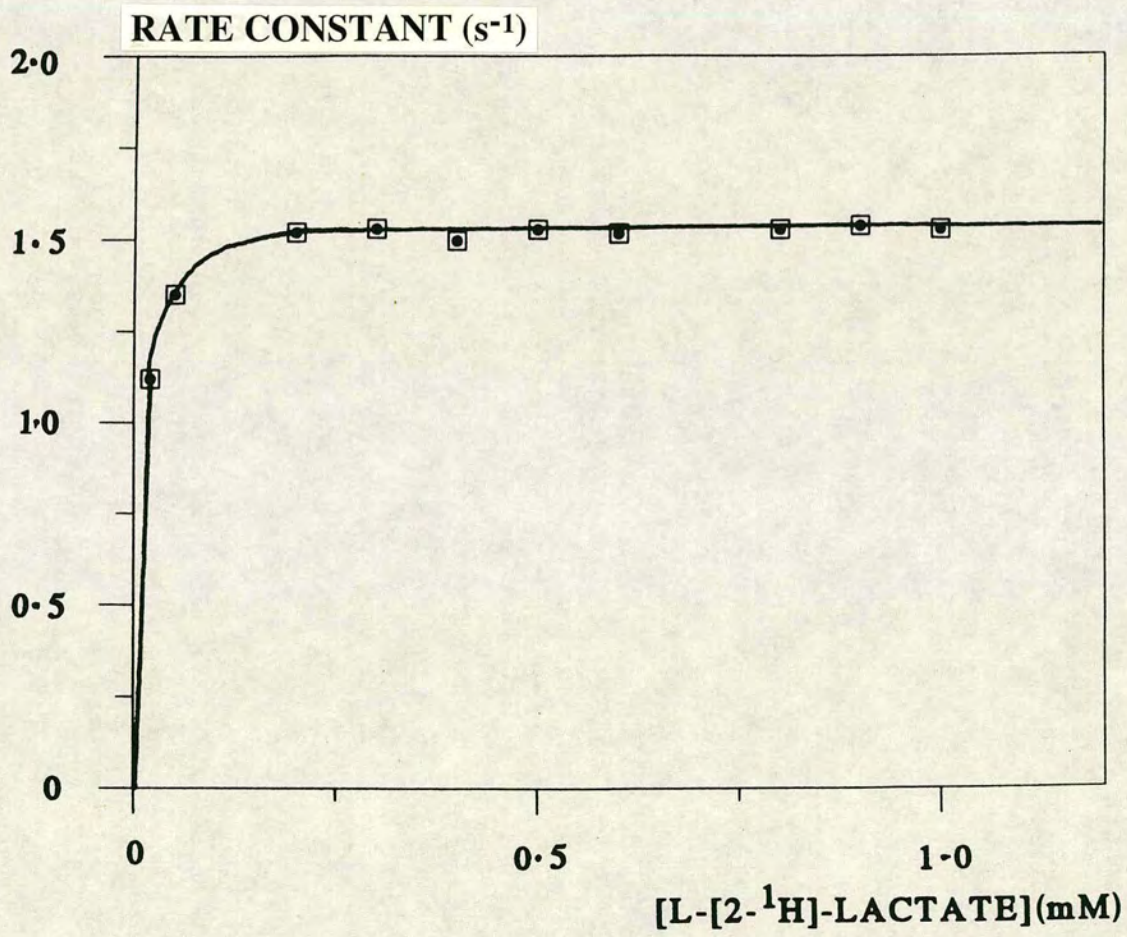

Experimental conditions are described in Section 2.2.3

values pertaining to this saturation which are quoted in Table 2.2), however, on increasing the substrate concentration substrate inhibition is observed as illustrated in Figure 2.5. The maximal rate of cytochrome *c* reduction occurs at the optimal substrate concentration of 0.56mM (S_{opt}) and the inhibition constant, K_I, that is the amount of inhibitor bound to the enzyme at which the rate is half of its maximum value, is equal to 17.5 ± 1.0mM. This inhibition could be attributed to enhanced affinity of substrate binding to a second site following saturation of primary binding sites.

Previously, by investigation of kinetic isotope effects, it has been shown that abstraction of the C-2 hydrogen of L-lactate as a proton is the overall rate-limiting step in the catalytic cycle for the *S.cerevisiae* wild-type enzyme (23,24). The kinetic isotope effect (KIE) values for the steady-state reduction of both acceptors by hinge-swap-b_2 are lower than for wild-type, of particular note is the fall from 3.0 for wild-type to 1.7 for the hinge-swap enzyme when using cytochrome *c* as acceptor. This observation indicates that a step/or steps occurring after the initial flavin reduction is/are partly rate-limiting since replacement of the C-2 hydrogen with deuterium has no great effect upon the rate constants of the later steps *i.e.* abstraction of the C-2 hydrogen is no longer the sole rate-limiting step in the overall catalytic cycle.

From Table 2.2 it can be seen that the Michaelis

FIGURE 2.5

MICHAELIS-MENTEN PLOT ILLUSTRATING THE SUBSTRATE INHIBITION EXHIBITED BY HINGE-SWAP FLAVOCYTOCHROME *b*2 UNDER STEADY-STATE CONDITIONS WITH CYTOCHROME *c* AS ACCEPTOR

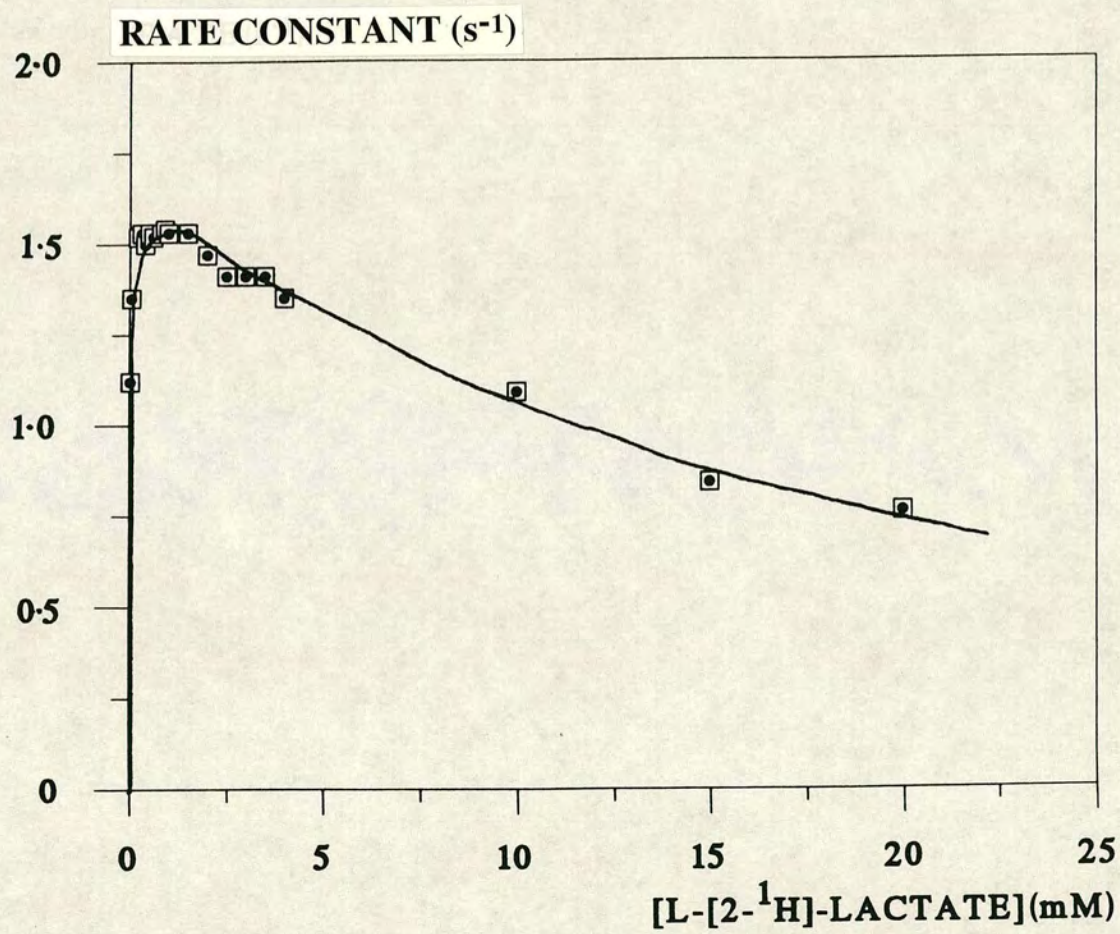

Experimental conditions are described in Section 2.2.3

constant, K_M, for wild-type and hinge-swap-b_2 do not differ significantly when ferricyanide is the electron acceptor. However when cytochrome *c* is the acceptor there is a large decline in the apparent K_M values for L-lactate. Steady-state parameters such as K_M are of a composite nature, representing a collection of rate constants for a series of steps in the catalytic pathway of the enzyme. Consequently it is not feasible to categorically relate this large drop in K_M to a substantial increase in substrate binding since K_M cannot be a direct reflection of the K_d for L-lactate as its value is obviously affected by steps occurring after L-lactate binding. Direct evidence that the K_M is not a true K_d comes from the catalytic efficiencies of the two enzymes, as expressed by k_{cat}/K_M (Table 2.3). Efficiency, for both enzymes, remains at approximately the same level for both ferricyanide and cytochrome *c* reduction *i.e.* the fall-off in value of k_{cat} is identical to the fall-off in value of the K_M. This proves that the K_M is controlled by the level of k_{cat} and is therefore not a sole indication of effectiveness of binding. The efficiencies for both enzymes with cytochrome *c* as the electron acceptor are slightly higher than with ferricyanide as the acceptor as would be expected since cytochrome *c* is the physiological electron acceptor.

Apparent K_M values for the electron acceptors themselves with both the hybrid and the wild-type enzymes are given in Table 2.4 (23). Here we see another difference between

TABLE 2.3

THE STEADY-STATE EFFICIENCY OF WILD-TYPE AND HINGE-SWAP FLAVOCYTOCHROMES *b*2 EXPRESSED BY k_{cat}/K_M

ENZYME	ELECTRON ACCEPTOR	$10^{-5}\,k_{cat}/K_M$ ($M^{-1}s^{-1}$) [^{1}H]LAC	[^{2}H]LAC	REF.
WT	FERRICYANIDE	8.16 ± 0.86	1.13 ± 0.11	(23)
HINGE	FERRICYANIDE	7.88 ± 1.05	1.02 ± 0.18	This work
WT	CYTOCHROME *c*	8.62 ± 1.50	1.46 ± 0.37	(23)
HINGE	CYTOCHROME *c*	8.10 ± 4.54	1.94 ± 1.30	This work

Abbreviations used : WT = wild-type-*b*2
HINGE = hinge-swap-*b*2
[^{1}H]LAC = L-[2-^{1}H]-lactate
[^{2}H]LAC = L-[2-^{2}H]-lactate

Experimental conditions : All experiments were carried out at 25°C in tris-HCl buffer, pH 7.5, I = 0.1M. The concentrations of ferricyanide used were 1mM and 8mM for WT and the hinge-swap enzymes respectively; cytochrome *c* concentrations were 50 μM and 15 μM respectively.

TABLE 2.4

K_M VALUES FOR THE EXTERNAL ELECTRON ACCEPTORS

ENZYME	ELECTRON ACCEPTOR	
	FERRICYANIDE K_M (mM)	CYTOCHROME *c* K_M (μM)
WILD-TYPE	<< 0.1	10 $\pm$ 1
HINGE-SWAP	1.16 $\pm$ 0.08	0.68 $\pm$ 0.08

Experimental conditions : All experiments were carried out at 25°C in tris-HCl buffer, pH 7.5, I = 0.1M. The concentration of L-[2-^{1}H]-lactate was at a constant level of 10mM throughout. This concentration was 95% saturating for WT-*b*2 with both acceptors, and for hinge-swap-*b*2 was >95% saturating for ferricyanide, but only 72% saturating with cytochrome *c*.

the two enzymes; a dependence of rate on the concentration of electron acceptor to varying extents. With cytochrome *c* as acceptor, the hinge-swap enzyme has a particularly low K_M of 0.68 μM when compared to the value of 10 μM for wild-type, which is approximately 15-fold higher. In other words acceptor saturation is more easily reached in the case of the hinge-swap enzyme. All steady-state experiments involving hinge-swap-*b*$_2$ were therefore performed at 15 μM cytochrome *c* (>95% saturation). Cytochrome *c* concentrations used with wild-type enzyme are given in the legend of Table 2.3 (23).

The hinge-swap enzyme has a degree of dependence on the concentration of ferricyanide as reflected by the apparent K_M of 1.16mM, which is at least 10-fold higher than for wild-type. As a result all steady-state assays using ferricyanide were performed at 8mM ferricyanide (90% saturation). The binding site for ferricyanide on flavocytochrome *b*$_2$ has been postulated by modelling studies (25) to be close to the domain interface. The presence of the shorter, more negatively charged *H.anomala* hinge region may cause disruption of this binding site, necessitating binding to a second, lower affinity site elsewhere on the protein, causing the apparent dependence on ferricyanide concentration.

2.3.2 STOPPED-FLOW KINETIC ANALYSIS

Stopped-flow kinetic studies were performed in order to

directly monitor the reduction of both the flavin and haem prosthetic groups using both L-[2-^{1}H]- and L-[2-^{2}H]-lactate. The kinetic parameters are summarised and compared to those previously obtained for the *S.cerevisiae* wild-type enzyme (23) in Table 2.5. Sample traces are shown in Figure 2.6 and examples of the Michaelis-Menten plots are illustrated in Figures 2.7 and 2.8. Flavin reduction was found to be monophasic at all lactate concentrations and haem reduction biphasic. This is in contrast to the wild-type enzyme in which both flavin and haem reductions are biphasic, at least at high lactate concentrations (23). Considering one protomer of the wild-type enzyme, FMN is initially reduced by one molecule of lactate (entry of two electrons into the protomer). The flavin group then passes one of its electrons to its partnering haem group resulting in fully reduced haem and the flavin semiquinone. In order to generate a fully reduced protomer a third electron must enter the system and it is postulated that this is regulated by interprotomer electron transfer between flavin moieties (24). This procedure happens in all four protomers, initially oxidising four molecules of lactate followed by oxidation of a further two molecules per tetramer as a result of the intramolecular rearrangement. This results in fully reduced flavocytochrome b_2, which requires 12 electrons in total. This is illustrated for a dimer in Figure 1.20. The initial reduction of the flavin by one molecule of lactate constitutes the first fast

TABLE 2.5

STOPPED-FLOW KINETIC PARAMETERS AND DEUTERIUM KINETIC ISOTOPE EFFECT VALUES FOR WILD-TYPE AND HINGE-SWAP FLAVOCYTOCHROME *b*2

ENZYME	PROSTHETIC GROUP REDUCTION	k_{cat} (s^{-1}) [^{1}H]LAC	k_{cat} (s^{-1}) [^{2}H]LAC	K_M (mM) [^{1}H]LAC	K_M (mM) [^{2}H]LAC	KIE	REF.
WT	FMN	604 ± 60	75 ± 5	0.84 ± 0.20	1.33 ± 0.28	8.1 ± 1.4	(23)
HINGE	FMN	240 ± 12	38 ± 2	0.37 ± 0.02	0.56 ± 0.01	6.3 ± 0.7	This work
WT	HAEM	445 ± 50	71 ± 5	0.53 ± 0.05	0.68 ± 0.05	6.3 ± 1.2	(23)
HINGE	HAEM	1.61 ± 0.42	1.00 ± 0.11	0.003 ± 0.001	0.003 ± 0.001	1.6 ± 0.7	This work

Abbreviations used : WT = wild-type-*b*2 ; HINGE = hinge-swap-*b*2 ; [^{1}H]LAC = L-[2-^{1}H]-lactate; [^{2}H]LAC = L-[2-^{2}H]-lactate.

Experimental conditions : All experiments were carried out at 25°C in tris-HCl buffer, pH 7.5, I = 0.1M. Values of k_{cat} are expressed in terms of number of prosthetic groups reduced per second.

FIGURE 2.6

STOPPED-FLOW KINETIC TRACES FOR THE REDUCTION OF THE PROSTHETIC GROUPS OF HINGE-SWAP FLAVOCYTOCHROME *b*2

(a) MONOPHASIC FLAVIN REDUCTION (438.3nm)

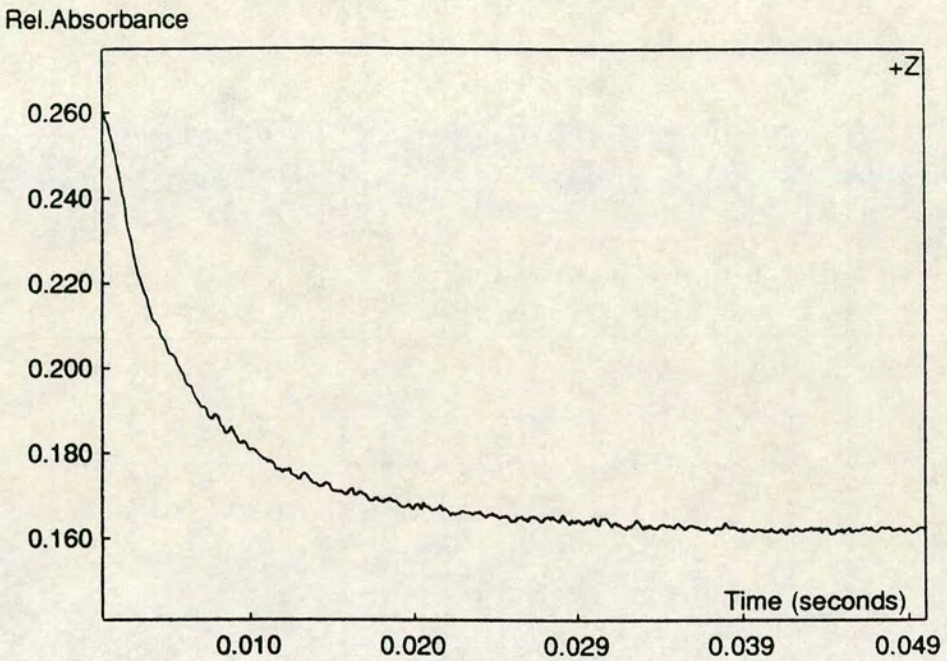

(b) BIPHASIC HAEM REDUCTION (557nm)

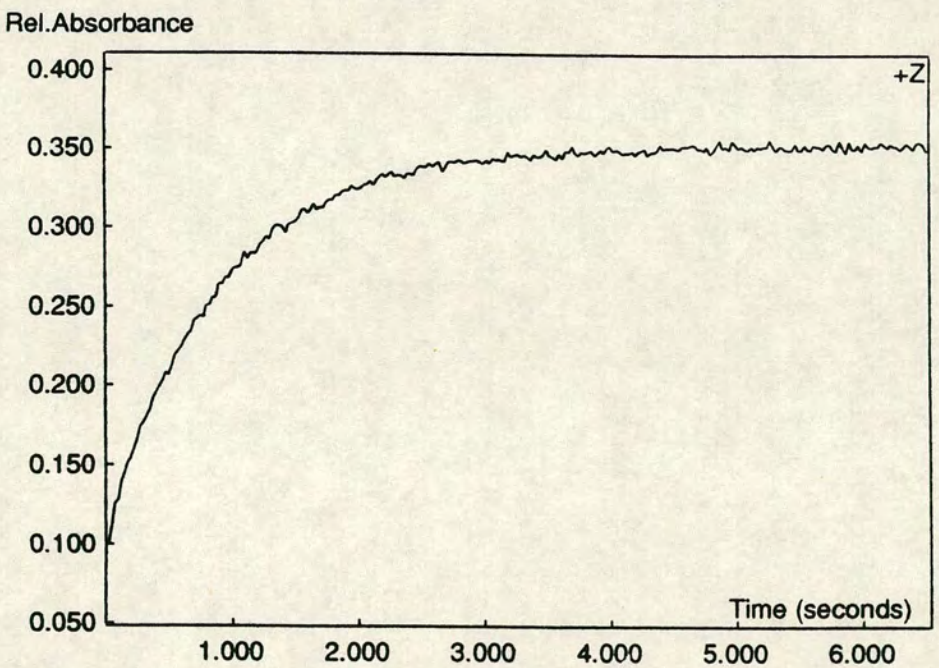

FIGURE 2.7

MICHAELIS-MENTEN PLOT FOR FLAVIN REDUCTION OF HINGE-SWAP FLAVOCYTOCHROME *b*$_2$ BY L-[2-^{1}H]-LACTATE UNDER STOPPED-FLOW CONDITIONS

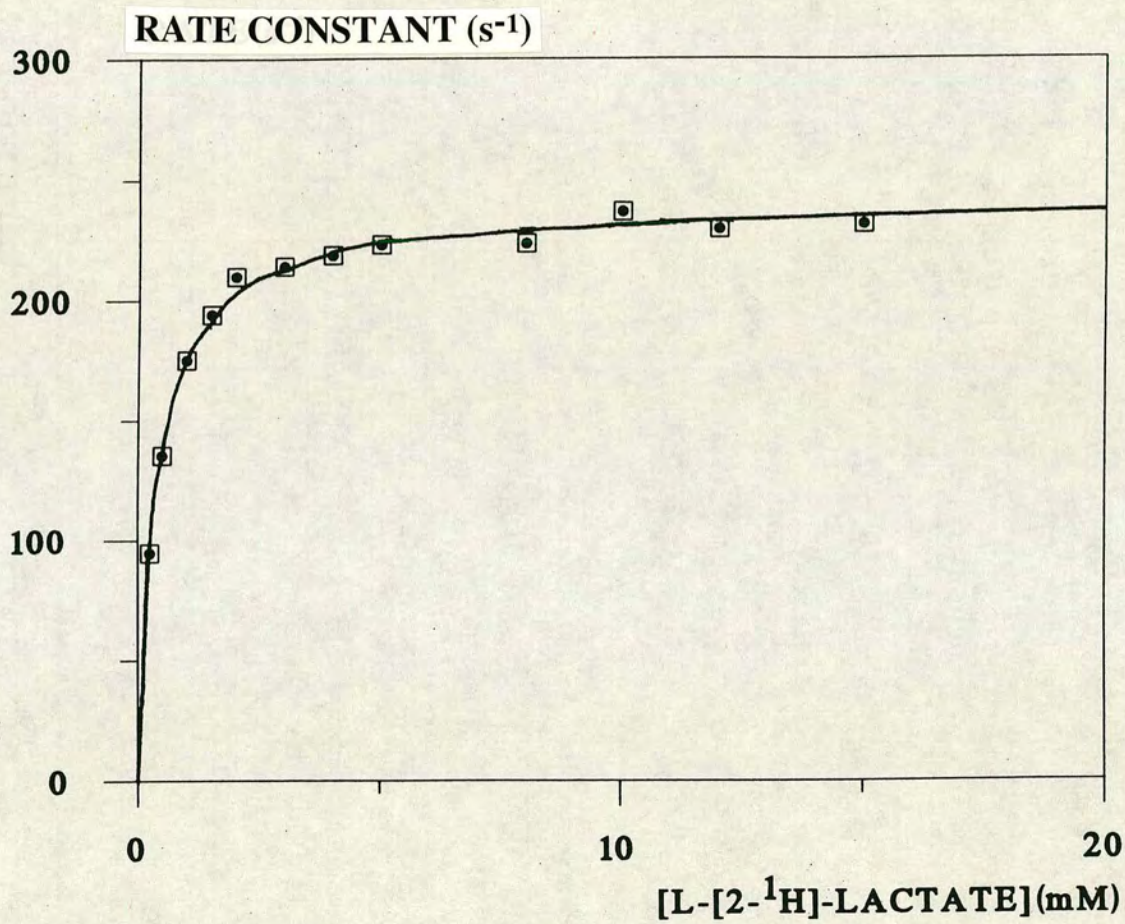

Experimental conditions are described in Section 2.2.3

FIGURE 2.8

MICHAELIS-MENTEN PLOT FOR HAEM REDUCTION OF HINGE-SWAP FLAVOCYTOCHROME *b*$_2$ BY L-[2-^{2}H]-LACTATE UNDER STOPPED-FLOW CONDITIONS

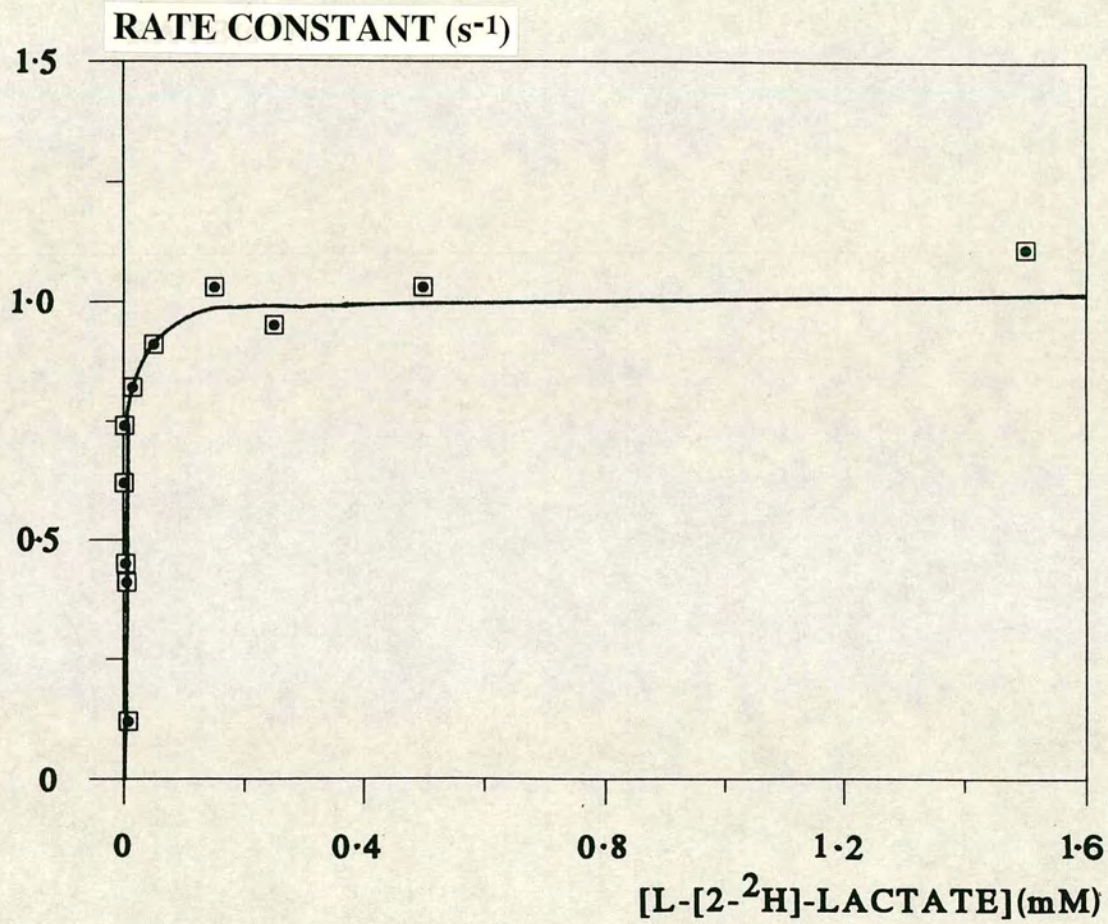

Experimental conditions are described in Section 2.2.3

phase, observed in stopped-flow experiments, which accounts for approximately 80% of the total absorbance change. The second phase, due to entry of the third electron, is so much slower than the first phase, approximately 20-fold slower, that it is considered to be kinetically irrelevant in catalytic turnover of the enzyme. Hence all data quoted, in the case of biphasic traces, correspond to the fast phase.

The monophasic nature of FMN reduction of the hinge-swap enzyme rules out the possibility of any interprotomer electron transfer on this timescale, inferring that flavin to haem electron transfer is very much slower than interprotomer electron transfer. This observation is supported by the dramatic effect on the rate of haem reduction, with k_{cat} for the hinge-swap enzyme being over 300-fold less than for the wild-type enzyme ($1.61s^{-1}$ and $445s^{-1}$ respectively). Hence introduction of the hinge-swap mutation has only a slight effect on the electron transfer from L-lactate to FMN, but a very major effect on electron transfer from FMN to haem. This conclusion is supported by the observed kinetic isotope effects (KIEs) as shown in Table 2.5. The KIE for FMN reduction drops only slightly in the hinge-swap enzyme compared to the wild-type enzyme (from 8.1 for WT to 6.3 for the hybrid) indicating that abstraction of the C-2 proton of L-lactate is rate-limiting over the timescale for flavin reduction. However there is a dramatic decrease in the KIE for haem reduction from 6.3 for the wild-type enzyme

to only 1.6 for the hybrid enzyme inferring that there has been a change in the overall rate-limiting step in the catalytic cycle from C-2-proton abstraction in wild-type to flavin to haem electron transfer in the hinge-swap enzyme. This is discussed further in Section 2.3.4. Michaelis constants, K_M, determined by the method of stopped-flow are more realistic than those obtained from steady-state kinetics as catalytic pathways are simplified. K_M values for flavin reduction of the wild-type and hinge-swap-*b*2 enzymes are similar indicating that the presence of the hinge mutation has no effect on formation of the Michaelis complex, as perhaps would be expected since no active site residues have been altered by the mutation. However, there is a large difference in the K_M values obtained for haem reduction, the value for the hybrid being approximately 200-fold lower than for wild-type for both L-[2-^{1}H] and L-[2-^{2}H]-lactate. The k_{cat}/K_M values are the same within experimental error, being, for example, $8.4 \times 10^5 M^{-1}s^{-1}$ for the wild-type enzyme and $5.3 \times 10^5 M^{-1}s^{-1}$ for hinge-swap-*b*2 for haem reduction with L-[2-^{1}H]-lactate (values calculated from data shown in Table 2.5). The fact that these values are similar again infers that K_M is controlled by the level of k_{cat}. Hence the low K_M values observed for hinge-swap-*b*2 are a consequence of the very low rate constant for haem reduction and are not an indication of efficient formation of the Michaelis complex.

2.3.3 REDOX POTENTIALS

There was the possibility that the vast decrease in rate of electron transfer from flavin to haem was caused by a change in the redox potential induced by the mutation. Obviously there can have been no change in the redox potential of the flavin group in the hinge-swap enzyme since the k_{cat} values for flavin reduction are not significantly altered; but a large decrease in the redox potential for the haem group could account for the lowering of the k_{cat} for haem reduction. The midpoint potentials for the haem groups for both wild-type and the hinge-swap enzyme were determined spectrophotometrically. Figure 2.9 shows the oxidative titration of hinge-swap-*b*2 and the Nernst plots for both oxidation and reduction of hinge-swap-*b*2 are illustrated in Figure 2.10. These two plots overlay exactly confirming the absence of hysteresis in the system *i.e.* oxidation/reduction is entirely reversible. The redox potential for the haem group of hinge-swap-*b*2 of -23$\pm$3mV, calculated from the oxidative titration, agrees within experimental error to that obtained for the haem group of *S.cerevisiae* wild-type of -20$\pm$2mV obtained under identical conditions. The latter is in agreement with that previously reported of -19mV (26).

FIGURE 2.9

REDOX POTENTIOMETRIC TITRATION SHOWING OXIDATION OF HINGE-SWAP FLAVOCYTOCHROME *b*2 ON ADDITION OF FERRICYANIDE

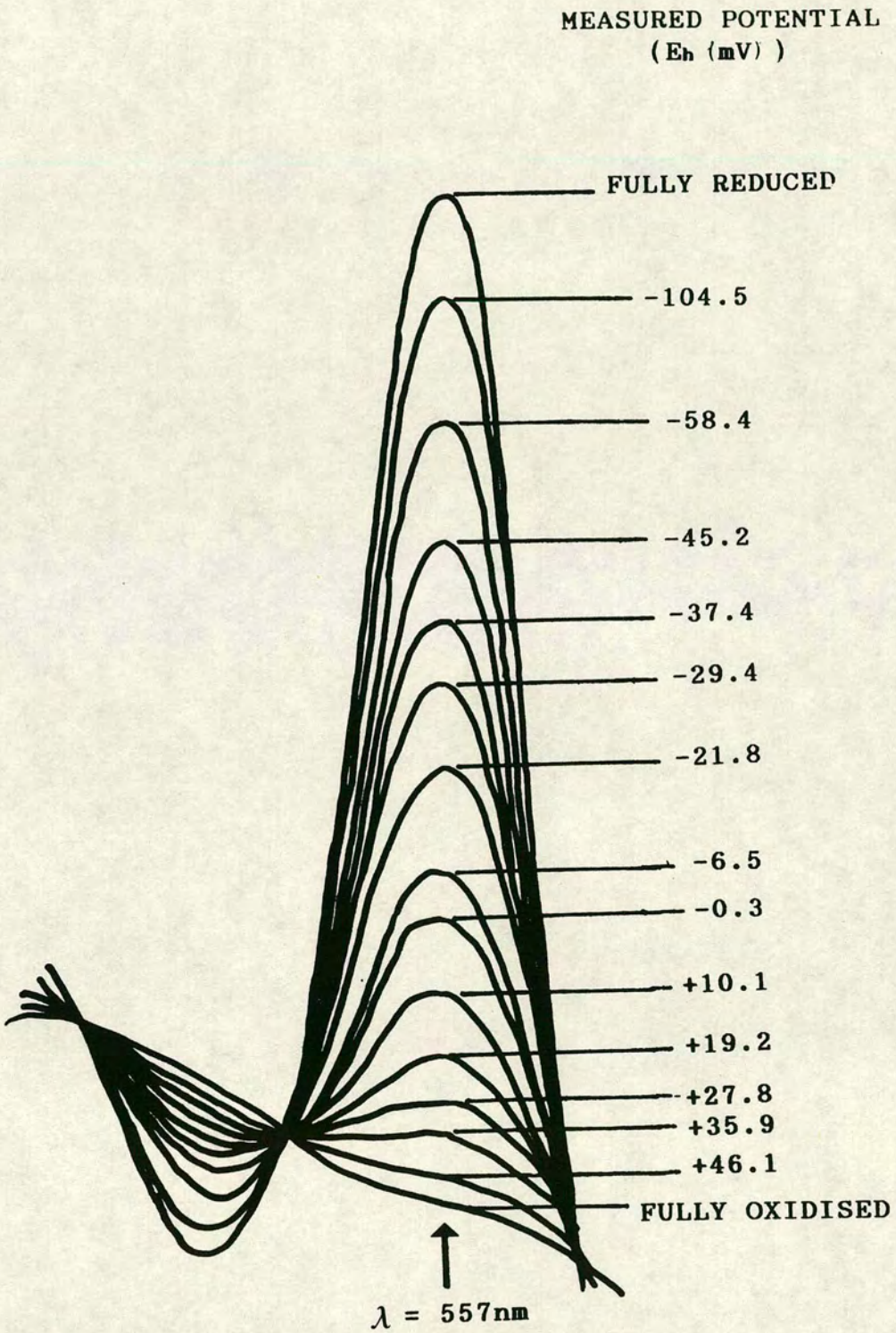

FIGURE 2.10

NERNST PLOTS USED TO DETERMINE THE HAEM REDOX POTENTIAL OF HINGE-SWAP FLAVOCYTOCHROME *b*2

(a) REDUCTION

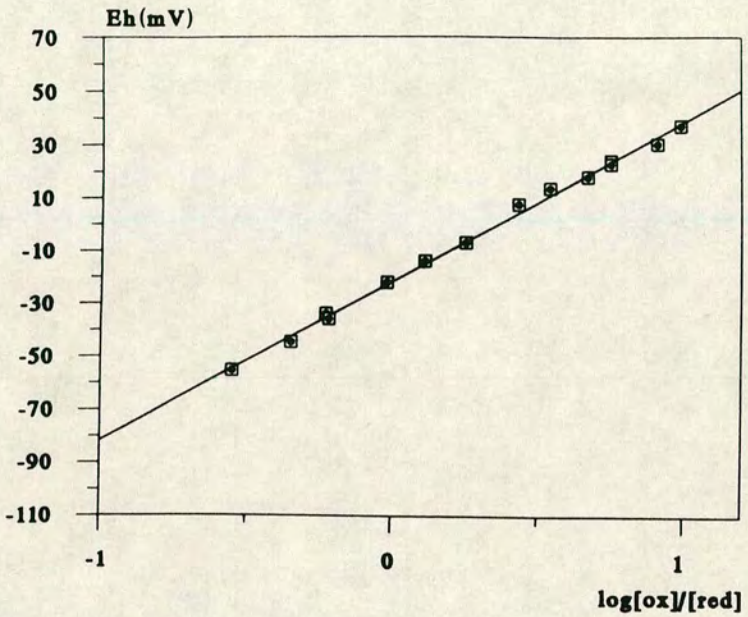

(b) OXIDATION

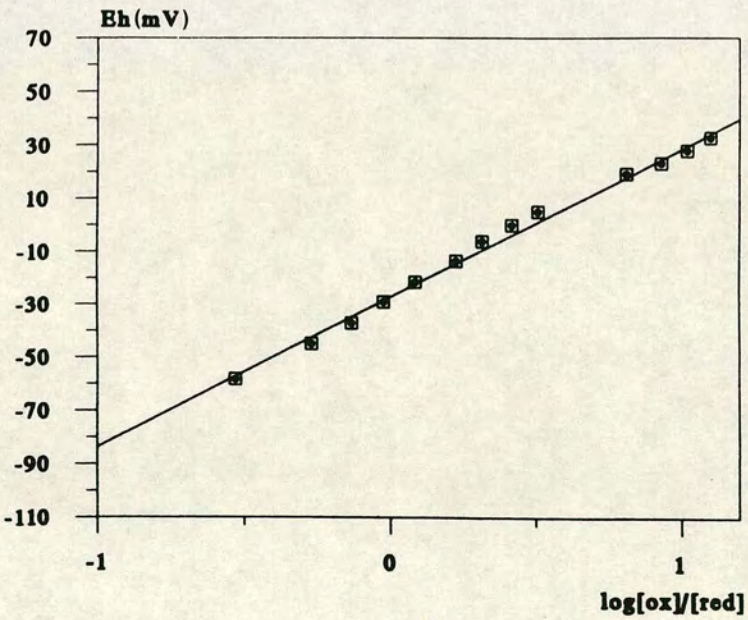

Gradients of the above plots are 60±2mV for the reduction and 57±2mV for the oxidation.
Both lines correspond to one electron processes.

2.3.4 DISCUSSION OF COMBINED RESULTS

The rate constants for *S.cerevisiae* wild-type (23) and hinge-swap flavocytochromes *b*2 are compared in Figure 2.11, which is a linear representation of the catalytic cycle of the enzyme. Similarly represented, in Figure 2.12, are the corresponding values of the kinetic isotope effects (KIEs).

Considering firstly the wild-type enzyme, the initial rate constant of $604s^{-1}$, for flavin reduction, gradually decreases along the enzyme's pathway ultimately reaching a third of its original value. This rate constant erosion is mirrored by the values for the KIE which fall from 8.1 for flavin reduction, to 6.3 for haem reduction, to 3.0 for cytochrome *c* reduction. The initial value, for flavin reduction, is high and drops along the electron transport chain, still being fairly significant for cytochrome *c* reduction. This proves that a substantial contribution to overall rate-limitation for *S.cerevisiae* wild-type flavocytochrome *b*2 is made by abstraction of the C-2 proton from L-lactate by the active site base, His-373.

Moving onto the hinge-swap enzyme we see a different behaviour. The initial rate constant, for flavin reduction is lower than for wild-type, being $240s^{-1}$, but moving along the chain, at the second step the rate constant has fallen by a massive amount to the minimum value which is invariant throughout the rest of the cycle. This large decrease indicates a disruption to

FIGURE 2.11

LINEAR REPRESENTATION OF THE CATALYTIC CYCLE OF FLAVOCYTOCHROME *b*2

COMPARING THE RATE CONSTANTS FOR WILD-TYPE AND HINGE-SWAP ENZYMES

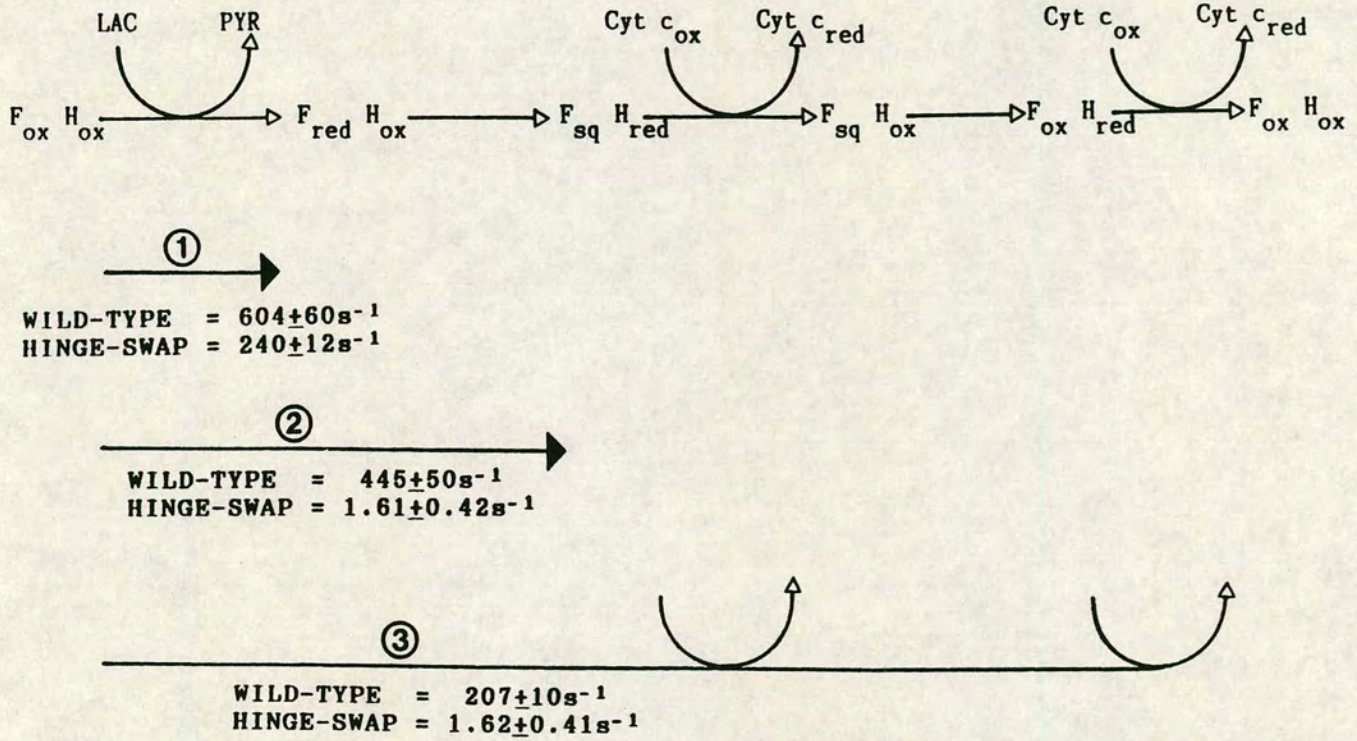

ABBREVIATIONS : LAC, LACTATE; PYR, PYRUVATE; F, FLAVIN; H, HAEM; Cyt c, CYTOCHROME *c*; ox, OXIDISED; red, REDUCED; sq, SEMIQUINONE.

FIGURE 2.12

COMPARISON OF THE DEUTERIUM KINETIC ISOTOPE EFFECTS FOR *S.cerevisiae* WILD-TYPE AND HINGE-SWAP FLAVOCYTOCHROMES *b*2

S.c. WT-*b*2	8.1±1.4	6.3±1.2	3.0±0.6
L-LACTATE---------->FLAVIN---------->HEME--------->CYTOCHROME *c*			
HINGE-SWAP-*b*2	6.3±0.7	1.6±0.7	1.7±1.3

electron flow between the two prosthetic groups, FMN and haem. This is supported by the KIEs. The KIE value for flavin reduction is 6.3 indicating that C-2 proton abstraction is still rate-limiting over the flavin reduction timescale but there is no significant isotope effect for haem reduction confirming that the transfer of electrons from FMN to haem has now become rate-limiting, and is in fact the rate-limiting step in the entire catalytic cycle since the KIE (and rate constant) for cytochrome *c* reduction are identical, within experimental error, to the values for haem reduction.

The presence of the *H.anomala* hinge in the bulk of the *S.cerevisiae* enzyme has caused a change in the rate-limiting step from C-2 proton abstraction from L-lactate by His-373 to flavin to haem electron transfer. It is interesting to note that the overall rate-limiting step in the wild-type enzyme from *H.anomala* is flavin to haem electron transfer (16), as discussed in Section 1.8.1, suggesting that it is the shorter, more acidic hinge region which is dominant in controlling the mobility of the domains and hence electron flow between them.

Although steps occurring after FMN reduction are severely disrupted, in essence the hinge-swap enzyme is still a good lactate dehydrogenase. The rate constant for flavin reduction of hinge-swap flavocytochrome b_2 is ~40% lower than that for the wild-type enzyme from *S.cerevisiae*. This difference may be due to restricted domain mobility resulting from the shorter hinge region which may have

the effect of either blocking the channel leading to the active site or, at the other extreme, not allowing encapsulation of substrate at the active site.

The discovery that flavin to haem electron transfer is rate-limiting in the hinge-swap enzyme leads us to a possible explanation of the ferricyanide dependency. It has previously been reported by Iwatsubo *et al.* (27) that de-haemo-b_2 shows a ferricyanide dependence. He suggested that in the absence of the haem group ferricyanide could accept an electron from both the flavin hydroquinone and the flavin semiquinone (electron transfer from the latter being 20-fold faster). Hence the apparent K_M for ferricyanide would have contributions from three steps: L-lactate to FMN, flavin hydroquinone to ferricyanide and flavin semiquinone to ferricyanide. In hinge-swap-b_2 we have an enzyme which, in effect, behaves as de-haemo-b_2 since the transfer of electrons to the haem is very much slower than any of the three processes mentioned above, hence during the time in which ferricyanide is reduced, the flavin does not "see" the haem as a suitable electron acceptor. In this hinge-swap enzyme ferricyanide must therefore bypass the haem and accept electrons from flavin hydroquinone and semiquinone in order to result in the relatively high rate constant observed with this acceptor. Such a scheme of electron transfer is illustrated in Figure 2.13, which depicts the differing pathways of electron transfer to ferricyanide which occur in the wild-type and hinge-swap enzymes. For hinge-swap-

FIGURE 2.13

POSTULATED MECHANISM OF ELECTRON TRANSFER TO FERRICYANIDE BY WILD-TYPE AND HINGE-SWAP FLAVOCYTOCHROMES *b*2

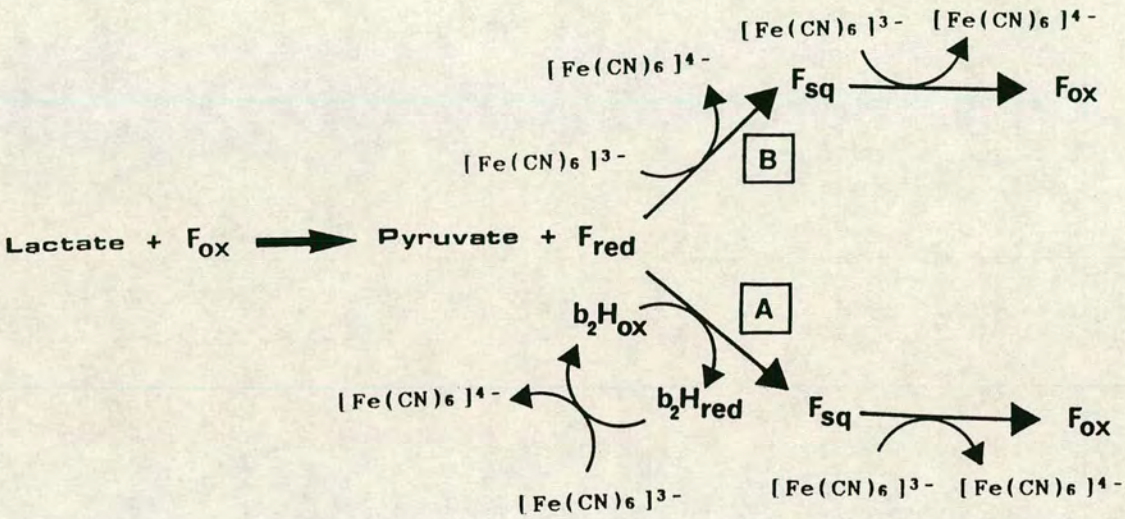

WILD-TYPE-*b*2 (ROUTE A) - Flavin is fully reduced by the two electrons it receives from lactate; it then passes one of these electrons to the *b*2-haem which can then reduce a molecule of ferricyanide. The resulting flavin semiquinone can subsequently reduce a second molecule of ferricyanide.

HINGE-SWAP-*b*2 (ROUTE B) - The fully reduced flavin (hydroquinone) passes electrons directly to ferricyanide, bypassing the haem. The semiquinone form of flavin is then oxidised by electron transfer to a second molecule of ferricyanide.

ABBREVIATIONS : F_{ox}, oxidised flavin; F_{red}, reduced flavin (hydroquinone), F_{sq}, flavin semiquinone; b_2H_{ox}, oxidised *b*2-haem; b_2H_{red}, reduced *b*2-haem.

*b*2 the situation is as described above, as for de-haemo-flavocytochrome *b*2; the turnover rate is limited at the level of lactate to flavin electron transfer and also by the step in which flavin hydroquinone is oxidised to flavin semiquinone by ferricyanide. The rate constant for the latter step is therefore dependent upon ferricyanide concentration, and the slower this rate the higher the K_M for the electron acceptor. This is in contrast to the wild-type enzyme in which this slow hydroquinone to semiquinone step is overcome by the rapid electron transfer between the flavin hydroquinone and the haem. The haem, or cytochrome *b*2, domain takes electrons from the flavin hydroquinone faster than ferricyanide is able to; and the haem itself then reacts very rapidly with ferricyanide, hence leading to a smaller value for the acceptor K_M. This accounts for the 10-fold difference in K_M (acceptor) between the hinge-swap and wild-type enzymes and also explains the dependence on ferricyanide concentration observed for the former.

Obviously the shorter, more acidic hinge region has had a drastic effect on electron transfer between flavin and haem. The closest edge-to-edge distance between the prosthetic groups is 9.7Å from flavin N-5 to haem C-2A. Dutton and co-workers (28,29) have suggested that it is edge-to-edge distance which controls electron transfer between redox centres. However simulation studies based on this theory predict flavin to haem electron transfer rates of 500-600s^{-1} for flavocytochrome *b*2 (30,31),

values which are much lower than would be expected if interdomain electron transfer was dominated by the edge-to-edge distance alone. Other factors which may be contributing to this lowering of rate are (i)the relative redox potentials of the prosthetic groups, (ii) the nature of the intervening medium, and (iii) mobility of the domains.

It was possible that the large decrease in interdomain electron transfer may have been caused by a decrease in the redox potential for the haem group making it a better electron donor, as mentioned in 2.3.3. This theory can be eliminated as our experimentation has shown that the haem redox potentials for the wild-type and hinge-swap enzymes are identical within experimental error.

The only covalent linkage of the domains is that involving the hinge region, so it has been assumed that at least part of the interdomain electron transfer is through space (10). Hence the nature of the intervening medium may be of importance. The most direct pathway from flavin to haem involves only solvent molecules which have been postulated to be less efficient at electron transfer by Mayo *et al.* (32). In this study Mayo suggested that aromatic amino-acid sidechains were the most feasible for electron transfer and it so happens that in flavocytochrome b_2 a tyrosine residue (Y143) bridges the flavin and haem groups. This residue may act as an electron pathway (1).

The most important factor in governing interdomain

electron transfer is the mobility of the domains with respect to one another. Evidence of this mobility comes from both the X-ray crystal structure (10) and from NMR studies (12). As the domains are mobile there can be no fixed edge-to-edge distance between the prosthetic groups. In the hinge-swap enzyme the domain mobility may be restricted by the shorter hinge region leading to disruption of interdomain contacts and increase of edge-to-edge distances resulting in poor overlap of acceptor/donor orbitals, in essence leading to less effective recognition between the domains.

2.4 CONCLUSIONS

In summary the role of the interdomain hinge has been probed by construction of the "hinge-swap" enzyme. Characterisation of this hybrid enzyme has enabled the following conclusions to be drawn:-

(1) the interdomain hinge has little influence on the lactate dehydrogenase function of flavocytochrome b_2, but it is important for its role as a cytochrome *c* reductase;

(2) the hinge is crucial in mediating the flow of electrons from flavin to haem;

(3) the hinge-swap mutation results in a change in the overall rate-limiting step from C-2 proton abstraction in the wild-type enzyme from *S.cerevisiae* to flavin-to-haem electron transfer (as in the wild-type enzyme from *H.anomala*);

(4) structurally the hinge is critical in ensuring efficient domain recognition.

2.5 REFERENCES

(1) Lesk, A.M. & Chothia, C., *J.Mol.Biol.*, **174**, 175 (1984).

(2) Huber, R. & Bennett, W.S., *Biopolymers*, **22**, 261 (1983).

(3) Anderson,B.F., Baker,H.M., Norris,G.E., Rumball,S.V. & Baker,E.N., *Nature*, **344**, 784 (1990).

(4) Janin,J. & Wodak,S., *Prog.Biophys.Mol.Biol.*, **42**, 71 (1983).

(5) Eklund,H., Samaha,J.-P., Wallen,L., Brändén,C.-I, Åkeson,A. & Jones,T.A.,*J.Mol.Biol.*, **146**, 561 (1981).

(6) Watson et al, *EMBO J.*, **1**, 1635 (1982).

(7) Faber,H.R. & Matthews,B.W., *Nature*, **348**, 263 (1990).

(8) Perham, R.N., *Biochemistry*, **30**, 8501 (1991).

(9) Argos, P., *J.Mol.Biol.*, **211**, 943 (1990).

(10) Xia, Z.-X. & Mathews, F.S., *J.Mol.Biol.*, **212**, 837 (1990).

(11) Miles, C.S., *Ph.D. thesis*, University of Edinburgh (1992).

(12) Brunt,C.E., Cox,M.C., Thurgood,A.G.P., Moore.G.R., Reid,G.A. & Chapman, S.K., *Biochem.J.*, **283**, 87 (1992).

(13) Labeyrie, F., Beloeil, J.C. & Thomas, M.A., *Biochim.Biophys.Acta.*, **953**, 134 (1988).

(14) Lederer,F., Cortial,S., Becam,A.M., Haumont, P.Y., & Perez,L., *Eur.J.Biochem.*, **152**, 419 (1985).

(15) Black,M.T., Gunn,F.J., Chapman,S.K. & Reid,G.A., *Biochem.J.*, **263**, 973 (1989).

(16) Capeillère-Blandin, C., Barber,M.J. & Bray,R.C., *Biochem.J.*, **238**, 745 (1986).

(17) Sambrook, J., Fritsch, E.F. and Maniatis, T., in *"Molecular Cloning: A Laboratory Manual"* , 2nd edition, Cold Spring Harbour Laboratory Press, Cold Spring Harbour, NY (1989).

(18) Reid, G.A., White, S.A., Black, M.T., Lederer, F., Mathews,F.S. & Chapman,S.K., *Eur.J.Biochem.*, **178**, 329 (1988).

(19) Mead, D.A., Szczesna-Skorupa, E. & Kemper, B., *Protein Eng.*, **1**, 67 (1986).

(20) Kunkel, T.A., *Proc.Natl.Acad.Sci.*, **82**, 488 (1985).

(21) White, P., Manson, F.D.C., Brunt, C.E., Reid, G.A. & Chapman,S.K., *Biochem.J.*, **291**, 89-94 (1993).

(22) Black,M.T., White,S.A., Reid,G.A. & Chapman,S.K., *Biochem.J.*, **258**, 255 (1989).

(23) Miles, C.S., Rouvière-Fourmy, N., Lederer, F., Mathews,F.S., Reid, G.A., Black, M.T. & Chapman, S.K., *Biochem.J.*, **285**, 187 (1992).

(24) Pompon,D., Iwatsubo,M. & Lederer,F., *Eur.J.Biochem.*, **104**, 479 (1980).

(25) Tegoni, M., Personal communication in White,S.A., *Ph.D. thesis*, University of Edinburgh (1989).

(26) Brunt, C.E., *Ph.D. thesis*, University of Edinburgh (1993).

(27) Iwatsubo, M., Mevel-Ninio, M. & Labeyrie, F., *Biochemistry*, **16**, 3558 (1977).

(28) Gunner,M.R. & Dutton,P.L.,*J.Amer.Chem.Soc.*,**111**, 3400 (1989).

(29) Moser,C.C., Warncke, K., Keske, J.M. & Dutton, P.L., *J.Inorg.Biochem.*, **43**, 91 (1991).

(30) Capeillère-Blandin,C., *Eur.J.Biochem.*, **56**, 91 (1975).

(31) Pompon, D., *Eur.J.Biochem.*, **106**, 151 (1980).

(32) Mayo, S.L., Ellis, W.R.Jnr., Crutchley, R.J. & Gray, H.B., *Science*, **233**, 948 (1986).

CHAPTER 3

INTRAMOLECULAR COMMUNICATION

THE IMPORTANCE OF STRUCTURAL INTEGRITY

3.1 INTRODUCTION

Knowledge of intramolecular electron transfer is of central importance in understanding the role of multiple redox centres in electron transport in biological systems. Tetrameric flavocytochrome *b*2 is one of these multiple redox systems, each monomer containing both flavin mononucleotide and haem protoporphyrin IX as prosthetic groups. Each of these moieties is bound in a functionally distinct domain (1). X-ray crystallography (2) has confirmed the existence of these two domains which are linked by a region of polypeptide chain which acts as a hinge. The structure of a monomer of flavocytochrome *b*2 is schematically represented in Figure 3.1. It has been proposed that flavocytochrome *b*2 arose as a result of gene fusion between a haemoprotein and an FMN-binding flavodehydrogenase (3). The cytochrome domain, located at the N-terminus of the amino-acid sequence, is homologous to microsomal cytochrome *b*5 (4) and the FMN-binding domain is related to spinach glycolate oxidase, a simple FMN-dependent α-hydroxy-acid-oxidising enzyme which has 40% sequence identity (5,6). Flavocytochrome *b*2 has been isolated and purified from two species of yeast, *Saccharomyces cerevisiae* and *Hansenula anomala*. Although only the enzyme from *S.cerevisiae* is of known three-dimensional structure (2), extensive kinetic studies have been carried out on the enzyme from *H.anomala* (7,8) and it has been shown that

FIGURE 3.1

SCHEMATIC REPRESENTATION OF A SUBUNIT OF FLAVOCYTOCHROME *b*$_2$ BASED ON THE KNOWN THREE-DIMENSIONAL STRUCTURE OF THE ENZYME FROM *S.cerevisiae*

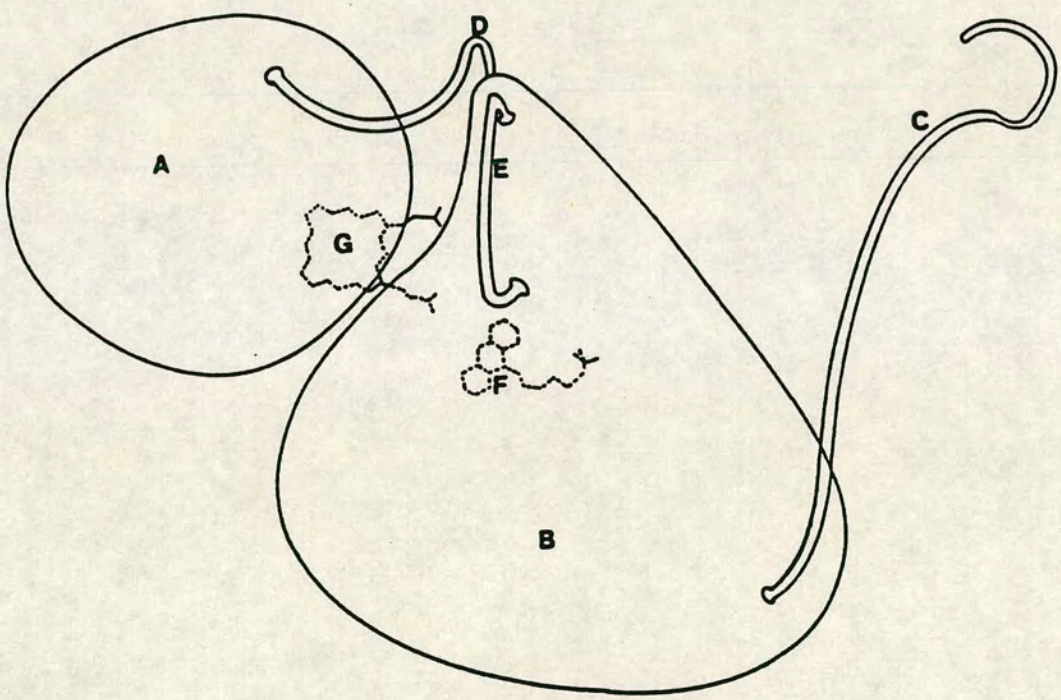

KEY : A, haem domain; B, flavodehydrogenase domain; C, C-terminal tail; D, interdomain hinge; E, protease-sensitive loop; F, FMN; G, protohaem IX.

the flavocytochromes *b*$_2$ from the two sources have significant differences in kinetic behaviour (Table 2.1). The molar activity of *H.anomala-b*$_2$ is several-fold higher than that of *S.cerevisiae-b*$_2$ and the enzymes from the two species of yeast have different rate-limiting steps; the rate-limiting step in *S.cerevisiae-b*$_2$ is abstraction of the C-2 hydrogen of L-lactate as a proton by the active site base, His-373, whereas in *H.anomala-b*$_2$ it is flavin to haem electron transfer (8). Determination of the amino-acid sequence of the *H.anomala* enzyme (10) and comparision to that of *S.cerevisiae-b*$_2$ (11) has led to the identification of regions of significant sequence divergence (10). The most striking differences were found in two surface loops of the protein: the interdomain hinge and a protease-sensitive region within the flavodehydrogenase domain.

The hinge region in *H.anomala* flavocytochrome *b*$_2$ (residues 88-96) is shorter and extremely acidic (net charge -6) compared to the corresponding region in the *S.cerevisiae* enzyme (residues 89-103, net charge of -1). The hinge regions are compared in Figure 3.2 and the effects of the shorter hinge are discussed in Chapter 2.

The protease-sensitive region in *S.cerevisiae* flavocytochrome *b*$_2$ comprises residues 300-312 and is quite basic having a net charge of +4. In *H.anomala-b*$_2$ the corresponding region (residues 288-298) is slightly shorter and is very acidic with net charge of -6. These regions are compared in Figure 3.2. In the crystal

FIGURE 3.2

COMPARISON OF THE AMINO-ACID SEQUENCES OF THE INTERDOMAIN HINGE AND PROTEASE-SENSITIVE LOOP REGIONS OF FLAVOCYTOCHROME *b*$_2$ FROM *S.cerevisiae* AND *H.anomala*

INTERDOMAIN HINGE

		LENGTH	NET CHARGE
	88 ... 103		
S.cerevisiae	- P E L V C P P Y A P G E T K	14	-1
H.anomala	E Q E E E E L S D - - - - - -	9	-6

PROTEASE-SENSITIVE LOOP

	288 ... 312		
S.cerevisiae	- - T K A G P K A M K K T N V	13	+4
H.anomala	D S D V Q G D D E D I - - - -	11	-6

structure of flavocytochrome *b*2 from *S.cerevisiae* this protease-sensitive region is unresolved implying that it has a degree of mobility. Its influence on catalytic activity has been indicated by kinetic studies of a mutant flavocytochrome *b*2 (12) and a protease-cleaved enzyme (13).

These structural and chemical differences probably form the basis for the kinetic differences between the flavocytochromes *b*2 from the two species of yeast. To investigate the specific roles of each of these regions, protein engineering has been used to generate four interspecies hybrid enzymes, which encompass hinge-swaps, loop-swaps and domain-swaps. These are illustrated in Figure 3.3.

Of these four hybrids, characterisation of the hinge-swap enzyme (pFM303) has been described in Chapter 2. Of the other hybrids, the most obvious to focus on is the "loop-swap" enzyme (pFM307); this enzyme consists of the bulk of the *S.cerevisiae* enzyme but with the protease-sensitive loop of the *H.anomala* enzyme. However, problems were encountered with the expression of this enzyme in *E.coli* which was at too low a level to allow the extraction of sufficient amounts of protein. Problems with expression of protein has been a feature observed with all of the hybrid enzymes, although, after much perseverance, suitable yields of pFM306 were achieved. This hybrid consists of the flavodehydrogenase domain from *H.anomala* and the hinge region and haem domain from

FIGURE 3.3

SCHEMATIC REPRESENTATION OF THE HYBRID ENZYMES BASED ON THE KNOWN THREE-DIMENSIONAL STRUCTURE OF THE SUBUNIT OF WILD-TYPE FLAVOCYTOCHROME *b*2 FROM *S.cerevisiae*

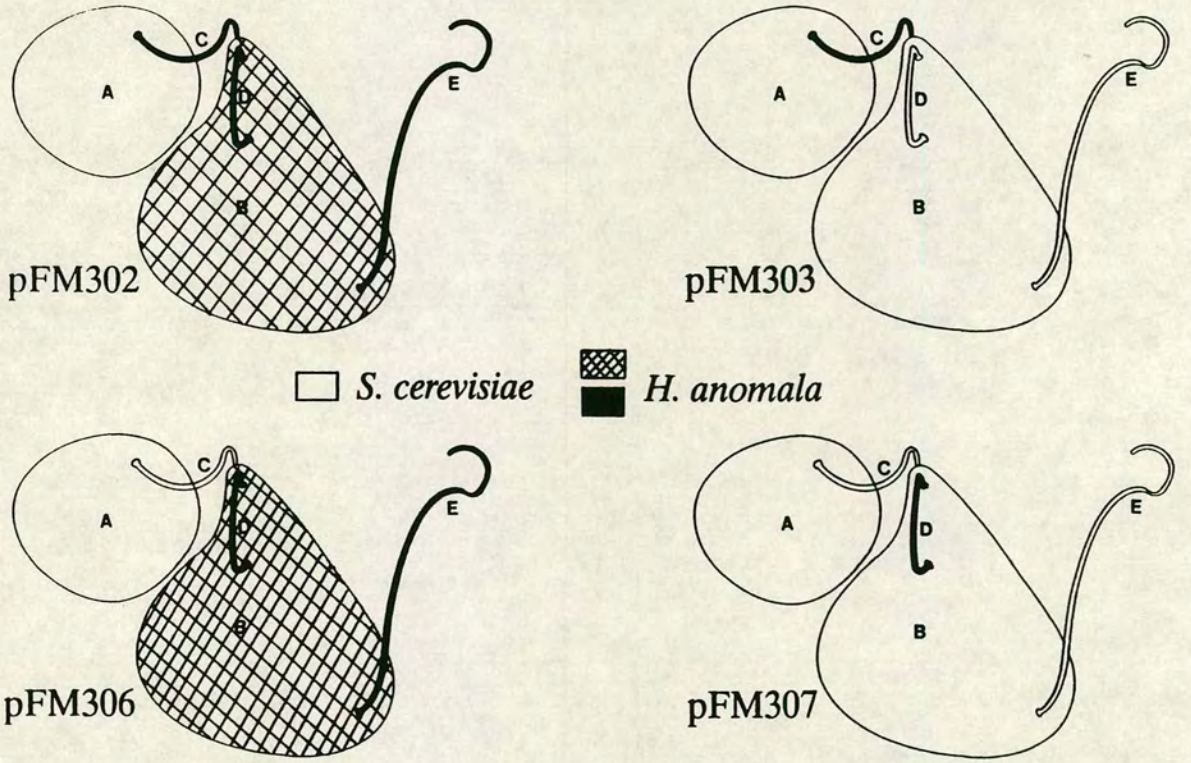

ABBREVIATIONS : A, haem domain; B, flavin domain; C, interdomain hinge; D, protease-sensitive loop; E, C-terminal tail; pFM303, hinge-swap-*b*2; pFM307, loop-swap-*b*2; pFM306, domain-swap-*b*2.
The coded boxes represent the source of the DNA used in mutagenesis.

S.cerevisiae and will hereafter be referred to as "domain-swap" flavocytochrome *b*$_2$. This chapter concentrates on the development of a purification procedure and characterisation of this enzyme. Part of this work was carried out in conjunction with an Honours project student, Duncan M.Short (14).

3.2 EXPERIMENTAL

3.2.1 CONSTRUCTION OF DOMAIN-SWAP FLAVOCYTOCHROME *b*$_2$ (DR.F.D.C.MANSON)

Standard methods for DNA manipulation were performed as described in Sambrook *et al.* (15). Modification of the genes encoding flavocytochrome *b*$_2$ from both *S.cerevisiae* and *H.anomala* is as described for the hinge-swap enzyme in Section 2.2.1 and the restriction map is shown in Figure 2.1(a). To construct the domain-swap enzyme (pFM306), the sequence encoding *S.cerevisiae*-*b*$_2$ was cleaved by *Xba*I and *Hin*dIII and the larger fragment containing the gene encoding the cytochrome domain and hinge region was isolated. Similarly the smaller fragment containing the flavodehydrogenase was isolated from the *H.anomala* sequence. The two fragments were ligated and the recombinant structure was verified by restriction enzyme analysis.

3.2.2 ISOLATION AND PURIFICATION PROCEDURE

S.cerevisiae wild-type and domain-swap flavocytochromes

*b*2 were expressed in *E.coli* (strain TG1) (16,17) which were grown as described in Section 7.1. Protein was isolated from cells which had been stored at -20°C by the method described in 7.4. The wild-type enzyme was purified by hydroxylapatite column chromatography as described in 7.4.4. Hydroxylapatite consists mainly of negatively charged material. Wild-type-*b*2 from *S.cerevisiae* has neutral surface charge and hence binds well to hydroxylapatite. *H.anomala-b*2, on the other hand, has a dense region of negative charge located on its flavodehydrogenase domain and as a result will not bind to hydroxylapatite. The domain-swap-*b*2 contains the flavodehydrogenase domain from the *H.anomala* enzyme, hence it does not bind to hydroxylapatite. Purification of the domain-swap enzyme was carried out by the method used for purification of *H.anomala-b*2, that is by ion-exchange column chromatography using DE52 (Whatman), a cellulose anion exchanger. The column was poured as summarised in 7.3.3 and was equilibrated in buffer A (50mM phosphate buffer, 5mM lactate, pH 7.0). Before loading the column the protein was dialysed against a large excess of half-strength buffer A at 0-4°C under nitrogen for approximately 20 hours during which time the dialysis buffer was renewed at least once. The protein was loaded onto the column and it bound in a tight band. After washing with 1-2 column volumes of buffer A the domain-swap-*b*2 was eluted with a 0-2% ammonium sulphate gradient. Fractions were collected and purity assessed by

absorbance ratio measurement as accounted in 7.4.4. Fractions with the lowest ratios were pooled and stored as an ammonium sulphate precipitate at 0-4°C under nitrogen. Protein of this purity was used for all steady-state measurements. Before stopped-flow measurements were made the protein was passed through a gel filtration column (G25 - see 7.3.4 and 7.9.2). Purity and structural integrity *i.e.* extent of proteolytic cleavage, were assessed by SDS-PAGE (Section 7.5).

On performing SDS-PAGE on the domain-swap enzyme it was found that the enzyme is subject to partial proteolytic cleavage over a period of time, resulting in bands at 39.4kDa and 14.2kDa, correlating to the N and (ϵ + ß) fragments as reported by Gervais *et al.* (18). This is in accordance with proteolysis of the hinge region having taken place.

Such proteolysis may be problematic kinetically, as a result the gene encoding the domain-swap enzyme has recently been transformed into protease-deficient *E.coli* (strain AR120) as for hinge-swap-*b2*.

3.2.3 KINETIC ANALYSIS

All experiments were carried out at 25±0.1°C in tris-HCl buffer at pH 7.5, except where stated otherwise. The buffer was 0.01M HCl and its ionic strength was adjusted to 0.10M by addition of NaCl.

A Beckmann DU-62 UV/visible spectrophotometer was used to

monitor the steady-state kinetics of the oxidation of L-lactate by the enzyme. The external electron acceptors used were either ferricyanide or cytochrome *c* as described in Section 7.8.

Stopped-flow measurements were performed using an Applied Photophysics SF.17MV spectrofluorimeter as reported in Section 7.9. Reduction of the prosthetic groups was monitored by observing absorbance changes at fixed wavelengths; 438.3nm for flavin reduction (a haem isosbestic point) and at either 423nm or 557nm for haem reduction (both wavelengths giving identical results). Data were collected and analysed using the SF.17MV software package in conjunction with an Archimedes 420/1 computer. Data were fitted to single exponentials for flavin reduction and to double exponentials for haem reduction.

For all kinetic measurements, k_{cat} and K_M were calculated using non-linear regression analysis.

Values of kinetic isotope effects (KIEs) were evaluated by comparing rates obtained using L-[2-^{1}H]-lactate to those obtained using L-[2-^{2}H]-lactate as substrate. The latter was synthesised by a coupled enzymatic procedure, the protocol for which is given in Section 7.7.2.

3.3 RESULTS AND DISCUSSION

3.3.1 STEADY-STATE KINETIC ANALYSIS

Results from the steady-state kinetic analysis of domain-

swap-*b*2 with ferricyanide as the electron acceptor are given in Table 3.1 where they are compared with those previously obtained for *S.cerevisiae* wild-type flavocytochrome *b*2 (17). A plot of rate versus substrate concentration is shown in Figure 3.4 which clearly illustrates the strong substrate inhibition observed at high L-lactate concentrations. Figure 3.5 shows the Michaelis-Menten plots, analysis of which enabled calculation of the kinetic parameters K_M and K_I. The K_I value is the concentration of inhibitor, in this case substrate, at which the rate is half the maximum.

The action of most enzymes is inhibited by a variety of substances. Inhibition may be a reversible or an irreversible process. In the former the functional regions of the enzyme do not change and enzyme and inhibitor equilibrate rapidly. Irreversible inhibition, on the other hand, can lead to complete inactivation (19) as a result of enzyme modification; an example of this is the action of 2-hydroxy-3-butynoate on flavocytochrome *b*2. This acetylene derivative of lactate results in an allenic carbanion which can then form a stable covalent adduct with the flavin group. This adduct is highly reactive and ultimately results in formation of an inactive modified flavin group (20,21). A scheme of this so called suicide inhibition is illustrated in Figure 1.17.

Reversible inhibitors may be categorised into three general classes: competitive, noncompetitive and

TABLE 3.1

A COMPARISON OF THE RESULTS FROM STEADY-STATE KINETIC ANALYSES OF *S.cerevisiae* WILD-TYPE AND DOMAIN-SWAP FLAVOCYTOCHROMES *b*$_2$ WITH FERRICYANIDE AS ELECTRON ACCEPTOR

	k_{cat} (s^{-1})	K_M (mM)	S_{opt} (mM)	K_I (mM)	k_{cat}/K_M ($M^{-1}s^{-1}$)
WILD-TYPE*	400±10	0.49±0.05	10	174±8	8.2×10^5
DOMAIN-SWAP#	190±10	0.62±0.10	5.6±1.0	55±11	3.0×10^5

Experimental conditions : All experiments were carried out in tris-HCl buffer, pH 7.5 at 25±0.1°C. The concentration of ferricyanide used was 1mM; this being >90% saturating for both enzymes.

k_{cat} is expressed in terms of number of electrons transferred per second per mole of enzyme.

References : *Reference (17); #This work.

FIGURE 3.4

GRAPHICAL ILLUSTRATION OF SUBSTRATE INHIBITION EXHIBITED BY DOMAIN-SWAP FLAVOCYTOCHROME b_2 WHEN USING FERRICYANIDE AS THE EXTERNAL ELECTRON ACCEPTOR

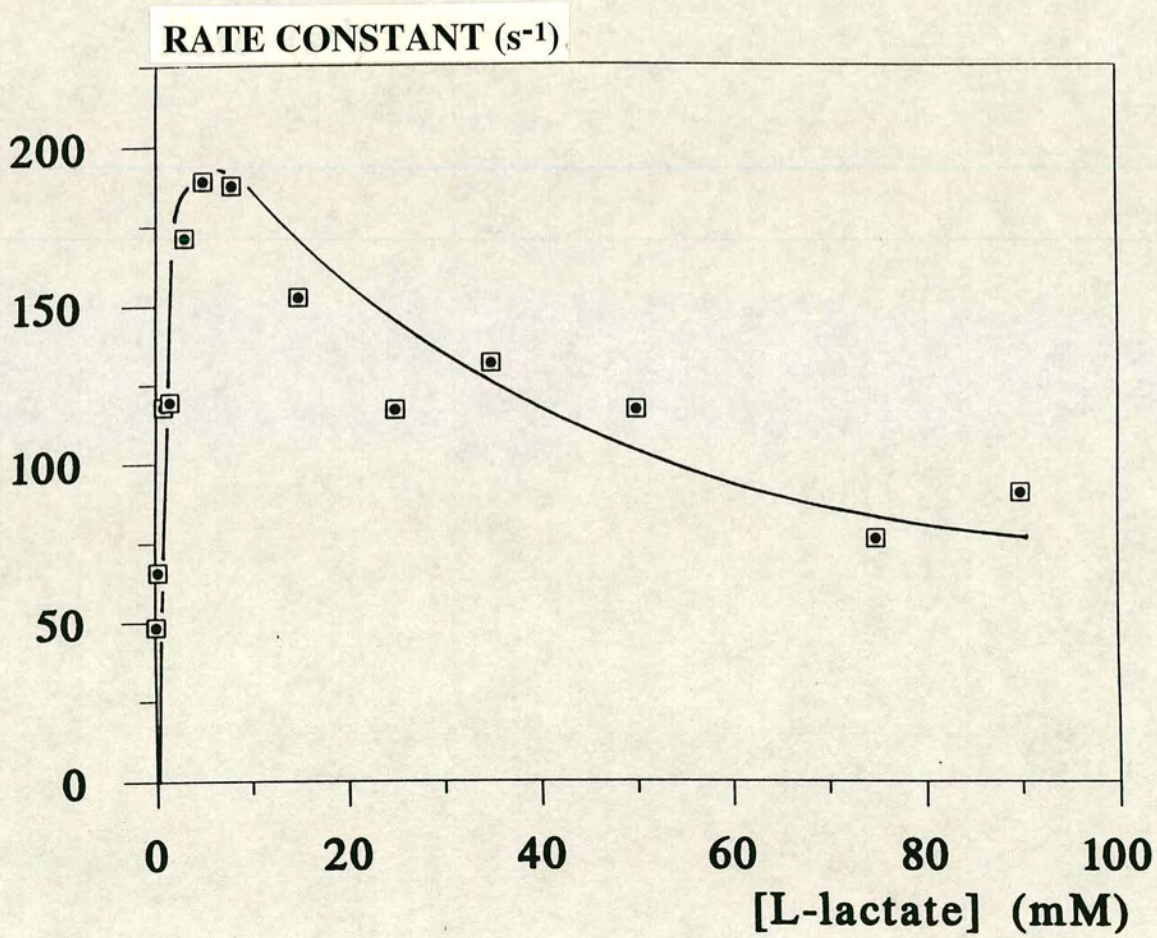

FIGURE 3.5

MICHAELIS-MENTEN PLOTS USED TO CALCULATE KINETIC PARAMETERS FOR THE STEADY-STATE REDUCTION OF FERRICYANIDE BY DOMAIN-SWAP FLAVOCYTOCHROME *b*2 WITH L-[2-^{1}H]-LACTATE

(a) DATA USED TO CALCULATE K_M

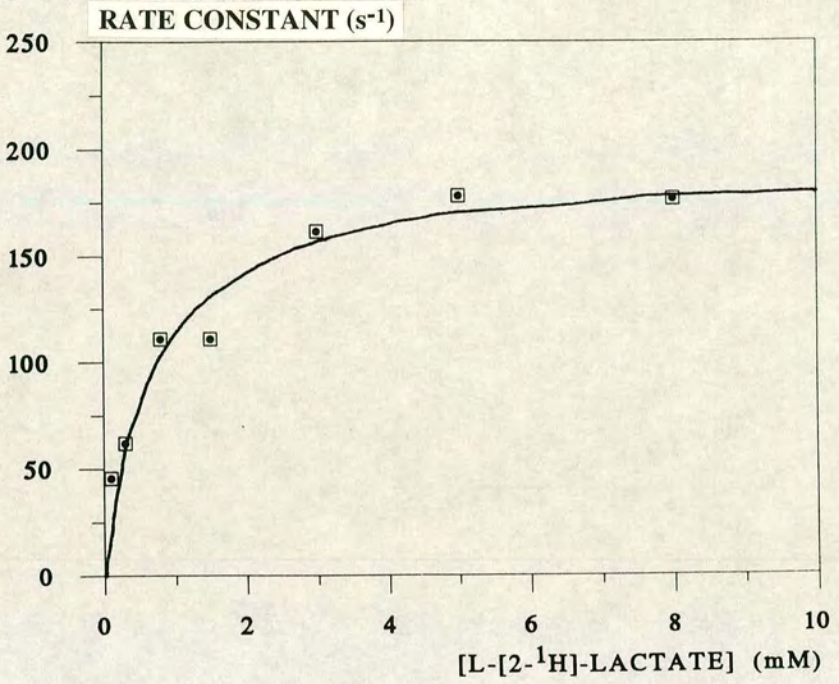

(b) DATA USED TO CALCULATE K_I

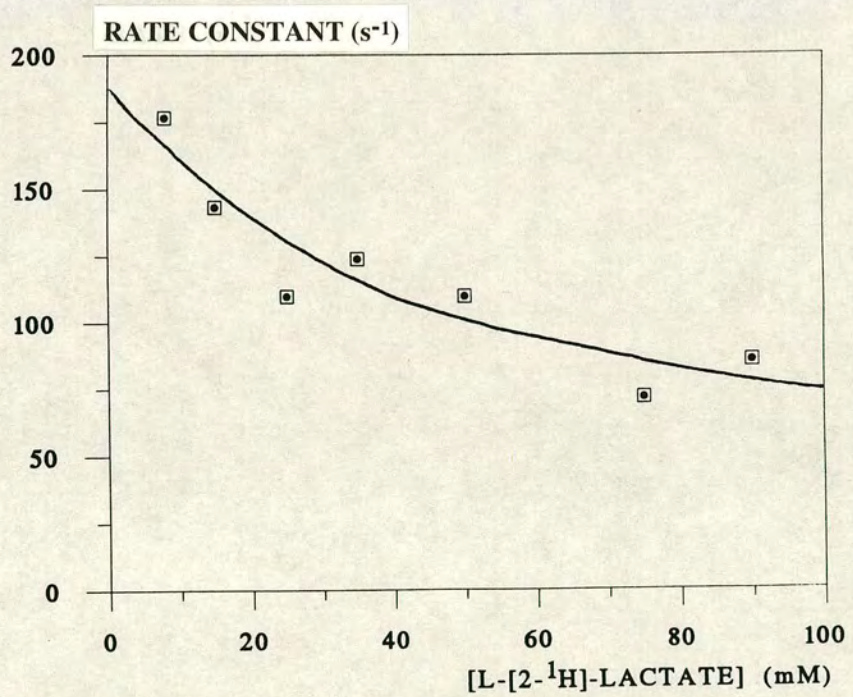

EXPERIMENTAL CONDITIONS AS DESCRIBED IN SECTION 3.2.3

uncompetitive. Uncompetitive inhibition occurs where the inhibitor binds to the enzyme-substrate complex and not to the enzyme. This type of inhibition rarely occurs in single-substrate systems.

In competitive inhibition, the inhibitor resembles the substrate sufficiently well to enable formation of interactions at the active site, but it is not sufficiently alike to take part in the reaction and to be released. Hence inhibitor and substrate compete for the active site of the enzyme and as a result less substrate binds to the enzyme.

Noncompetitive inhibition occurs in the case where inhibitor and substrate occupy different binding sites on the enzyme surface *i.e.* both can bind simultaneously to the enzyme molecule. Such inhibition decreases the turnover number of the enzyme (k_{cat}) whereas competitive inhibition diminishes the number of enzyme molecules that have bound substrate (K_M). Cases in which both k_{cat} and K_M are both altered are termed mixed inhibition. Catalysis by *S.cerevisiae* wild-type-*b*$_2$ is inhibited at excess concentrations of L-lactate (22). This substrate inhibition is weaker (K_I = 174$\pm$8mM) than that observed for the domain-swap enzyme (K_I = 55$\pm$11mM). The inhibition caused in the latter enzyme may be due to either presence of a second, lower affinity binding site or to complexation of excess substrate with the flavin semiquinone (23). These two options will be discussed later in the combined results section (3.3.3).

The domain-swap enzyme is still an efficient L-lactate dehydrogenase. This is evident from the results with ferricyanide as acceptor which are given in Table 3.1. The value of k_{cat} for *S.cerevisiae* wild-type-*b*2 is only twice that of the value for the domain-swap enzyme ($400s^{-1}$ as opposed to $190s^{-1}$).

Steady-state analysis using cytochrome *c* as the electron acceptor is very revealing (see Table 3.2 and Figure 3.6). The domain-swap enzyme is a very poor cytochrome *c* reductase; there is a large decrease in the value of k_{cat} for cytochrome *c* reduction, from $207s^{-1}$ for wild-type to only $0.41s^{-1}$ for the domain-swap enzyme (a 500-fold decrease). The domain-swap enzyme's poor ability as a cytochrome *c* reductase suggests that, like the hinge-swap enzyme, steps occurring after substrate binding, such as flavin to haem electron transfer, are affected.

Comparison of k_{cat} values for both external electron acceptors for the wild-type enzyme from *S.cerevisiae* gives a good indication that there are different electron pathways through the enzyme to the acceptor (24, 3). Electrons are transferred to cytochrome *c* only from the cytochrome *b*2 haem (25) whereas ferricyanide can accept electrons from both flavin and haem. Thus when the rate of flavin to haem electron transfer is decreased the ratio of k_{cat}(cyt.*c*)/k_{cat}(ferri.) is also decreased since electron transfer from flavin to ferricyanide contributes more to the overall rate. The suggestion that the rate of flavin to haem electron transfer is slower in the domain-

TABLE 3.2

COMPARISON OF THE RESULTS FROM THE STEADY-STATE KINETIC ANALYSES FOR *S.cerevisiae* WILD-TYPE, HINGE-SWAP AND DOMAIN-SWAP FLAVOCYTOCHROMES *b*$_2$ WITH CYTOCHROME c AS ELECTRON ACCEPTOR

	k_{cat} (s^{-1})	K_M (mM)	k_{cat}/K_M ($M^{-1}s^{-1}$)	$\frac{k_{cat}(c)}{k_{cat}(f)}$
WILD-TYPE*	207±10	0.24±0.04	8.6×10^5	0.52
HINGE-SWAP§	1.62±0.41	0.002±0.001	8.1×10^5	0.013
DOMAIN-SWAP#	0.41±0.03	0.043±0.012	9.5×10^3	0.002

Abbreviations used : c = cytochrome *c*; f = ferricyanide

Experimental conditions : All experiments were carried out at 25±0.1°C in tris-HCl buffer, pH 7.5, I=0.1M. The concentrations of ferricyanide used were 1mM for wild-type and domain-swap (>90% saturating) and 8mM for hinge-swap (87% saturating). The cytochrome *c* concentrations were 50 μM for wild-type (~90% saturating), 15 μM for hinge-swap (>95% saturating) and 16 μM (>95% saturating) for domain-swap.

k_{cat} is expressed in terms of electrons transferred per second per mole of enzyme.

References : *Reference (17);§This work (Chapter 2);#This work.

FIGURE 3.6

MICHAELIS-MENTEN PLOT FOR THE STEADY-STATE REDUCTION OF CYTOCHROME *c* BY DOMAIN-SWAP FLAVOCYTOCHROME *b*$_2$ WITH L-[2-^{1}H]-LACTATE

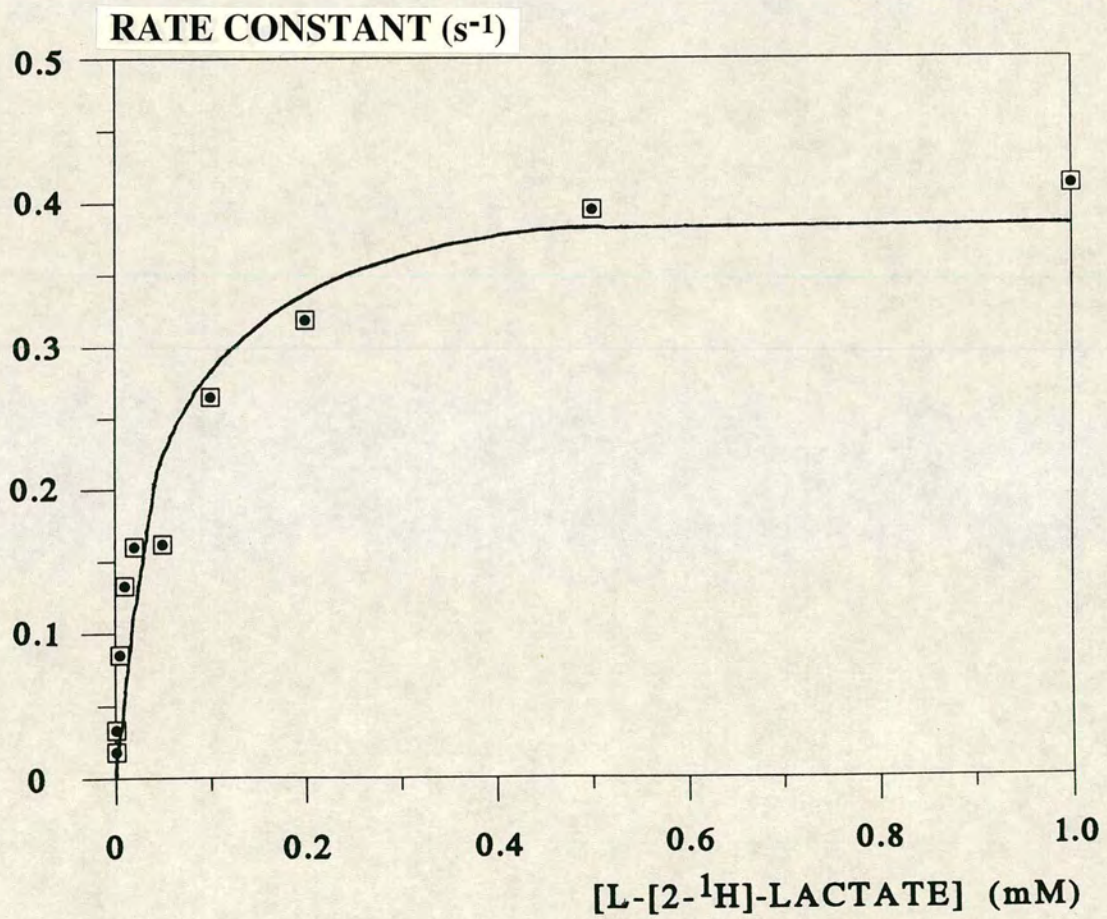

EXPERIMENTAL CONDITIONS AS DESCRIBED IN SECTION 3.2.3

swap enzyme is supported by comparison of the ratios k_{cat}(cyt.*c*)/k_{cat}(ferri.) which range from 0.52 for the *S.cerevisiae* wild-type enzyme to 0.013 for hinge-swap to 0.002 for the domain-swap enzyme, inferring that flavin to haem electron transfer is even more affected in the domain-swap than in the hinge-swap enzyme. Concentrating once more on ferricyanide as the acceptor and looking in particular at the value of the Michaelis constant, K_M for L-lactate, we see that this value is, within experimental error, the same as that for the *S.cerevisiae* wild-type enzyme. As stated in the previous chapter, the K_M is not an indication of a K_d for L-lactate since it is a composite value of a number of catalytic steps. This is supported by the fact that the catalytic efficiencies of the domain-swap and wild-type enzymes (expressed by k_{cat}/K_M and shown in Table 3.1) are identical *i.e.* the fall-off in k_{cat} is mirrored by a fall-off in K_M.

With cytochrome *c* as acceptor a low K_M is observed (0.043mM for domain-swap as opposed to 0.24mM for wild-type) but again this similarity cannot be assigned as a true K_d for L-lactate.

3.3.2 STOPPED-FLOW KINETIC ANALYSIS

Stopped-flow kinetics were performed on the domain-swap enzyme in order to monitor reduction of the individual prosthetic groups using both L-[2-^{1}H]- and L-[2-^{2}H]-

lactate. The results are summarised in Table 3.3 where they are compared to results previously obtained for *S.cerevisiae* wild-type (17) and hinge-swap flavocytochromes b_2 (Chapter 2). Sample traces for each reduction are shown in Figure 3.7 and the corresponding Michaelis-Menten plots are illustrated in Figures 3.8 and 3.9.

Flavin reduction in the domain-swap enzyme was found to be monophasic at all L-lactate concentrations and haem reduction biphasic, as opposed to both flavin and haem reductions being biphasic in the wild-type enzyme from *S.cerevisiae*. This was in accordance with the results for the hinge-swap enzyme and, as discussed in Section 2.3.2, precludes interprotomer electron transfer in domain-swap-b_2 since the second phase, which would normally be due to entry of the final electron into the monomer by means of interflavin electron transfer, is no longer present. This infers that an essential step subsequent to substrate binding is much slower than interprotomer electron transfer; this step can only be flavin to haem electron transfer.

Closer examination of the stopped-flow kinetic data confirms this theory. Flavin reduction is barely affected by the mutation, being only one-fifth slower than *S.cerevisiae* wild-type ($490s^{-1}$ for the domain-swap as opposed to $604s^{-1}$ for the wild-type enzyme). The domain-swap enzyme remains a very effective L-lactate dehydrogenase, as is reflected in the efficiencies, as

TABLE 3.3

COMPARISON OF THE RESULTS FROM STOPPED-FLOW KINETIC ANALYSES OF *S.cerevisiae* WILD-TYPE, HINGE-SWAP AND DOMAIN-SWAP FLAVOCYTOCHROMES *b2*

(a) FLAVIN REDUCTION

	L-[2-^{1}H]-lactate			L-[2-^{1}H]-lactate			
	k_{cat} (s^{-1})	K_M (mM)	k_{cat}/K_M ($M^{-1}s^{-1}$)	k_{cat} (s^{-1})	K_M (mM)	k_{cat}/K_M ($M^{-1}s^{-1}$)	K.I.E.
S.c. WILD-TYPE[a]	604±60	0.84±0.20	7.2×10^5	75±5	1.33±0.28	6.0×10^4	8.1±1.4
HINGE-SWAP[b]	240±12	0.37±0.02	6.5×10^5	38±2	0.56±0.01	6.5×10^4	6.3±0.7
DOMAIN-SWAP[c]	490±20	1.82±0.26	2.7×10^5	185±5	4.81±0.25	3.8×10^4	2.6±0.1

(b) HAEM REDUCTION

	L-[2-^{1}H]-lactate			L-[2-^{2}H]-lactate			
	k_{cat} (s^{-1})	K_M (mM)	k_{cat}/K_M ($M^{-1}s^{-1}$)	k_{cat} (s^{-1})	K_M (mM)	k_{cat}/K_M ($M^{-1}s^{-1}$)	K.I.E.
S.c. WILD-TYPE[a]	445±50	0.53±0.05	8.4×10^5	71±5	0.68±0.05	1.0×10^5	6.3±1.2
HINGE-SWAP[b]	1.61±0.42	0.003±0.001	5.4×10^5	1.00±0.11	0.003±0.001	3.3×10^5	1.6±0.7
DOMAIN-SWAP[c]	0.99±0.05	0.022±0.007	4.5×10^4	0.64±0.01	0.08±0.02	0.8×10^4	1.6±0.1

Abbreviations : *S.c.* = *S.cerevisiae*; K.I.E. = KINETIC ISOTOPE EFFECT.

References : [a] Reference 17; [b] Chapter 2; [c] This work.

Experimental Conditions : All experiments were carried out at 25±0.1°C in tris-HCl buffer, pH 7.5, I=0.1M. k_{cat} values are expressed as number of prosthetic groups reduced per second.

FIGURE 3.7

STOPPED-FLOW KINETIC TRACES FOR THE REDUCTION OF THE PROSTHETIC GROUPS OF DOMAIN-SWAP FLAVOCYTOCHROME *b*2

(a) MONOPHASIC FLAVIN REDUCTION (438.3nm)

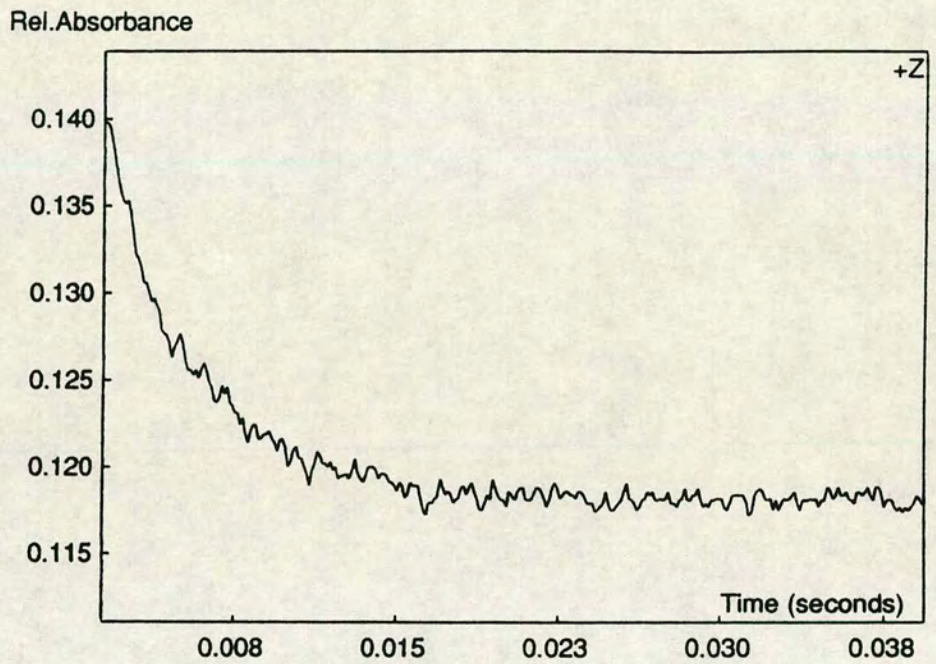

(b) BIPHASIC HAEM REDUCTION (423nm)

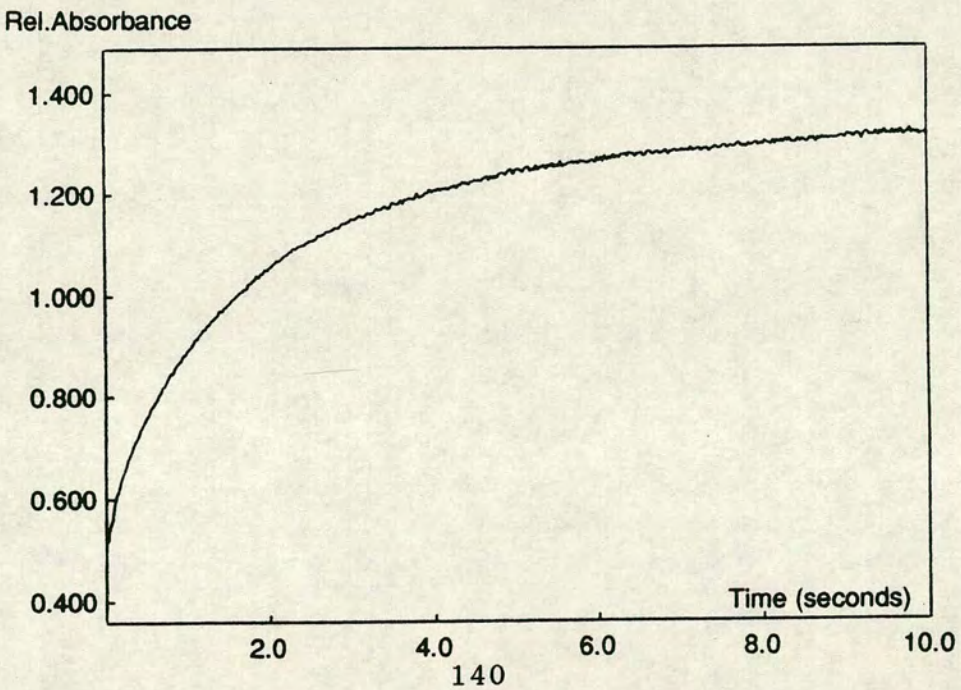

FIGURE 3.8

MICHAELIS-MENTEN PLOT FOR FLAVIN REDUCTION OF DOMAIN-SWAP FLAVOCYTOCHROME *b*$_2$ BY L-[2-^{1}H]-LACTATE UNDER STOPPED-FLOW CONDITIONS

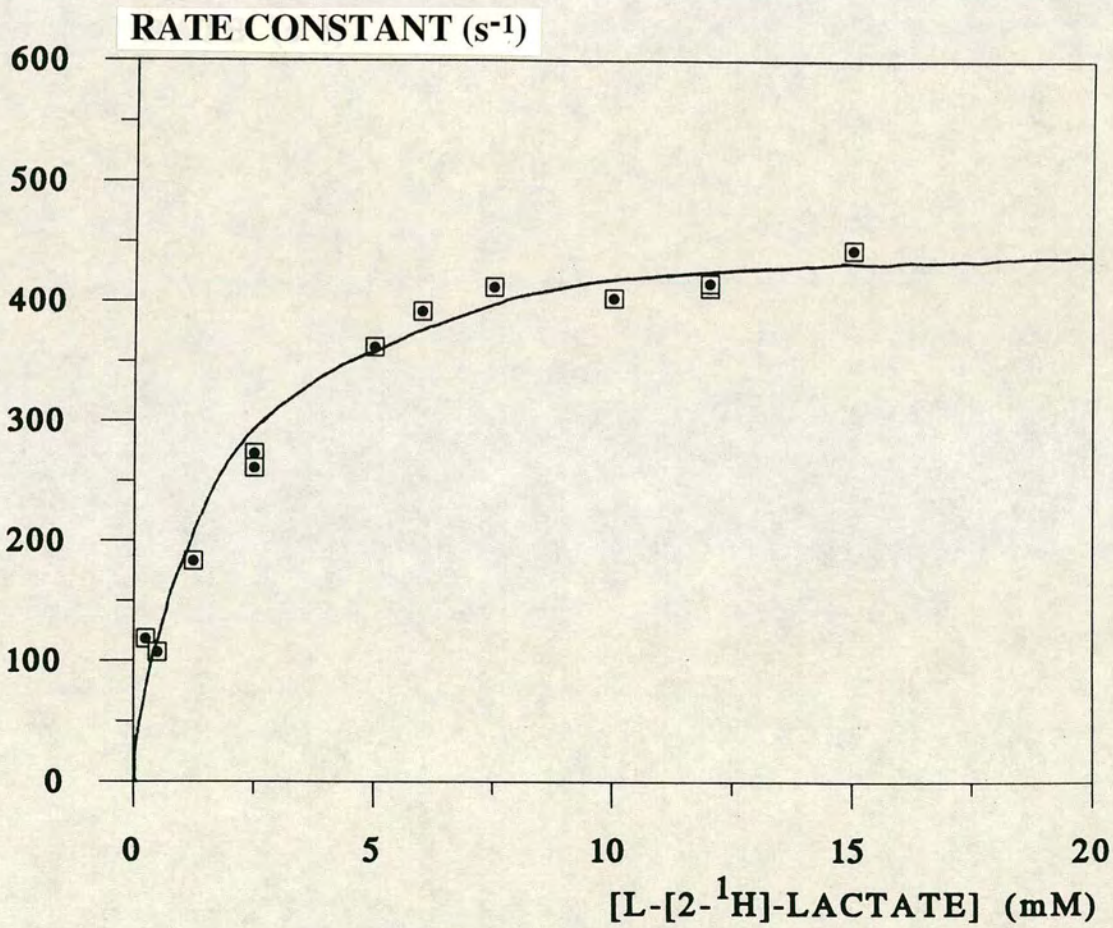

EXPERIMENTAL CONDITIONS AS DESCRIBED IN SECTION 3.2.3

FIGURE 3.9

MICHAELIS-MENTEN PLOT FOR HAEM REDUCTION OF DOMAIN-SWAP FLAVOCYTOCHROME *b*2 WITH L-[2-^{1}H]-LACTATE UNDER STOPPED-FLOW CONDITIONS

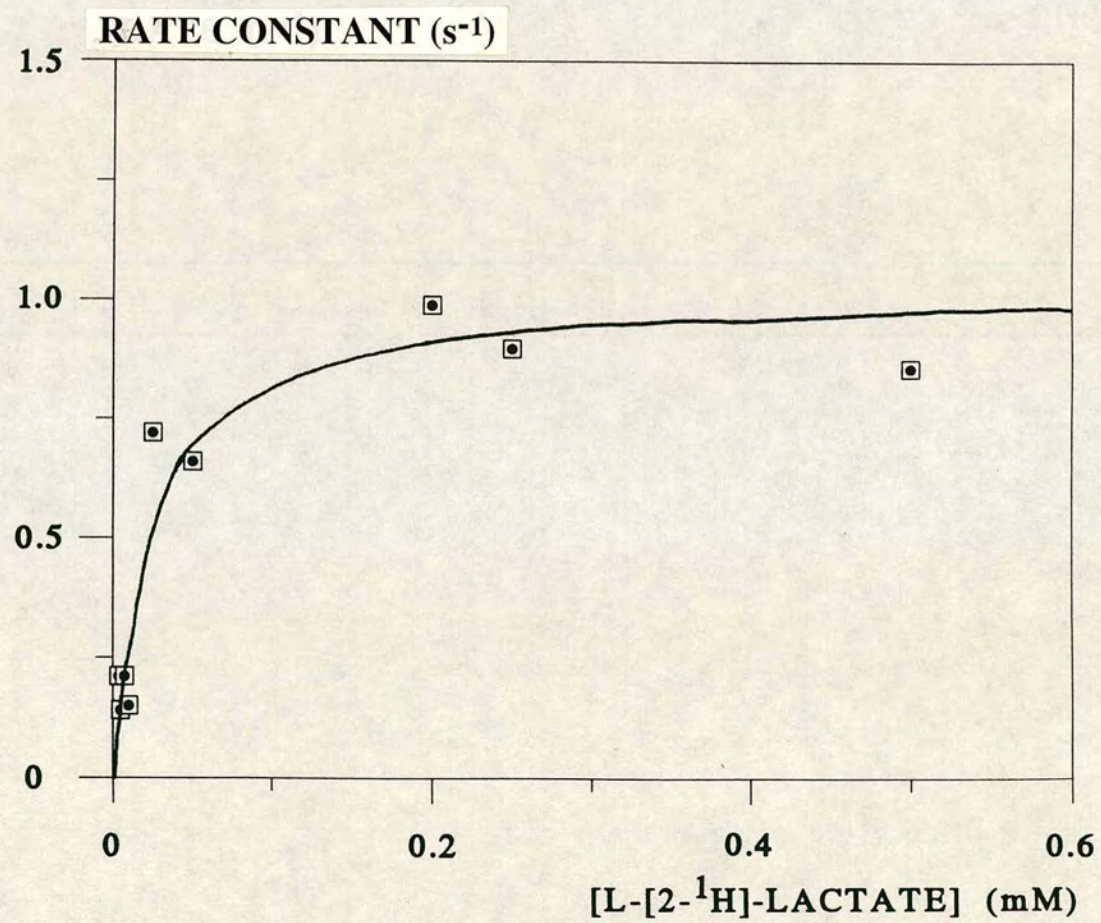

EXPERIMENTAL CONDITIONS AS DESCRIBED IN SECTION 3.2.3

expressed by k_{cat}/K_M, which are almost identical to those for the wild-type enzyme from *S.cerevisiae*.

That flavin to haem electron transfer has been considerably slowed down is proven by the dramatic decline in the rate constants observed for haem reduction; there has been a 450-fold decrease from $445s^{-1}$ for *S.cerevisiae* wild-type to only $0.99s^{-1}$ for the domain-swap enzyme. The domain-swap enzyme, like the hinge-swap enzyme, is a very poor cytochrome *c* reductase, the mutation having little effect on the rate of electron transfer from L-lactate-to-flavin but a severe effect on the subsequent steps which necessitate domain-domain electron transfer. This is further supported by the values of the kinetic isotope effects (KIEs) for each step which are discussed in Section 3.3.3.

Turning to the K_M, the Michaelis constant, we do see a slight difference in the values obtained for flavin reduction for the domain-swap compared to *S.cerevisiae* wild-type. As mentioned in Chapter 2, K_M values are not the ideal way to obtain an estimate of substrate binding as they are of a composite nature. In this case the fall-off in K_M is directly reflected by decrease in k_{cat} as evidenced from the fact that the catalytic efficiencies of flavin reduction (as expressed by k_{cat}/K_M) for both domain-swap and wild-type enzymes are the same within experimental error. This proves that the observed differences in K_M values do not give any conclusive indication of strength and mode of L-lactate binding.

Characterisation of domain-swap-*b*2 has focussed on a comparison with the wild-type enzyme from *S.cerevisiae*. Ideally results should also be compared to those for the enzyme from *H.anomala*, particularly at the level of flavin reduction. This has proved difficult since although *H.anomala* has undergone total kinetic characterisation, this was performed at 5°C (26) as opposed to our 25°C, and is not directly comparable with our results. Consequently, some preliminary stopped-flow experiments were performed in this study for flavin reduction of the domain-swap enzyme at 5°C and 25°C in order to attempt to make some comparisions with wild-type *H.anomala*-*b*2. One might expect results for flavin reduction to be the same for both enzymes as they both contain the same flavodehydrogenase domain. The results showed a linear dependence on rate with temperature (as previously reported for *H.anomala* wild-type (8)) and identical KIE values were obtained at both temperatures (2.6 ± 0.1 as shown in Table 3.3a). The rates obtained at 5°C with L-[2-^{1}H]-lactate were however approximately four-fold lower than those obtained for the wild-type enzyme from *H.anomala* ($97 s^{-1}$ compared to $393 s^{-1}$ (25)).

3.3.3 DISCUSSION OF THE COMBINED KINETIC RESULTS

Figure 3.10 is a linear representation of the catalytic cycle of flavocytochrome *b*2 which shows rate constants for the various steps for both *S.cerevisiae* wild-type

FIGURE 3.10

LINEAR REPRESENTATION OF THE CATALYTIC CYCLE OF FLAVOCYTOCHROME *b*2

COMPARING THE RATE CONSTANTS FOR WILD-TYPE AND DOMAIN-SWAP ENZYMES

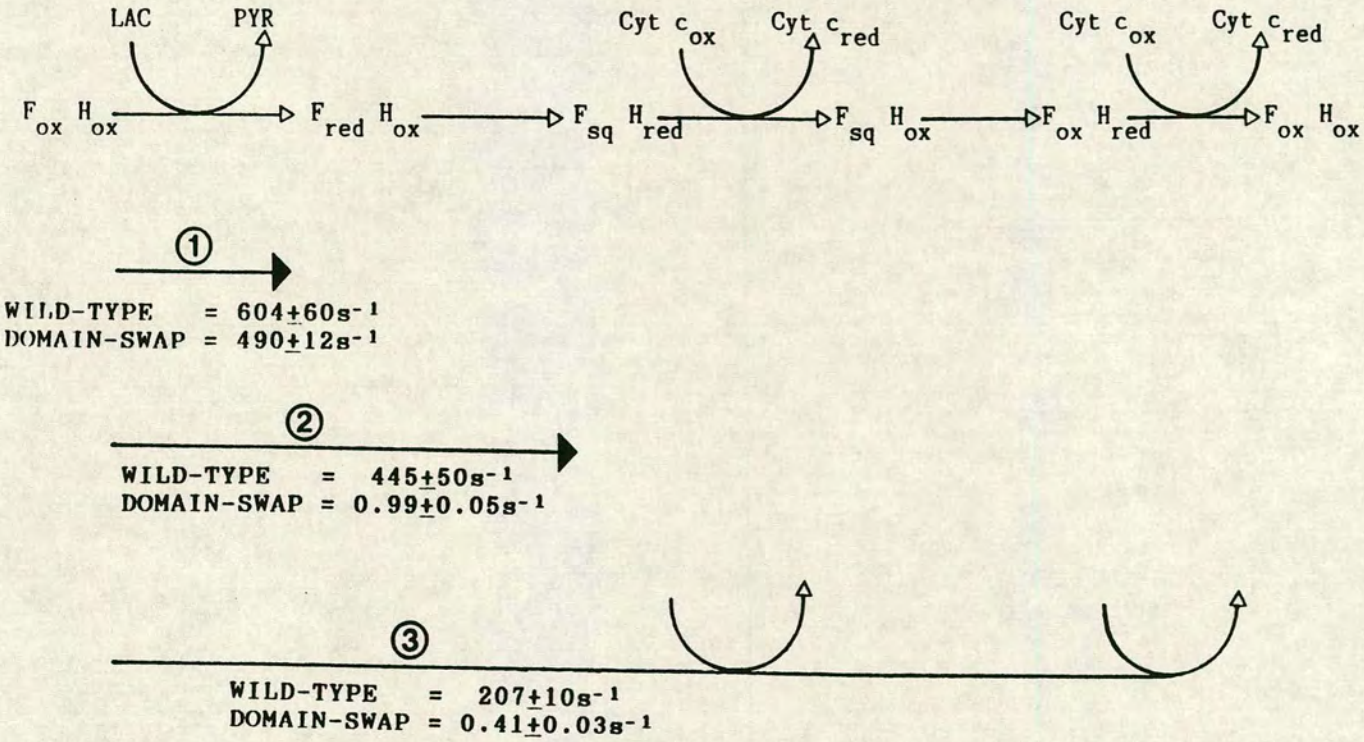

ABBREVIATIONS : LAC, LACTATE; PYR, PYRUVATE; F, FLAVIN; H, HAEM; Cyt c, CYTOCHROME *c*; ox, OXIDISED; red, REDUCED; sq, SEMIQUINONE.

(17) and the domain-swap enzymes. The corresponding values of the kinetic isotope effects (KIEs) for each step are similarly represented in Figure 3.11.

Considering firstly the rate constants, the *S.cerevisiae* wild-type enzyme has an initial rate constant for flavin reduction of $604s^{-1}$, this gradually declines over the catalytic cycle eventually reaching a third of its original value ($207s^{-1}$ for cytochrome *c* reduction). This decrease is also seen in the values of the KIEs which fall from 8.1 for flavin reduction to 6.3 for haem reduction to 3.0 for cytochrome *c* reduction. The KIEs are determined by comparison of the rates obtained when using normal L-lactate to those using L-lactate which has been deuterated at the C-2 position. Hence the values obtained for wild-type enzyme from *S.cerevisiae* indicate that flavin reduction *i.e.* abstraction of the C-2 hydrogen as a proton by the active site base, His-373, is rate-limiting and is indeed rate-limiting over the entire catalytic cycle since the KIE values erode gradually, still being at a significant value for cytochrome *c* reduction.

The domain-swap enzyme behaves differently. It still has a fairly high rate constant for flavin reduction, similar to that for *S.cerevisiae* wild-type, but this undergoes a massive 500-fold drop to a value of only $0.99s^{-1}$ for haem reduction inferring that flavin to haem electron transfer has been greatly disrupted. This is supported by the KIE values. The value for flavin reduction is 2.6 which is

FIGURE 3.11

COMPARISON OF THE DEUTERIUM KINETIC ISOTOPE EFFECTS FOR *S.cerevisiae* WILD-TYPE AND DOMAIN-SWAP FLAVOCYTOCHROMES *b*2

S.c. WT-*b*2	8.1±1.4	6.3±1.2	3.0±0.6
L-LACTATE---------->FLAVIN---------->HEME---------->CYTOCHROME *c*			
DOMAIN-SWAP-*b*2	2.6±0.7	1.6±0.1	1.5±0.2

lower than for *S.cerevisiae* wild-type but still indicates that this step is partly rate-limiting over this timescale. However, the KIE drops to below two for haem reduction and remains at this level for the rest of the cycle, inferring that abstraction of the C-2 hydrogen as a proton by His-373 has little or no rate-limiting contribution to catalytic steps occurring after flavin reduction *i.e.* there has been an alteration in the overall rate-limiting step towards flavin to haem electron transfer.

This change in rate-limitation is a result of the enzyme having domains from different species of yeast; the flavodehydrogenase domain from *H.anomala* and the hinge region and haem domain from *S.cerevisiae*. In the case of the hinge-swap enzyme, in which the hinge of the *S.cerevisiae* enzyme was replaced with the shorter, more acidic hinge from the *H.anomala* enzyme, it was postulated that the presence of this shorter hinge in some way restricts the mobility of the domains with respect to one another in such a way as to severely impair domain/domain communication. In the domain-swap enzyme we have again disrupted flavin to haem electron transfer but this enzyme contains the longer, presumably more flexible, hinge region from *S.cerevisiae* , so, assuming that the domains remain in the same relative positions as in *S.cerevisiae* wild-type, the drastic effect upon flavin to haem electron transfer must arise as a result of lack of structural integrity: the *H.anomala* flavin domain cannot

physically recognise the *S.cerevisiae* haem domain enough to promote efficient electron transfer between the two. The decreased rate of electron flow from flavin to haem observed for the domain-swap enzyme enables us to draw an analogy with hinge-swap-b_2. In both of these hybrid enzymes the flavin group cannot efficiently recognise the haem group to the extent that the enzymes can effectively be regarded as behaving as de-haemo-b_2. In the absence of haem, Iwatsubo *et al.* (27) suggested that ferricyanide could accept an electron from both flavin hydroquinone and flavin semiquinone (electron transfer from the latter being 20-fold faster). This is indeed the case for the hinge-swap enzyme and this enzyme's rate of turnover is limited by the step in which flavin hydroquinone is oxidised to flavin semiquinone by the ferricyanide (Figure 2.13). This step is hence dependent upon the concentration of ferricyanide. The rate constant for the domain-swap enzyme with ferricyanide as the acceptor is twice as slow as *S.cerevisiae* wild-type ($190s^{-1}$ as opposed to $400s^{-1}$ respectively), this suggests that in the domain-swap enzyme the ferricyanide must be bypassing the haem and must be accepting electrons from both the flavin hydroquinone and the flavin semiquinone as is the case for hinge-swap-b_2. However, the domain-swap enzyme does not show any dependence upon the concentration of ferricyanide, but instead shows strong substrate inhibition at high L-lactate concentrations with this electron acceptor. Thus the reaction scheme proposed for

the hinge-swap enzyme must in some way be altered. Supposing excess substrate bound to the flavin semiquinone, this eventuality would require dissociation of pyruvate from the active site and a subsequent molecule of lactate to bind before the flavin semiquinone would donate its electron to ferricyanide (22). In this case we have effectively limited ferricyanide reduction to acceptance of electrons from only the flavin hydroquinone thus there can be no ferricyanide dependence since this is reliant upon ferricyanide being able to accept electrons from both the hydro- and semiquinone in the absence of haem. Thus the substrate inhibition observed for the domain-swap enzyme with ferricyanide as electron acceptor must be a result of complexation of excess substrate with the flavin semiquinone as was postulated in Section 3.3.1. This theory is supported by the fact that substrate inhibition is not observed when using cytochrome *c* as external electron acceptor.

3.4 CONCLUSIONS

The importance of structural integrity within an enzyme system has been investigated by construction of a hybrid enzyme of flavocytochrome b_2 which constitutes an interspecies domain-swap. Full kinetic characterisation of this enzyme and comparision with both the holoenzymes and hinge-swap-b_2 has enabled the following conclusions to be drawn:-

(1) the domain-swap has little effect on the enzyme's capacity to be a L-lactate dehydrogenase but greatly lowers its effectiveness as a cytochrome *c* reductase;

(2) the rate of electron flow from flavin to haem has been dramatically decreased in the domain-swap enzyme to the extent that this step becomes rate-limiting as opposed to C-2 proton abstraction in the wild-type enzyme from *S.cerevisiae*;

(3) structural integrity is of crucial importance in allowing efficient domain/domain communication *i.e.* recognition and subsequent electron transfer.

3.5 REFERENCES

(1) Appleby,C.A. & Morton,R.K.,*Nature (London)*, 173, 749 (1954).

(2) Xia, Z.-x. & Mathews, F.S., *J.Mol.Biol.*, 212, 837 (1990).

(3) Lederer, F., in *"Chemistry and Biochemistry of Flavoenzymes"*, II, 153, Franz Miller(ed.),CRC Press Inc.,Boca Raton (1991).

(4) Guiard, B., Groudinsky, O. & Lederer, F., *Proc.Natl.Acad.Sci. U.S.A.*, 71, 2539 (1974).

(5) Volokita,M, & Somerville,C.R.,*J.Biol.Chem.*,282,15825 (1988).

(6) Cederlund, E., Lindquist, Y., Söderlund, G., Brändén, C.-I. & Jörnvall, H., *Eur.J.Biochem.*, 173, 523 (1988).

(7) Tegoni,M., Silvestrini, M.C., Labeyrie,F. & Brunori, M., *Eur.J.Biochem.*, 140, 39 (1984).

(8) Capeillère-Blandin,C., Barber,M.J. & Bray, M.C., *Biochem.J.*, 238, 745 (1986).

(9) Labeyrie,F., Baudras, A. & Lederer, F., in *"Methods in Enzymology"*, 53, 238, Fleischer,S. & Packer,L. (eds.), Academic Press, NY (1978).

(10) Black, M.T., Gunn, F.J., Chapman, S.K. & Reid, G.A., *Biochem.J.*, 263, 973 (1989).

(11) Lederer, F., Cortial, S., Becam, A.-M., Haumont, P.-Y. & Perez,L., *Eur.J.Biochem.*, 152, 419 (1985).

(12) Reid, G.A., White, S.A., Black,M.T., Lederer,F., Mathews,F.S. & Chapman,S.K., *Eur.J.Biochem.*, **178**, 329 (1988).

(13) Pompon, D., Iwatsubo, M. & Lederer, F., *Eur.J.Biochem.*, **104**, 479 (1980).

(14) Short, D.M., *Honours Project Report*, University of Edinburgh (1993).

(15) Sambrook, J., Fritsch, E.F. & Maniatis, T., in *"Molecular Cloning: A Laboratory Manual"*, 2nd edition, Cold Spring Harbour Press, Cold Spring Harbour, NY (1989).

(16) Black, M.T., White, S.A., Reid, G.A. & Chapman, S.K., *Biochem.J.*, **258**, 255 (1989).

(17) Miles, C.S., Rouvière-Fourmy, N., Lederer, F., Mathews,F.S., Reid,G.A., Black,M.T. & Chapman,S.K., *Biochem.J.*, **285**, 187 (1992).

(18) Gervais,M., Groudinsky,O., Risler,Y. & Labeyrie,F., *Biochem.Biophys.Res.Commun.*, **77**, 1543 (1977).

(19) Rando, R.R., *Science*, **185**, 320 (1974).

(20) Pompon, D. & Lederer, F., *Eur.J.Biochem.*, **148**, 145 (1985).

(21) Walsh, C.T., *Annu.Rev.Biochem.*, **47**, 881 (1978).

(22) Somlo, M. & Slonimski, P.P., *Bull.Soc.Chim.Biol.*, **48**, 1221 (1966).

(23) Tegoni, M., Janot, J. -M. & Labeyrie, F., *Eur.J.Biochem.*, **190** ,329 (1990).

(24) Chapman, S.K., White, S.A. & Reid, G.A., *Adv.Inorg.Chem.*, **36**, 257 (1991).

(25) Dubois, J., Chapman, S.K., Mathews, F.S., Reid, G.A. & Lederer, F., *Biochemistry*, **29**, 6393 (1990).

(26) Capeillère-Blandin, C., *Biochem.J.*, **274**, 207 (1991).

(27) Iwatsubo, M., Mével-Ninio, M. & Labeyrie, F., *Biochemistry*, **16**, 3558 (1977).

CHAPTER 4

INTERMOLECULAR COMMUNICATION

THE ROLE OF THE C-TERMINAL TAIL IN CYTOCHROME *c* BINDING

4.1 INTRODUCTION

Cytochrome *c* was first suggested to be the physiological electron acceptor for yeast mitochondrial flavocytochrome b_2 by Appleby and Morton (1) and this protein partnership was later shown to be part of a short electron transport chain, also involving cytochrome *c* oxidase, which ultimately enabled the yeast to respire on L-lactate (2). Complex formation has been shown to take place both in solution and in the crystalline form (3) and several workers have shown this complexation to be dependent on the pH and ionic strength of the surrounding media (3-6). Such ionic strength-dependence indicates that electrostatic interactions are of importance in the formation and stability of the complex.

Cytochrome *c* has sequentially and structurally conserved lysine residues which form an uninterrupted ring of positive charge located near the exposed haem edge and it has been postulated that these residues take part in the complementary ionic interaction between cytochrome *c* and its respective oxidoreductases (7). Studies of electron transfer rates between flavocytochrome b_2 and chemically-modified cytochromes *c* have demonstrated that these lysine residues are important in the association of the two proteins (8). However, no complementary region on flavocytochrome b_2 has yet been identified. Considering the interaction of cytochrome *c* with cytochrome b_5 (which is structurally homologous to the cytochrome b_2 core),

these two proteins associate face to face via the exposed haem edges; the result being that the two haem groups are constrained in an almost co-planar arrangement at a closest edge-to-edge approach of 8.4Å (7) (Figure 4.1). A similar interaction may at first seem favourable for association of cytochrome *c* with flavocytochrome b_2 since the former can only accept electrons from the cytochrome b_2-binding domain of the enzyme (9). This, however, is impossible, since unlike cytochrome b_5, the haem edge of cytochrome b_2 is not exposed to solvent because it is sterically blocked by the flavodehydrogenase domain. For such an association to occur, one would require a large amount of reorganisation energy in order to permit movement of the cytochrome domain with respect to the flavodehydrogenase domain.

Cytochrome *c* must obviously bind to the enzyme somewhere and we can begin to search for these areas by identifying complementary association regions *i.e.* surface regions with dense negative charge localisation. Such a region is located at the end of the C-terminal tail (two glutamates and an aspartate) which is highlighted in Figure 4.2. Previous studies (10) carried out on a mutant of flavocytochrome b_2, in which the 23 residues constituting the C-terminal tail were deleted (hereafter referred to as TD-b_2), have shown that deletion of the tail region has a significant effect upon the enzyme's affinity for cytochrome *c*.

Thus the tail may have a crucial role in complexation of

FIGURE 4.1

MODEL OF THE INTERACTIONS BETWEEN CYTOCHROME b_5 AND CYTOCHROME *c* BASED ON SALEMME'S MODEL (7)

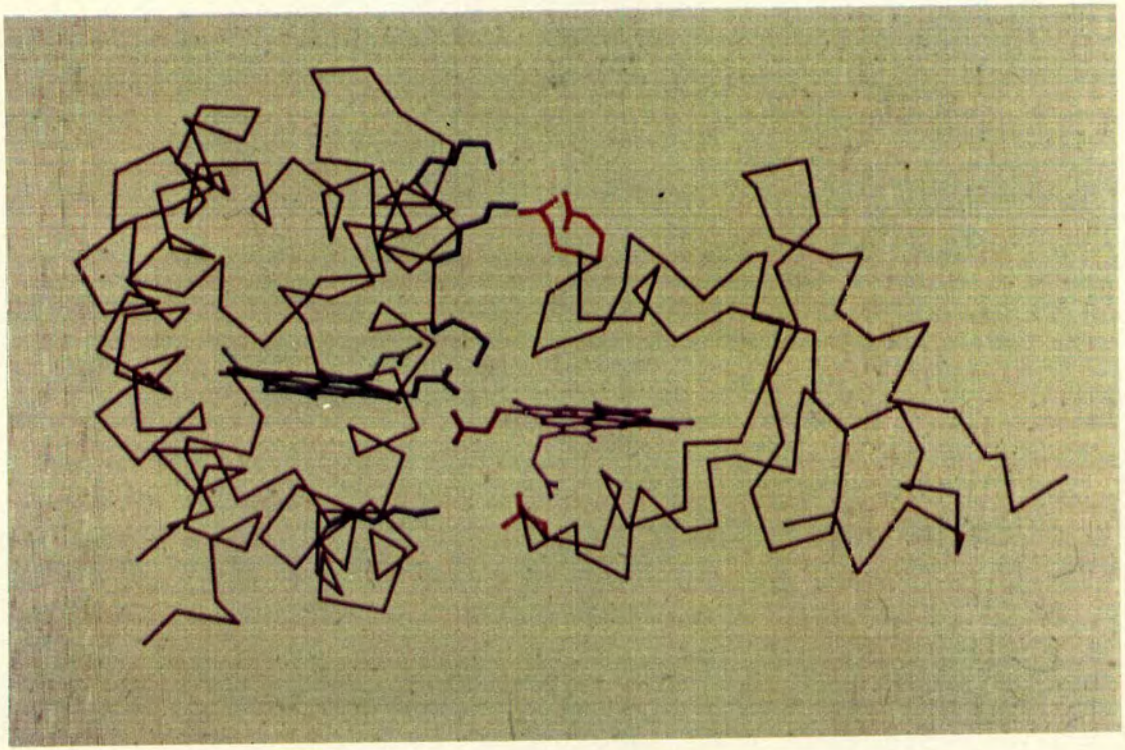

The model shows negatively-charged residues on cytochrome b_5 (red) interacting with positively-charged residues on cytochrome *c* (blue).

FIGURE 4.2

THE AMINO-ACID SEQUENCE OF THE C-TERMINAL TAIL OF FLAVOCYTOCHROME *b*$_2$ ILLUSTRATING THE MUTATIONS MADE IN THIS REGION

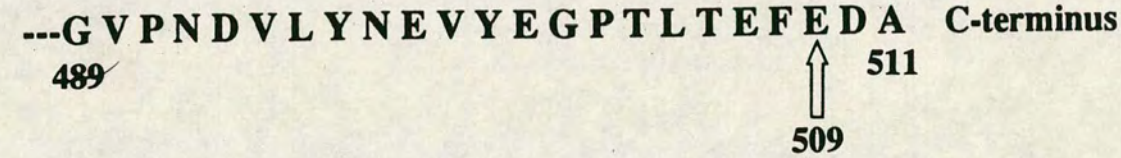

Mutations made in this region
(the amino-acids are represented as side-chain R in $RCH(\overset{+}{N}H_3)C\bar{O}_2$)

Tail-deleted-b_2	**complete 23 residue deletion**
E509*	**residues 509-511 deleted**
E509K	**Glutamic acid --------> Lysine**

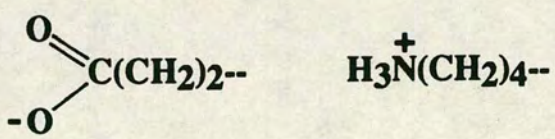

E509Q	**Glutamic acid --------> Glutamine**

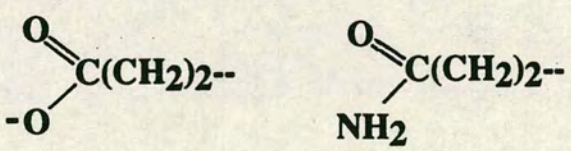

and subsequent electron transfer to cytochrome *c*, possibly forming part of a complementary surface. To investigate this further other mutant enzymes have been generated by site-directed mutagenesis which focus on the three residues at the end of the C-terminal tail. These comprise a deletion (E509*) in which these last three residues have been deleted, and two charge-change point mutations: E509Q - glutamic acid to glutamine (a negative to neutral charge change) and E509K - glutamic acid to lysine (a negative to positive charge change). These mutations are illustrated in Figure 4.2. This chapter is concerned with the characterisation of these tail-mutated enzymes which should enable us to elucidate whether or not the end of the C-terminal tail is involved in the interaction between cytochrome *c* and flavocytochrome *b*$_2$ and to what extent these residues contribute to electrostatic interactions, if at all.

4.2 EXPERIMENTAL

4.2.1 CONSTRUCTION OF TAIL-MUTATED FLAVOCYTOCHROMES *b*$_2$ (DRS. M.T.BLACK AND F.D.C.MANSON)

The genes encoding TD-*b*$_2$ (Dr.M.T.Black), E509*, E509Q and E509K (Dr.F.D.C.Manson) were generated by the double primer method of Zoller and Smith (11) as described in (12). Standard methods of DNA manipulation were used as described in Sambrook *et al.* (13). The following oligonucleotides, synthesised on an Applied Biophysics

model 380B DNA synthesiser (Oswel DNA service, University of Edinburgh), were used for mutagenesis:- (GAACAGTTTGAGTACCA) for TD-*b*2, and TAACAGAATTT(T,C or A)AGGATGCAT for E509*, E509Q and E509K respectively; the first two (TD-*b*2 and E509*) involving introduction of stop codons in place of Gly-489 and Glu-509 respectively. Wild-type and tail-mutated flavocytochromes *b*2 were over-expressed in *E.coli* as described in (12).

4.2.2 ENZYME PREPARATION AND PURIFICATION

Wild-type (14) and tail-mutated flavocytochromes *b*2 were isolated from *E.coli* and were purified on hydroxylapatite columns as described in Section 7.4. All protein preparations were performed in 0.1M phosphate buffer (pH 7.0 5mM L-lactate, 1mM EDTA) which has an ionic strength of 0.22M, but phosphate buffer of differing ionic strength (25mM phosphate, I=0.06M) was used with the deletion mutants in order to obtain protein binding to the column and hence efficient purification. Protein was stored as a 70% ammonium sulphate pellet under nitrogen at 0-4°C for up to a month for WT, E509Q and E509K but long-term storage of the deletion mutants was avoided because of protein instability due to FMN loss.

4.2.3 KINETIC ANALYSIS

All experiments were carried out at 25±0.1°C in tris-HCl buffer at pH 7.5. The buffer concentration was 0.01M in

HCl with the ionic strength adjusted to 0.10M by addition of NaCl.

Steady-state kinetic measurements involving the enzymatic oxidation of L-lactate were performed using either Beckmann DU-62 or Pye-Unicam SP8-400 UV/visible spectrophotometers. The external electron acceptors used were ferricyanide and cytochrome *c*; reduction of these acceptors by the enzyme was monitored at 420nm and 550nm respectively, in the manner described in Section 7.8.

Pre-steady-state, or stopped-flow, kinetic measurements were carried out as described in Section 7.9 using an Applied Photophysics SF.17MV stopped-flow spectrofluorimeter. Flavin reduction was monitored at 438.3nm (a haem isosbestic point) and haem reduction at either 423nm or 557nm (results at both wavelengths being identical). The SF.17MV software package was used to collect and analyse data on an Archimedes 420/1 computer. Traces for both flavin and haem reductions were fitted to double exponentials, with the exception of traces for flavin reduction at low concentrations of L-lactate which were fitted to single exponentials.

For both steady-state and stopped-flow data, k_{cat} and K_M parameters were determined using non-linear regression analysis.

Kinetic isotope effect values (KIEs) were measured by comparing rate constants obtained when using L-[2-^{1}H]-lactate to those obtained when using L-[2-^{2}H]-lactate, which was synthesised and purified as described in

Section 5.7.7.2.

4.2.4 GEL FILTRATION

In order to determine whether TD-*b*2 was tetrameric or monomeric, gel filtration on a Sephacryl S-300 (Sigma) column (150x2.5cm) was carried out at 0-4°C in 0.1M phosphate buffer (pH 7.0, 5mM L-lactate, I=0.22M). The procedures for column preparation, equilibration and calibration are described in Section 7.3.4. A typical sample loaded onto the column consisted of blue dextran (M_R 2,000kDa), TD-*b*2 (M_R unknown) and ferricyanide (M_R 330Da). Several columns were run in order to elucidate the molecular weight of TD-*b*2 at specific stages in the purification and under various conditions such as differing ionic strength.

4.2.5 IONIC STRENGTH DEPENDENCE

A small scale experiment was carried out on freshly prepared TD-*b*2 to discern the effect of ionic strength on activity. *E.coli* containing over-expressed TD-*b*2, which had been stored at -20°C, were lysed at 0-4°C in phosphate buffer, pH 7.0 of varying ionic strength from I=0.06M to I=0.22M. Steady-state activity measurements were carried out, as described in Section 7.8, at 25$\pm$0.1°C in tris-HCl buffer, pH 7.5 (I=0.1M - see buffer preparation in Section 7.2.2) with ferricyanide as the external electron acceptor.

4.2.6 FMN REINCORPORATION

As previously reported (10), TD-*b*2 loses activity as a result of FMN loss with time. FMN reincorporation was attempted to try to regain enzyme activity. The protocol for this is given in Section 7.6. Activity measurements under the conditions given in Section 2.2.5 were carried out as described in Section 7.8.

4.3 RESULTS AND DISCUSSION

4.3.1 STEADY-STATE KINETIC ANALYSIS

Results obtained from steady-state kinetic measurements using L-[2-^{1}H]- and L-[2-^{2}H]-lactate as substrates with ferricyanide and cytochrome *c* as external electron acceptors are given in Tables 4.1 and 4.2, where they are compared to results previously obtained for the wild-type (14) and tail-deleted flavocytochromes *b*2 (10). All of the enzymes exhibited saturating kinetics with ferricyanide as electron acceptor, but showed some variation with cytochrome *c* as will be discussed later. A typical Michaelis-Menten plot for one of the enzymes with ferricyanide as electron acceptor is shown in Figure 4.3. Comparison of the rate constants obtained for enzymatic L-lactate oxidation using ferricyanide as the external electron acceptor shows that all tail-mutated enzymes are efficient L-lactate dehydrogenases. The rate constant drops to its lowest value, which is only half that of

TABLE 4.1

STEADY-STATE KINETIC PARAMETERS AND DEUTERIUM KINETIC ISOTOPE EFFECT VALUES FOR WILD-TYPE AND TAIL-MUTATED FLAVOCYTOCHROMES *b*2 WITH FERRICYANIDE AS ELECTRON ACCEPTOR

ENZYME	k_{cat} (s^{-1})		K_M (mM)		K.I.E.	REFERENCE
	[^{1}H]LAC	[^{2}H]LAC	[^{1}H]LAC	[^{2}H]LAC		
WT	400 ± 10	86 ± 5	0.49 ± 0.05	0.76 ± 0.06	4.7 ± 0.4	(14)
TD-*b*2	330 ± 12	-	0.96 ± 0.06	-	3.6 ± 0.4	(10)
TD-*b*2	38 ± 2	-	1.04 ± 0.14	-	-	This work
E509A	205 ± 4	43 ± 1	1.11 ± 0.09	1.16 ± 0.12	4.7 ± 0.1	This work
E509Q	308 ± 25	62 ± 1	0.45 ± 0.04	0.98 ± 0.15	5.0 ± 0.4	This work
E509K	361 ± 3	108 ± 10	0.30 ± 0.02	0.88 ± 0.20	3.4 ± 0.5	This work

Abbreviations used : WT, wild-type flavocytochrome *b*2 ; TD-*b*2 ,tail-deleted flavocytochrome *b*2 ; [^{1}H]LAC, L-[2-^{1}H]-lactate; [^{2}H]LAC, L-[2-^{2}H]-lactate.

k_{cat} is expressed in terms of number of electrons transferred per second per mole of enzyme (since L-lactate is a two electron donor these values can be halved to express them in terms of moles of substrate reduced per second).

Experimental conditions : All experiments were carried out at 25°C in tris-HCl buffer, pH 7.5, I = 0.1M. The concentration of ferricyanide used in all cases was 1mM which was >90% saturating.

TABLE 4.2

STEADY-STATE KINETIC PARAMETERS AND DEUTERIUM KINETIC ISOTOPE EFFECT VALUES FOR WILD-TYPE AND TAIL-MUTATED FLAVOCYTOCHROMES *b*2 WITH CYTOCHROME *c* AS ELECTRON ACCEPTOR

ENZYME	k_{cat} (s^{-1})		K_M (mM)		K.I.E.	REFERENCE
	[^{1}H]LAC	[^{2}H]LAC	[^{1}H]LAC	[^{2}H]LAC		
WT	207 ± 10	70 ± 10	0.24 ± 0.04	0.48 ± 0.10	3.0 ± 0.6	(14)
E509Q	72 ± 2	36 ± 1	0.10 ± 0.02	0.77 ± 0.43	1.9 ± 0.1	This work
E509K	48 ± 2	19 ± 1	0.47 ± 0.06	0.44 ± 0.06	2.5 ± 0.1	This work

Abbreviations used : WT, wild-type flavocytochrome *b*2 ; [^{1}H]LAC, L-[2-^{1}H]-lactate; [^{2}H]LAC = L-[2-^{2}H]-lactate.

k_{cat} is expressed in terms of number of electrons transferred per second per mole of enzyme (since L-lactate is a two electron donor these values can be halved to express them in terms of moles of substrate reduced per second).

Experimental conditions : All experiments were carried out at 25°C in tris-HCl buffer, pH 7.5, I = 0.1M. The concentrations of cytochrome *c* used were as follows:- 50 μM for WT; 16 μM for E509Q and 150 μM for E509K (all of which are ~90% saturating). No results are shown for TD-*b*2 or E509* as both these enzymes were non-saturating with cytochrome *c*.

FIGURE 4.3

MICHAELIS-MENTEN PLOT FOR THE STEADY-STATE REDUCTION OF FERRICYANIDE BY E509K FLAVOCYTOCHROME *b*$_2$ WITH L-[2-^{1}H]-LACTATE

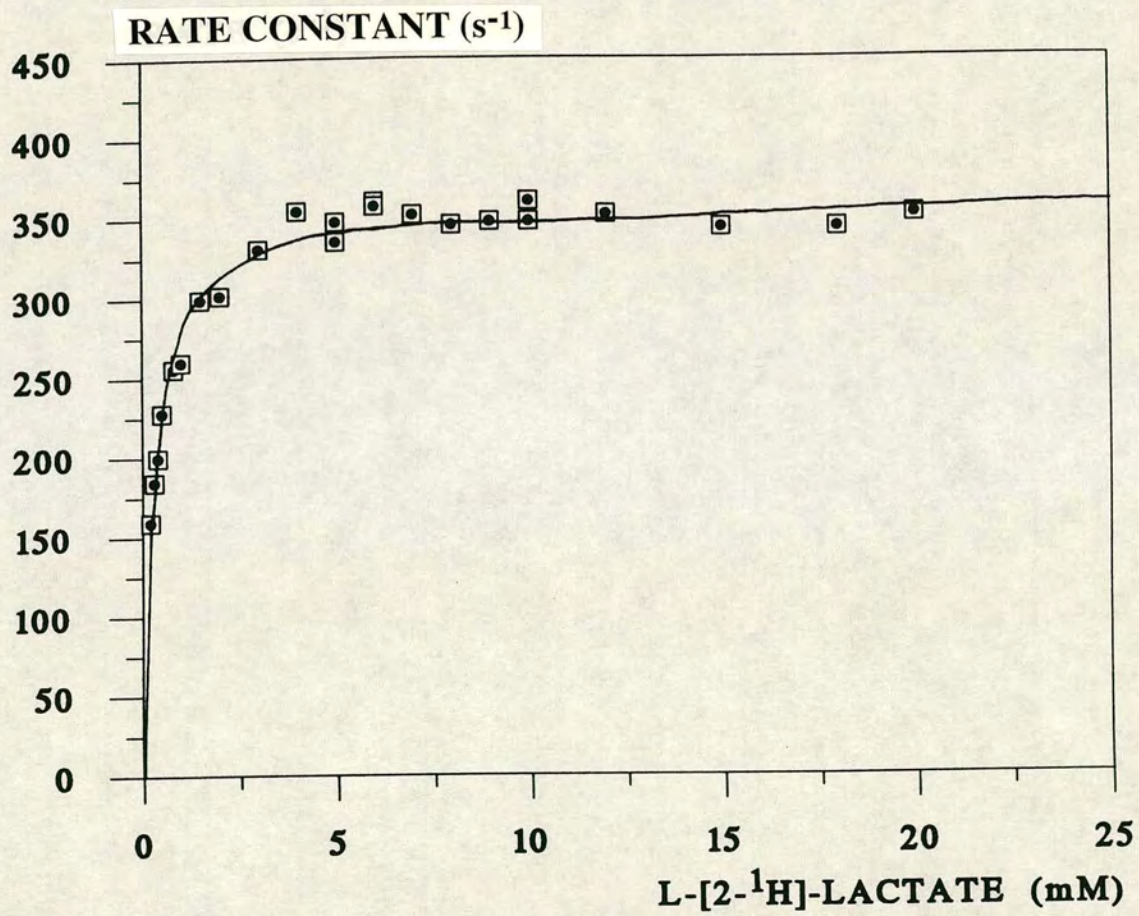

EXPERIMENTAL CONDITIONS ARE DESCRIBED IN 4.2.3.

wild-type, for the E509* mutant enzyme. However, as has previously been reported, TD-*b*2 (10) has slightly unusual behaviour with ferricyanide as acceptor in that the rate of L-lactate oxidation by TD-*b*2 decreases long before L-lactate or ferricyanide have been depleted. This was manifested in the form of curving (biphasic), as opposed to linear, assay traces. Initial rates were measured at differing L-lactate concentrations and these gave rise to typical saturating kinetics as illustrated in Figure 4.3. White *et al.* (10) reported that the deactivation was due to FMN loss and not to dissociation of the protein into monomers. Deactivation proceeds in a biphasic manner; the first fast phase is dependent on L-lactate concentration and has been postulated to lead to a partially deactivated, conformationally altered enzyme. The conformational alteration then leads to FMN loss, which constitutes the second substrate independent phase of the deactivation. After total activity loss, White *et al.* reported that 60% of the activity could be regained by FMN reincorporation.

In contrast, the small three-residue deletion in the tail (E509*) has some effect on L-lactate oxidation with ferricyanide as the electron acceptor. There has been a two-fold decrease in the k_{cat} value from $400s^{-1}$ for wild-type to $205s^{-1}$ for E509*, and an increase in the K_M value from 0.49mM for wild-type to 1.11mM for E509*. These differences are also seen, albeit to varying extents, for TD-*b*2 and are consistent with a general destabilisation

of the enzyme resulting from a conformational change.

The deactivation kinetics of TD-*b*$_2$ and the k_{cat} and K_M observations for TD-*b*$_2$ and E509* infer that the entire C-terminal tail has an important influence on protein structure distant from it, particularly at the active site.

The point mutations in the tail (E509Q and E509K) have little effect upon L-lactate oxidation: k_{cat} and K_M values are not significantly altered. This is also reflected in the efficiencies (as expressed by k_{cat}/K_M, Table 4.3) which are identical to wild-type within experimental error. However, the efficiencies for TD-*b*$_2$ and E509* are slightly lower than for wild-type and the point mutants, further supporting the above conclusions.

Kinetic isotope effect (KIE) values were measured for each enzyme to discern whether changes to the tail have any effect upon rate-limitation in the enzyme. The results are given in Table 4.1 and show that, within experimental error, the KIE values are identical for wild-type and the tail-mutated enzymes, proving that any conformational change incurred has no effect on rate-limitation *i.e.* the major rate limiting step is still abstraction of the C-2 hydrogen as a proton by the active site base, His-373.

Turning to the physiological electron acceptor, cytochrome *c*, there are significant differences in the steady-state behaviour of the tail-mutated enzymes compared to the wild-type enzyme. The major effects are

TABLE 4.3

THE STEADY-STATE EFFICIENCIES OF WILD-TYPE AND TAIL-MUTATED FLAVOCYTOCHROMES *b*2 EXPRESSED BY k_{cat}/K_M

ENZYME	ELECTRON ACCEPTOR	$10^{-5} k_{cat}/K_M$ ($M^{-1}s^{-1}$) [^{1}H]LAC	[^{2}H]LAC	REFERENCE
WT	FERRICYANIDE	8.16 ± 0.86	1.13 ± 0.11	(14)
TD-*b*2	FERRICYANIDE	3.44 ± 0.25	-	(10)
TD-*b*2	FERRICYANIDE	0.37 ± 0.05	-	This work
E509*	FERRICYANIDE	1.85 ± 0.15	0.37 ± 0.04	This work
E509Q	FERRICYANIDE	6.84 ± 0.82	0.63 ± 0.10	This work
E509K	FERRICYANIDE	12.03 ± 0.81	1.23 ± 0.30	This work
WT	CYTOCHROME *c*	8.62 ± 1.50	1.46 ± 0.37	(14)
E509Q	CYTOCHROME *c*	7.15 ± 1.44	0.47 ± 0.26	This work
E509K	CYTOCHROME *c*	1.02 ± 0.14	0.43 ± 0.06	This work

Abbreviations used : WT, wild-type flavocytochrome *b*2; [^{1}H]LAC, L-[2-^{1}H]-lactate; [^{2}H]LAC, L-[2-^{2}H]-lactate.

Experimental conditions : All experiments were carried out at 25°C in tris-HCl buffer, pH 7.5, I = 0.1M. The concentration of ferricyanide used in all cases was 1mM which was >90% saturating and the concentrations of cytochrome *c* used were as follows:- 50 μM for WT; 16 μM for E509Q and 150 μM for E509K (all of which are ~90% saturating). No efficiencies are shown for TD-*b*2 or E509* with cytochrome *c* as acceptor as both of these enzymes are non-saturating with this acceptor.

observed for the tail-deletion mutants, TD-*b*2 and E509*. Neither of these enzymes show saturation with cytochrome *c*; this is illustrated in Figure 4.4 in the form of a Michaelis-Menten plot for E509*. As a result no kinetic parameters can be estimated for either of these enzymes and this steady-state data implicates the C-terminal tail region, and in particular the last three residues of this tail, as being involved in the formation of the flavocytochrome *b*2/cytochrome *c* complex.

The role of the end of the C-terminal tail can be investigated by monitoring the manner in which the point mutations of residue Glu-509 influence the cytochrome *c* reductase activity of flavocytochrome *b*2.

Firstly considering E509Q, which constitutes a negative to neutral charge-change. Cytochrome *c* saturation is observed with this enzyme, giving an apparent acceptor K_M of 11±3 μM, which is the same as for the wild-type enzyme within experimental error. The saturating kinetics hence enabled determination of kinetic parameters for E509Q with regards to cytochrome *c* reduction; these are tabulated in Table 4.2 and an example is illustrated in Figure 4.5. Comparing the results to those of wild-type we see that there is a three-fold drop in the k_{cat} value, from 207s^{-1} for WT to 72s^{-1} for E509Q, in other words the enzyme still has cytochrome *c* reductase capability. The drop in k_{cat} is mirrored by a decrease in the K_M value which is thus not indicative of a true dissociation constant for L-lactate. The fall in both parameters means

FIGURE 4.4

PLOT OF RATE VERSUS SUBSTRATE CONCENTRATION FOR E509* FLAVOCYTOCHROME *b*2 ILLUSTRATING THE NON-SATURATION SHOWN BY THIS ENZYME WITH CYTOCHROME *c* AS ELECTRON ACCEPTOR

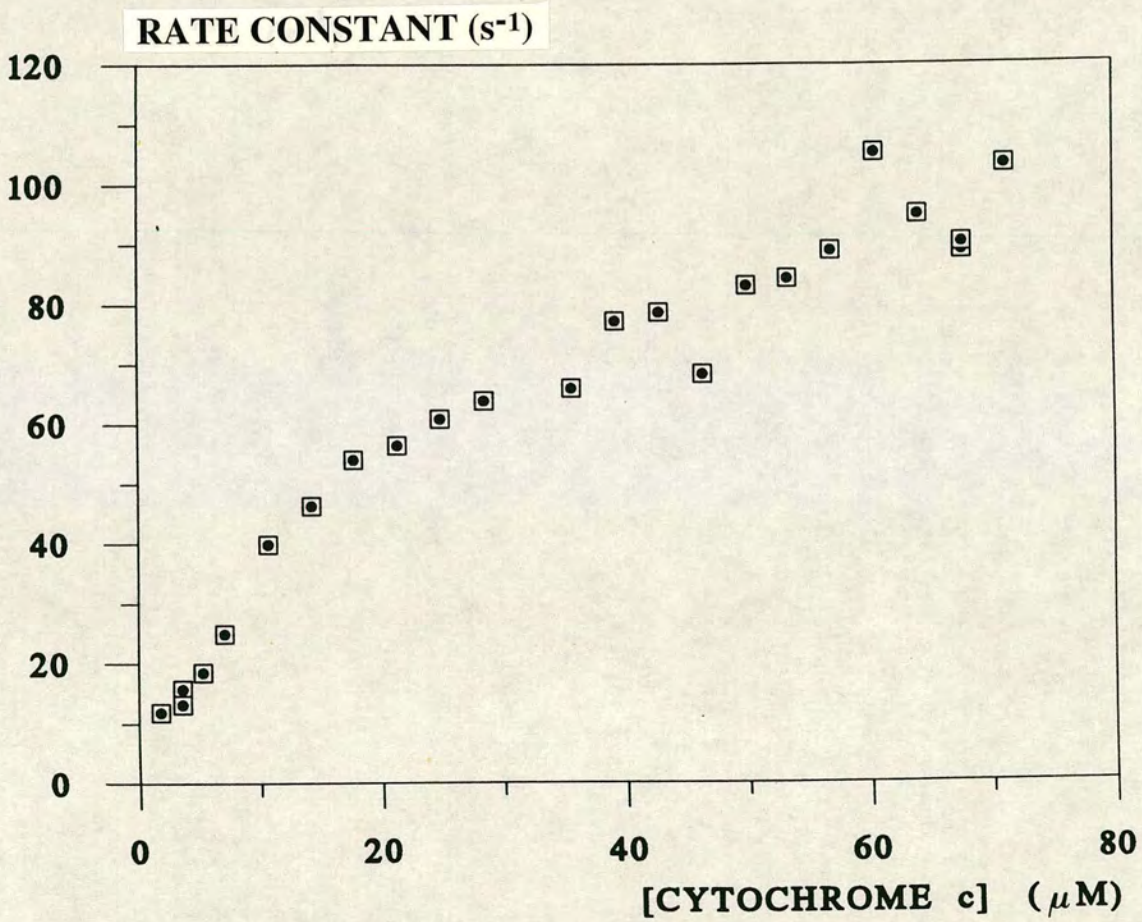

EXPERIMENTAL CONDITIONS ARE DESCRIBED IN 4.2.3

FIGURE 4.5

MICHAELIS-MENTEN PLOT FOR THE STEADY-STATE REDUCTION OF CYTOCHROME *c* BY E509Q FLAVOCYTOCHROME *b*$_2$ WITH L-[2-^{1}H]-LACTATE

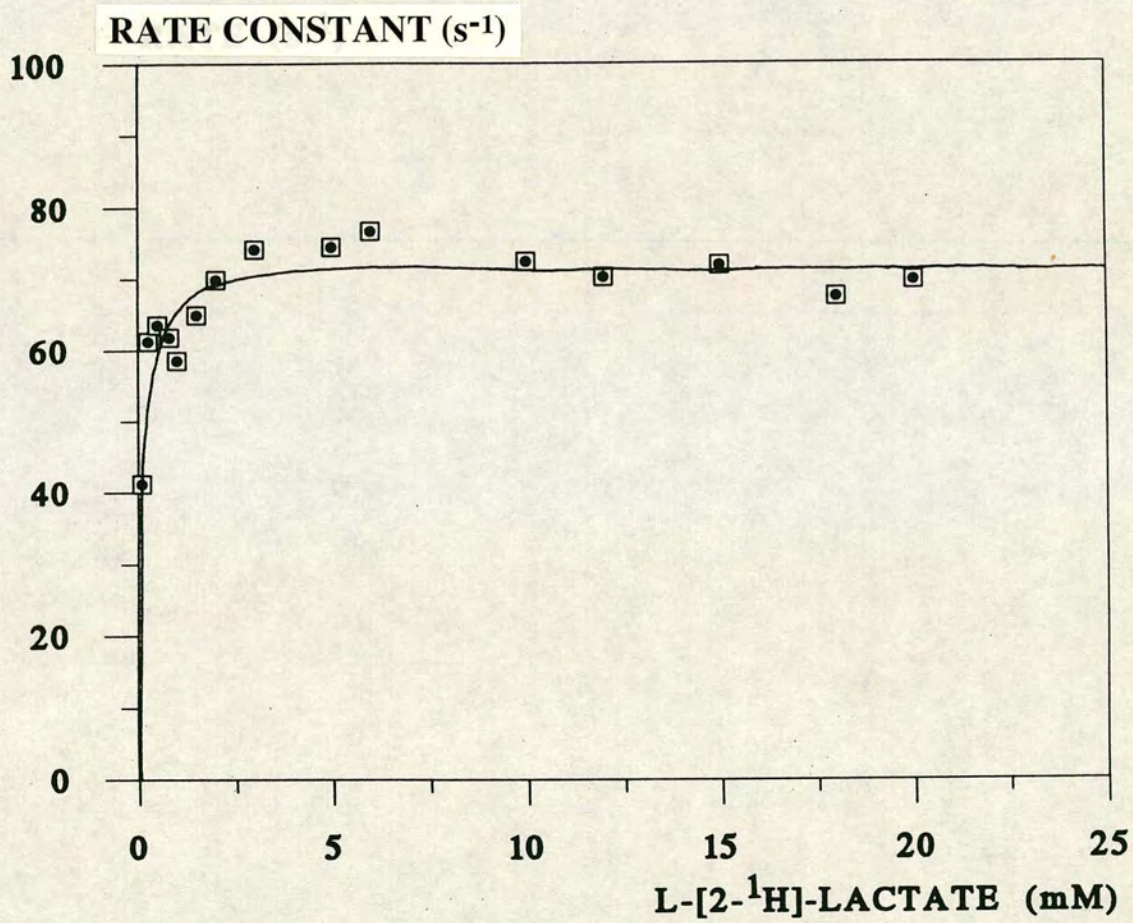

EXPERIMENTAL CONDITIONS ARE DESCRIBED IN 4.2.3.

that the steady-state efficiency of the enzyme E509Q is almost identical to that of WT (results are given in Table 4.3).

At first glance it appears that E509Q is not too different from the wild-type enzyme with regards to cytochrome *c* reduction. There is, however, one significant difference between the two enzymes and this is illustrated by the values of the kinetic isotope effects (KIEs) which decrease from 3.0 for WT to 1.9 for E509Q. In the WT enzyme the KIE values erode along the electron transfer chain from 8.3 for flavin reduction to 3.0 for cytochrome *c* reduction. The fact that there is an erosion is indicative of each step having some contribution to rate-limitation even though it may not necessarily be the overall rate-limiting step in the catalytic cycle. This point mutation constitutes a negative to neutral charge change and assuming that it is this region of the C-terminal tail which associates with the dense region of positive charge located on cytochrome *c*, we might expect to see some evidence to indicate loss of an electrostatic interaction between the two proteins. This evidence comes from the observation that cytochrome *c* reduction is slightly more rate-limiting for E509Q than for wild-type. Also the fact that the rate constant for flavin reduction is lower than for wild-type (Table 4.4) suggests that, in generating this point mutant, there has been some effect upon protein structure at the active site presumably due to alteration of the tail, which is

thought to act as a "conformational anchor" (10).

The other point mutant, E509K, shows different characteristics. It proved much more difficult to attain cytochrome *c* saturation with this enzyme resulting in a higher apparent acceptor K_M (21 ± 3 μM) than for E509Q or WT. This mutant enzyme constitutes a negative to positive charge-change; if this residue is involved in cytochrome *c* binding, electrostatic repulsion may account for the high concentrations of cytochrome *c* required for saturation. This enzyme shows an even larger difference in k_{cat} values than E509Q: the value for E509K is four-fold lower than that for WT ($48 s^{-1}$ as opposed to $207 s^{-1}$ respectively). The K_M value is slightly higher for E509K than for WT but this is most probably a reflection of the decreased rate of reduction of cytochrome *c* rather than an effect on substrate binding. These differences are reflected by the steady-state efficiency (expressed as k_{cat}/K_M) which is eight-fold lower for E509K than for WT (Table 4.3). The value of the KIE for cytochrome *c* reduction for E509K is identical to that for WT, within experimental error, indicating that this particular point mutation does not increase the rate-limiting contribution of this step.

A further numerical comparison can be made between the point mutations; that is by means of the ratio of the k_{cat} values when using the different electron acceptors *i.e.* k_{cat}(cytochrome *c*)/k_{cat}(ferricyanide). The value of this ratio for WT is 0.52, for E509Q this decreases

slightly to 0.23, and there is a further decrease to 0.13 for E509K. In general, the smaller the value of this ratio, the greater the emphasis upon different electron transfer pathways through the enzyme. However, in this case this is not true and the decrease in value reflects the decrease in rate of cytochrome *c* reduction.

To summarise the steady-state results, it is obvious that the tail region, and in particular Glu-509, is of importance in the formation of a catalytically-competent complex, although it may not be the sole point of association between the two proteins.

4.3.2 STOPPED-FLOW KINETIC ANALYSIS

Stopped-flow kinetics were performed in order to monitor the individual reductions of the prosthetic groups of the enzyme. The results obtained are shown in Table 4.4 where they are compared to results previously obtained for the wild-type enzyme under identical conditions (14). Sample traces are shown in Figure 4.6 and typical examples of Michaelis-Menten plots are illustrated in Figures 4.7 and 4.8. No results are given for either of the tail-deleted enzymes as both these enzymes were prone to complete FMN loss, resulting in total activity loss over a short period of time. Both flavin and haem reductions for the point mutations were found to be biphasic, at least at high L-lactate concentrations. This is in accordance with the wild-type enzyme (14) as already discussed in Section

TABLE 4.4

COMPARISON OF THE RESULTS FROM STOPPED-FLOW KINETIC ANALYSES OF WILD-TYPE AND TAIL-MUTATED FLAVOCYTOCHROMES *b*2

(a) FLAVIN REDUCTION

	L-[2-^{1}H]-lactate			L-[2-^{2}H]-lactate				
	k_{cat} (s^{-1})	K_M (mM)	k_{cat}/K_M ($M^{-1}s^{-1}$)	k_{cat} (s^{-1})	K_M (mM)	k_{cat}/K_M ($M^{-1}s^{-1}$)	K.I.E.	REFERENCE
WILD-TYPE	604±60	0.84±0.20	7.2×10^5	75±5	1.33±0.28	6.0×10^4	8.1±1.4	(14)
E509Q	648±80	0.90±0.20	7.2×10^5	73±9	1.28±0.23	5.7×10^4	8.9±0.2	THIS WORK
E509K	600±117	1.53±0.23	3.9×10^5	81±3	3.41±0.27	2.4×10^4	8.6±0.1	THIS WORK

(b) HAEM REDUCTION

	L-[2-^{1}H]-lactate			L-[2-^{2}H]-lactate				
	k_{cat} (s^{-1})	K_M (mM)	k_{cat}/K_M ($M^{-1}s^{-1}$)	k_{cat} (s^{-1})	K_M (mM)	k_{cat}/K_M ($M^{-1}s^{-1}$)	K.I.E.	REFERENCE
WILD-TYPE	445±50	0.53±0.05	8.4×10^5	71±5	0.68±0.05	1.0×10^5	6.3±1.2	(14)
E509Q	436±20	1.09±0.13	4.0×10^5	67±1	0.91±0.05	0.7×10^5	6.5±0.2	THIS WORK
E509K	510±20	0.56±0.09	9.1×10^5	83±2	0.87±0.07	1.0×10^5	6.1±0.3	THIS WORK

Abbreviations : K.I.E. = KINETIC ISOTOPE EFFECT.

Experimental conditions : All experiments were carried out at 25±0.1°C in tris-HCl buffer, pH 7.5, I=0.1M. k_{cat} values are expressed as number of prosthetic groups reduced per second.

FIGURE 4.6

STOPPED-FLOW KINETIC TRACES FOR THE REDUCTION OF THE PROSTHETIC GROUPS OF E509K AND E509Q FLAVOCYTOCHROMES *b*2

(a) E509K FLAVIN REDUCTION (438.3nm)

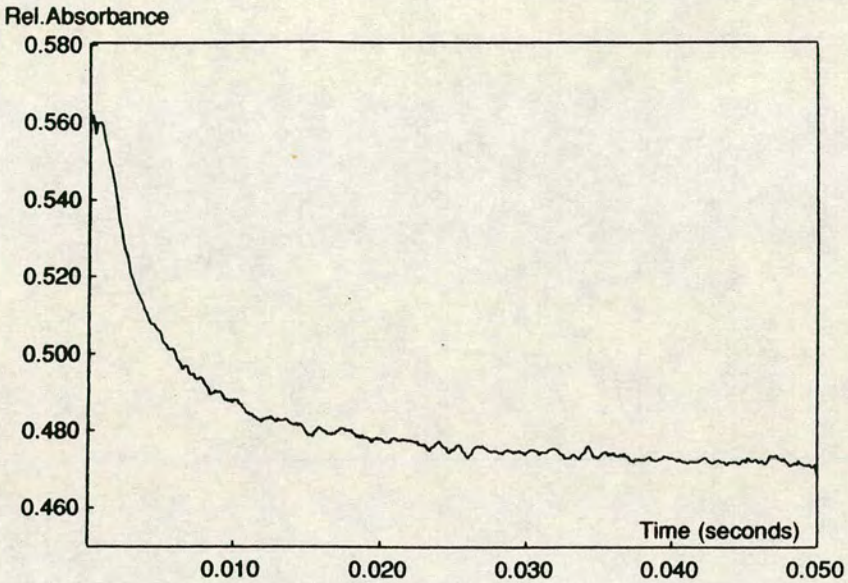

(b) E509Q HAEM REDUCTION (423nm)

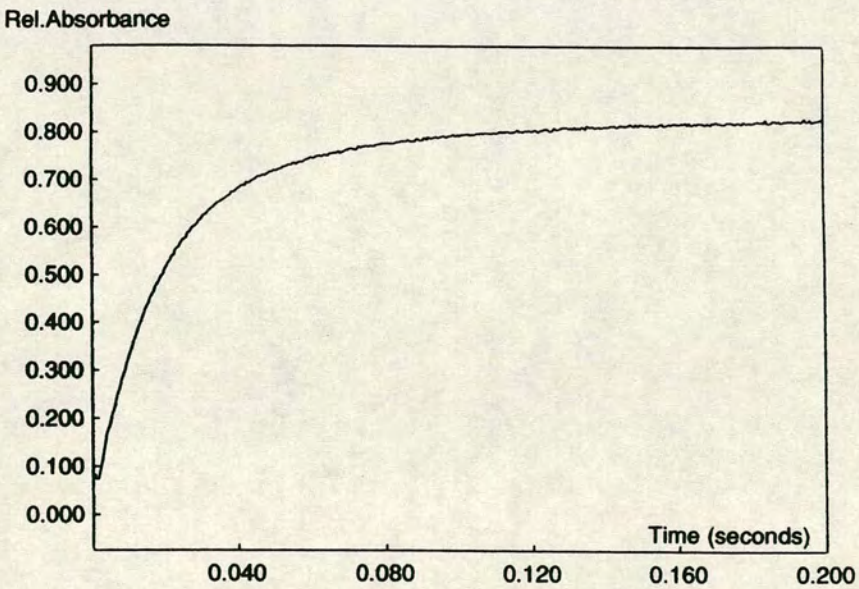

EXPERIMENTAL DETAILS GIVEN IN 4.2.3

FIGURE 4.7

MICHAELIS-MENTEN PLOT FOR FLAVIN REDUCTION OF E509K FLAVOCYTOCHROME *b*$_2$ BY L-[2-^{1}H]-LACTATE UNDER STOPPED-FLOW CONDITIONS

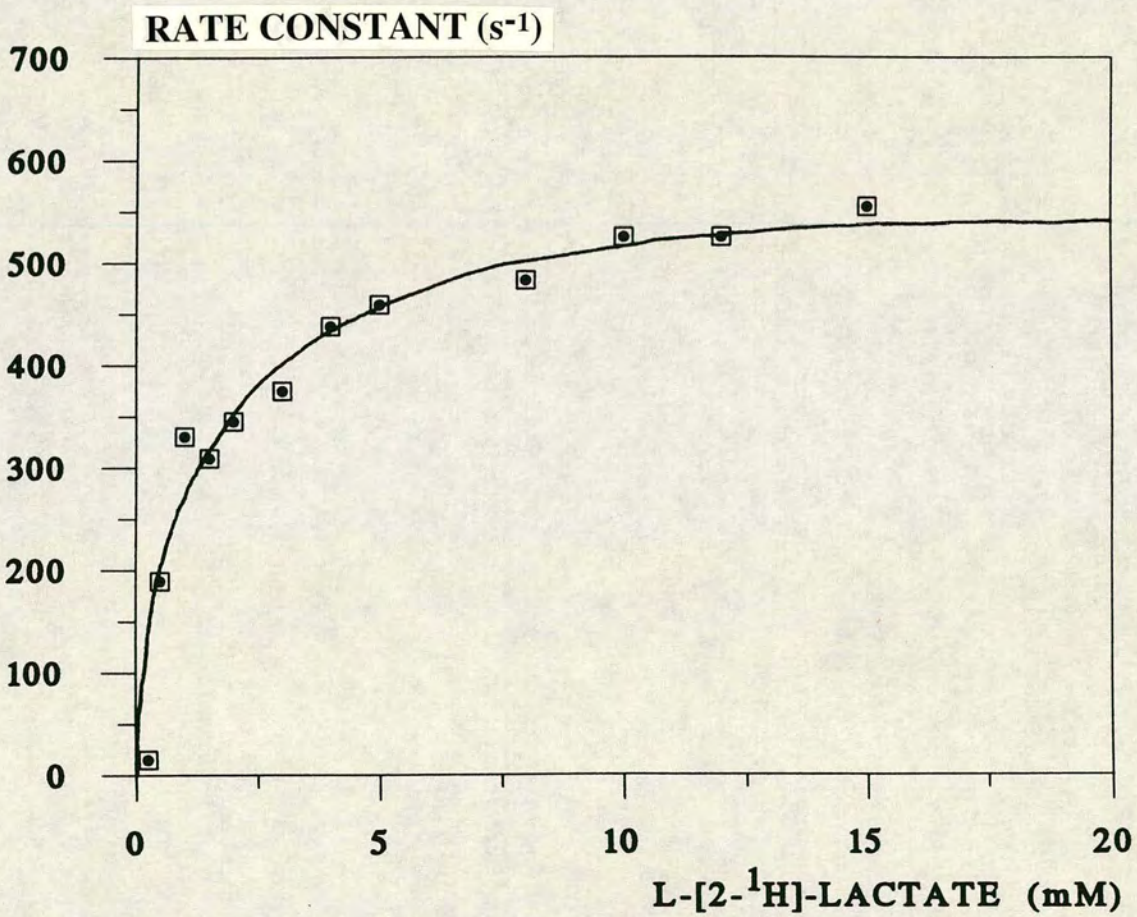

EXPERIMENTAL CONDITIONS ARE DESCRIBED IN 4.2.3.

FIGURE 4.8

MICHAELIS-MENTEN PLOT FOR HAEM REDUCTION OF E509Q FLAVOCYTOCHROME *b*$_2$ BY L-[2-^{2}H]-LACTATE UNDER STOPPED-FLOW CONDITIONS

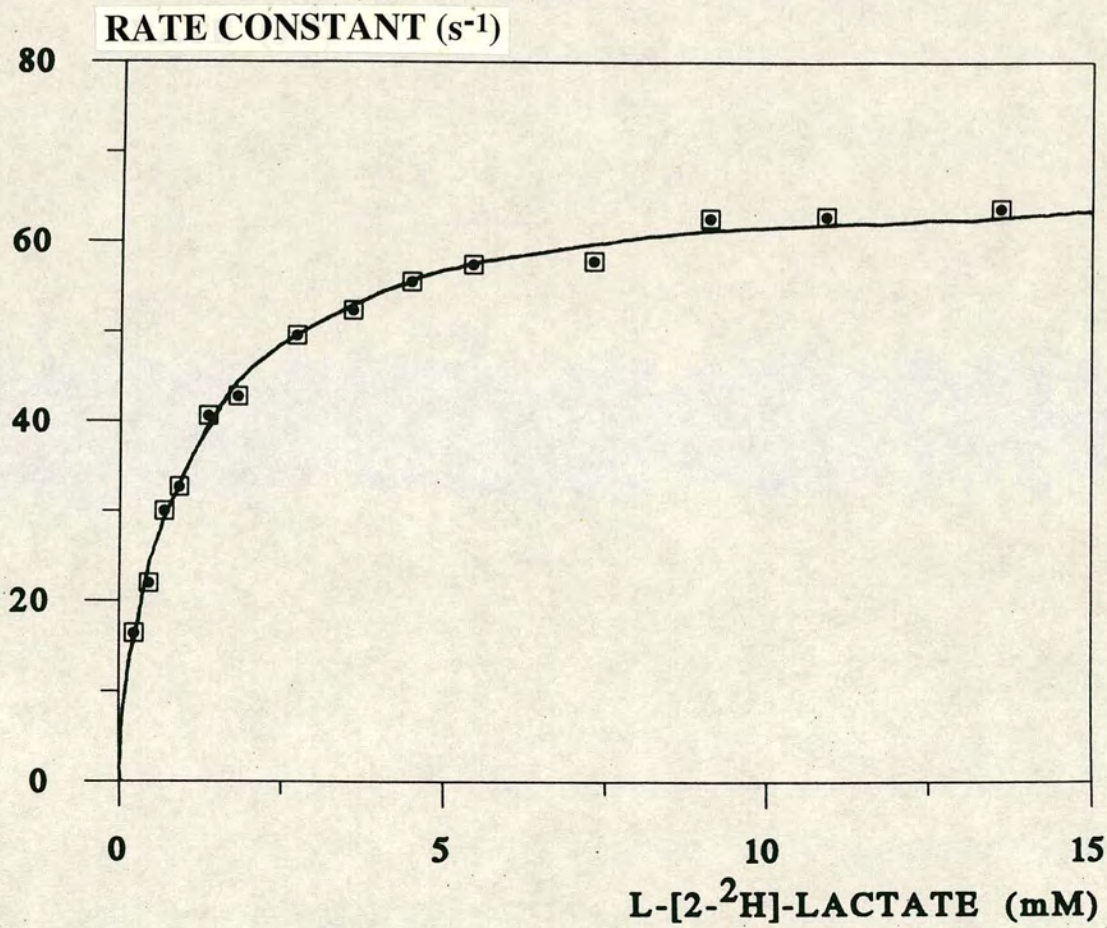

EXPERIMENTAL CONDITIONS ARE DESCRIBED IN 4.2.3.

2.3.2. Concentrating on the first stage of catalytic turnover, electron transfer from L-lactate to FMN, the point mutant E509Q is kinetically identical to the wild-type enzyme in every respect. For the E509K enzyme the situation is slightly different; the rate constant for flavin reduction is identical to that for the wild-type and E509Q enzymes, indicating that all three enzymes are very efficient L-lactate dehydrogenases. However, the K_M for L-lactate for E509K is almost twice as large as that for wild-type (1.53mM as opposed to 0.84mM), this results in a lower efficiency, as expressed by k_{cat}/K_M. This higher K_M value may be indicative of a slight structural perturbation at the active site induced by the charge change near to the end of the C-terminal tail.

As mentioned above the rate constants for haem reduction are not affected by either of the point mutations; flavin to haem electron transfer is not altered as a result of mutations to the tail. This is further supported by the KIE values which are all identical, proving that the contribution of this step to rate-limitation does not significantly increase.

4.3.3 DISCUSSION OF COMBINED KINETIC RESULTS

A linear representation of the catalytic cycle of flavocytochrome *b*$_2$ is shown in Figure 4.9 in which the rate constants for each step for the wild-type, E509Q and E509K enzymes are compared. A similar scheme is

FIGURE 4.9

LINEAR REPRESENTATION OF THE CATALYTIC CYCLE OF FLAVOCYTOCHROME *b*2

COMPARING THE RATE CONSTANTS FOR WILD-TYPE, E509Q AND E509K ENZYMES

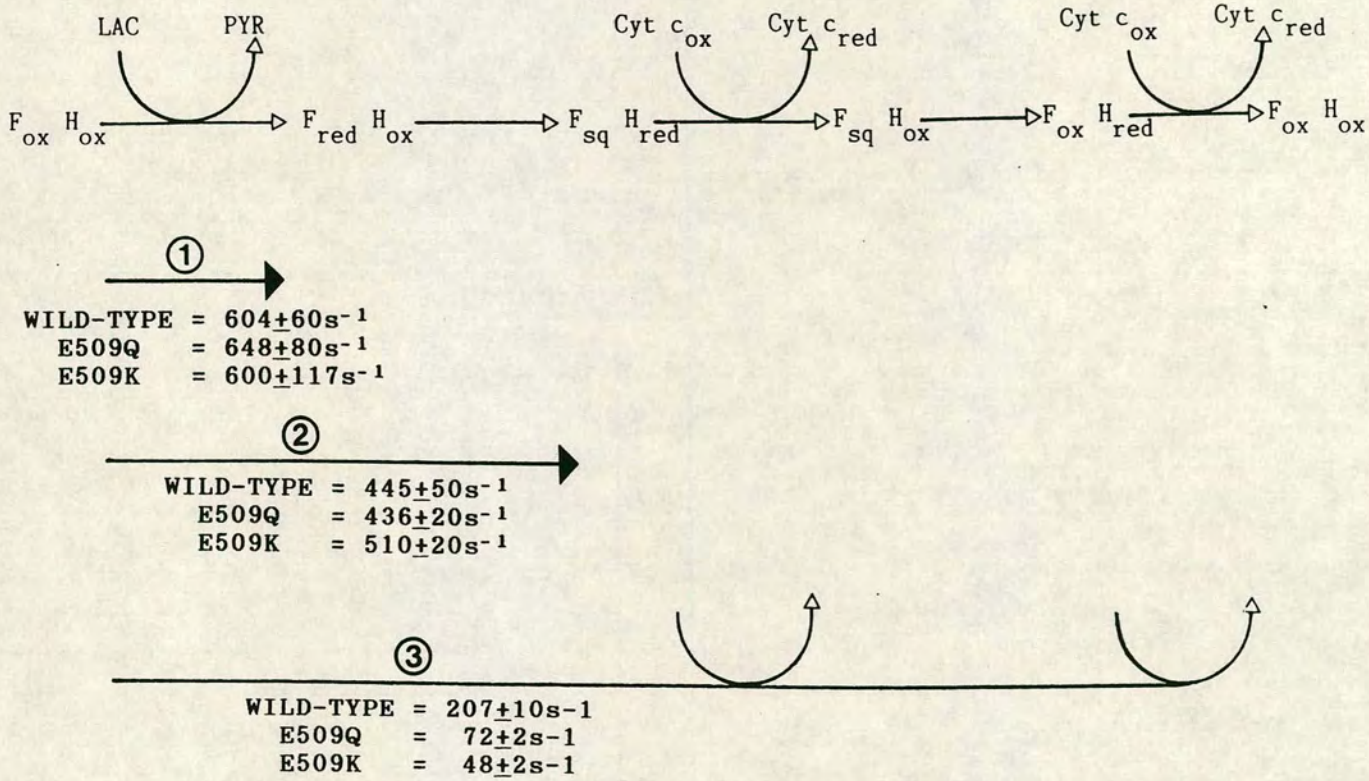

ABBREVIATIONS : LAC, LACTATE; PYR, PYRUVATE; F, FLAVIN; H, HAEM; Cyt c, CYTOCHROME *c*; ox, OXIDISED; red, REDUCED; sq, SEMIQUINONE.

illustrated in Figure 4.10 showing the values of the kinetic isotope effects (KIEs).

The rate constants for the wild-type enzyme decline slowly throughout catalysis from $604s^{-1}$ for flavin reduction eventually reaching a third of this value at $207s^{-1}$ for cyt. *c* reduction. This behaviour is also seen for the KIE values which erode along the electron transport chain from 8.1 for flavin reduction to 3.0 for cytochrome *c* reduction. Such values indicate that it is flavin reduction, or more precisely, abstraction of the C-2 hydrogen of L-lactate as a proton by the active site base, His-373, which is the overall rate-limiting step in the catalytic cycle, although the following two steps do contribute slightly to rate-limitation.

For both point mutations the situation is similar, but there are subtle differences. Both E509Q and E509K show a gradual decline in rate constant along the chain except that the fall in rate from haem reduction to cytochrome *c* reduction is larger in the point mutants than in the wild-type enzyme; the rate constants for cytochrome *c* reduction being approximately one-ninth and one-twelfth of the original value for flavin reduction for E509Q and E509K respectively. This is mirrored by the KIE values which again erode along the chain but undergo a significant drop for cytochrome *c* reduction, particularly for E509Q. This indicates that cytochrome *c* reduction is in some way affected by these point mutations such that cytochrome *c* reduction has a greater contribution to

FIGURE 4.10

COMPARISON OF THE DEUTERIUM KINETIC ISOTOPE EFFECTS FOR WILD-TYPE, E509Q AND E509K FLAVOCYTOCHROMES *b*2

WILD-TYPE	8.1±1.4	6.3±1.2	3.0±0.6
L-LACTATE---------->FLAVIN---------->HEME--------->CYTOCHROME *c*			
E509Q	8.9±0.2	6.5±0.2	1.9±0.1
E509K	8.6±0.1	6.1±0.3	2.5±0.1

overall rate-limitation than in the wild-type enzyme, although it must be pointed out that the overall rate-limiting step in the catalytic cycle is still C-2 hydrogen abstraction.

The above data are consistent with the end of the C-terminal tail being involved in the electrostatic interactions associating flavocytochrome *b*2 and cytochrome *c*, and in the electron transfer between these two proteins. However, it is unlikely that this association via the tail is the only interaction involved in formation of the catalytically-competent complex.

4.3.4 INSTABILITY OF TAIL-DELETED FLAVOCYTOCHROME *b*2

Initial steady-state kinetics for TD-*b*2 with ferricyanide as electron acceptor are given in Table 4.1. It was observed that k_{cat} values for L-lactate were approximately 9-fold lower than had previously been reported by White *et al.* (10). It was postulated that this decrease in activity was due to FMN loss with time. Previous studies (10) had reported that TD-*b*2 was tetrameric even after complete FMN loss; in order to confirm this and to probe the mechanisms controlling activity loss, the molecular weight of TD-*b*2 was determined by a non-denaturing method at various stages of purification and at differing ionic strengths. Molecular weight determination was carried under conditions of varying ionic strength because preparations

of TD-*b*2 would only bind to hydroxylapatite at low ionic strengths and the initial activity was dependent upon the ionic strength of the lysing buffer. This is illustrated in Figure 4.11 which is a plot of TD-*b*2 activity versus ionic strength of the lysing buffer.

Gel filtration on Sephacryl S-300 (Sigma) showed that the preparations of TD-*b*2 in this study were monomeric. The calibration plot for the column is shown in Figure 4.12 and results in M_R 53.6±1.0 kDa for TD-*b*2 (the theoretical value for the monomer being 54.3 kDa). TD-*b*2 was shown to be monomeric under all of the following conditions:- (i) after purification on hydroxylapatite at low ionic strength (I=0.06M),(ii) after 70% ammonium sulphate fractionation at low ionic strength (I=0.06M) and storage under nitrogen at 0-4°C, and (iii) immediately after fresh preparation from *E.coli* in phosphate buffer with I=0.22M. All protein proven to be monomeric was completely inactive and activity could not be restored by either addition of excess free FMN to the assay solution or by attempted FMN reincorporation by denaturation/refolding.

To summarise, our preparation of TD-*b*2 is particularly unstable, completely losing activity as a result of FMN loss and monomerisation. It is possible that this occurs as a result of low ionic strength of the lysing and purification buffers, but whether or not these processes occur simultaneously or consequently is as yet unknown.

The results obtained for the smaller deletion mutant

FIGURE 4.11

PLOT TO ILLUSTRATE THE IONIC STRENGTH DEPENDENCE OF THE ACTIVITY OF TAIL-DELETED FLAVOCYTOCHROME *b*2

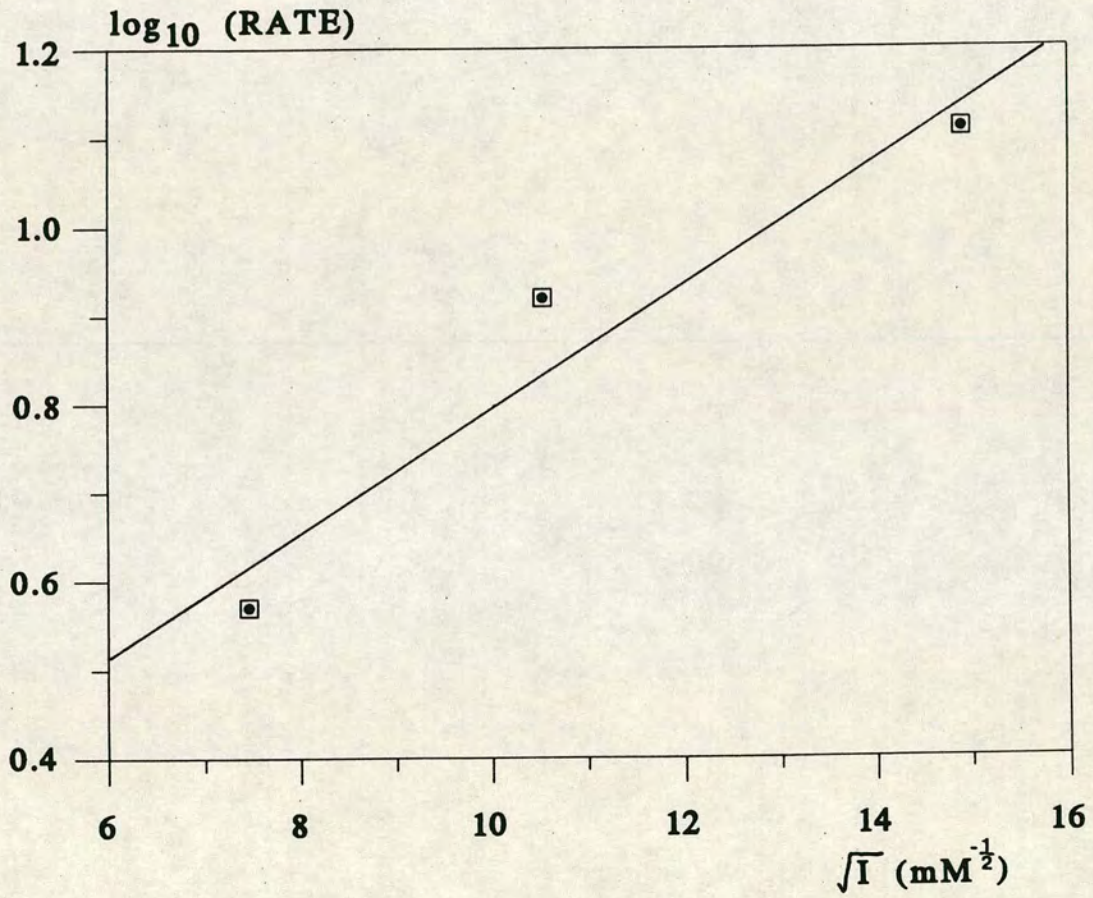

Experimental conditions : *E.coli* containing tail-deleted flavocytochrome *b*2 were lysed in phosphate buffer of varying ionic strength (pH 7.0) at 4°C. The activity of the enzyme was then assessed by the steady-state reduction of ferricyanide under saturating conditions at 25±0.1°C in tris-HCl buffer, pH 7.5, I=0.1M.

FIGURE 4.12

CALIBRATION CURVE FOR SEPHACRYL (S300) GEL FILTRATION COLUMN USED IN MOLECULAR WEIGHT DETERMINATION OF TAIL-DELETED FLAVOCYTOCHROME *b*2

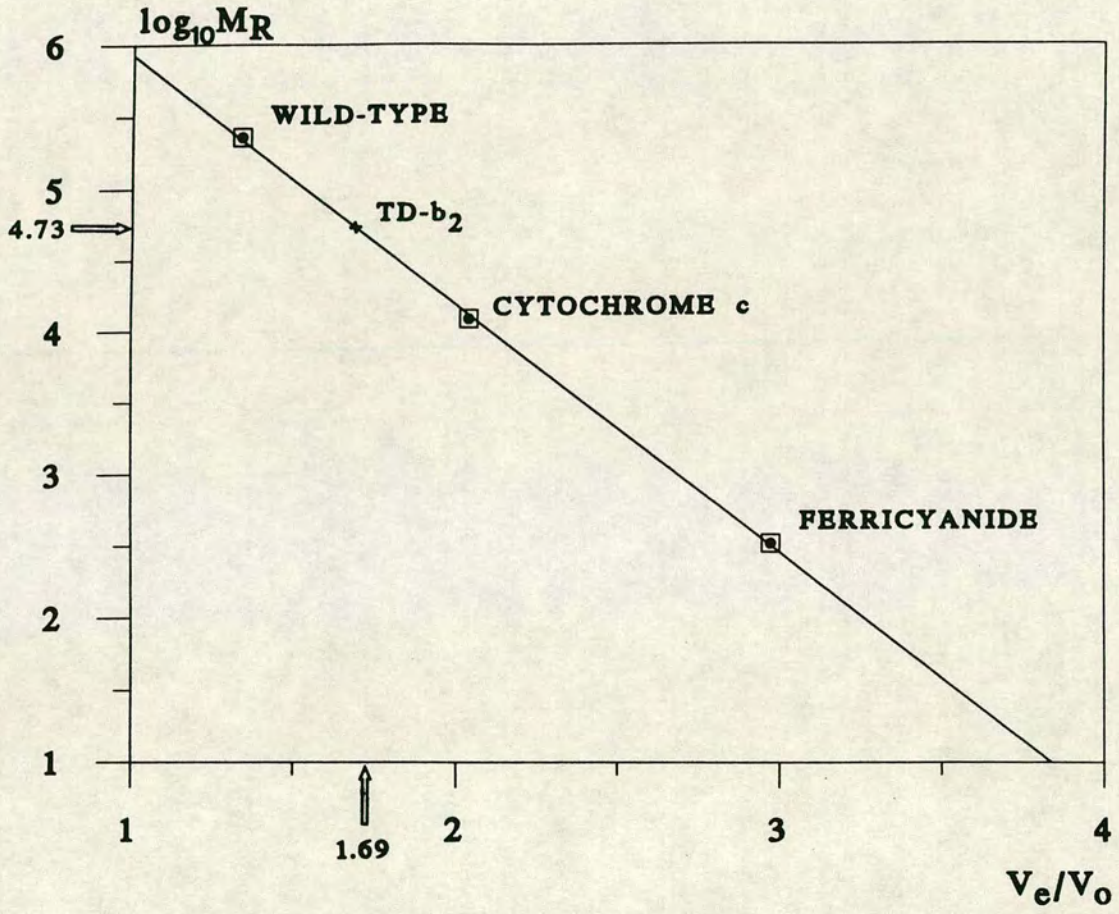

Abbreviations : TD-b2, tail-deleted flavocytochrome *b*2; MR, molecular weight; Ve/Vo, elution volume ratio.

Experimental details are given in 4.2.4.

(E509*) suggest that this process is occurring for this enzyme also. As yet this is unsubstantiated, but it may be that the small deletion causes FMN loss, but may not disrupt the structure sufficiently enough to cause subunit dissociation.

The TD-*b*2 enzyme was originally generated with a view to creating a monomer of flavocytochrome *b*2 as it was thought that the C-terminal tail was responsible for holding the subunits together as a tetramer (10). This study suggests that the tail does influence quaternary structure; probably as a result of the tail being of importance in maintaining structural integrity at the active site: disruption to the tail leading to FMN loss and breakdown of tetrameric structure.

4.4 CONCLUSIONS

Characterisation of the tail-mutated flavocytochromes *b*2 leads us to the following conclusions:-

(1) the C-terminal tail is of importance for structural integrity within the enzyme; without it the enzyme is more susceptible to destabilisation via FMN loss and subunit dissociation;

(2) the last three residues of the C-terminal tail are involved in association with and electron transfer to cytochrome *c* *i.e.* are directly involved in formation of a catalytically-competent complex;

(3) mutations made in the C-terminal tail do not alter rate-limitation of flavocytochrome *b*2 although they may cause a small degree of conformational change localised at the active site;

(4) the C-terminal tail is not the only region on flavocytochrome *b*2 which is involved in the binding of cytochrome *c*.

4.5 REFERENCES

(1) Appleby, C.A. & Morton, R.K., *Nature (London)*, **173**, 749 (1954).

(2) Pajot, P. & Claisse, M., *Eur.J.Biochem.*, **49**, 275 (1974).

(3) Baudras, A., Krupa, M. & Labeyrie, F., *Eur.J.Biochem.*, **20**, 58 (1971).

(4) Capeillère-Blandin, C., *Eur.J.Biochem.*, **128**, 533 (1982).

(5) Tegoni, M., Mozzarelli, A., Rossi, G.L. & Labeyrie, F., *J.Biol.Chem.*, **258**, 5424 (1983).

(6) Albani, J., *Arch.Biophys.Biochem.*, **243**, 292 (1985).

(7) Salemme, F.R., *J.Mol.Biol.*, **102**, 563 (1976).

(8) Matsushima, A., Yoshimura, T. & Aki, K., *J.Biochem.(Tokyo)*, **100**, 543 (1986).

(9) Iwatsubo, M., Mevel-Ninio, M. & Labeyrie, F., *Biochemistry*, **16**, 3558 (1977).

(10) White, S.A., Black, M.T., Reid, G.A. & Chapman, S.K., *Biochem.J.*, **263**, 849 (1989).

(11) Zoller, M.J. & Smith,M., *DNA*, **3**, 479 (1984).

(12) Black, M.T., White, S.A., Reid, G.A. & Chapman, S.K., *Biochem.J.*, **258**, 255 (1989).

(13) Maniatis, T., Fritsch, E.F. & Sambrook, J., in *"Molecular Cloning:A Laboratory Manual"*, Cold Spring Harbour Laboratory Press,Cold Spring Harbour (1982).

(14) Miles, C.S., Rouvière-Fourmy, N., Lederer, F., Mathews, F.S., Reid, G.A. & Chapman, S.K., *Biochem.J.*, **285**, 187 (1992).

CHAPTER 5

INTERMOLECULAR COMMUNICATION

INVESTIGATION OF CYTOCHROME *c* BINDING SITE BY KINETIC AND SPECTROSCOPIC TECHNIQUES

5.1 INTRODUCTION

Cytochrome *c* is known to form a stable complex with its physiological partner, flavocytochrome b_2, both in solution and in the crystalline state (1-5). Formation of this complex has been shown to be highly dependent on ionic strength indicating that important interactions between the two proteins are electrostatic (3). Cytochrome *c* associates with flavocytochrome b_2 by way of its ring of positively-charged lysine residues occurring near to the haem edge (6) and a distance of 18Å between the haem centres has been reported by Vanderkooi *et al.* (7).

Investigation of the electron transfer pathway through flavocytochrome b_2 has shown that cytochrome *c* can only accept an electron from the haem domain (8). It was therefore postulated that the main association area for cytochrome *c* on flavocytochrome b_2 was the haem domain. However fluorescence studies carried out by Thomas *et al.* (9) demonstrated that cytochrome *c* can bind to both the flavin and the haem domains; the affinity to the flavin domain being higher than to the haem domain.

Different values have been reported in the literature for the stoicheometry of the complex between cytochrome *c* and flavocytochrome b_2. Baudras *et al.* (3,4) reported a ratio of one cytochrome *c* per flavocytochrome b_2 tetramer for the cleaved *S.cerevisiae* enzyme both in solution and in co-crystals of the two proteins. More recently, Tegoni *et*

al. (2) have obtained complexation by diffusion of cytochrome *c* through channels in crystals of intact *S.cerevisiae-b2* and have obtained a ratio of four cytochrome *c* molecules per flavocytochrome *b2* tetramer. Tegoni *et al.* went on to generate a hypothetical model for the interaction of flavocytochrome *b2* and cytochrome *c* using molecular modelling and energy minimisation techniques (10). As a means of discrimination between proposed models, several criteria were adhered to:- (i) that the ring of lysines surrounding the exposed haem edge on the front of the cytochrome *c* molecule were involved in the association with flavocytochrome *b2* (6); (ii) that electrostatic interactions were formed between these positively-charged lysines and complementary surface charges, such as Asp and Glu, on flavocytochrome *b2* (11); (iii) that the prosthetic haem groups facing each other in the complex were parallel with edge-to-edge distance ranging from 8.4 - 16Å; (iv) that the stoicheometry was feasible; (v) that both domains were involved (9); and (vi) that more than one subunit could interact with a single cytochrome *c* molecule.

The resulting model is illustrated in Figures 5.1, 5.2 and 5.3 and contains four cytochrome *c* molecules interacting with a tetramer of flavocytochrome *b2*. The *b2* and *c* haems are co-planar with an edge-to-edge distance of 14Å. Cytochrome *c* is located at the border between the cytochrome *b2* core and the flavodehydrogenase domain, a site which corresponds to an electrostatically favourable

FIGURE 5.1

MOLECULAR MODEL OF THE INTERACTION BETWEEN FLAVOCYTOCHROME *b*2 AND CYTOCHROME *c*, SHOWING FOUR CYTOCHROME *c* MOLECULES BOUND TO THE TETRAMER (10)

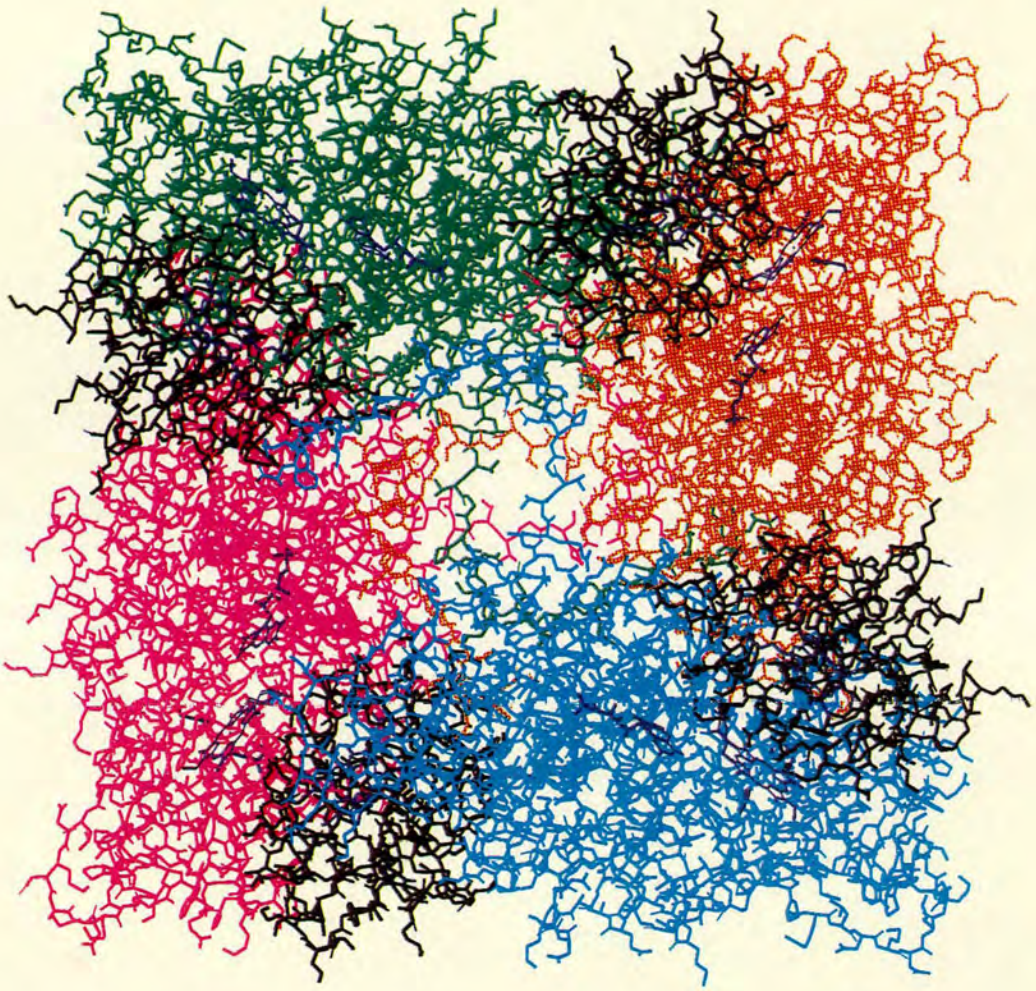

The four subunits of the *b*2 tetramer are shown in blue, green, orange and pink, with the prosthetic groups in dark blue. The four cytochrome *c* molecules bound to the tetramer are shown in black.

FIGURE 5.2

SIDE VIEW OF THE MOLECULAR MODEL OF THE INTERACTION BETWEEN FLAVOCYTOCHROME *b*2 AND CYTOCHROME *c*

The *b*2 tetramer, with bound cytochrome *c* molecules (black), is viewed from the side, perpendicular to the four-fold axis.

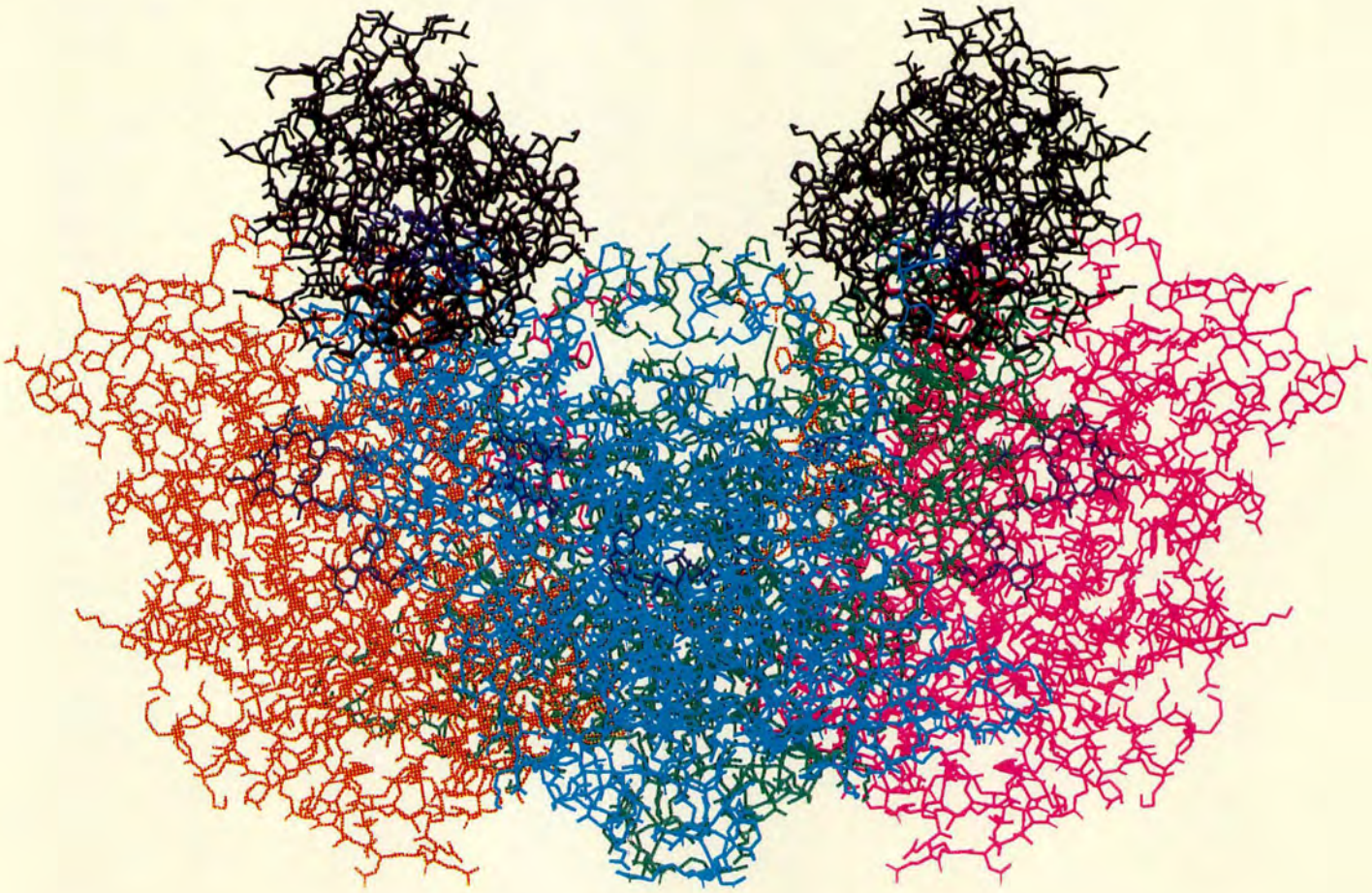

FIGURE 5.3

CRYSTAL PACKING REPRESENTATION OF THE COMPLEX FORMED BETWEEN A DIMER OF FLAVOCYTOCHROME *b*2 AND TWO CYTOCHROME *c* MOLECULES (10)

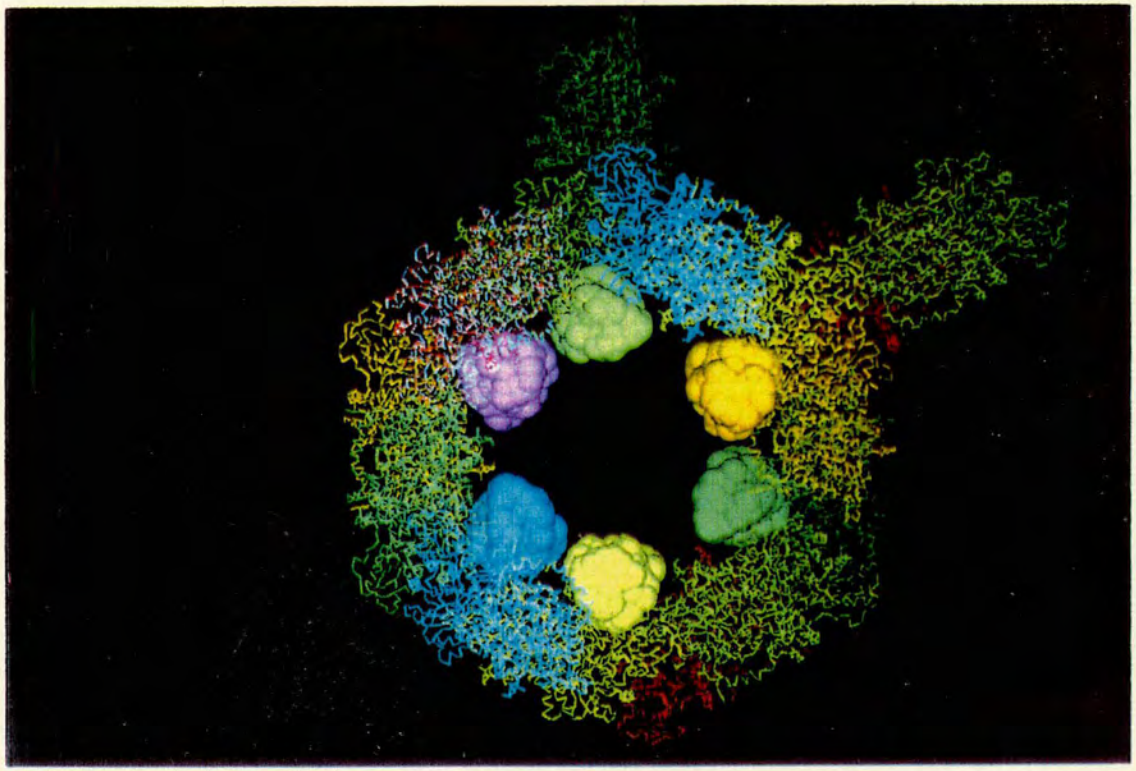

Flavocytochrome *b*2 is represented as a C_α-backbone model, and cytochrome *c* as space-filling models.

region (Figure 5.4). Each cytochrome *c* interacts with three of the four subunits having association points with the cytochrome *b*2 core (residues 1-17) of one subunit, the interdomain hinge (residues 86-91) of a second subunit, and a region near to the end of the C-terminal tail in the flavodehydrogenase domain (residues 505-510) in a third subunit. The contacts are polar, consisting of ion-pairs and hydrogen bonds.

Site-directed mutagenesis of each of these three regions may help to confirm this hypothesis and to elucidate the strength of the particular associations. The mutant flavocytochromes *b*2 which are discussed in this chapter concern two of the regions mentioned above: the interdomain hinge and the C-terminal tail. The respective mutants are the hinge-swap enzyme (see Chapter 2) and E509K, the negative to positive charge-change point mutation in the C-terminal tail (see Chapter 4).

Both of these enzymes have been fully characterised by steady-state analysis and both show peculiarities with respect to kinetic behaviour with cytochrome *c*. The hinge-swap enzyme has k_{cat} for cytochrome *c* reduction which, at a value of $1.62s^{-1}$, is 130-fold lower than the wild-type enzyme from *S.cerevisiae* ($207s^{-1}$). This rate-lowering is a result of major disruption in flavin to haem electron transfer. E509K is partially unsaturating with cytochrome *c* and also shows a decreased rate constant for reduction of the acceptor. These investigations were under steady-state conditions and

FIGURE 5.4

THE INTERACTING WATER ACCESSIBLE SURFACES OF FLAVOCYTOCHROME b_2 (BLUE) AND CYTOCHROME *c* (PINK) (10)

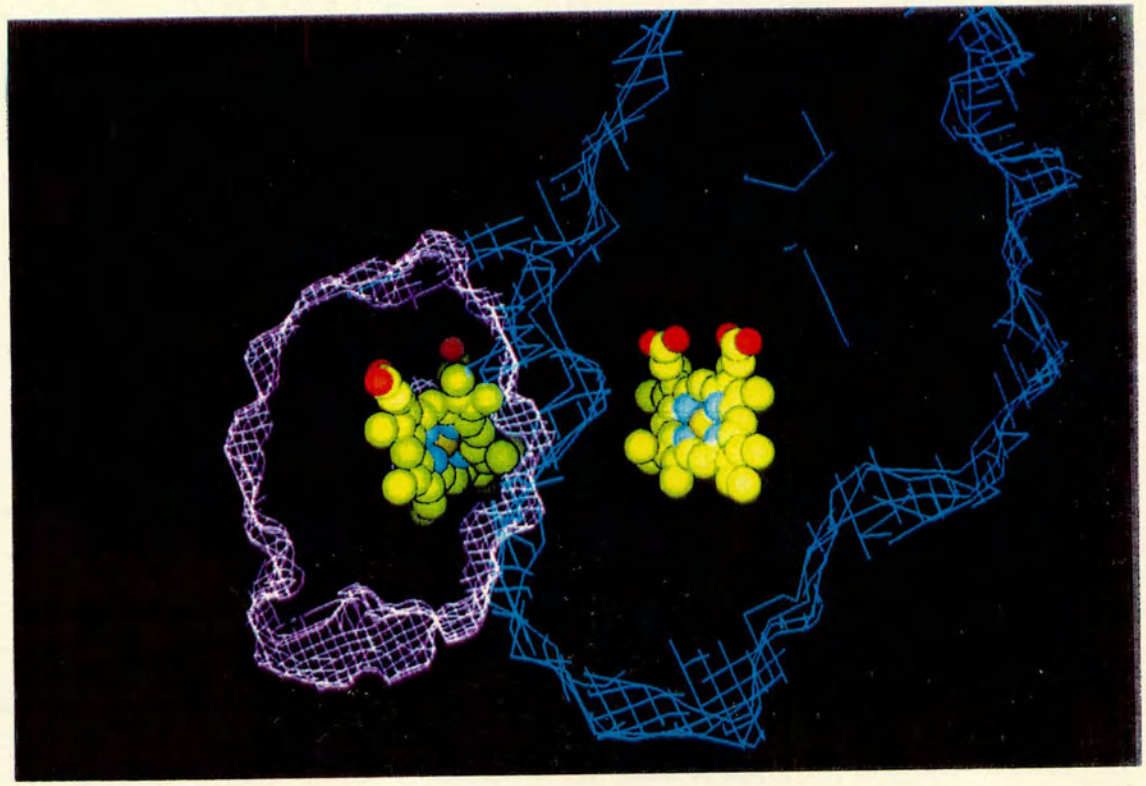

correspond to the electron transfer from L-lactate through to cytochrome *c*, with no direct evidence for the rate of electron transfer from the cytochrome *b*2 domain to cytochrome *c* or the nature and strength of cytochrome *c* binding. These properties have been investigated by means of stopped-flow kinetics and NMR spectroscopy respectively. To enable direct comparisons to be made, these experiments were also carried out on wild-type flavocytochrome *b*2 by R. Eryl Sharp (12).

5.2 EXPERIMENTAL

5.2.1 CONSTRUCTION OF MUTATED FLAVOCYTOCHROMES *b*2 (DR.F.D.C.MANSON)

The hinge-swap and E509K mutant flavocytochromes *b*2 (Dr.F.D.C.Manson) were generated by site-directed mutagenesis using the double primer method of Zoller and Smith (13). Standard methods of DNA manipulation were used, as given in Sambrook *et al.* (14). Construction of these enzymes is described in more detail in Sections 2.2.1 and 4.2.1 respectively. Wild-type and mutant flavocytochromes *b*2 were over-expressed in *E.coli*; the protease-deficient strain AR120 proving most efficient for high level over-expression of the intact flavocytochrome *b*2 containing the mutation in the hinge region.

5.2.2 ENZYME PREPARATION AND PURIFICATION

Enzymes were isolated from *E.coli* which had been stored at -20°C as described in Section 7.4. Purification was achieved by hydroxylapatite chromatography in 0.1M phosphate buffer (5mM L-lactate, 1mM EDTA, pH 7.0), followed by gel-filtration on Sephadex G-25 equilibrated in tris-HCl buffer, pH 7.5. This buffer was 0.01M in HCl and the ionic strength was adjusted to 0.10M by addition of NaCl (see Section 7.4.4). Protein at this stage of purification was ready for use in stopped-flow kinetic experiments and was fully reduced by addition of excess L-lactate.

Prior to NMR spectroscopy, protein was dissolved in a minimal amount of 20mM phosphate/D_2O buffer (pH 7.0, I=0.04M) and solvent exchange was carried out using Amicon centricon microconcentrators in the manner described in Section 7.12.3.

5.2.3 STOPPED-FLOW KINETIC ANALYSIS

All experiments were carried out at 25±0.1°C in tris-HCl buffer, pH 7.5. This buffer was 0.01M in HCl with the ionic strength adjusted to 0.10M by addition of NaCl. Stopped-flow kinetics were performed in the general manner described in Section 7.9 using an Applied Photophysics SF.17MV stopped-flow spectrofluorimeter, except that fully reduced flavocytochrome b_2 solution was placed in one syringe and fully oxidised cytochrome *c*

solution in the other. During the stopped-flow reaction, equal microvolumes of the two protein solutions were mixed and the change in absorbance associated with cytochrome *c* reduction was monitored at 416.5nm (a flavocytochrome b_2 isosbestic point). The concentration of flavocytochrome b_2 was varied throughout the experiment, with the maximum resulting in an approximately 20-fold excess over cytochrome *c* concentration; sufficient to ensure that pseudo-first order kinetics were observed. The SF.17MV software package was used to collect and analyse data on an Archimedes 420/1 computer. Traces were fitted to single exponentials. Results were plotted in the form of maximal rate versus flavocytochrome b_2 concentration and second order rate constants were determined by using linear regression analysis.

5.2.4 NMR SPECTROSCOPY

All 1D proton NMR spectra were recorded at 25°C in 20mM phosphate/D_2O buffer (pH 7.0, I=0.04M) using a Varian VXR600S spectrometer operating at 600MHz. The D_2O peak occurring at 4.8ppm (pH 7.0, 25°C) was used as an internal reference. An unperturbed resonance was identified in each flavocytochrome b_2 spectrum (probably due to a solvent impurity) and was referenced to the D_2O peak.

Initial spectra of free 0.1mM oxidised cytochrome *c* and

of free 0.1mM oxidised flavocytochrome *b*2 tetramer (0.4mM monomer concentration) were collected. These enabled an addition spectra to be computed by use of the Varian VXR600S software. 1D proton NMR spectra of flavocytochrome *b*2 were recorded after subsequent additions of small aliquots of a ~16mM stock solution of oxidised cytochrome *c* (horse heart, Type VI - Sigma) in 20mM phosphate/D_2O buffer, pH 7.0. Aliquots of cytochrome *c* were calculated such that a cytochrome *c* titration was performed with an increasing integral ratio of cytochrome *c* haems to flavocytochrome *b*2 haems up to an excess of six cytochrome *c* haems per flavocytochrome *b*2 tetramer. Linewidths of the resonances corresponding to cytochrome *c* haem methyls 3 and 8, at 32.5ppm and 35.5ppm respectively, were measured. A linewidth broadening factor of 10Hz was added to all resonances with the exception of some of the resonances for E509K as indicated in Table 5.2.

5.3 RESULTS AND DISCUSSION

5.3.1 STOPPED-FLOW KINETIC ANALYSIS

An example of a typical stopped-flow trace for cytochrome *c* reduction is shown in Figure 5.5. The second order rate constants for cytochrome *c* reduction by wild-type and mutant flavocytochromes *b*2 are given in Table 5.1 and are illustrated in graphical form in Figure 5.6. The hinge mutant has the lowest second-order rate constant which,

FIGURE 5.5

TYPICAL STOPPED-FLOW KINETIC TRACE FOR THE REDUCTION OF CYTOCHROME *c* BY E509K FLAVOCYTOCHROME *b*2

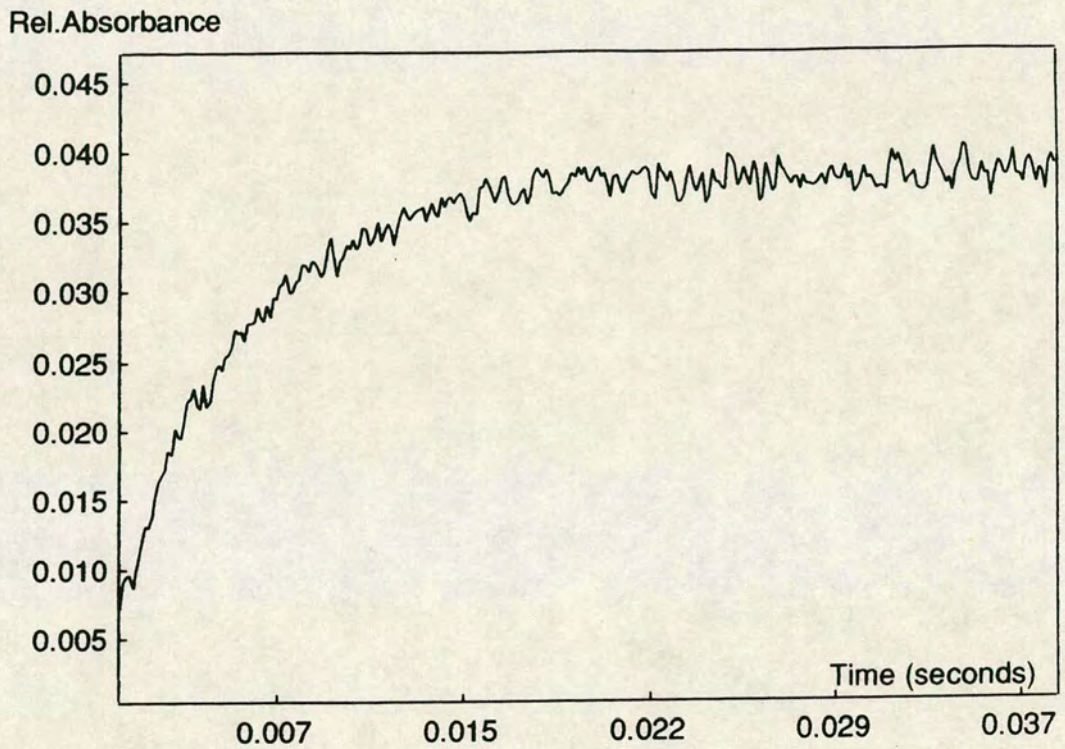

Experimental conditions : Experiments were carried out at 25±0.1°C in Tris-HCl, pH 7.5, I=0.1M. This particular trace shows the reduction of cytochrome *c* by E509K-*b*2 which is in 5-fold excess. Absorbance change was monitored at 416.5nm.
Further details can be found in 5.2.3.

TABLE 5.1

SECOND ORDER RATE CONSTANTS FOR THE REDUCTION OF CYTOCHROME *c* BY WILD-TYPE AND MUTANT FLAVOCYTOCHROMES *b*$_2$

ENZYME	SECOND ORDER RATE CONSTANT ($10^{-6}/M^{-1}s^{-1}$)
WILD-TYPE	47.0 ± 1.0
E509K	24.0 ± 1.3
HINGE-SWAP	3.3 ± 0.3

Experimental conditions : All experiments were carried out at 25 ± 0.1°C in tris-HCl buffer, pH 7.5, I = 0.1M. The buffer concentration was 0.01M in HCl.

FIGURE 5.6

PLOT OF MAXIMAL RATE VERSUS ENZYME CONCENTRATION USED IN THE DETERMINATION OF THE SECOND-ORDER RATE CONSTANTS FOR CYTOCHROME c REDUCTION UNDER STOPPED-FLOW CONDITIONS

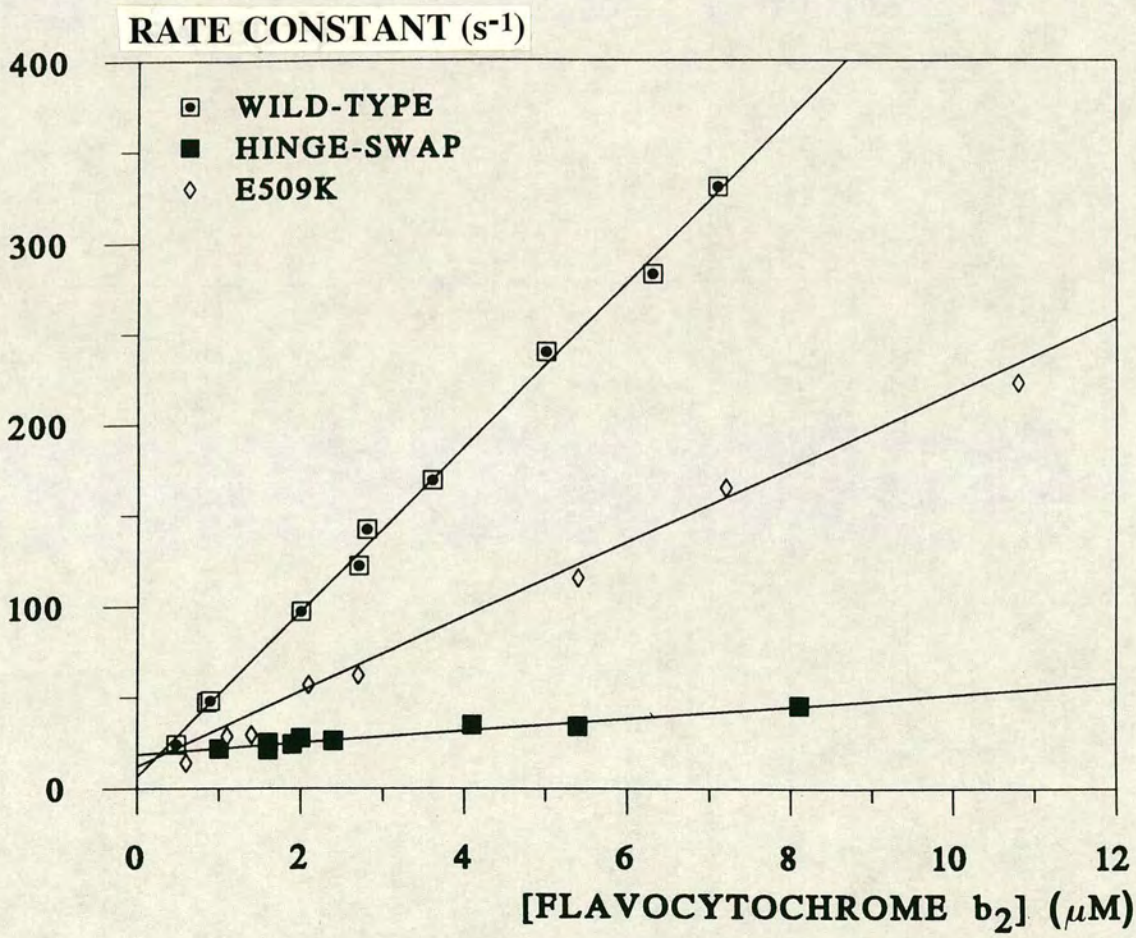

Experimental conditions are described in 5.2.3. The second-order rate constants were calculated by linear regression analysis and are quoted in Table 5.1.

at a value of 3.3 x $10^6 M^{-1}s^{-1}$, is an order of magnitude lower than wild-type flavocytochrome *b*2. This result is not surprising when one considers the large structural changes introduced (as previously discussed in Chapter 2) and suggests that the hinge is involved in electron transfer to cytochrome *c*, although from this data alone, it is impossible to draw any conclusions regarding the extent and strength of any interprotein interactions. The E509K mutant enzyme has a second order rate constant which is comparable to that for wild-type flavocytochrome *b*2. This suggests that efficient electron transfer can occur within the flavocytochrome *b*2:cytochrome *c* complex which is not surprising since this enzyme comprises only a small point mutation which is unlikely to have caused much structural change within the enzyme. This correlates with the kinetic analysis of E509K discussed in the previous chapter; whereby the mutation did not drastically affect the cytochrome *c* reductase ability of the enzyme. However, there did appear to be slightly greater contribution to overall rate-limitation of the catalytic step in which cytochrome *c* is reduced. which could be due to the effect of the charge-change on cytochrome *c* binding.

5.3.2 NMR SPECTROSCOPY

Proton NMR spectra for cytochrome *c* titrations are shown for the wild-type and E509K mutant enzymes in Figures 5.7 and 5.8 respectively. In the case of the wild-type

FIGURE 5.7

NMR SPECTRA SHOWING TITRATION OF CYTOCHROME c TO WILD-TYPE FLAVOCYTOCHROME *b*2

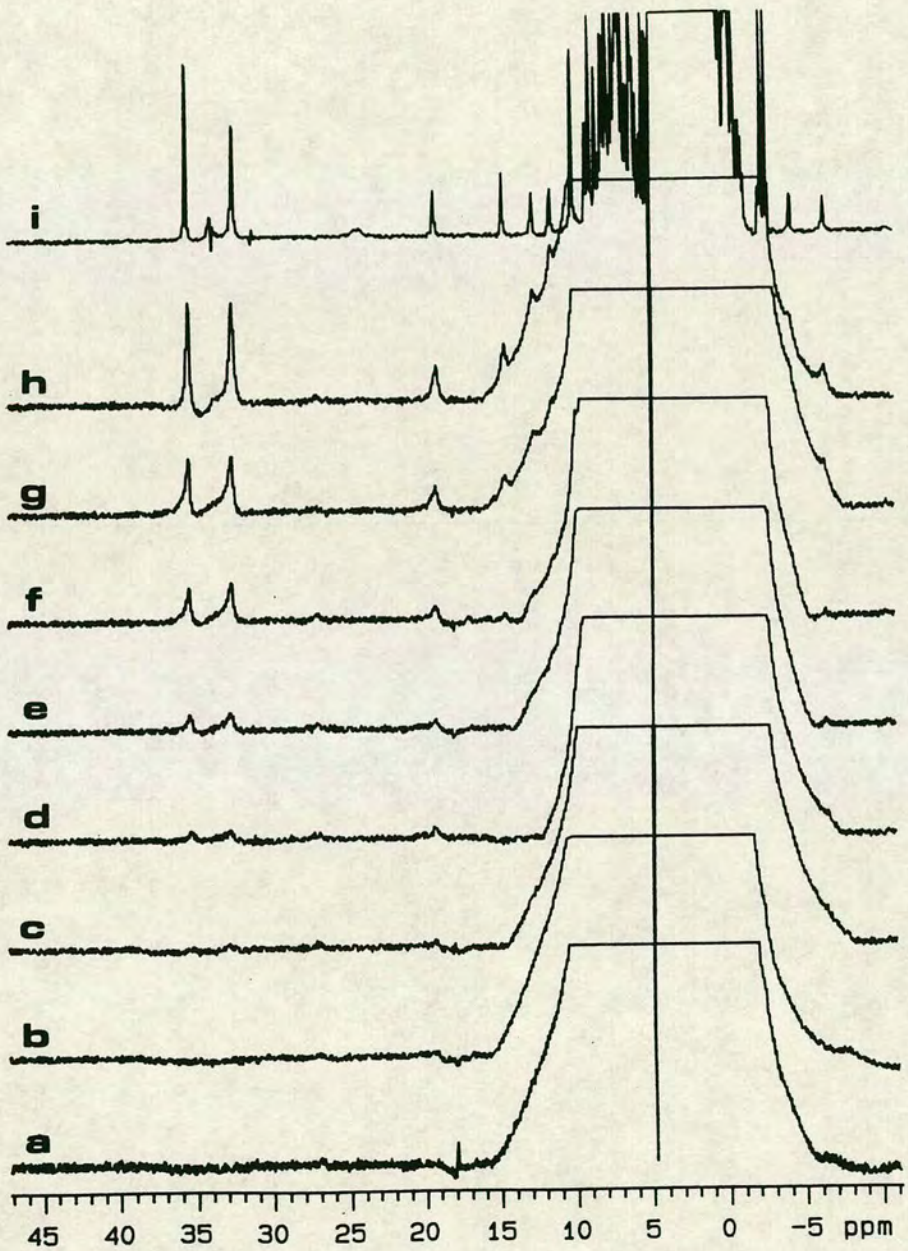

600MHz spectra were recorded at 25°C in 20mM phosphate/D_2O buffer, pH 7.0. Spectrum (a) is of 0.4mM wild-type-*b*2 subunit (0.1mM tetramer); (b) an 8:1 mixture of wild-type-*b*2 and cytochrome *c* respectively (0.4mM wild-type-*b*2 subunit and 0.05mM cytochrome *c*); (c) 4:1; (d) 8:3; (e) 4:2; (f) 4:3; (g) 4:4; (h) 4:6; and (i) is an electronic addition spectrum of free wild-type flavocytochrome *b*2 and cytochrome *c*.

FIGURE 5.8

NMR SPECTRA SHOWING TITRATION OF CYTOCHROME *c* TO E509K FLAVOCYTOCHROME *b*$_2$

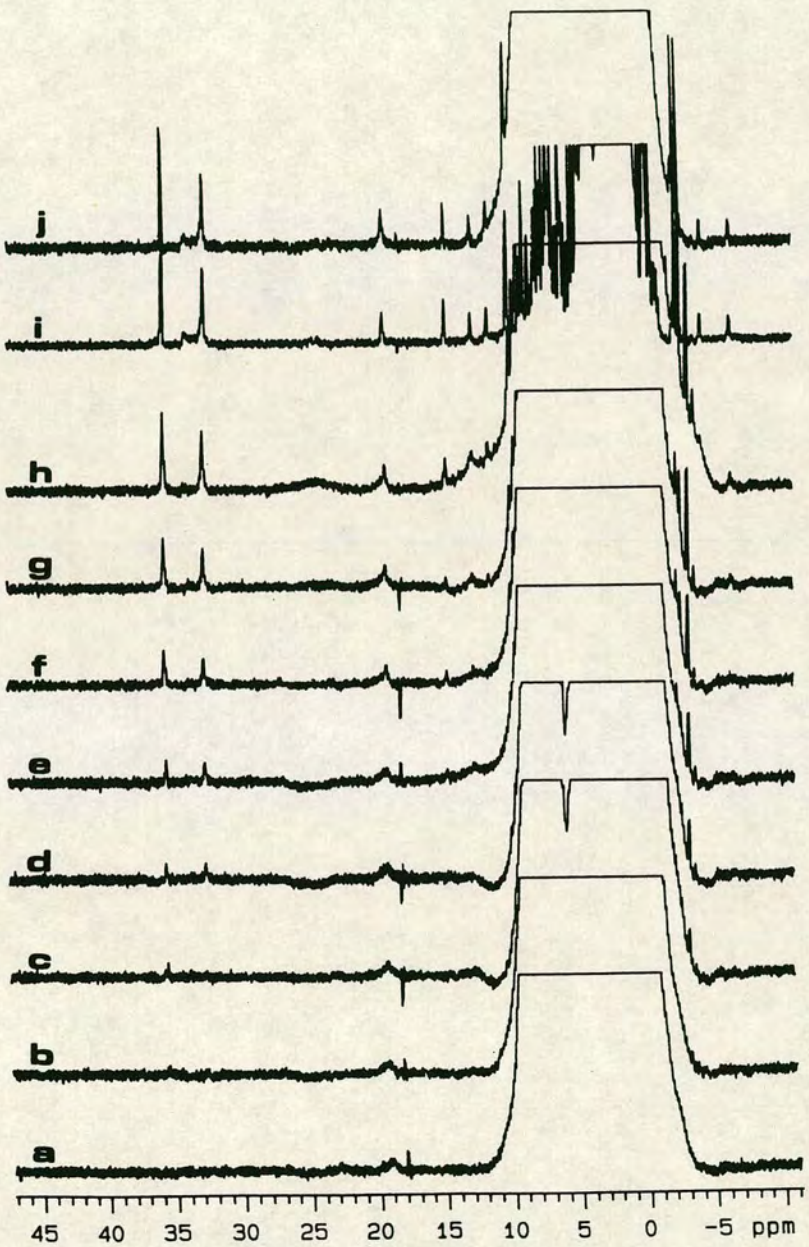

600MHz spectra were recorded at 25°C in 20mM phosphate/D_2O buffer, pH 7.0. Spectrum (a) is of 0.4mM E509K-*b*$_2$ subunit (0.1mM tetramer); (b) an 8:1 mixture of E509K-*b*$_2$ and cytochrome *c* respectively (0.4mM E509K-*b*$_2$ subunit and 0.05mM cytochrome *c*); (c) 4:1; (d) 8:3; (e) 4:2; (f) 4:3; (g) 4:4; (h) 4:6; (i) is a spectrum of 0.1mM cytochrome *c*; and (j) is an electronic addition spectrum of free E509K flavocytochrome *b*$_2$ and cytochrome *c*.

flavocytochrome b_2, as the stoicheometry of cytochrome *c* increases, the proportion of occupied binding sites on flavocytochrome b_2 will also increase, until at higher ratios of cytochrome *c* to flavocytochrome b_2, these sites become saturated. At this stage the spectrum starts to resemble the electronic addition spectrum of free flavocytochrome b_2 and cytochrome *c*. The broadness of the linewidths is indicative of the extent of binding of cytochrome *c* to flavocytochrome b_2. Binding results in formation of a larger molecular species which has a slower tumbling time, and this, as a direct result of the diminished relaxation times, leads to linewidth broadening.

The degree of broadening can thus be used as a qualitative guide to the amount of cytochrome *c* binding to flavocytochrome b_2. This is illustrated in Figure 5.9 which is a comparison of the 4:3 (flavocytochrome b_2 : cytochrome *c*) binding spectra along with the electronic addition spectrum of the two proteins free in solution. It is clear that for wild-type and for all the mutant enzymes the linewidths are broader than in the addition spectra. This implies that cytochrome *c* is binding to all of the enzymes although to differing extents; wild-type > E509K = hinge-swap.

In an attempt to quantify this data, the linewidths of the resonances corresponding to haem methyls 3 and 8 of cytochrome *c* (at 32.5 and 35.5ppm respectively) were measured (Table 5.2) and graphs were plotted of linewidth

FIGURE 5.9

NMR SPECTRA SHOWING COMPARISON OF LINEWIDTH BROADENING DUE TO CYTOCHROME *c* BINDING TO WILD-TYPE AND MUTANT FLAVOCYTOCHROMES *b*2

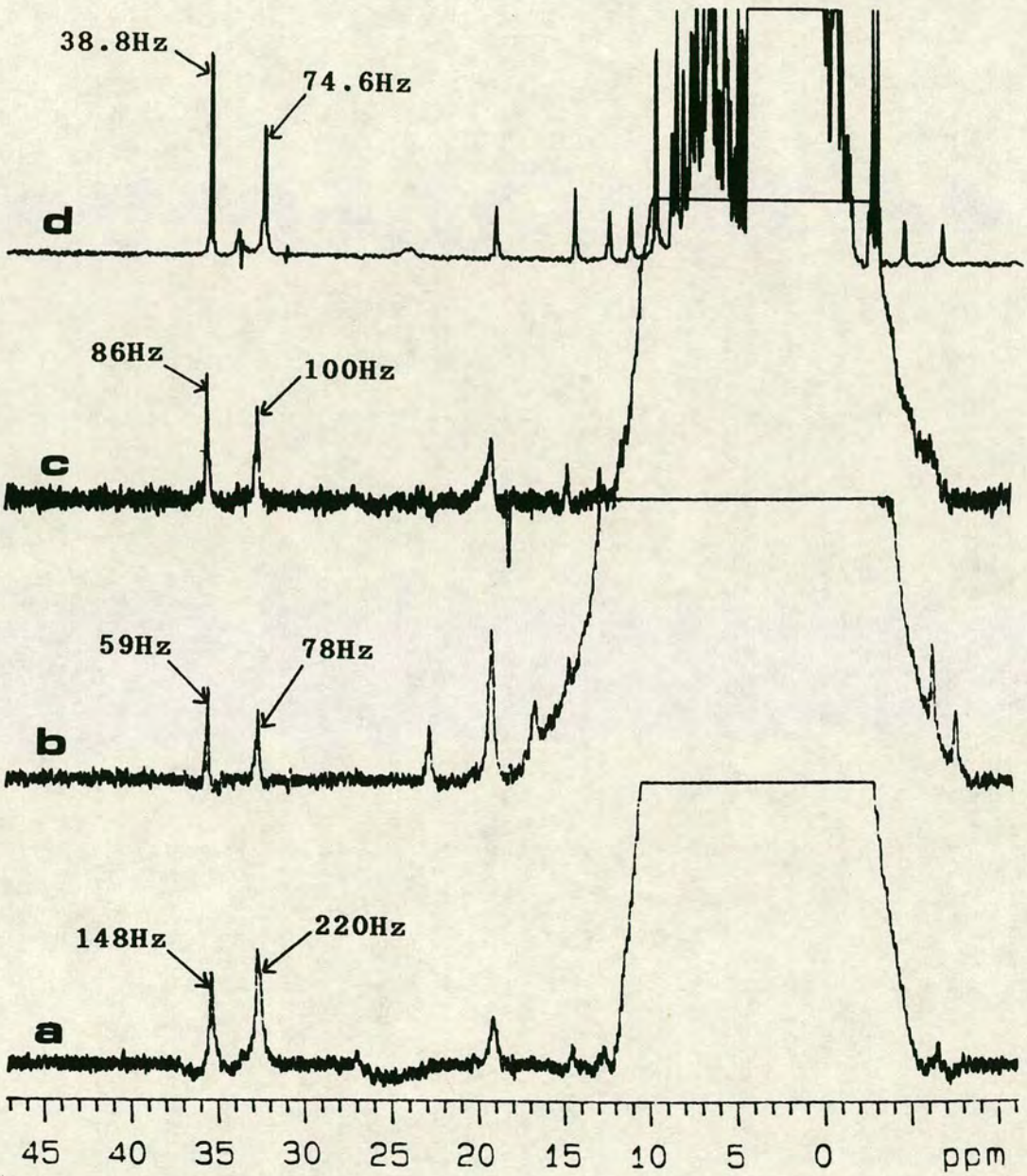

600MHz spectra were recorded at 25°C in 20mM phosphate/D_2O, pH 7.0. Each spectrum is of a 4:3 mixture of flavocytochrome *b*2 to cytochrome *c*. Spectrum (a) wild-type (b) hinge-swap (c) E509K and (d) is an electronic addition spectrum of free wild-type flavocytochrome *b*2 and cytochrome *c*.
The values given indicate the linewidths of the particular peaks.
Further experimental details are given in 5.2.4.

TABLE 5.2

LINEWIDTH BROADENING OF CYTOCHROME *c* HEME METHYL RESONANCES FOR WILD-TYPE AND MUTANT FLAVOCYTOCHROMES *b*$_2$

(a) RESONANCE AT 32.5ppm (HAEM METHYL-3)

[cyt.*c*] (mM)	1/[cyt.*c*] (mM^{-1})	LINEWIDTH (Hz)		
		WT	HINGE	E509K
0.1 (free)	0	74.6	74.6	74.6
0.6	1.67	202	110	95 (5)
0.4	2.50	215	94	100 (5)
0.3	3.33	220	78	100
0.2	5.00	300	102?	120
0.15	6.79	-	87?	112 (15)

(b) RESONANCE AT 35.5ppm (HAEM METHYL-8)

[cyt.*c*] (mM)	1/[cyt.*c*] (mM^{-1})	LINEWIDTH (Hz)		
		WT	HINGE	E509K
0.1 (free)	0	38.8	38.8	38.8
0.6	1.67	137	74	69 (5)
0.4	2.50	138	74	76 (5)
0.3	3.33	148	59	86
0.2	5.00	200	74	75
0.15	6.79	-	62	71 (15)

Abbreviations used : WT, wild-type; HINGE, hinge-swap mutant; E509K, point mutation in C-terminal tail; cyt.*c*, cytochrome *c*.

Experimental conditions : All proton NMR spectra were recorded at 25°C in 20mM phosphate/D_2O, pH 7.0. Linewidth broadening factors of 10Hz were applied to all resonances, with the exception of some of the resonances in the E509K spectra, which were as indicated in parentheses.

(Hz) versus 1/[cytochrome *c*] (mM^{-1}). These are shown in Figure 5.10. The degree of binding is indicated by the gradient of the line fitted to a linear regression analysis. The steepness of the gradient decreases in the order wild-type > E509K = hinge-swap. At present we can still only ascertain qualitative information from this data *i.e.* estimates of the relative strength of cytochrome *c* binding to the respective enzymes. The hinge-swap enzyme binds cytochrome *c* very weakly although this is probably not an accurate reflection of the contribution of the hinge region to cytochrome *c* binding in view of the large structural changes imposed. The E509K enzyme would appear to bind cytochrome *c* as weakly as does hinge-swap-b_2. One would not expect there to be major structural changes resulting from the point mutation in the E509K enzyme. The observed decrease in cytochrome *c* binding compared to the wild-type enzyme must be a direct consequence of the negative-to-positive (Glu→Lys) charge change which presumably results in electrostatic repulsion between cytochrome *c* and flavocytochrome b_2. This result supports the idea that the C-terminal tail, and in particular the region at the end of this tail, is crucial for cytochrome *c* binding.

FIGURE 5.10

PLOTS OF THE LINEWIDTHS OF NMR RESONANCES FOR HAEM METHYLS OF CYTOCHROME *c* VERSUS THE RECIPROCAL OF CYTOCHROME *c* CONCENTRATION

(a) HAEM METHYL-3 (32.5ppm)

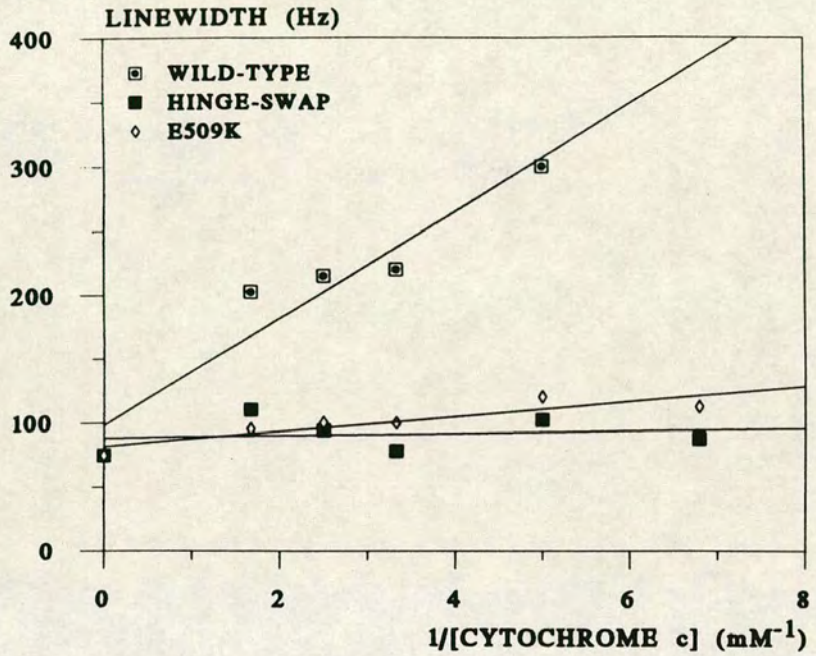

(b) HAEM METHYL-8 (35.5ppm)

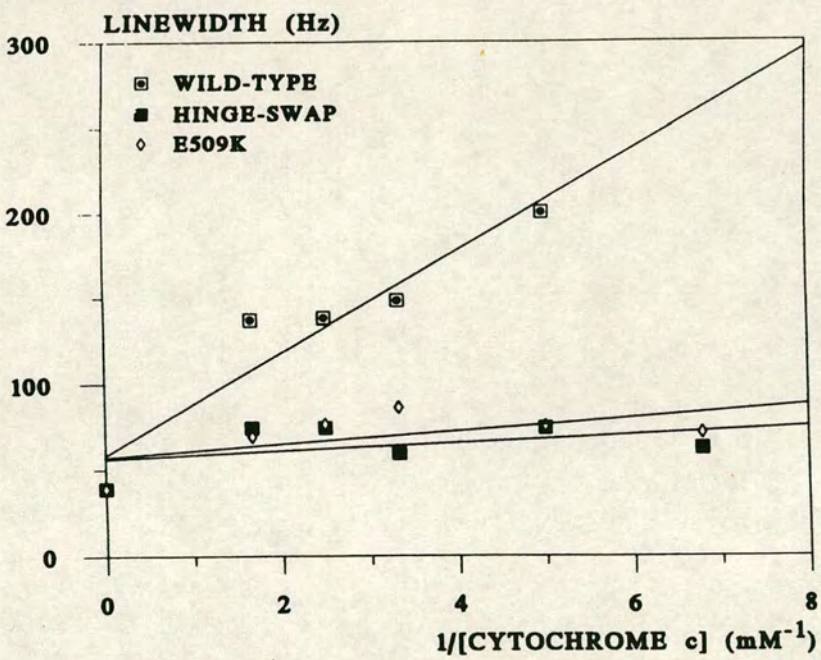

Experimental conditions are described in 5.2.4. The degree of binding of cytochrome *c* to each enzyme was assessed by gradient determination.

5.4 CONCLUSIONS

The following conclusions can be drawn from the investigation of intermolecular electron transfer discussed in this chapter:-

(1) the C-terminal tail, in particular the last three residues, is important for cytochrome *c* binding;

(2) structural integrity within the hinge region appears to be of importance for cytochrome *c* binding and electron transfer to the acceptor;

(3) a complex formed which possesses strong binding may not necessarily have the most efficient electron transfer *i.e.* it may not be the optimal catalytically-competent complex.

5.5 REFERENCES

(1) Prats, M., *Biochimie*, **60**, 77 (1978).

(2) Tegoni, M., Mozarelli, A., Rossi, G.L. and Labeyrie, F., *J.Biol.Chem.*, **258**, 5424 (1983).

(3) Baudras, A., Krupa, M. and Labeyrie, F., *Eur.J.Biochem.*, **20**, 58 (1971).

(4) Baudras, A., Capeillère-Blandin, C., Iwatsubo, M. and Labeyrie, F., in *"Structure and Function of Oxidation Reduction Enzymes"* (Åkeson, Å. and Ehrenberg, Å, eds.), pp.273, Pergammon, Oxford (1972).

(5) Yoshimura, T., Matsushima, A., Aki, K. and Kakiuchi, K., *Biochim.Biophys.Acta*, **492**, 331 (1977).

(6) Matushima, A., Yoshimura, T. and Aki, K., *J.Biochem.(Tokyo)*, **100**, 543 (1986).

(7) Vanderkooi, J.M., Glatz, P., Casadel, J. and Woodrow, G.V., *Eur.J.Biochem.*, **110**, 189 (1980).

(8) Iwatsubo, M., Mevel-Ninio, M. and Labeyrie, F., *Biochemistry*, **16**, 3558 (1977).

(9) Thomas, M.-A., Gervais, M., Favaudon, V. and Valat, P., *Eur.J.Biochem.*, **135**, 577 (1983).

(10) Tegoni, M., White, S.A., Roussel, A., Mathews, F.S. and Cambillau, C., *Proteins: Structure, Function and Genetics*, **16**, 408 (1993).

(11) Salemme, F.R., *J.Mol.Biol.*, **102**, 563 (1976).

(12) Sharp, R.E., White, P., Chapman, S.K. and Reid, G.A., *Biochemistry* (in preparation) (1993).

(13) Zoller, M.J. and Smith, M., *DNA*, **3**, 479 (1984).

(14) Sambrook, J., Fritsch, E.F. and Maniatis, T., *"Molecular Cloning: A Laboratory Manual"*, 2nd edition, Cold Spring Harbour Press, Cold Spring Harbour, NY (1989).

CHAPTER 6

EFFECT OF pH ON ELECTRON TRANSFER IN FLAVOCYTOCHROME *b*$_2$

6.1 INTRODUCTION

6.1.1 PREVIOUS WORK

In the early twentieth century Michaelis and Davidsohn (1) and Michaelis and Pechstein (2) suggested that the reversible loss of enzyme activity observed in more acidic or more basic solutions resulted from ionisation of acidic and basic groups in the enzyme which affected the reaction. Hence a plot of V_{max} versus pH would give a "bell-shaped" curve from which the ionisation constants of the two groups could be obtained using a suitable equation. This assumed that it was possible to distinguish between reversible loss of activity and irreversible loss of activity due to denaturation (3). The latter may be avoided by measuring relative activity immediately after the enzyme is subjected to the extreme pH *i.e.* no incubation period.

More detailed work on the effect of pH on the affinities of enzymes for substrates and inhibitors was published by Dixon in 1953 (4). In this work he presented a set of rules to facilitate interpretation of kinetic data in this field. The principle of his method was that if pK_M or log V_{max} are plotted against pH the resulting graph consists of a number of straight line portions interconnected by curves. The change in gradient of successive straight line portions is dependent on unit charge change of the enzyme and the point at which extrapolations of the straight line portions meet

corresponds to the pK_as of the groups concerned with enzyme-substrate complexation (pK_M versus pH plot) or involved in the enzyme-catalysed reaction (log V versus pH plot). At the time of writing this paper however Dixon could find very few examples of work on variation of K_M with pH.

In 1954 Alberty and Massey furthered this work by concentrating on the mathematical interpretation of the variation of maximal initial velocity (V_{max}) with pH, considering only irreversible activity loss (5). The result of their steady-state treatment, expressed in terms of the Michaelis equation (6) (see Appendix I) was as follows:-

$$v = \frac{V}{1 + K_M/[S]} \qquad \text{where } V = \frac{k_3[E_0]}{\{1 + [H^+]/K_{aES} + K_{bES}/[H^+]\}}$$

where
- v = initial velocity
- V = maximum initial velocity
- K_M = Michaelis constant
- $[S]$ = substrate concentration
- $[E]_0$ = initial enzyme concentration
- k_3 = rate constant between enzyme-substrate complex and products
- K_{aES}, K_{bES} = ionisation constants of E-S complex in acidic/basic regions

N.B. the denominator term shown in parentheses is known as the Michaelis pH function.

The classical treatment of hydrogen ion titration curves of globular proteins regarded the molecule as an impenetrable sphere with surface amino-acid residues grouped so as to give uniformly distributed charge (7). More recently, since pK_a perturbation of buried groups on globular proteins are complex functions of the size and shape of the protein and also of the ionic strength of

the solution (8), electrostatic theories have come into play which take into account these buried groups and solvent accessibility (9).

One of the first studies of the effect of pH on the proteolytically-cleaved form of flavocytochrome b_2 from baker's yeast was carried out by Boeri and Tosi (10) who investigated variation of pK values with differing external electron acceptors, postulating that their observed pK value of 5.65 was due to a group close to the active site.

In 1962, Hasegawa, studying the effects on the enzyme's activity over a pH range of 5.0 to 9.5 at 20°C using methylene blue as the electron acceptor, proposed an optimum pH of 7.2-7.6 (11). Table 6.1 summarises these and other findings.

Hinkson and Mahler investigated the effect of pH on the binding of different substrates (12). Their results implied the presence of a free group on the enzyme with a pK_a of 6.5-7.0, which could not be due to lactic acid (pK_a = 3.86 (13)). This moiety appeared to be concerned with binding the groups attached to the α-carbon of the substrate and product.

Ogura *et al.* used pH dependency as a key to obtaining an insight into the mechanistic action of yeast L-lactate dehydrogenase (14). They investigated the effect on the overall reaction in the pH range from 5.0 to 9.0, taking precautions to avoid the occurrence of irreversible activity loss. They observed an upward shift in the

TABLE 6.1

PREVIOUS pH STUDIES ON FLAVOCYTOCHROME *b*2

FORM OF ENZYME	pH_{opt}	TEMP. °C	pK_a	ELECTRON ACCEPTOR	REFERENCE
E-S	5.2	20	-	methylene blue	(17)
E-S	5.57	20	-	methylene blue	(18)
E-S	7.5	20	-	ferricyanide	(18)
E-S	8.0	20	-	ferricyanide	(19)
E-S	7.2-7.6	20	-	methylene blue	(11)
E-S	7.0-7.5	20	-	other e- acceptor	(11)
E	8.0	20	6.5-7.0	acceptor independent	(12)
E	8.0	20	6.3	ferricyanide	(12)
E-S	8.0	20	5.68	ferricyanide	(12)
E-S	7.2	25	5.2,8.9	other e- acceptors	(14)
E-S	7.2	15	5.1,9.2	other e- acceptors	(14)
E-S	7.2	15	6.0,9.2	ferricyanide	(14)
E-S	7.2	25	6.1	any acceptor	(15)
E-S	7.2	25	$5.3,9.7^{f}$	ferricyanide	(16)
E	7.2	25	$6.0,8.8^{h}$	ferricyanide	(16)

* other electron acceptors include thionine[11,14], methylene blue[14], cytochrome *c*[14] and 2-6-dichlorophenol-indophenol[14].

Superscripts f and h represent pK_a values pertaining to flavin and haem prosthetic groups respectively.
(E, enzyme; E-S, enzyme-substrate complex)

acidic pK_a value when decreasing the concentration of substrate used.

In a slightly later paper (15), Ogura *et al.*, on performing stopped-flow kinetic studies, observed that the rate of reduction of protohaem decreased with increasing hydrogen ion concentration in the medium, in other words the rate of flavin to haem electron transfer is pH dependent. Ogura along with Suzuki then went on to compare the effects of pH on the rates of reduction of both flavin and haem prosthetic groups (16). They found pK values for both the enzyme-substrate complex and for the oxidised enzyme unit. Hence they postulated that there were two kinds of ionisable groups in the enzyme unit which were essential for activity; the acidic values being due to the imidazole of a histidine and the basic values to amino groups in the protein moiety of the enzyme unit. They also suggested that hydrogen transfer from the substrate to bound FMN was inhibited by association and dissociation of the protons of these essential groups.

6.1.2 PRESENT WORK

Although enzymes contain many ionizing groups, plots of maximal rate versus pH are usually in the form of simple single or double ionisation curves, inferring that the only ionisations which are of importance are those directly involved at the active site or those groups

concerned with maintaining the active conformation of the enzyme. Studies of the effects of pH on kinetic parameters can therefore be very useful in determining which residues are directly involved in substrate binding and in the elucidation of the subsequent catalytic mechanism.

Most enzymes are only active over a narrow pH range, having a definite pH optimum with sharp activity falloff on either side of this point. This optimum is due to a combination of several effects:-

(a) loss of enzyme stability at pH extremes due to irreversible structural damage, for example, disruption of tertiary structure by charging or discharging of ionisable groups;

(b) lowered affinity of the enzyme for substrate at non-optimum pHs where substrate saturation may be significantly altered;

(c) alteration of mode and strength of substrate binding to the enzyme and on reactivity in catalysis.

The first two of these effects can easily be distinguished and compensated for experimentally; the first by measuring activities immediately after the enzyme is subjected to the extreme pH, and the second by ensuring that highly saturating concentrations of substrate are used at all pH values.

It is with this in mind that a study of the effect of pH on the kinetic behaviour of wild-type flavocytochrome *b*$_2$ from *Saccharomyces cerevisiae* was undertaken. The active

site residues thought to be of most importance for binding of substrate are His-373, Tyr-254, Tyr-143 and Arg-376. Ionisation of these side-chains must therefore be of great significance in catalysis. To investigate the mechanism of action of the enzyme and to elucidate the important ionising groups, wild-type and enzymes with point mutations of the above residues were studied. The mutations investigated were Tyr143→Phe (Y143F-*b*2), Tyr254→Phe (Y254F-*b*2) and His373→Gln (H373Q-*b*2). A point mutation of Arg-376 has been constructed, namely Arg-376→Lys, but this enzyme has no measurable activity. These point mutants have previously undergone full kinetic characterisation (20) and the resulting information regarding the importance of these residues at the active site is summarised in Section 1.7.2.2. Since each amino-acid side-chain gives rise to a particular pK_a value, we can postulate that any difference in pK_a in a mutant compared to the wild-type would be due to lack or gain of ionisable side-chain at that point - implying that particular residue's catalytic importance.

Previously pK_a values of 4.8 and 4.6 had been obtained for the haem propionates of the isolated cytochrome *b*2 core domain using NMR spectroscopy (21). These were consistent with the propionate groups being exposed to solvent (Section 1.6.3.4). As Y143 is both an active site residue and is in contact with haem propionate-7, an NMR/pH study of WT and various mutants may be

informative. Resonances in the proton NMR spectrum of the wild-type tetrameric protein (M_R 230kDa) are too broad to notice subtle chemical shift changes. However NMR spectroscopy can and has been used to follow a pH titration of the monomeric form of tail-deleted flavocytochrome *b*2 (M_R 55kDa) (TD-*b*2) which has a 23 amino-acid deletion of the C-terminal tail (22).

It is important to note that all previous pH studies on flavocytochrome *b*2, as reported above, were carried out on the proteolytically "cleaved" form of the enzyme; this study is carried out on the recombinant intact enzyme.

In our study several assumptions were made in order to simplify kinetic analysis (23):-

(i) the ionising groups act as perfectly titrating acids and bases;

(ii) only one ionic form of the enzyme is active;

(iii) all intermediates are in protonic equilibrium *i.e.* chemical steps are slower than proton transfer;

(iv) the rate determining step does not change with pH, although this may break down with interesting consequences.

6.2 EXPERIMENTAL

6.2.1 CONSTRUCTION OF THE MUTANT ENZYMES (DRS.M.T.BLACK AND F.D.C.MANSON)

Y143F-*b*2, Y254F-*b*2, TD-*b*2 (Dr.M.T.Black) and H373Q-*b*2

(Dr.F.D.C.Manson) were generated by site-directed mutagenesis, using the double primer method of Zoller and Smith (24) as described in (25). The oligonucleotides used were synthesised on an Applied Biosystems model 380B DNA synthesiser and were as follows :- Y143F-*b*2 (GTGGGCCTTCTATTCCT), Y254F-*b*2 (CCAACTATTTGTTAACTC), TD-*b*2 (GAACAGTTTGAGTACCA) and H373Q-*b*2 (TCCAATCAAGGTGGTAG). Wild-type flavocytochrome *b*2 and all the mutant enzymes were over-expressed in *E.coli* as described in (25), producing vastly increased yields over isolation from yeast.

6.2.2 ENZYME PREPARATION AND PURIFICATION

The point mutation enzymes (Y143F, Y254F and H373Q), along with the wild-type enzyme, were isolated from *E.coli* and purified on hydroxylapatite columns as described in Section 7.4.4. The pure enzyme could then be stored without significant activity loss for approximately one month as a 70% ammonium sulphate precipitate at 0-4°C under nitrogen. The purification for TD-*b*2 differed slightly in that conditions of lower ionic strength were required in order for the enzyme to bind to the hydroxylapatite column (Section 4.3.4) and this enzyme was particularly unstable with respect to FMN loss.

6.2.3 KINETIC ANALYSIS

All steady-state experiments were carried out at 25±0.1°C using ferricyanide as the external electron acceptor, as described in Section 7.8.3. All activity measurements were made at constant ionic strength, I=0.1M. Due to the wide pH range used (4 to 13) several buffering systems were used, as detailed in Figure 6.1. Full nomenclature and method of preparation of buffers is given in Section 7.2.

Activity measurements were made at 10mM L-[2-^{1}H]-lactate, *i.e.* under saturating substrate conditions, to obtain pH profiles for WT, Y143F, Y254F and H373Q. Michaelis constants (K_M) were determined over the pH range in which there was measurable activity for WT and Y143F.

Pre-steady-state kinetics (stopped-flow) (Section 7.9) were used to measure kinetic isotope effects (KIE) at 25±0.1°C for both flavin and haem prosthetic groups, using 15mM L-[2-^{1}H]- and L-[2-^{2}H]-lactate; the latter being synthesised and purified as described in Section 7.7.2. The isotope effects were measured at pH values of 5.0 (phthalate), 7.5 (tris-HCl) and approximately 9.7 (CAPS); the latter being achieved by a "pH-jump" whereby enzyme at pH 9.0 is simultaneously rapidly-mixed with substrate at pH 11.0.

6.2.4 NMR SPECTROSCOPY

Highly purified tail-deleted flavocytochrome *b*$_2$ (TD-*b*$_2$)

FIGURE 6.1

BUFFERS USED AND THEIR pH RANGE

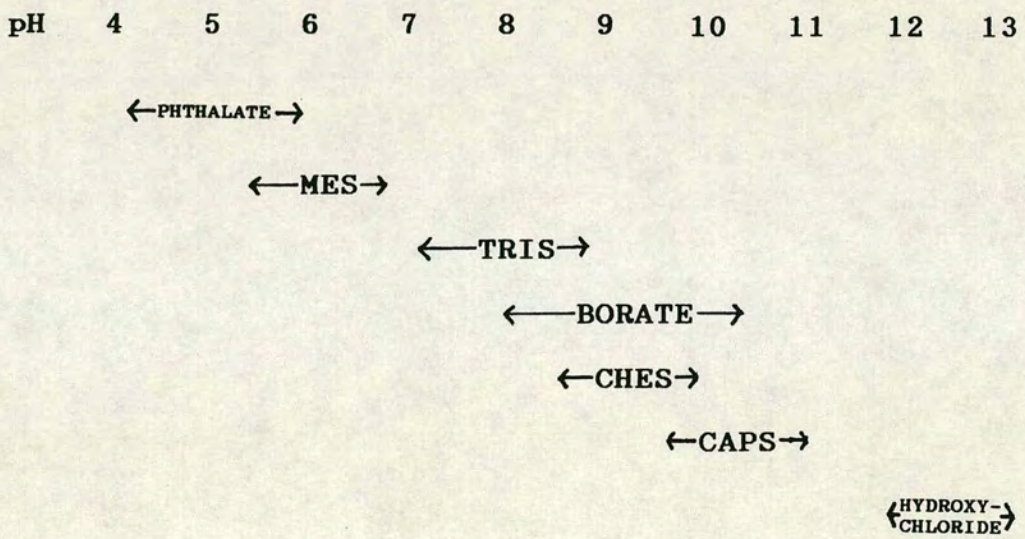

Buffer preparation is described in Section 7.2

was exchanged into D_2O as described in Section 7.12.3 and 1D proton NMR spectra were recorded at 25°C using a Varian VXR 600S spectrometer operating at 600MHz. The D_2O peak occuring at 4.8 (pH 7,25°C) was used as a reference peak. A stationary peak was then identified in each of the *b*2 spectra, probably due to a solvent impurity, which was then referenced to the D_2O peak. A pH titration was observed by acidification of the sample by addition of small aliquots of a 1% solution of DCl. Reported pH values were recorded directly from the meter and were not corrected for the small isotope effect - they are hence designated pH*.

6.3 RESULTS AND DISCUSSION

6.3.1 STEADY-STATE KINETICS

In accordance with the effects discussed in Section 6.1, all steady-state experiments were carried out under saturating substrate concentrations. Enzyme activity was measured immediately after exposure to the extreme pH by means of injecting a small amount of enzyme stock solution, kept at pH 7.5, into the relatively large volume of the assay vial which was at the pH under investigation.

The effects of pH on wild-type flavocytochrome *b*2 were examined first in order to obtain a basis for comparison of the mutants and to ensure the validity of the buffer systems chosen. Values of V_{max} were determined over the

pH range 4-11.5, statistical analysis of which produced a typical symmetrical bell-shaped curve (Figure 6.2) from which pK_a values for the enzyme-substrate complex of 5.40 ± 0.12 and 10.92 ± 0.11 were calculated using a non-linear least squares regression programme (Table 6.2).

Due to the amount of activity still remaining at pH 11.5, the pH range was extended by use of hydroxy-chloride buffer (pH 12-13), however at such extremities of pH enzyme activity was very low and hence difficult to measure to any degree of accuracy.

Values of K_M were determined over the entire pH range except where activity was too low to be measured, and a plot of K_M versus pH allowed calculation of pK_a values in good agreement with those obtained from V_{max} data (see Figure 6.3 and Table 6.2). The pH dependencies of both V_{max} and K_M are concerned with the enzyme-substrate complex *i.e.* ionisation of groups involved in both substrate binding and catalysis. Providing that the substrate is non-ionising those groups involved in substrate binding alone may be identified from the observed pK_a by plotting the reciprocal of K_M versus pH. For wild-type flavocytochrome *b*$_2$ this results in a biphasic plot at high pH producing a new pK_a value of 8.15 ± 0.02, as determined by the method of Dixon (4) (see Figure 6.4). Assuming that the higher pK value is due to protein denaturation, the original value of 10.92 ± 0.11, as observed on the V_{max}/pH plot, must be a combination of effects due to this newly found ionising group and

FIGURE 6.2

DEPENDENCE OF MAXIMAL RATE WITH pH FOR WILD-TYPE FLAVOCYTOCHROME *b*$_2$

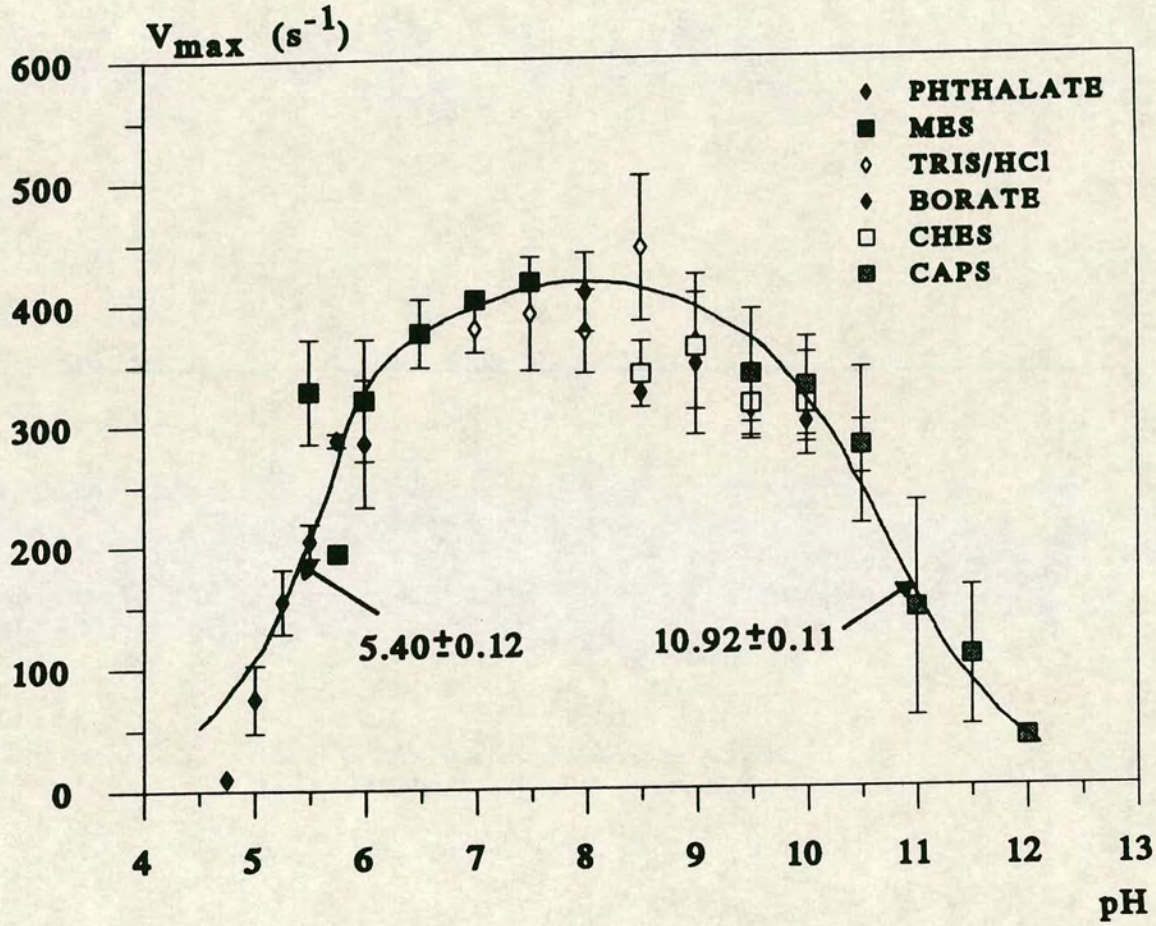

Experimental conditions : Kinetic data were obtained from the steady-state reduction of ferricyanide under saturating conditions at 25±0.1°C in the appropriate buffer (I=0.1M) as indicated by the above key.
Error bars indicate averaging of data collected at the particular pH value.
Further experimental details can be found in 6.2.3.
Values shown correspond to the calculated pK$_a$ values (Table 6.2)

TABLE 6.2

CALCULATED pKa VALUES FROM PLOTS OF KINETIC PARAMETERS VERSUS pH

ENZYME	SOURCE	pKa VALUES		
WT	V_{max}	5.40±0.12	-	10.92±0.11
	K_M	4.69±0.38	-	11.09±0.10
	$1/K_M$	6.30±0.08	8.15±0.02	10.43±0.20
Y143F	V_{max}	4.75±0.20	8.87±0.51	11.88±0.64
	K_M	5.73±0.38	-	-
	$1/K_M$	6.25±0.10	-	-
Y254F	V_{max}	4.87±0.09	-	12.36±0.23

Experimental conditions : Data were obtained from the steady-state reduction of ferricyanide under saturating conditions at 25±0.1°C in the appropriate buffer, I=0.1M. Further details can be found in 6.2.3.

FIGURE 6.3

DEPENDENCE UPON pH OF THE MICHAELIS CONSTANT FOR WILD-TYPE FLAVOCYTOCHROME *b*2

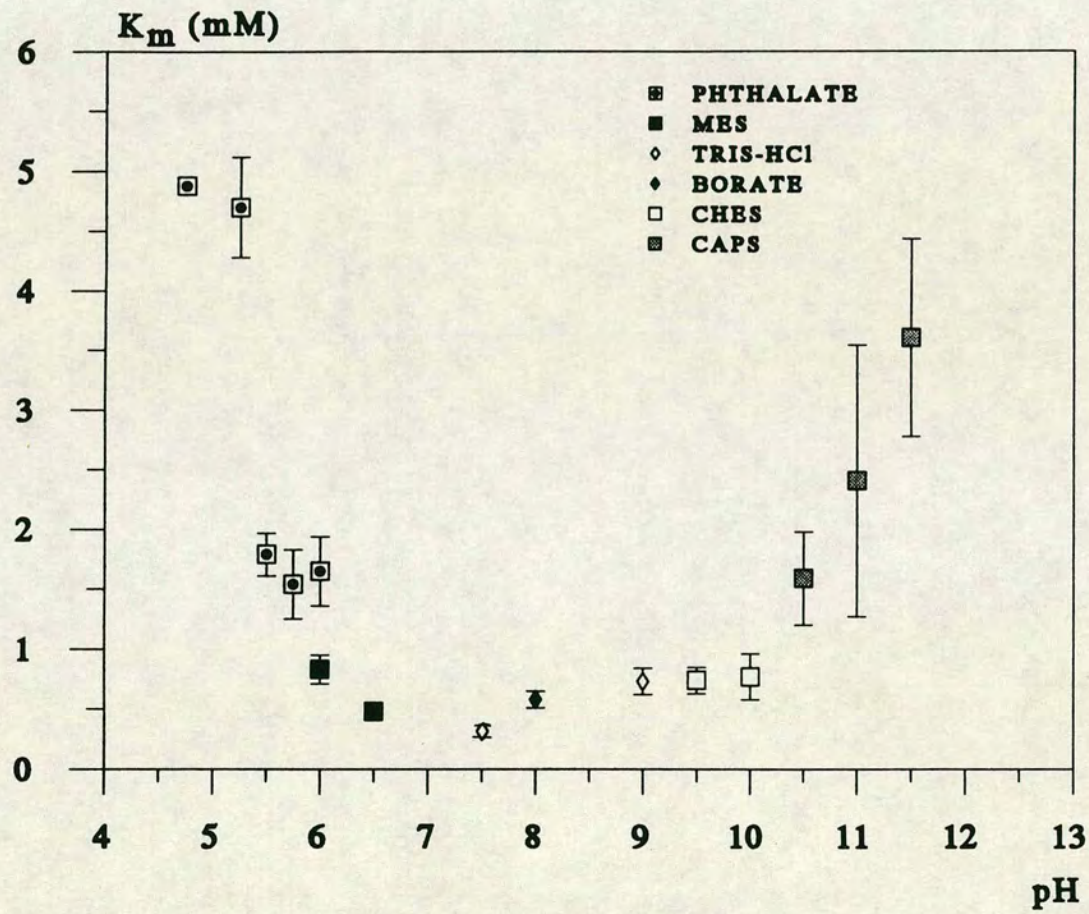

Experimental conditions : Data were obtained from Michaelis-Menten plots for the steady-state reduction of ferricyanide with L-[2-^{1}H]-lactate. Experiments were carried out at 25±0.1°C in the buffer indicated (I=0.1M). Error bars indicate averaging of data collected at particular pH value.
Further experimental details can be found in 6.2.3.

FIGURE 6.4

DEPENDENCE UPON pH OF THE RECIPROCAL OF THE MICHAELIS CONSTANT FOR WILD-TYPE FLAVOCYTOCHROME b_2

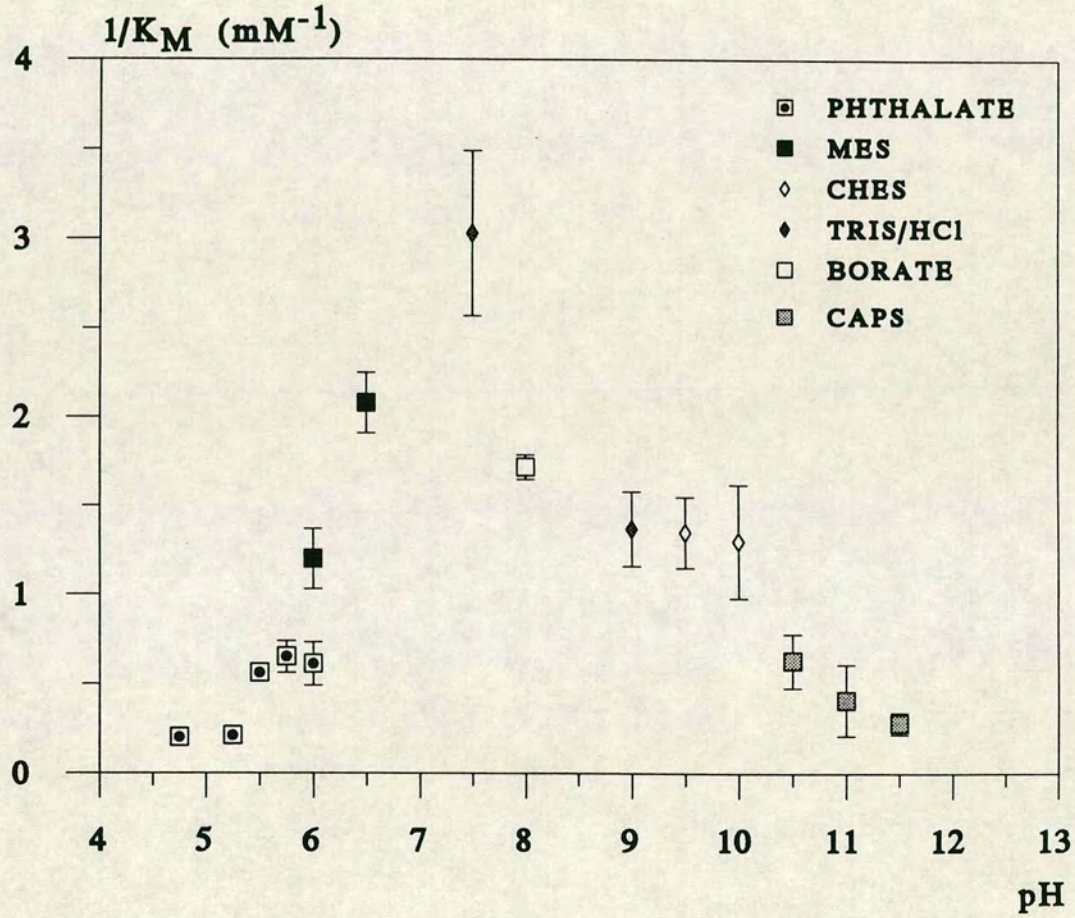

Experimental conditions : Data were obtained from Michaelis-Menten plots for the steady-state reduction of ferricyanide with L-[2-^{1}H]-lactate. Experiments were carried out at 25±0.1°C in the buffer indicated (I=0.1M). Error bars indicate averaging of data collected at particular pH value.
Further experimental details can be found in 6.2.3.

denaturation.

At this stage we could postulate that the pK_a value observed at low pH (5.40±0.12), which is in agreement with that of Suzuki and Ogura (16), is due, at least in part, to protonation of the active-site histidine (His-373) since free histidine has a pK_a value of 6.04 (26). The most obvious mutant enzyme to study to confirm this would be H373Q-*b*2. Replacement of the active site base results in an enzyme with a drastically decreased rate of L-lactate dehydrogenation, in fact 10^4 times slower than wild-type. Such residual rates were impossible to measure to any degree of accuracy hence this pK_a could not be categorically assigned to protonation of His-373 on the basis of steady-state data. Further analysis (pre-steady-state and NMR studies) were necessary in order to confirm or discount this and the results from these studies are reported later.

Considering the higher pH region, substrate ionisation can categorically be eliminated for the pK value of 8.15±0.02 since free lactic acid has a pK_a of only 3.86 (13). The observed pK_a must therefore be due to ionisation of a group important for substrate binding within the free enzyme, for example, a tyrosine residue. The crystal structure shows two tyrosine residues located at the active site (30), both of which play important roles in complexation and catalysis. These are Tyr-143 and Tyr-254; the hydrogen bonding capability of these residues has been removed by replacing tyrosine with

phenylalanine using the technique of site-directed mutagenesis. Kinetic investigation of these mutant enzymes (Y143F and Y254F) should enable us to determine whether either of these residues are responsible for the observed pK_a value.

Kinetic parameter versus pH plots were obtained for Y143F-*b*2. The plot of V_{max} versus pH (Figure 6.5) showed a biphasic curve at high pH as did the plot of $1/K_M$ versus pH for wild-type. The pK value at low pH, 4.75 ± 0.20, was similar to that obtained for wild-type, any difference possibly being due to a disruption of the hydrogen bonding network involving Tyr-143, which includes a direct hydrogen bond to haem propionate-7 as described in more detail in 6.3.3. Again, the value at very high pH can be ascribed to denaturation. However, the appearance of a pK_a at 8.87 ± 0.51, which is within experimental error the same as that for wild-type, leads us to believe that Tyr-143 is not the group identified as being important for substrate binding since removal of its hydrogen-bonding capability has not affected the pK_a observed for wild-type. In other words, there is another group which is more important for substrate binding than Tyr-143, this could possibly be Tyr-254. A V_{max} versus pH plot for Y254F-*b*2 (Figure 6.6) supports this as the enzyme has increased resistance to high pH with a pK so high that it must be predominantly due to denaturation and there is no evidence of the presence of the ionising group responsible for the pK value of ~8.

FIGURE 6.5

DEPENDENCE OF MAXIMAL RATE ON pH FOR Y143F FLAVOCYTOCHROME *b*$_2$

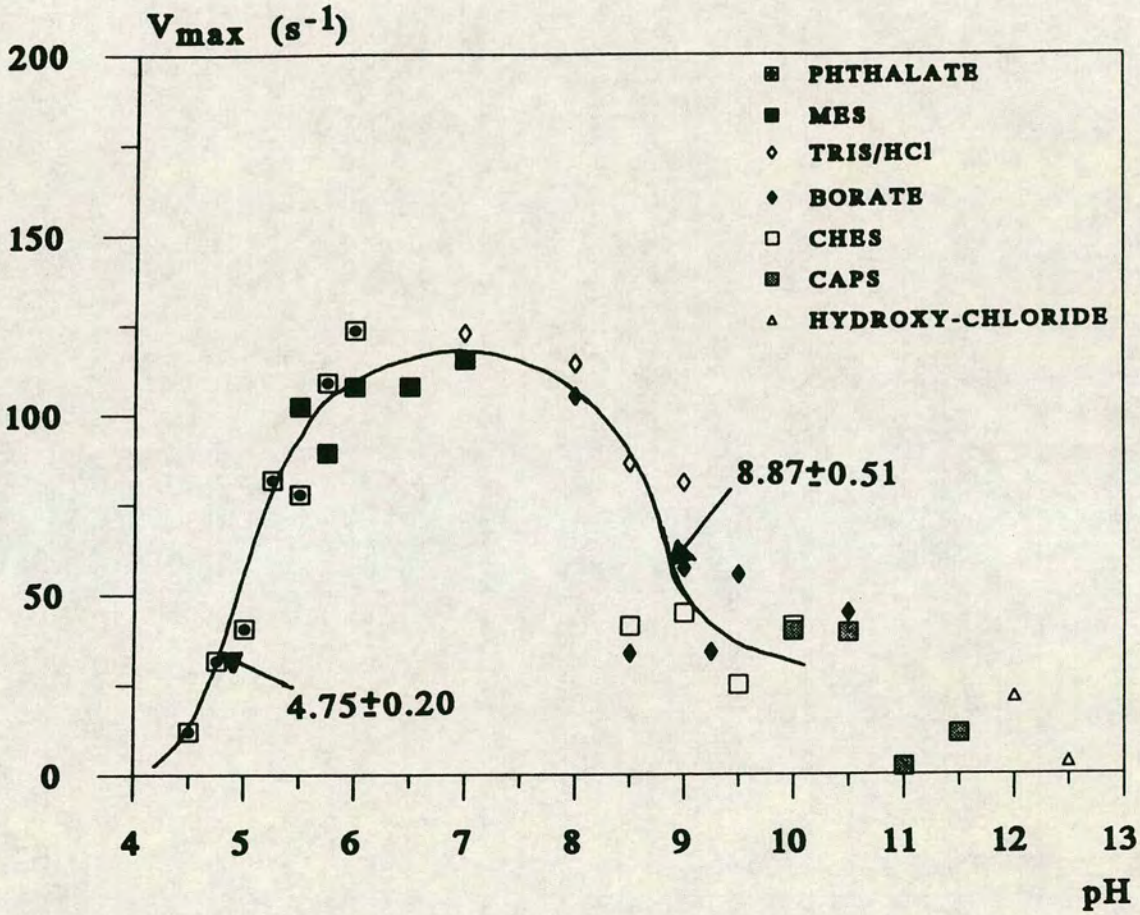

Experimental conditions : Kinetic data were obtained from the steady-state reduction of ferricyanide under saturating conditions at 25±0.1°C in the appropriate buffer (I=0.1M) as indicated by the above key.
Further experimental details can be found in 6.2.3.

Values shown correspond to the calculated pK_a values (Table 6.2)

FIGURE 6.6

DEPENDENCE OF MAXIMAL RATE WITH pH FOR Y254F FLAVOCYTOCHROME *b*2

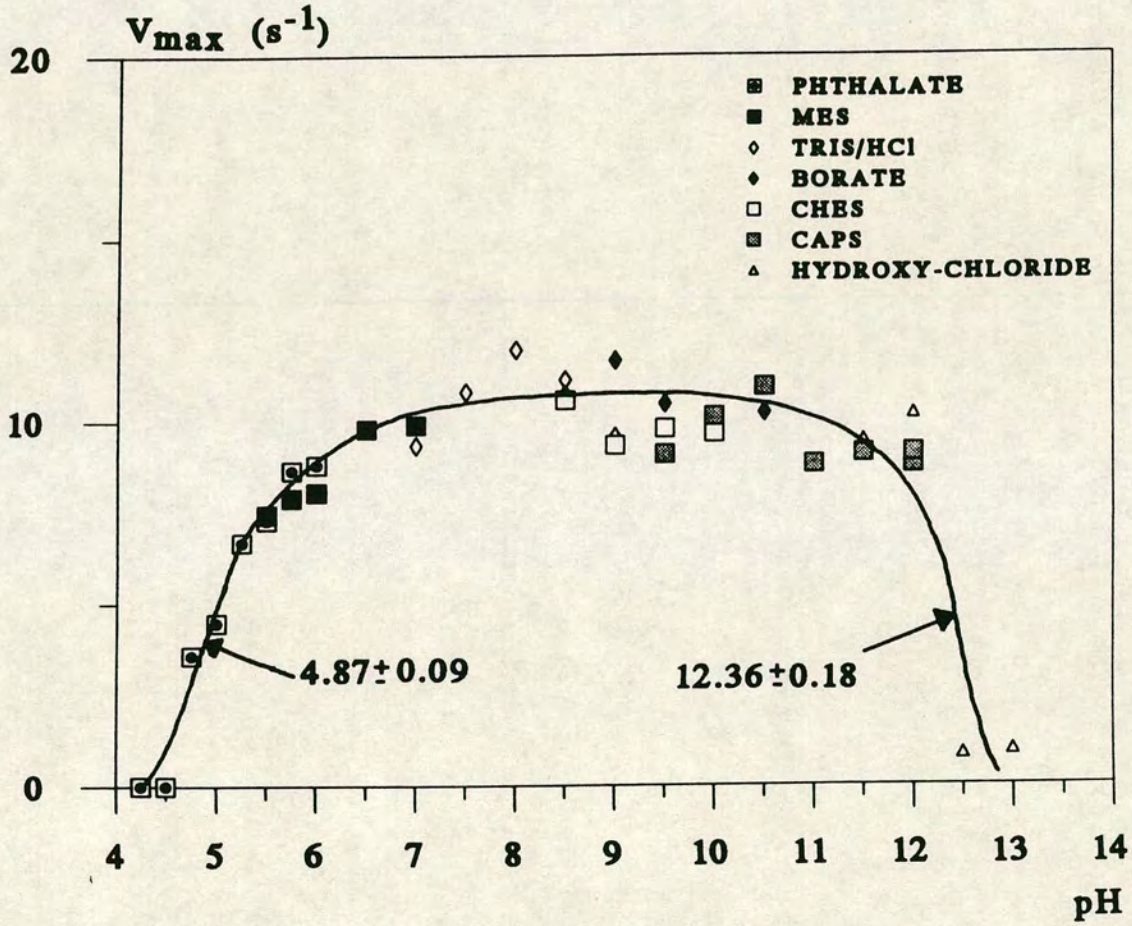

Experimental conditions : Kinetic data were obtained from the steady-state reduction of ferricyanide under saturating conditions at 25±0.1°C in the appropriate buffer (I=0.1M) as indicated by the above key.
Further experimental details can be found in 6.2.3.
Values shown correspond to the calculated pKa values (Table 6.2)

Suzuki and Ogura (16) found a pK_a of 8.8 for the free "cleaved" enzyme-unit when using stopped-flow to monitor reduction of the prosthetic groups. They attributed this pK_a to ionisation of amino-groups in the free enzyme, which could result in the inhibition of substrate to FMN electron transfer.

Efficiency plots (k_{cat}/K_M versus pH) for both wild-type and Y143F-*b*2 are shown in Figure 6.7. Both followed similar shapes, having a definite optimum and an apparent biphasic nature at high pH. Optimal pH was found to be 7.5 for both enzymes although Y143F-*b*2 appears to have a wider range at the optimum of *c.a.* pH 6-8.

All of the above experiments were carried out using ferricyanide as the external electron acceptor. This is preferable to using the physiological acceptor, cytochrome *c*, since cytochrome *c* has many ionising groups of its own which may interfere with the determination of pK_a values due solely to groups within flavocytochrome *b*2.

6.3.2 STOPPED-FLOW KINETICS

Stopped-flow (pre-steady-state) kinetics allows collection of a large amount of data over a single turnover. This enables reduction of both the flavin and haem prosthetic groups to be monitored by observing the change in absorbance at a haem isosbestic (438.3nm) for the former and at haem peaks (557/423nm) for the latter.

FIGURE 6.7

CATALYTIC EFFICIENCIES OF WILD-TYPE AND Y143F FLAVOCYTOCHROMES *b*2 UNDER VARYING pH CONDITIONS, EXPRESSED AS THE RATIO k_{cat}/K_M

(a) WILD-TYPE

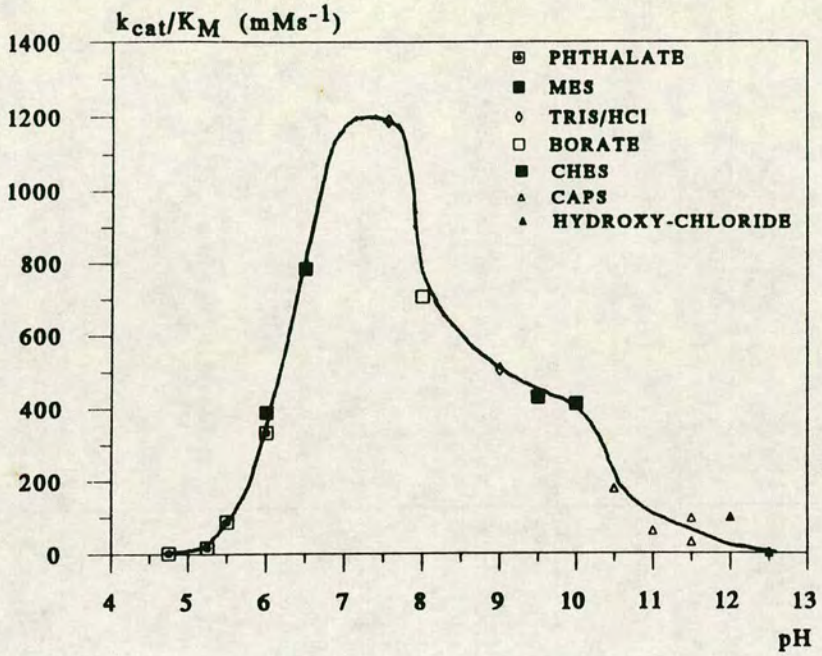

(b) Y143F

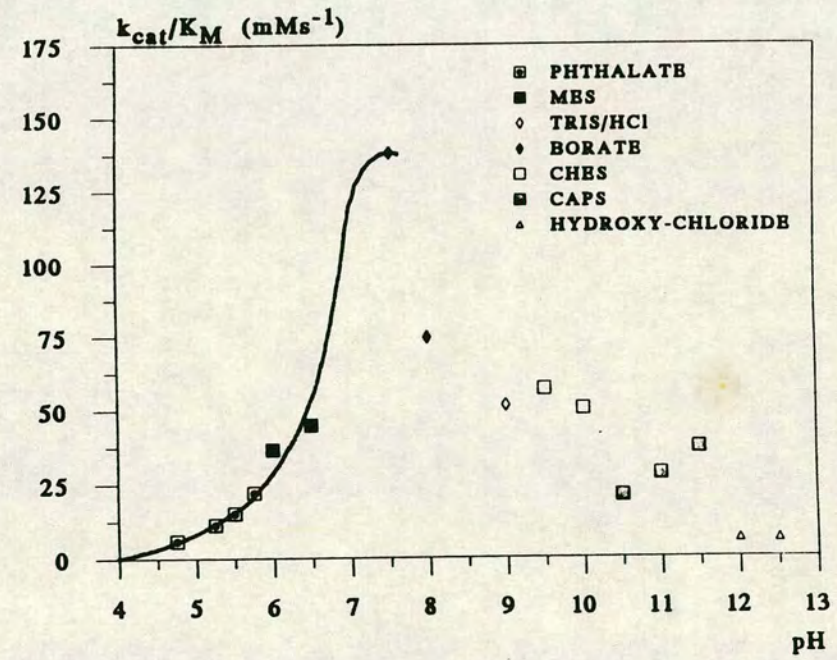

Experimental conditions : Data were obtained from Michaelis-Menten plots for the steady-state reduction of ferricyanide with L-[2-^{1}H]-lactate. Experiments were carried out at 25±0.1°C in the buffer indicated (I=0.1M). Further experimental details can be found in 6.2.3.

Typical traces for these reductions are illustrated in previous chapters.

Kinetic isotope effects (KIEs) can be observed by comparing rate constants with L-[2-^{1}H]-lactate to those obtained with L-[2-^{2}H]-lactate *i.e.* lactate which has been deuterated at the C-2 position. A value greater than two for this ratio constitutes a significant isotope effect. A previous study on *S.cerevisiae* wild-type-b_2 (28) resulted in values for the KIE for each step in the catalytic cycle as shown in Figure 6.8. It can be seen that for the first step in catalysis, flavin reduction, there is a KIE value of 8.1±1.4, indicating that, over the flavin reduction timescale, abstraction of the C-2 hydrogen is totally rate-limiting, this observation was in accordance with previous results (27). The fact that the isotope effect erodes along the electron transport chain, still having a significant value for cytochrome *c* reduction of 3.0±0.5, proves that the overall rate-limiting step in the catalytic cycle is abstraction of the hydrogen at C-2 of lactate by the active site base, His-373. A similar study was performed on the Y143F enzyme (28), results for which are shown in Figure 6.8. Abstraction of the C-2 hydrogen of lactate is still rate-limiting over the timescale for flavin reduction, but the large drop in KIE value from 6.3±1.2 to 1.6±0.5 for haem reduction, and subsequently cytochrome *c* reduction, proves that the overall rate-limiting step in the catalytic cycle is now flavin to haem electron transfer.

FIGURE 6.8

COMPARISON OF THE DEUTERIUM KINETIC ISOTOPE EFFECTS FOR WILD-TYPE AND Y143F FLAVOCYTOCHROMES *b*$_2$

This information comes from reference 28.

WILD-TYPE	8.1±1.4	6.3±1.2	3.0±0.6
L-LACTATE--------->FLAVIN---------->HEME--------->CYTOCHROME *c*			
Y143F	4.3±0.8	1.6±0.5	1.7±0.5

By measuring KIE values for reduction of the prosthetic groups of the WT, Y143F and Y254F enzymes at differing pH values, any pH-induced changes in rate-limitation will become evident. The pH values used were 5.0, 7.5 and approximately 9.7. The latter being achieved by the "pH-jump" as described in 6.2.4. The basis behind such a jump is that diffusion-controlled rate is much faster than enzyme turnover hence the rate of diffusion of the two differing pH buffers is much faster ($>10^8 s^{-1}$) than any chemical step, thus the enzyme will react at the desired pH.

Results obtained for WT-b_2 at 25$\pm$0.1°C are shown in Table 6.3. Curves were fitted to double exponentials since at high lactate concentrations both flavin and haem reductions are biphasic. The first fast phase is due to the initial reduction and the second slower phase occurs as a result of inter-subunit electron transfer. This slow phase is kinetically irrelevant as already described in Section 1.7.3, hence only the fast phase corresponding directly to the reduction in question has been used to calculate the KIE values, by taking a fixed percentage of the reaction. The KIE values at pH 7.5 agree, within experimental error, to those reported previously (28). In all cases the rate of flavin reduction is faster than the rate of haem reduction as expected. The KIE value for flavin reduction shows values greater than 6 at all pH values indicating that, over the flavin reduction timescale,abstraction of the C-2 hydrogen of L-lactate is

TABLE 6.3

EFFECT OF pH ON PROSTHETIC GROUP REDUCTION AS OBSERVED BY VARIANCE IN KINETIC ISOTOPE EFFECTS

pH	ENZYME	FLAVIN REDUCTION	HAEM REDUCTION
5.0	WT	6.61±0.32	2.41±0.08
5.0	Y143F	3.48±0.03	1.32±0.03
7.5	WT	8.45±0.20	6.45±0.16
7.5	Y143F	4.03±0.05	1.76±0.03
9.65	WT	8.11±0.34	6.09±0.12
9.52	Y143F	3.22±0.09	1.55±0.05

Experimental conditions : Kinetic isotope effects were measured under stopped-flow conditions at 25±0.1°C in the appropriate buffer using saturating concentrations of L-[2-^{1}H]- and L-[2-^{2}H]-lactate. The wavelength of observation was 438.3nm for flavin reduction and either 423 or 557nm for haem reduction. Further experimental details are given in 6.2.3 and 7.9.

rate-limiting and in the case of pH 7.5 and 9.65 this step is rate-limiting for the entire catalytic cycle. This observation clearly rules out any contribution from protonation of His-373 to the pK_a of 5.40±0.12 observed for wild-type under steady-state conditions. However at pH 5.0 the KIE for haem reduction has decreased to 2.41±0.08, this is a barely significant isotope effect and suggests that, at this low pH, flavin to haem electron transfer is making a more important contribution to rate-limitation; in other words protonation of a residue lying between the two prosthetic groups, such as Tyr-143 or the haem propionates, is responsible for the pK_a of 5.40±0.12.

The results obtained for Y143F-*b*2 are also shown in Table 6.3 and those at pH 7.5 again show good agreement to those reported in (28) *i.e.* that the rate-limiting step in Y143F is flavin to haem electron transfer, and this is unaltered over the pH range from 5.0 to 9.6. Preliminary data for Y254F-*b*2 showed that there did not appear to be any pH-induced change in rate-limitation.

6.3.3 NMR SPECTROSCOPY

Initial NMR studies on flavocytochrome *b*2 from *S.cerevisiae* have already been discussed in Section 1.6.3.4. NMR spectroscopy has been carried out on the isolated *b*2 cytochrome domain (cytochrome *b*2 core), and by means of a combination of techniques including 2D-NMR,

the haem resonances have been assigned (21). These assignments are illustrated in Figures 6.9 and 6.10 and in Table 6.4. The cytochrome *b*2 core shows high stability to pH, the optical spectrum being unaltered over the pH range 4 to 10. This enabled determination of pK_a values for both of the haem propionate groups by use of high-field NMR (21). Figure 6.11 shows a range of spectra in the highly-shifted upfield region, 8-30 ppm, produced with differing pH*. The haem propionate peaks are labelled 1a,1b,2a and 2b and their positions shift significantly with decreasing pH*, as they pick up hydrogen ions from solution and the protons of the group undergo changes in chemical environment. By plotting chemical shift versus pH*, typical sigmoidal curves are obtained, as shown in Figure 6.12, for haem propionate resonances 1a and 2a (corresponding to haem propionates-7 and -6 respectively). These curves may be analysed by means of Hill plots, which are plots of pH* against a logarithmic function of chemical shift, as shown in Figure 6.13. Both propionates give linear plots with gradients equal to one, indicative of a single ionisation. The intercepts with the pH*-axis result in two pK_as of 4.80 and 4.56 for haem propionates-7 and -6 respectively. Values which are consistent with the propionates being exposed to solvent (*c.f.* pK_a of ~4.8 for free porphyrin propionic groups in water (29)) as predicted by X-ray crystallography.

Values for the exposed propionates in the cytochrome *b*2

FIGURE 6.9

THE PROTOHAEM IX PROSTHETIC GROUP SHOWING AXIAL LIGANDS AND HAEM PROTONS

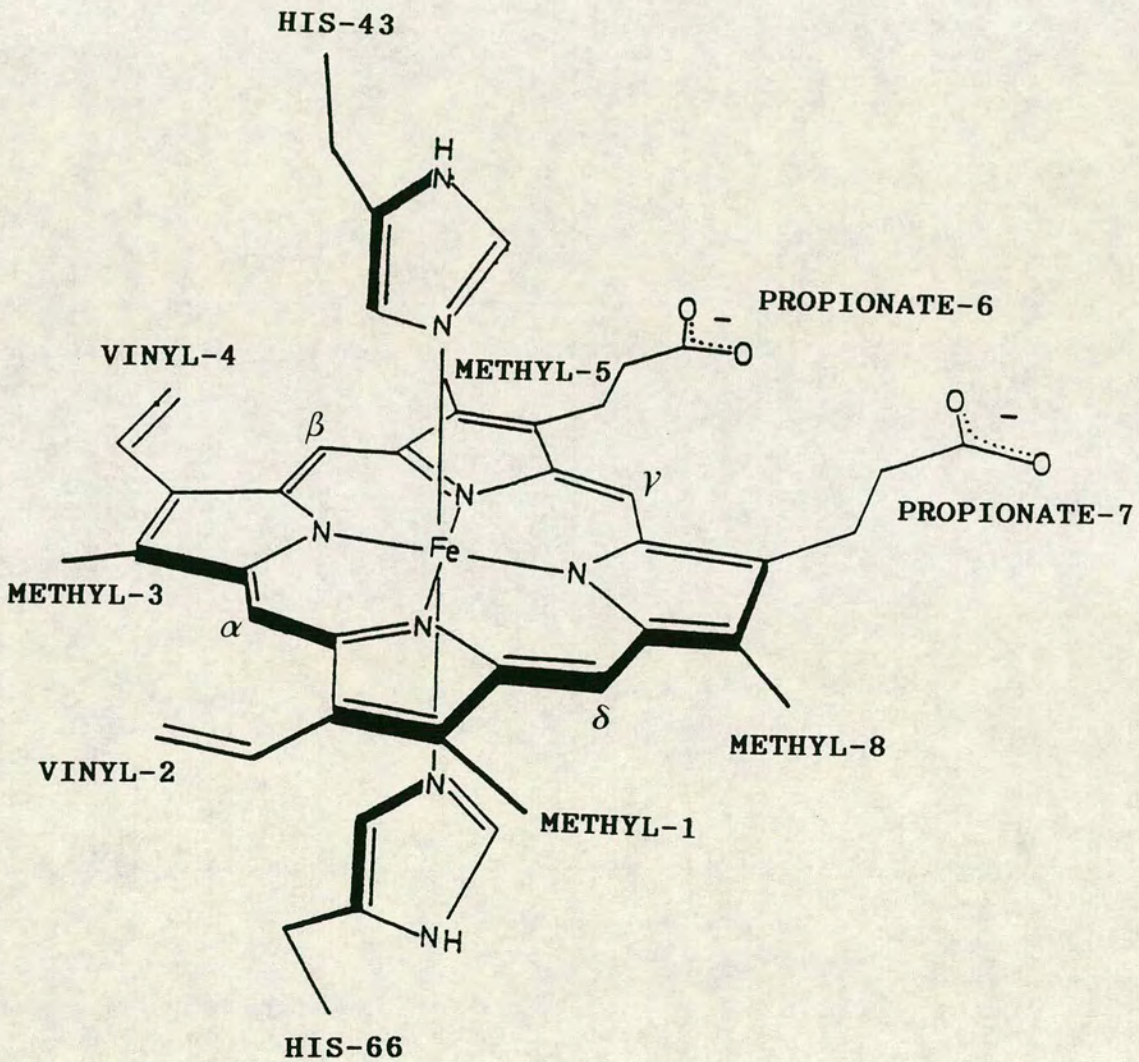

FIGURE 6.10

1D NMR SPECTRUM OF OXIDISED CYTOCHROME b_2 CORE ILLUSTRATING ASSIGNED HAEM PROTON RESONANCES (21)

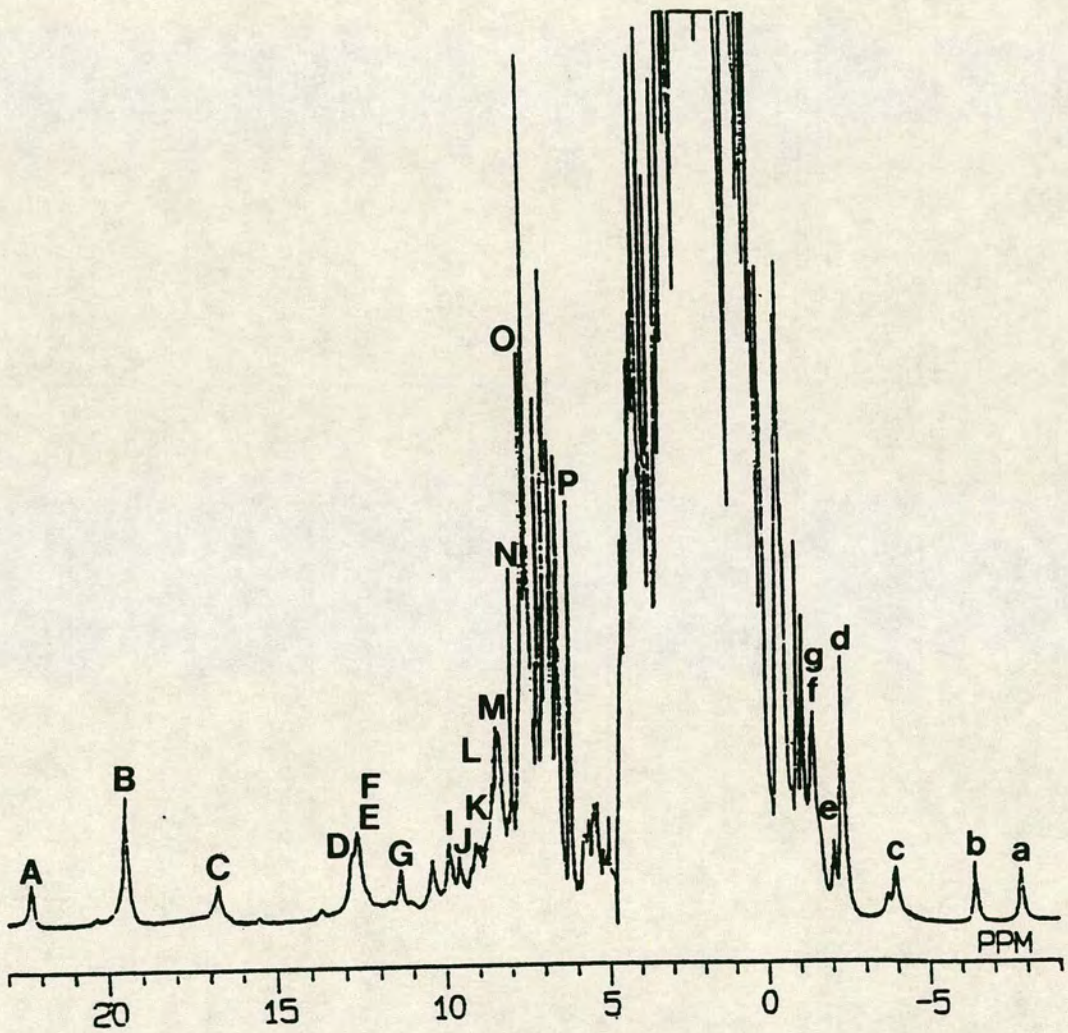

This 400MHz spectrum was taken at 25°C in 50mM phosphate/D_2O buffer, pH 7.0. The assignments of the labelled resonances are given in Table 6.4.

TABLE 6.4

ASSIGNMENT OF HAEM PROTON RESONANCES IN THE NMR SPECTRUM OF OXIDISED CYTOCHROME *b*$_2$ CORE

LABEL IN FIGURE 6.10	δ (ppm)	ASSIGNMENT
A	22.2	VINYL-2α
B	19.4	METHYL-3
E	12.6	PROPIONATE-7α
F	12.5	PROPIONATE-7α
G	11.4	PROPIONATE-6α
J	9.6	PROPIONATE-6α
M	8.3	METHYL-8
O	7.5	METHYL-5
P	6.1	METHYL-1
a	-7.2	VINYL-2β
b	-6.5	VINYL-2β
d	-2.3	PROPIONATE-6β
e	-2.0	PROPIONATE-6β
f	-1.3	PROPIONATE-7β
g	-1.2	PROPIONATE-7β

FIGURE 6.11

NMR pH TITRATION OF CYTOCHROME *b*2 CORE

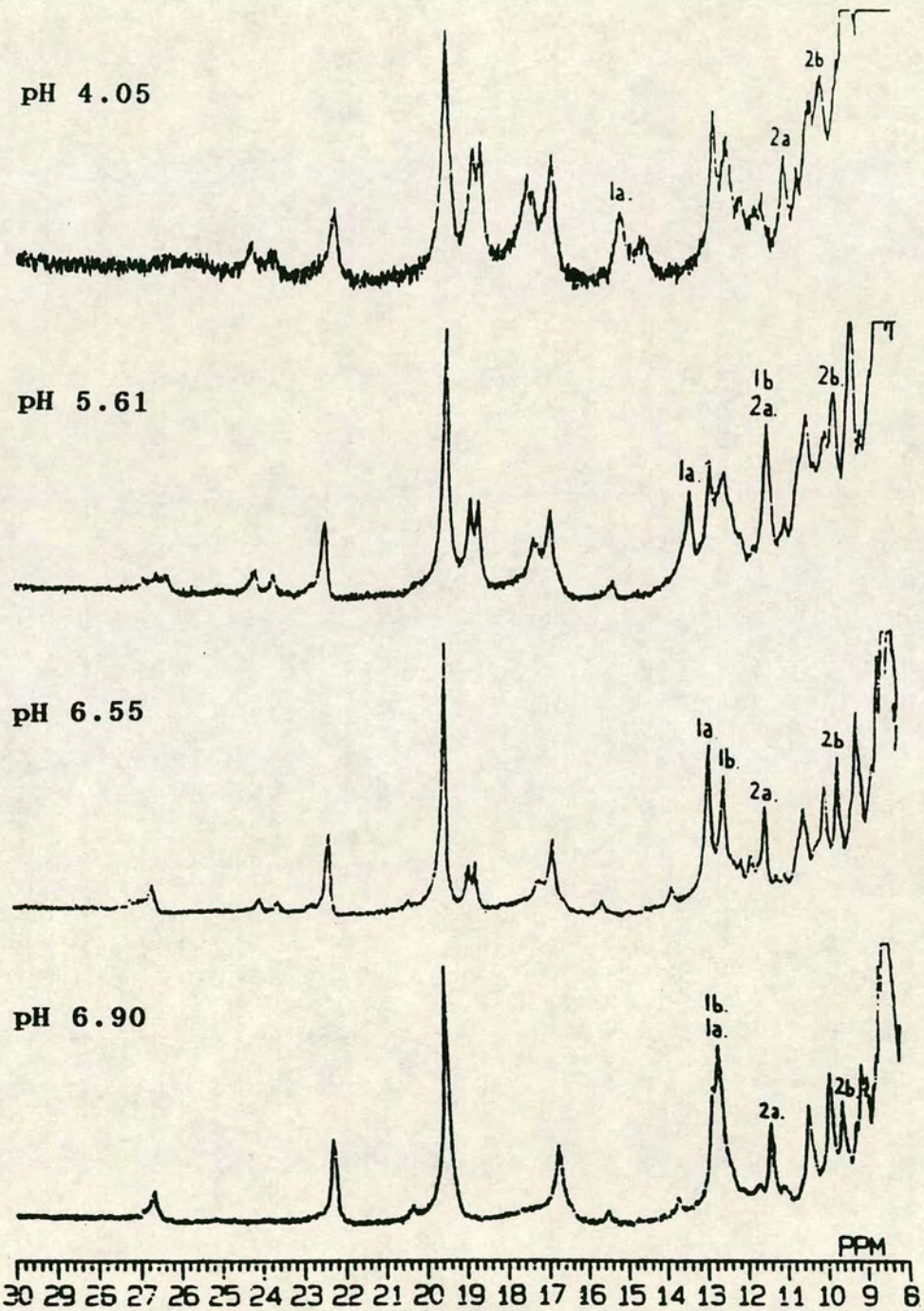

The pH titration was carried out in 5mM phosphate/D_2O buffer at 25°C. The shifts in resonances for haem propionate α-protons (1a, 1b, 2a and 2b) were monitored by 400MHz NMR spectroscopy.
This information was taken from reference 21.

FIGURE 6.12

PLOTS OF CHEMICAL SHIFT VERSUS pH* FOR NMR RESONANCES OF THE HAEM PROPIONATES OF CYTOCHROME b_2 CORE

(a) pH TITRATION OF RESONANCE 1a IN FIGURE 6.11

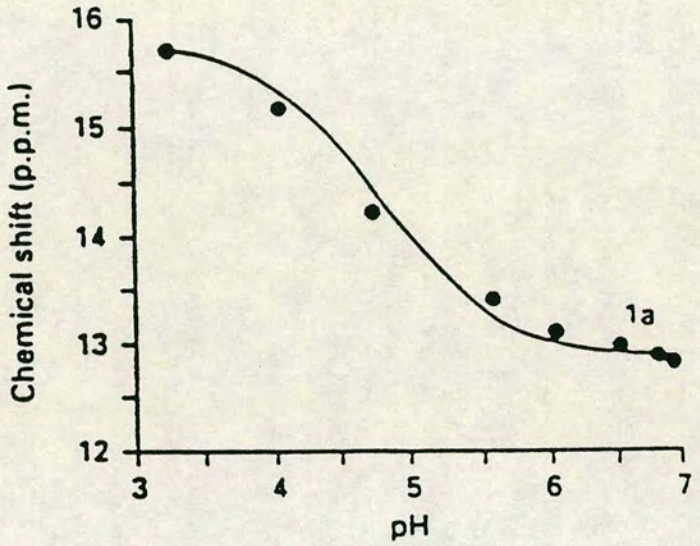

(b) pH TITRATION OF RESONANCE 2a IN FIGURE 6.11

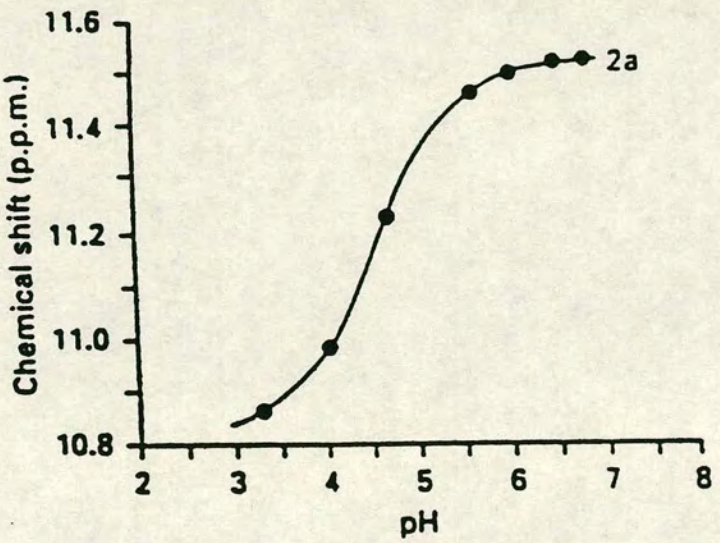

This information was taken from reference 21.

FIGURE 6.13

DETERMINATION OF pKa VALUES FOR HAEM PROPIONATES OF CYTOCHROME *b*2 CORE BY USE OF HILL PLOTS

The Hill plots correspond to the pH titration of the NMR resonances for haem propionate-6 (resonance 2a) and haem propionate-7 (resonance 1a) (Figures 6.11 and 6.12). Both lines have gradients equal to one and the pKa values are given by the intercepts with the *x*-axis as indicated. This information was taken from reference 21.

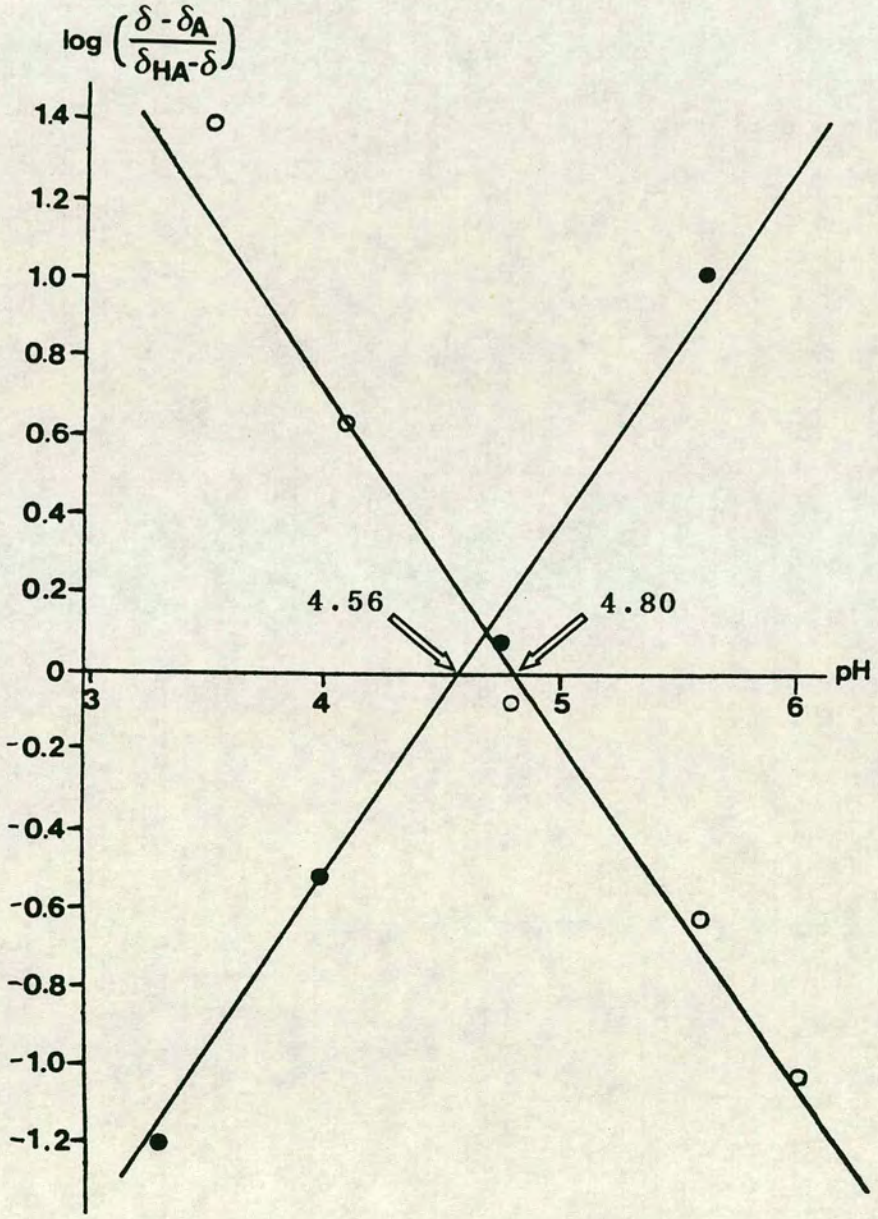

core were close to those observed kinetically for wild-type, hence an NMR study on the holoenzyme would enable us to determine to what extent the presence of the flavin domain affects the propionate groups, and whether this has any effect on the observed pK_as. Such a study was impossible on the tetrameric wild-type and Y143F enzymes due to their high molecular weights (*c.a.* 230kDa) and hence slow tumbling rate in solution, which leads to broad linewidths. Tail-deleted flavocytochrome b_2 (TD-b_2) is a tetrameric mutant in which the 23 amino-acid residues which constitute the C-terminal tail have been removed. TD-b_2, however, is monomeric under certain conditions, this has allowed observation of pH effects on a b_2 protomer. Presence of the monomer was confirmed by gel filtration as described in Section 4. Initial experiments on this form of TD-b_2 at 400MHz, carried out in collaboration with Dr.G.R.Moore's group at University of East Anglia, showed a particularly sharp proton NMR spectrum coincidental with the monomeric nature. TD-b_2 was then used for pH* titration at Edinburgh using a 600MHz NMR spectrometer. Figure 6.14 is a stack plot of the spectra obtained. Some denaturation was observed but since all major peaks in the spectrum at pH* 7 are still evident in the lowest pH* spectrum one can assume that the majority of the protein remains in its native state throughout the titration.

Three peaks of the spectra were concentrated upon : A - α-proton of haem propionate-7; B - α-proton of haem

FIGURE 6.14

NMR pH TITRATION OF TAIL-DELETED FLAVOCYTOCHROME *b*$_2$

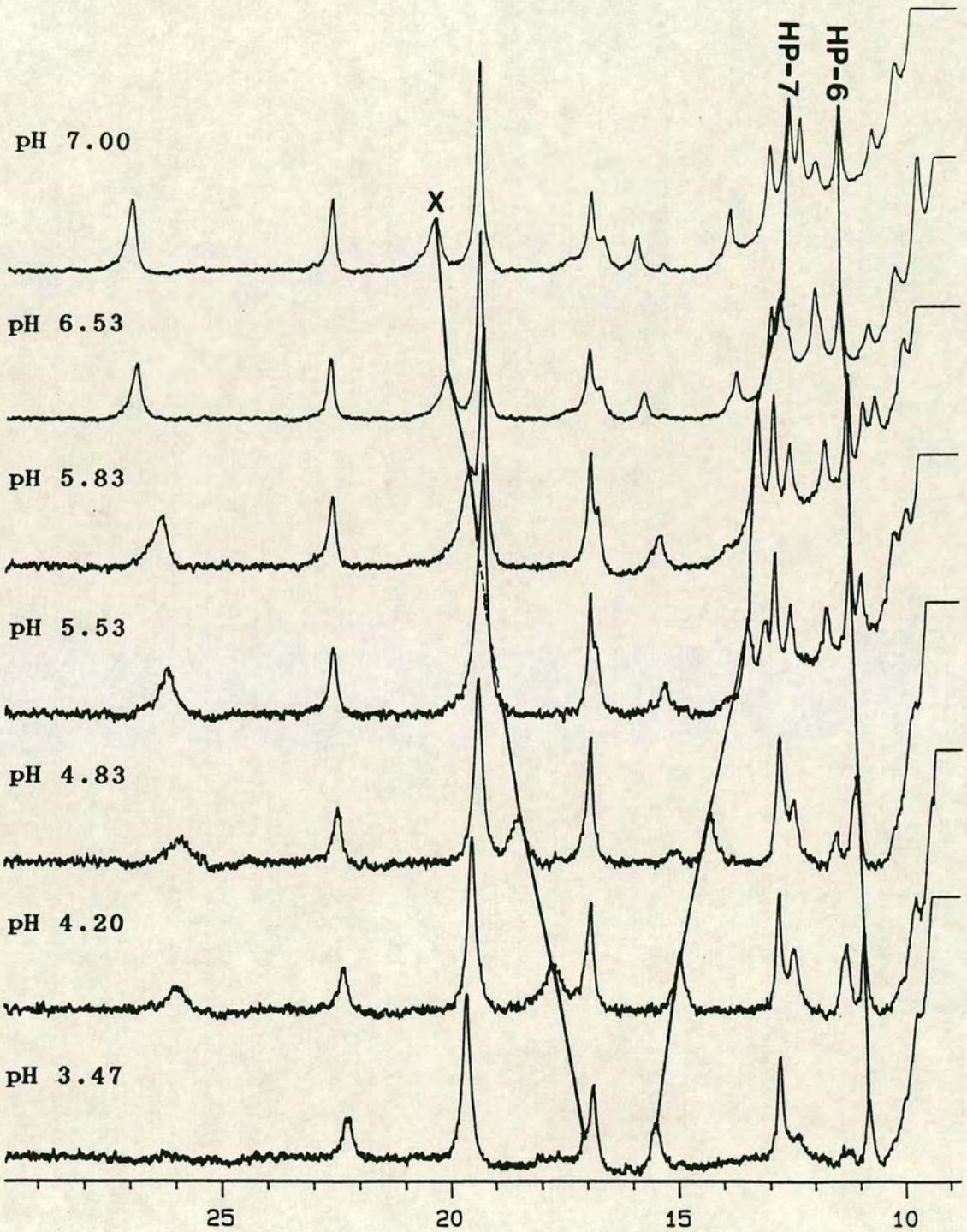

The pH titration was carried out in 20mM phosphate/D_2O buffer at 25°C. The shifts in resonances for haem propionate α-protons (labelled HP-6 and HP-7) and for resonance X were monitored by 600MHz NMR spectroscopy.

propionate-6; and X, an unassigned peak, believed to be due to a propionate. The chemical shift changes of each of these resonances were calculated and when plotted against pH* gave sigmoidal curves (Figure 6.15). Hill plots (Figure 6.16) were linear with gradients equal to one and gave the following pK_a values :- 5.0±0.3 for haem propionate-7; 5.3±0.5 for haem propionate-6 and 5.0±0.3 for peak X. The Hill plots for haem propionate-7 and resonance X overlay exactly, therefore one can categorically assign peak X to haem propionate-7. Its appearance is concerned with greater protein exposure due to the monomeric nature of the enzyme. A COSY (correlated spectroscopy) experiment was performed at 600MHz (data not shown) to provide further confirmation of the identity of this peak, however no clear crosspeaks could be observed.

The pK_a results suggest, as expected, that the haem propionates are less accessible to solvent than in the cytochrome *b*2 core, but haem propionate-6 is less accessible than haem propionate-7. This makes sense, as the latter is closer to the active site of the enzyme.

In steady-state kinetics for WT-*b*2 a pK_a of 5.40±0.12 was observed. This value is in good agreement with those obtained by NMR for haem propionate ionisation, hence one can postulate that this pK_a is due to protonation of a haem propionate group. This is further supported by the observed pK_a for Y143F of 4.75±0.20. The fact that this value is lower suggests that the haem propionate is more

FIGURE 6.15

PLOTS OF CHEMICAL SHIFT VERSUS pH* FOR NMR RESONANCES OF THE HAEM PROPIONATES OF TAIL-DELETED FLAVOCYTOCHROME *b*2

(a) pH TITRATION OF THE RESONANCE FOR HAEM PROPIONATE-6 (SEE FIGURE 6.14)

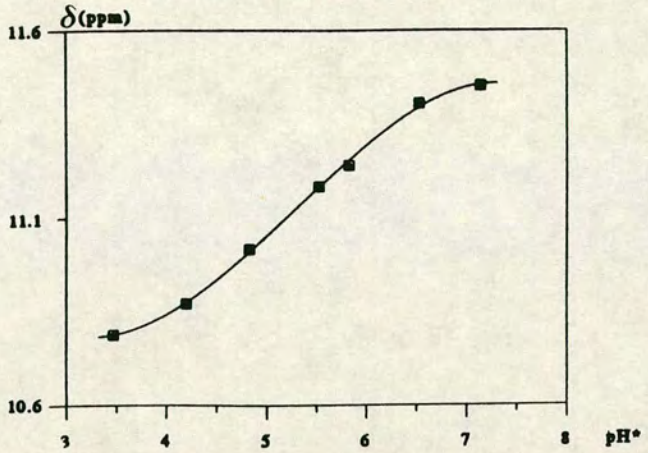

(b) pH TITRATION OF THE RESONANCE FOR HAEM PROPIONATE-7 (SEE FIGURE 6.14)

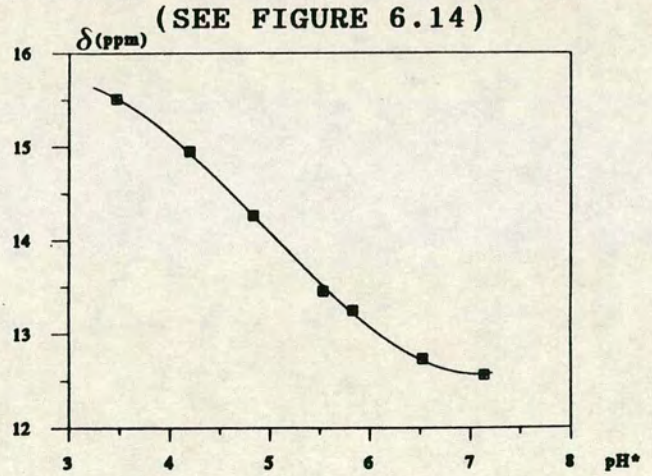

(c) pH TITRATION OF THE RESONANCE LABELLED X (SEE FIGURE 6.14)

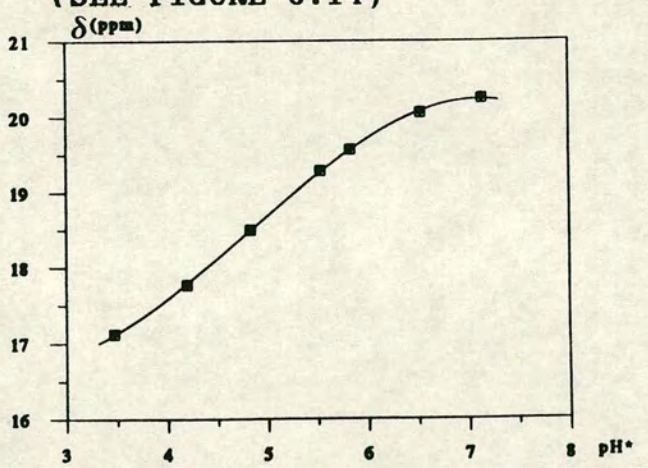

FIGURE 6.16

DETERMINATION OF pK_a VALUES FOR THE HAEM PROPIONATES OF TAIL-DELETED FLAVOCYTOCHROME *b*$_2$ BY USE OF HILL PLOTS

The Hill plots correspond to the pH titration of the NMR resonances for both haem propionates and resonance X (Figures 6.14 and 6.15).
All lines have gradients equal to one and the pK_a is given by the intercept with the x-axis (as indicated by arrows).

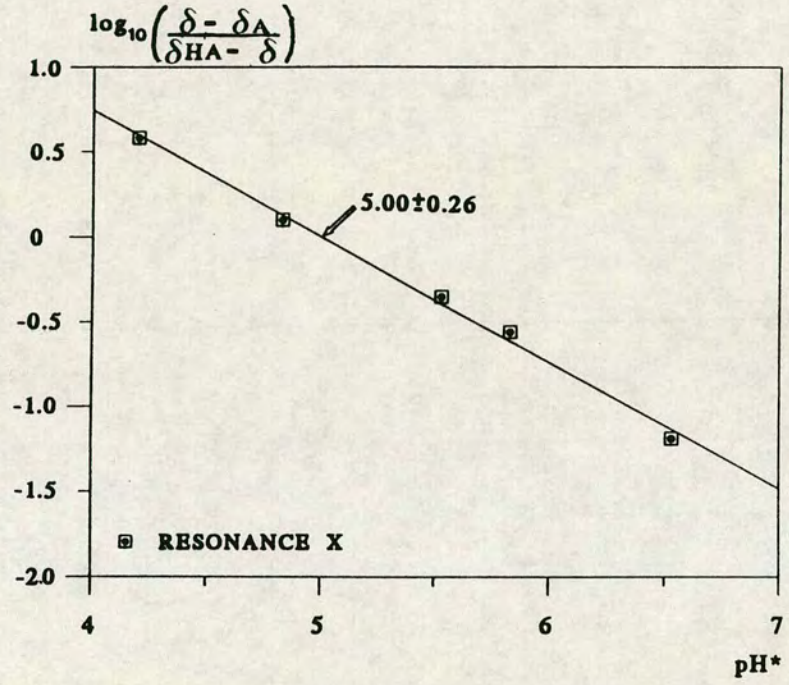

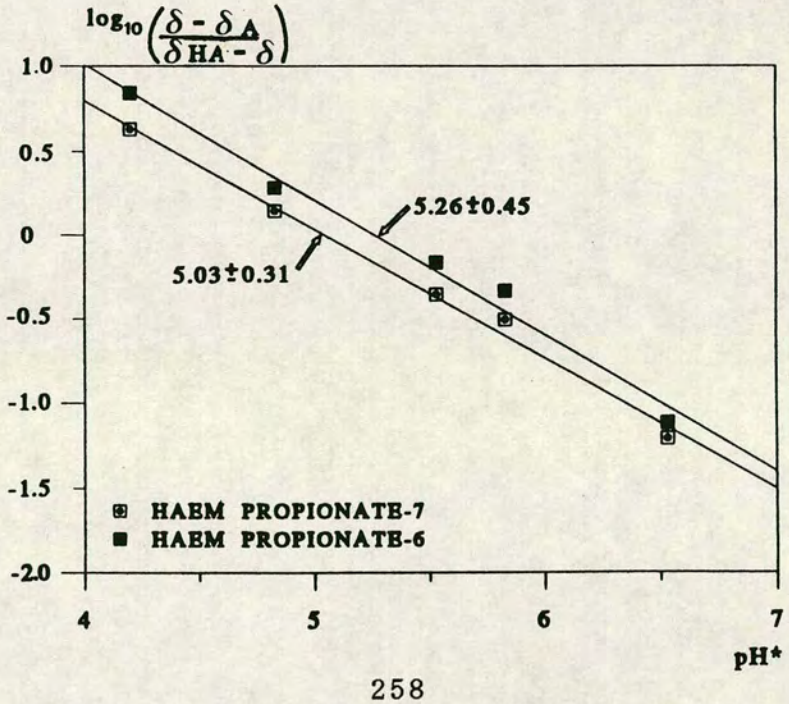

exposed to solvent, which would be the case on removal of the hydroxyl group of Tyr-143, since in subunit 1 (pyruvate absent) of the X-ray crystal structure (30), Tyr-143 is hydrogen-bonded to haem propionate-7 (see Figure 1.21).

6.4 CONCLUSIONS

We can draw several conclusions from this study of the effect of pH on recombinant intact flavocytochrome *b*$_2$:-

(1) the recombinant intact flavocytochrome *b*$_2$ expressed in and isolated from *E.coli* shows greater stability to extremes of pH than the proteolytically cleaved enzyme isolated directly from the yeast, *S.cerevisiae*;

(2) the pK_a value at low pH has categorically been assigned to protonation of haem propionate-7;

(3) the higher pK_a value, of approximately 8, is postulated to be due to deprotonation of a group important in substrate binding. This is most likely a tyrosine residue and the most obvious candidate is Tyr-254;

(4) at low pH in the wild-type enzyme there is a change in rate-limitation with flavin to haem electron transfer playing a more significant role. The ionisation of haem propionate-7 has disrupted the network of hydrogen bonds, particularly between itself and Tyr-143, with the result that the rate of interdomain electron transfer has been lowered.

6.5 REFERENCES

(1) Michaelis,L. & Davidsohn,H., *Biochem.Z.*, **35**, 386 (1911).

(2) Michaelis,L. & Pechstein,H., *Biochem.Z.*, **59**, 77 (1914).

(3) Johnson,M.J., in *"Respiratory Enzymes"*, H.A.Lardy, Burgess Publishing Co., Minneapolis, pg 51 (1949).

(4) Dixon,M., *Biochem.J.*, **55**, 161 (1953).

(5) Alberty,R.A. & Massey,V., *Biochim. Biophys. Acta*, **13**, 347 (1954).

(6) Michaelis,L. & Menten,M.L., *Biochem.Z.*, **49**, 1333 (1913).

(7) Linderstrøm-Lang,K., *C.R.Trav.Lab.Carlsberg*, **15**, 70 (1924).

(8) Matthew,J.B., Friend,S.H. & Gurd,F.R.N., *Biochem.*, **20**, 571 (1981).

(9) Voet, J.G., Coe,J., Epstein,J., Matossian,V. & Shipley,T., *Biochem.*, **20**, 7182 (1981).

(10) Boeri,E. & Tosi,L., *Arch. Biochem. Biophys.*, **60**, 463 (1956).

(11) Hasegawa,H., *J.Biochem.*, **52**, 12 (1962).

(12) Hinkson,J.W. & Mahler,H.R., *Biochemistry*, **2**, 216-220 (1963).

(13) Weast,R.C. (editor), in *"CRC Handbook of Chemistry and Physics"* (62nd edition), CRC Press Inc., Bocov Raton, Florida, D-145 (1981).

(14) Ogura,Y., Ohta,Y. & Nakamura,T., *J.Biochem.*, **60**, 63 (1966).

(15) Ogura,Y. & Nakamura,T., *J.Biochem.*, **60**, 77 (1966).

(16) Suzuki,H. & Ogura,Y., *J.Biochem.*, **67**, 277 (1970).

(17) Bach,S.J., Dixon,M. & Zerfas,L.G., *Biochem.J.*, **40**, 229 (1946).

(18) Boeri,E. & Tosi,L., *Arch.Biochem.Biophys.*, **60**, 463 (1956).

(19) Appleby,C.A. & Morton,R.K., *Biochem.J.*, **71**, 492 (1959).

(20) Miles,C.S., *Ph.D. thesis*, University of Edinburgh (1992).

(21) Brunt,C.E., Cox,M.C., Thurgood,A.G.P., Moore,G.R., Reid,G.A. & Chapman,S.K., *Biochem.J.*, **283**, 87 (1992).

(22) White,S.A., Black,M.T., Reid.G.A. & Chapman,S.K., *Biochem.J.*, **263**, 849 (1989).

(23) Fersht, A., in *"Enzyme Structure and Mechanism"* (second edition), W.H.Freeman and Co., New York (1985).

(24) Zoller,M.J. & Smith,M., *DNA*, **3**, 479 (1984).

(25) Black,M.T., White,S.A., Reid,G.A. & Chapman,S.K., *Biochem.J.*, **258**, 255 (1989).

(26) Dawson, R.M.C., Elliot, D.C., Elliot, W.H. & Jones,K.M., in *"Data for Biochemical Research"*, 2nd edition, Oxford Uni.Press (1969).

(27) Pompon,D., Iwatsubo,M. & Lederer,F., *Eur.J.Biochem.*, **104**, 479 (1980).

(28) Miles, C.S., Rouvière-Fourmy, N., Lederer, F., Mathews, F.S., Reid, G.A., Black, M.T. & Chapman,S.K., *Biochem.J.*, **285**, 187 (1992).

(29) Moore,G.R. & Pettigrew,G.W., in *"Cytochromes c - Evolutionary, Structural and Physicochemical Aspects"*, Springer-Verlag (1990).

(30) Xia,Z.-x. & Mathews,F.S., *J.Mol.Biol.*, **212**, 837 (1990).

CHAPTER 7

METHODS AND MATERIALS

7.1 GROWTH OF CELLS

7.1.1 EXPRESSION AND DNA MANIPULATION

E.coli strain TG1 was used for plasmid propagation and expression of flavocytochrome b_2, except for the hinge-swap mutation which was, at a later stage, expressed in the proteolytically deficient AR120 strain. Standard methods for growth of *E.coli*, plasmid purification, DNA manipulation and transformation were carried out as described in references 1 and 2 by Dr.F.D.C.Manson.

7.1.2 MEDIA PREPARATION

Deionised water, purified by reverse osmosis and ion-exchange to a resistivity of 18.3 MΩ (Millipore Mill-QSP reagent water system), was used to prepare Luria Broth (LB) according to the following recipe :-

10g/l tryptone (Difco)

5g/l yeast extract (Difco)

5g/l sodium chloride (Fisons)

All media was autoclaved before use in a Denley Sovereign autoclave (122°C, 20 minutes, 16 p.s.i.). Immediately prior to innoculation, a solution of antibiotic, either 50 μg/ml carbenicillin or 100 μg/ml ampicillin (both Sigma), was added to the media via a sterile Millipore filter (Millex-GS 0.22 μm).

7.1.3 PREPARATION OF CULTURE PLATES

Equal volumes of double-strength LB and bacto-agar

(Difco-15g/l normal strength) were autoclaved separately, allowed to cool and then mixed. Carbenicillin was added in the manner described above and plates (Sterilin) could then be poured. *E.coli* were kept on such plates for a duration of up to one month.

7.1.4 GROWTH CONDITIONS

Single colonies of plasmid-bearing *E.coli* were innoculated into antibiotic-containing media by means of a sterile loop. *E.coli* were grown at 37°C on an incubated orbital shaker (Luckham) at 250rpm for approximately 12 hours. *E.coli* (AR120) were grown under similar conditions but for up to 24 hours.

7.1.5 CELL HARVESTING

Cells were harvested from growth media by centrifugation at 16,000g for 4 minutes at 0-4°C, using a Sorval RC-5B refridgerated centrifuge. The resulting "wet pellet" of cells was stored at -20°C until required. Yields of wet cells varied substantially, however the average was approximately 3g of wet cells per litre of LB.

7.2 BUFFER PREPARATION

7.2.1 GENERAL

Deionised water, purified by reverse osmosis and ion-exchange to a resistivity of 18.3 MΩ (Millipore Mill-QSP

reagent water system) was used to prepare all buffers. Measurements of pH were made using a standard glass electrode connected to a digital pH meter (WPA CD620). The pH electrode was calibrated in the ranges pH 4 to 7 and pH 7 to 10 using BDH colour-coded buffers (accurate to $\pm$0.02 at 20°C). The range of calibration depended upon the pK_a of the buffer in question. All buffers were adjusted to an ionic strength of 0.1M by addition of sodium chloride (Fisons), except where indicated otherwise. Buffering ranges of the individual buffers are shown below in parentheses.

7.2.2 TRIS-HCl (pH 7.1-8.9)

To 500ml of deionised water were added 10ml of 1M HCl (Fisons) and 5.265g sodium chloride, to give final concentrations of 0.01M HCl and 0.09M NaCl. The resulting solution was titrated to the required pH with an aqueous solution of tris (hydroxymethyl) aminomethane (Trizma base - Sigma) and adjusted to a volume of 1l using a volumetric flask.

7.2.3 MES (pH 5.4-6.8); CHES (pH 8.6-10.0) AND CAPS (pH 9.7-11.1)

The IUPAC nomenclature for these buffers are, respectively, N-morpholinoethane sulphonic acid, 2-[N-cyclohexylamino]-1-propanesulphonic acid and 3-[cyclohexyl]-1-propanesulphonic acid, all of which were

obtained from Sigma. These buffers were prepared in the same way as described in 7.2.2, except that 0.01M sodium hydroxide (Fisons) was used as opposed to 0.01M HCl.

7.2.4 BORATE (pH 8.0-10.5)

Borate buffer was again prepared as above, except that whether the buffer was adjusted to either 0.01M HCl or 0.01M NaOH depended on the pH required, since the pK_a of the borate used in titration (disodium tetraborate - BDH) was 9.3.

7.2.5 HYDROXY-CHLORIDE (pH 12.0-13.0)

This buffer was prepared by titration of 0.1M NaCl with 0.1M NaOH to achieve the required pH.

7.2.6 PHTHALATE (pH 4.1-5.9)

Since phthalate is doubly charged, buffer of I=0.1M was made by keeping the concentration of phthalate constant at 0.01M, adding a calculated amount of sodium chloride (see Figure 7.1 and Table 7.1) and titrating with NaOH to the required pH.

7.2.7 PHOSPHATE : pH 7.0

Aqueous solutions of monobasic sodium phosphate and dibasic sodium phosphate (both Sigma) were combined to give a buffered solution of pH 7.0. The ionic strength of

FIGURE 7.1

EXAMPLE CALCULATION TO DETERMINE THE AMOUNT OF NaCl TO BE ADDED TO PHTHALATE BUFFER AT VARIOUS pH VALUES

$$H_2Pht \;\text{====>}\; {}^{-}HPht + H^{+} \;\text{====>}\; Pht^{2-} + H+$$
$$pK_a = 5.41$$

$$K_a = \frac{[Pht^{2-}][H^{+}]}{[HPht^{-}]} = 3.89 \times 10^{-6} \quad ...(a)$$

At pH = 6.0, in (a):-

$$3.89 = \frac{[Pht2-]}{[HPht^{-}]} \qquad [Pht^{2-}] + [HPht^{-}] = 0.01$$

e.g. say $[Pht^{2-}] = 0.008$ and $[HPht^{-}] = 0.002$

$$I = \frac{1}{2}\sum (0.01 \times 1^2)_{K^+} + (0.008 \times 2^2)_{Pht^{2-}} + (0.002 \times 1^2)_{HPht^{-}} + (0.008 \times 1^2)_{Na^+}$$

$$= \underline{0.026M}$$

Hence must add NaCl => 0.074M i.e. 0.1083 g in 25ml

TABLE 7.1

ADDITION OF NaCl TO PHTHALATE BUFFER (I = 0.1M)

In each 25 ml of buffer, there is 0.01M potassium hydrogen phthalate (Sigma) i.e. 0.511 g.

The required amount of NaCl was calculated using the method illustrated in Figure 7.1.

pH	$\frac{[Pht^{2-}]}{[HPht^{-}]}$	$[HPht^{-}]$	$[Pht^{2-}]$	I (M)	NaCl I (M)	NaCl (g)
4.25	0.0692	9.35×10^{-3}	6.47×10^{-4}	0.0113	0.0887	0.1296
4.50	0.1230	8.90×10^{-3}	1.10×10^{-3}	0.0122	0.0878	0.1283
4.75	0.2188	8.20×10^{-3}	1.80×10^{-3}	0.0136	0.0864	0.1262
5.00	0.3890	7.20×10^{-3}	2.80×10^{-3}	0.0156	0.0844	0.1233
5.25	0.6918	5.91×10^{-3}	4.09×10^{-3}	0.0182	0.0818	0.1195
5.50	1.2301	4.48×10^{-3}	5.52×10^{-3}	0.0210	0.0790	0.1154
5.75	2.1875	3.14×10^{-3}	6.86×10^{-3}	0.0237	0.0763	0.1115
6.00	3.8900	2.04×10^{-3}	7.96×10^{-3}	0.0259	0.0741	0.1083

the buffer was altered by using different concentrations of starting solutions. The final ionic strength was calculated in a similar manner to that shown in Figure 7.1 using the following equation :-

$$I = 1/2 \sum c_i z_i^2 \qquad (i)$$

where c_i represents the concentration of each species present and z_i represents the charges of these species. For example, 25mM phosphate solutions would result in a buffer of ionic strength equal to 55.6mM.

For protein isolation and purification techniques, phosphate buffer was used in the presence of varying quantities of the disodium salt of diaminoethanetetra-acetic acid (EDTA - Fisons) and the lithium salt of L(+) lactic acid (Sigma) - hereafter referred to as L-lactate. The former acted as a chelating agent for any metal ions released by cell lysis and the latter ensured that the enzyme remained in the more stable reduced form.

7.3 COLUMN CHROMATOGRAPHY

7.3.1 GENERAL

All columns were poured by slurrying the column material in the required buffer and introducing this slurry to the column, making certain that the column was completely vertical so as to ensure a smooth, even loading surface. Columns were poured and equilibrated at 0-4°C. A small piece of glass wool was used at the bottom of the column

to prevent loss of column material. Flow was regulated by means of head height alteration and a tap at the column base.

7.3.2 HYDROXYLAPATITE

Hydroxylapatite is the crystalline form of $Ca_{10}(PO_4)_6(OH)_2$. Binding is believed to take place through the phosphate groups and proteins are eluted by varying the ionic strength of the eluting buffer. As the column material consists of a majority of negatively-charged groups, neutral and positively-charged groups bind well whereas more negatively-charged groups do not. This explains why hydroxylapatite binds *S.cerevisiae-b2* very well but binds the more negatively-charged *H.anomala-b2* very poorly. Column protocol is described in Section 7.4.4. The column material was regenerated by passing 200ml of 1M NaCl through, prior to re-equilibration.

7.3.3 ION EXCHANGE RESINS

Ion exchange resins consist of a cross-linked polymer matrix to which ionised or ionisable groups are attached. Most ion exchange resins are based on a matrix of either polystyrene or polymethacrylic acid cross-linked by divinylbenzene. Pore size is dependent on the degree of cross-linkage of the resin. Dowex 1x8-200 (Sigma) is an example of a strongly basic anion exchange resin

based on a polystyrene matrix. This material is used in the purification of deuterolactate (see 7.6.2).

Cellulose ion exchangers are made from microgranular cellulose, which is cellulose which has been treated to increase the proportion of micro-crystalline cellulose and then cross-linked by diepoxides. Exchange capacity may be influenced by a wide range of factors, including pH and ionic strength. An example of a cellulose anion exchanger is DE52 (Whatman), which is used in the purification of *H.anomala-b*$_2$, and hence the hybrid enzyme, pFM306, which contains the flavin domain from *H.anomala-b*$_2$.

Pre-swollen DE52 was slurried in the required buffer and adjusted to pH 7.0 by addition of HCl (BDH). A 70x25mm column was then poured in the normal way described in 7.3.1. Column regeneration was achieved by sequential washes of 0.5M HCl (BDH), deionised water, 0.5M NaOH (Fisons) and deionised water, followed by re-equilibration with buffer.

7.3.4 GEL FILTRATION

The principle behind gel filtration is that a material with a defined pore size will retain lower molecular weight molecules within the pores whilst macromolecules will pass through the material and be eluted in decreasing order of molecular weight.

Sephadex G25 (Sigma) has a fractionation range and

exclusion limit of M_R 1,000 to 5,000 for globular proteins. In this study, a 100x10mm column, equilibrated in buffer at the required pH, was used to remove small molecules such as lactate and pyruvate from the protein prior to pre-steady-state kinetics. The column was regenerated by large volumes of buffer.

Sephacryl S-300 (Sigma) was used to determine non-denatured protein molecular weights, having a fractionation range and exclusion limit for proteins of 10,000 to 1,500,000. Column material was swollen for several hours in excess equilibration buffer (0.1M phosphate, pH 7, 5mM lactate) and a long column (150x2.5cm) was poured as described in 7.3.1. The length of the column ensures complete separation of the different molecular weight entities. After use the column material was recovered by washing with 200ml of 0.2M NaOH If the column was to be stored 0.02% sodium azide (Fisons) was added as a bacteriostatic agent.

After column equilibration, a solution of blue dextran (M_R 2,000kDa) was passed through to reveal any irregularities such as air bubbles; this also enabled the void volume, V_o, of the column to be calculated. Possible molecular markers for calibration include ß-amylase (200kDa), alcohol dehydrogenase (150kDa), bovine serum albumin (66kDa), carbonic anhydrase (29kDa), myoglobin (17.5kDa) and cytochrome *c* (12.5kDa). However, such a broad range was not necessary in this study as S-300 columns were only used to estimate molecular weights in

order to distinguish between monomeric and tetrameric proteins. The loaded sample consisted of blue dextran (Sigma), cytochrome *c* (Sigma), wild-type flavocytochrome b_2, potassium ferricyanide (Fisons) and the protein under investigation. The volume at which each eluted, V_e, was determined by means of UV/vis absorbance and activity measurements. Elution profiles were recorded as V_e/V_o. From the linear plot of $\log_{10} M_R$ versus V_e/V_o, the molecular weight of the protein being investigated could be determined.

7.4 PROTEIN ISOLATION AND PURIFICATION

7.4.1 CELL LYSIS

Frozen plasmid-bearing cells were allowed to defrost and were suspended in buffer A (0.1M phosphate, pH 7.0, 1mM EDTA and 5mM L-lactate). Lysozyme from chicken egg albumin (Sigma) was added to a concentration of approximately 0.2 mg/ml and the mixture was stirred for 30 minutes at 0-4°C. After this time the cell debris and any unlysed cells were removed from suspension by centrifugation at 39,000g for 15 minutes. A pink-red colour in the supernatant indicated the presence of haem-containing flavocytochrome b_2. The pellet of solids recovered was subjected to further lyses, all resulting supernatants being pooled.

7.4.2 AMMONIUM SULPHATE FRACTIONATION

The first stage in purification is ammonium sulphate fractionation. This has its basis in the "salting-out" principle (3) whereby increasing salt concentration selectively precipitates macromolecules out of solution. Ammonium sulphate is generally used for this purpose as it has high solubility and does not significantly alter the pH of the solution.

The supernatant after lysis was firstly adjusted to 30% saturation by addition of ammonium sulphate (Fisons). This precipitated out a large amount of protein, which was removed as a pellet by centrifugation at 39,000g for 10 minutes. The supernatant was then taken to 70% ammonium sulphate saturation, which was sufficient to precipitate flavocytochrome b_2 which was again removed from solution by centrifugation. The resulting enzyme-containing pellet could be stored without significant activity loss for several weeks at 0-4°C under nitrogen. Enzyme at this stage of purity was used for all steady-state experiments (2), except where otherwise specified.

7.4.3 DIALYSIS

Prior to further purification by column chromatography, the protein had to be dialysed to remove any small molecule contaminants such as ammonium sulphate. Seamless dialysis tubing (Sigma) was used, with a molecular weight exclusion limit of 12,000. Protein was resuspended in

buffer A and was sealed into a piece of dialysis tubing which had previously been soaked and thoroughly washed in deionised water. The protein was dialysed overnight against a large volume of half-strength buffer A under nitrogen at 0-4°C. The dialysis buffer was renewed halfway through if deemed necessary.

7.4.4 PURIFICATION BY COLUMN CHROMATOGRAPHY

After dialysis the protein was centrifuged to remove any insolubles and was loaded onto a 70x25mm hydroxylapatite column (Biorad) which had previously been equilibrated with two column volumes of buffer A. The protein bound in a tight band at the top of the column. The major impurity, a yellow protein, was completely eluted by a thorough washing with buffer A. Flavocytochrome *b*$_2$ was then eluted using a 0-10% ammonium sulphate gradient and fractions were collected either manually or by a Biorad Model 2110 fraction collector. Purity of the fractions was assessed by measurement of absorbances at 269nm and 423nm for reduced protein (275nm and 413nm if oxidised). The most pure protein had a ratio $A_{269}/A_{423} < 0.5$ ($A_{275}/A_{413} < 1.0$). The fractions with the lowest ratios were pooled, adjusted to 70% ammonium sulphate saturation and centrifuged at 39,000g for 10 minutes. The resulting pellet was stored as previously described in 7.4.2.

7.5 SODIUM DODECYL SULPHATE-POLYACRYLAMIDE GEL ELECTROPHORESIS (SDS-PAGE)

7.5.1 GENERAL

Most biological polymers are electrically charged and will therefore move in an electric field. Electrophoresis is the transport of particles through a solvent by such a field.

The molecular weights of many proteins can be determined by measuring their mobility in sodium dodecyl sulphate-containing polyacrylamide gels (4). In a solution of neutral pH, containing 1% sodium dodecyl sulphate (SDS) and 0.1M mercaptoethanol, most multichain proteins will bind SDS and dissociate, with disulphide linkages being broken by mercaptoethanol. The complexes consisting of SDS and protein subunits adopt a random coil configuration. Such complexes behave as though they have uniform shape and equal charge-to-mass ratio since the amount of SDS bound per unit weight of protein is constant. Effective mobility directly relates to molecular weight because of the molecular sieving properties of the gel.

Electrophoresis of known molecular weight proteins on a column gel will result in a number of separate bands and a plot of distance migrated versus $\log_{10} M_R$ will give a linear calibration "curve" which can be used to identify unknown molecular weights of other proteins run on the same gel.

7.5.2 ELECTROPHORESIS BUFFERS

7.5.2.1 STACKING BUFFER
(stored as a two-fold concentrate)

Tris-HCl, pH 6.8	0.125M
SDS (Sigma)	0.1%

7.5.2.2 RESOLVING BUFFER
(stored as a two-fold concentrate)

Tris-HCl, pH 8.8	0.375M
SDS (Sigma)	0.1%

7.5.2.3 RESERVOIR BUFFER
(stored as a five-fold concentrate)

Tris-HCl, pH 8.8	0.025M
Glycine (Sigma)	0.19M
SDS (Sigma)	0.1%

7.5.2.4 SAMPLE BUFFER

Tris-HCl, pH 6.8	0.125M
SDS (Sigma)	2.0%
Glycerol (Fisons AR grade)	10%
ß-mercaptoethanol (Sigma)	10%
Bromophenol blue (BDH)	0.01%

7.5.3 STAINS AND DESTAINS

7.5.3.1 GEL STAIN

Isopropanol (Fisons)	v/v	25%
Acetic acid (May & Baker)	v/v	10%
Coomassie blue (Sigma)		0.1%

7.5.3.2 GEL DESTAIN

Three successive destains were used, in order of decreasing strength of isopropanol, as follows:-

(i)	Isopropanol (Fisons)	v/v	25%
	Acetic acid (May & Baker)	v/v	10%
(ii)	Isopropanol (Fisons)	v/v	10%
	Acetic acid (May & Baker)	v/v	10%
(iii)	Acetic acid (May & Baker)	v/v	10%

7.5.4 ELECTROPHORESIS EQUIPMENT

SDS-PAGE was perfomed using a vertical gel box system (BRL). The potential across the gel was controlled by a Biorad 200/0.2 power supply.

7.5.5 RESOLVING GEL PREPARATION

A solution of volume 40ml was made up using resolving buffer containing 12% acrylamide (BDH) and 10% ammonium persulphate (Sigma). This solution was filtered and degassed. TEMED (N,N,N',N'-tetramethylethylenediamine - Sigma) was added to a concentration of 0.5 μl/ml; this acted as a crosslinker. The resulting mixture was poured and allowed to set.

7.5.6 STACKING GEL PREPARATION

A 20ml solution was prepared using stacking buffer and 6% acrylamide. TEMED (20μl) was added and the solution was

poured over a well mould placed directly above the resolving gel.

7.5.7 SAMPLE PREPARATION

Molecular weight markers and proteins were dissolved in sample buffer, boiled for two minutes and allowed to cool. Samples (5-25 μl) were injected into individual wells.

7.5.8 ELECTROPHORESIS

Both reservoirs were filled with reservoir buffer. A current of 0.03A was applied across the gel and the gel was run until the dye front was approximately 5mm from the base of the gel (about five hours). The gel was stained overnight and then destained by two or three sucessive washes of each destain.

7.6 FLAVIN REINCORPORATION

For tetrameric protein deactivated by FMN loss, for example TD-*b*$_2$, approximately 60% of the activity can be restored by reincorporating FMN. The deactivated protein was partially denatured in a small volume of solution B (0.1M phosphate buffer, 5mM lactate, 1mM EDTA, 4M urea (BDH)). A ten-fold excess of FMN (Sigma) was added and reincorporation was facilitated by dialysis against solution B (minus urea) under nitrogen at 0-4°C for 20 hours.

7.7 PREPARATION OF SUBSTRATES

7.7.1 L-[2-^{1}H]-LACTATE

All solutions were made up as standards by addition of the required buffer (see Section 7.2) to the calculated amount of the lithium salt of L-lactic acid (Sigma). All weighings were carried out using a Sartorius analytical balance.

7.7.2 SYNTHESIS OF L-[2-^{2}H]-LACTATE

A coupled enzymatic procedure was utilised to synthesize L-[2-^{2}H]-lactate, essentially by the method of Shapiro *et al.* as described in (5).

The following starting solution was prepared:- 50ml of 10mM phosphate buffer (pH 8), 1.8mM nicotinamide adenine dinucleotide (NAD^{+}- Sigma), 70mM pyruvate (sodium salt - Fluka), 90mM hexadeuteroethanol (Sigma). To this were added 2mg of yeast alcohol dehydrogenase (Sigma) and 12mg of beef heart lactate dehydrogenase (Sigma). The reaction mixture was incubated, with shaking, at 37°C for 24 hours, after which time the reaction was quenched by boiling for three minutes. The solution was filtered and allowed to cool. An 180x25mm Dowex 1x8-200 column (Section 7.3.3) equilibrated in deionised water was used to purify the deuterolactate, using a linear eluting gradient of deionised water and 3.6M formic acid. The fractions were adjusted to pH 7.5 and presence of

labelled lactate was determined by WT-*b*2 activity measurements. The degree of contamination by pyruvate was assessed by use of a pyruvate diagnostic kit (Sigma). All pyruvate-free fractions were pooled and concentrated to a volume of approximately 2ml using a high vacuum trigol/cardice rotary evaporator. Isotopic purity was confirmed by mass spectrometry. The concentrated stock was then successively diluted by the appropriate buffer. Concentration of L-[2-^{2}H]-lactate was determined by injecting a known amount of labelled lactate solution into an assay containing 1mM ferricyanide and a limiting concentration of flavocytochrome *b*2. The total absorbance change, monitored at 420nm by UV/vis spectrophotometry, could then be used to calculate the stock concentration of L-[2-^{2}H]-lactate.

7.8 STEADY-STATE KINETICS

7.8.1 GENERAL BACKGROUND

"Steady-state" usually refers to the case in dynamic situations where rate of formation is balanced by rate of removal. In enzyme kinetics the steady-state is an approximation since the substrate is generally being depleted but as activity measurements are taken over relatively short time periods any concentration change is negligible and the steady-state is a very good approximation.

The initial rate of an enzyme-catalysed reaction, v,

tends towards a limiting value, V_{max}, with increasing substrate saturation as illustrated in Figure 7.2. Such behaviour can be analysed by the basic equation governing enzyme kinetics, the Michaelis-Menten equation (6), as shown below.

$$v = \frac{[E]_o[S]\ k_{cat}}{K_S + [S]} \qquad \text{(ii)}$$

This can be converted to linear form by means of a double reciprocal or Lineweaver-Burk plot (7):-

$$\frac{1}{v} = \frac{K_M}{V_{max}} \cdot \frac{1}{[S]} + \frac{1}{V_{max}} \qquad \text{(iii)}$$

Derivations and symbol definitions for both of these equations are given in Appendix I.

The kinetic parameters which can be determined experimentally are K_M and k_{cat}, the former being the Michaelis constant which in many cases is effectively K_S, the dissociation complex of the enzyme-substrate complex. The catalytic turnover number, k_{cat}, represents the maximum number of substrate molecules converted to products per active site per unit time.

7.8.2 KINETIC PARAMETER DETERMINATION FOR FLAVOCYTOCHROME *b*2

Flavocytochrome *b*2 catalyses a two electron oxidation. The enzyme's turnover rate can therefore be measured by

FIGURE 7.2

PLOTS ILLUSTRATING METHODS OF ANALYSIS OF ENZYME KINETICS

(a) MICHAELIS-MENTEN

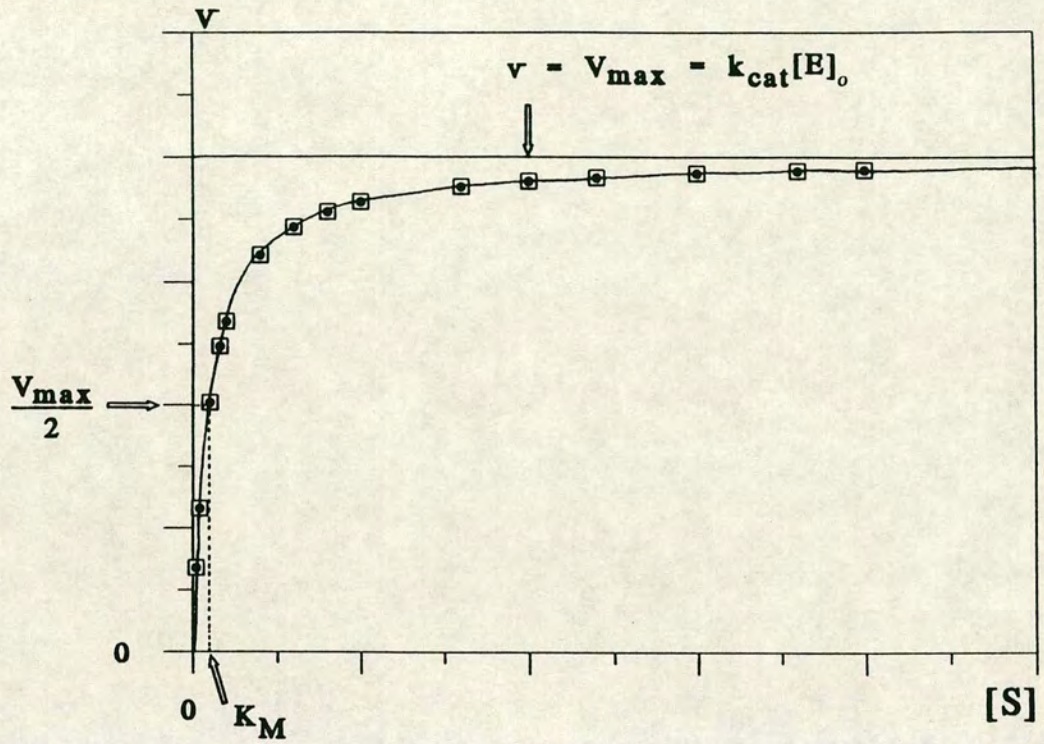

(b) LINEWEAVER-BURK

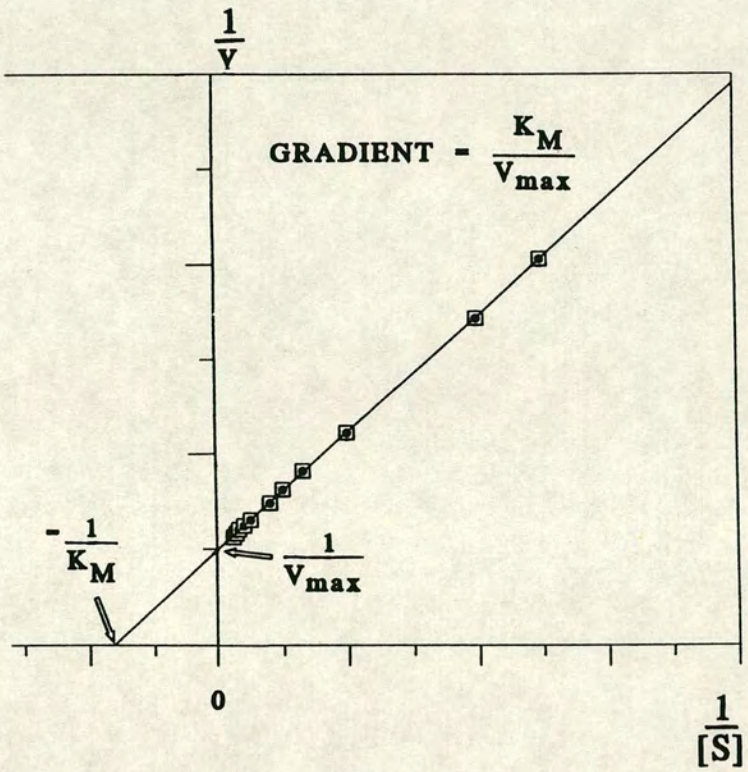

monitoring reduction of an external electron acceptor under saturating conditions. The physiological electron acceptor is cytochrome *c*, but artificial acceptors such as ferricyanide can also be used. The rate of acceptor reduction can be followed spectrophotometrically by recording change in absorbance with time.

Assays were performed in high quality glass/quartz cuvettes (Sigma) with path lengths of either 1cm or 0.2cm, using Beckmann DU-62 or Pye Unicam SP8-400 spectrometers, thermostatically controlled to 25.0±0.1°C. All assay constituents were made up in the required buffer at I=0.1M. Enzyme solutions were in tris-HCl, pH 7.5, I=0.1M and were stored on ice. Volume measurements were made to accuracy of 0.8% using a Rainin edp2 digital pipette (E2-1000).

In order to determine K_M for substrate, assays were performed varying substrate concentration between 0 and 15mM under saturating conditions of electron acceptor and vice versa to elucidate K_m for the acceptor.

7.8.3 FERRICYANIDE AS THE ACCEPTOR

Stock solutions of 3mM and 12mM potassium ferricyanide (Fisons) were made up in the appropriate buffer. The higher concentration being used in 0.2cm path length cells to enable assays to be made at ferricyanide concentrations of up to 8mM. This was to determine whether a particular mutant enzyme exhibited a

ferricyanide concentration dependence. If there was no such dependence then assays were carried out in a volume of 3ml in 1cm cuvettes at 1mM ferricyanide. Absorbance decrease was monitored at a wavelength of 420nm. An extinction coefficient of 1010 $M^{-1}cm^{-1}$ (ϵ_{ox-red}) was used to calculate initial rates.

7.8.4 CYTOCHROME *c* AS THE ACCEPTOR

Solutions of horse heart cytochrome *c* (type VI - Sigma) were freshly made up in the required buffer. Concentrations were determined by absorbance measurement at 550nm with ϵ_{ox}=8160$M^{-1}cm^{-1}$ and were varied between 0 and 150μM to elucidate the point of acceptor saturation. Assays were carried out in 1cm cuvettes at this level of saturation, varying substrate between 0 and 15mM. The reaction was followed by monitoring absorbance increase at 550nm using ϵ_{ox-red}= 22,640$M^{-1}cm^{-1}$.

7.8.5 PROTEIN CONCENTRATION DETERMINATION

A stock solution of enzyme in tris-HCl, pH 7.5, I=0.1M was prepared. The concentration of this stock was determined by means of its optical spectrum using the published extinction coefficients (8). The majority were measured using the Soret peak at 423nm in the reduced spectrum with an extinction coefficient equal to

183,000$M^{-1}cm^{-1}$. A known amount of the enzyme stock was injected into each assay by means of a Hamilton syringe.

7.9 STOPPED-FLOW KINETICS

7.9.1 GENERAL BACKGROUND

The stopped-flow technique allows analysis of a single turnover of the enzyme in its pre-steady-state. The principle of operation is shown in Figure 7.3. The two syringes are controlled by a gas-driven piston. On triggering the apparatus, the syringes are compressed to expel 25 μl each and then they are mechanically stopped. The period of time between the trigger and the stopping of the flow is the dead time of the instrument and is typically $\leq$ 1ms. After this time the solution ages normally with time and the events occurring are detected by suitable spectroscopic methods.

7.9.2 PRACTICAL APPLICATION

An Applied Photophysics SF.17MV MicroVolume stopped-flow Spectrofluorimeter was used in the transmission mode for all measurements. The light source was a 150W xenon arc lamp and the syringes were driven by a pneumatic ram drive under an average operating pressure of 70 p.s.i. The syringes and photometric cell were kept at 25.0$\pm$0.1°C by means of a thermostatted circulator bath. Prior to each measurement both syringes and cell were flushed with

FIGURE 7.3

TYPICAL SET-UP OF STOPPED-FLOW APPARATUS

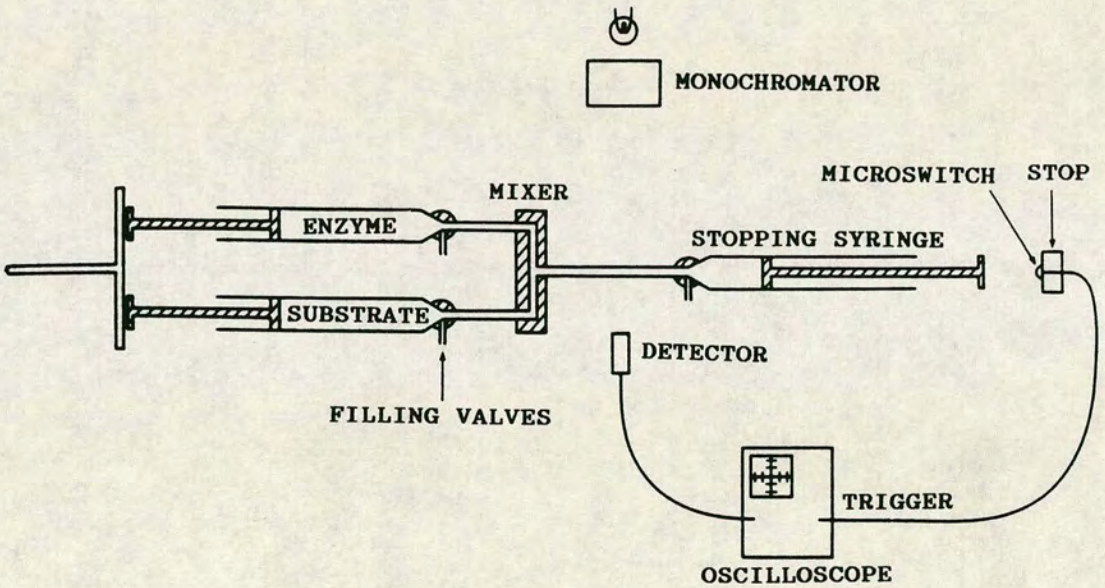

Details of the principle of operation are given in 7.9.

the solution to be used. Data were collected and displayed in the absorbance mode and were processed using the SF.17MV spectrofluorimeter software package.

Reduction of the flavin prosthetic group was followed by monitoring the decrease in absorbance at 438.3nm, an haem isosbestic, and reduction of the haem group was observed by monitoring increase in absorbance at either 557 or 423nm. The software package allowed rapid non-linear regression analysis of traces to analytical equations, including multiple exponentials. Data could thence be used to estimate kinetic parameters as described in Section 7.8.

7.10 UV/VISIBLE ABSORPTION SPECTROMETRY

7.10.1 GENERAL

The absorption of ultraviolet or visible radiation generally leads to excitation of specific bonding electrons and as a consequence the wavelength of absorption peaks can be correlated with the types of bonds that exist in the species under study.

The absorbance of dilute solutions, A, usually follows Beer's Law as shown in equation 4:-

$$A = \log_{10}\frac{I_0}{I} = \epsilon.c.l \qquad \text{(iv)}$$

The absorbance, A, is a function of the intensity of light incident on the sample, I_0, and the intensity of the light transmitted through the sample, I. It can be

seen that the degree of absorbance is dependent on three factors, solution concentration (c), the path length of the cell (l) and the molar extinction coefficient (ϵ). This law is the basis of all UV/visible absorption spectroscopic studies described in this work and has been used in the calculation of protein concentrations and activities.

Absorption spectroscopy can be used as a means of classification and identification of cytochromes, for example the spectrum of reduced flavocytochrome b_2 shows sharp peaks at 557, 528 and 423nm which are characteristic of a *b*-type cytochrome.

7.10.2 EXPERIMENTAL

All measurements were carried out using either Beckmann DU-62 or Pye Unicam SP2-800 UV/visible spectrophotometers, thermostatically controlled to 25.0±0.1°C. Protein spectra were recorded between 250 and 700nm. Kinetic data were collected by measuring absorbance change at fixed wavelengths of 420nm (ferricyanide) and 550nm (cytochrome *c*).

7.11 REDOX POTENTIOMETRY

7.11.1 GENERAL

Redox potential is a measure of the tendency of a redox couple to donate or accept electrons. Its value gives an

indication of the relative stability of the oxidised and reduced states. Any factor which results in stabilisation of the reduced form will make the couple a better electron acceptor and will give rise to a more positive redox potential. It is therefore important to monitor the redox potential of the prosthetic groups in flavocytochrome b_2 to make certain that effects observed in mutant enzymes are real and not an artefact of an altered redox potential.

The method of Dutton (9) coupled with spectrophotometry was used to measure the mid-point potential of the haem groups of the wild-type and hinge-swap enzymes. Measurements were carried out in a 3ml quartz cuvette adapted to hold the platinum working electrode, which was used in conjunction with an Ag/AgCl reference electrode. Prior to use the electrode was washed with acetone and dried. The spectrometer was fitted with a magnetic stirring device and a small bar magnet was placed in the cell to ensure thorough mixing. All potentials were measured under anaerobic conditions with stirring.

7.11.2 PREPARATION OF REDOX STANDARD SOLUTIONS

7.11.2.1 IRON (III)/ EDTA SOLUTION

EDTA (40mM - Fisons) was dissolved in deionised water and the resulting solution was neutralised to pH 7.0. Iron (III) ammonium sulphate (2mM - Aldrich) was dissolved in this solution by heating gently.

7.11.2.2 IRON (II) SOLUTION

Iron (II) ammonium sulphate (100mM - Aldrich) was dissolved in degassed deionised water. This solution was covered with a rubber septum and thoroughly degassed, as it was essential to keep this solution anaerobic.

7.11.2.3 DITHIONITE SOLUTION

Immediately before use, sodium dithionite (30mg - Fisons) was dissolved in tris-HCl, pH 7.5, I= 0.1M (5ml). The resulting solution was covered with a rubber septum and thoroughly degassed.

7.11.2.4 FERRICYANIDE SOLUTION

Potassium ferricyanide (30mg - Fisons) was dissolved in tris-HCl, pH 7.5, I=0.1M (5ml).

7.11.2.5 REDOX MEDIATORS

The redox centres of biological molecules are often shielded by protein and hence there can be no intimate contact with the electrode surface. Redox mediators are small organic or inorganic redox reagents which act as "go-betweens" between the biological redox couple and the measuring electrode. The mediators must be stable to decomposition, react reversibly and take no part in any chemical modification of the biological redox couple. The mediators chosen are those with E_m values in the range of

the biological redox couple.

The mediators used for the redox potential determination of the haem group of flavocytochrome *b*2 are listed below. Stock solutions (5mM) were made up in deionised water (with 20% ethanol for DAD and HNQ) and were kept in darkness as they all have a certain degree of light sensitivity.

Mediator	E_m (mV)
flavin mononucleotide (FMN)	-200
2-hydroxy-1,4-napthaquinone (HNQ)	-140
phenazine methosulphate (PMS)	+80
2,3,5,6-tetramethyl-p-phenylenediamine (DAD)	+220

7.11.3 CALIBRATING THE ELECTRODE

The calibration solution in the cuvette (5ml) was 0.3mM iron (III) ammonium sulphate solution and 0.25M acetate buffer (pH 5.0). Prior to use this was degassed for at least 10 minutes using saturated argon. Iron (II) ammonium sulphate solution (10μl) was injected via a port and the steady potential reading was noted; a further 15μl were injected, bringing the solution to a concentration of 0.5mM Fe^{3+}, and the potential was recorded. This gave two points on a Nernst plot from which values for slope and intercept could be found. These should ideally be 59mV and 108mV respectively.

7.11.4 SAMPLE PREPARATION

Protein was fully purified as described in 7.4.4 and stored as an ammonium sulphate precipitate. It was required in the oxidised state for redox potential determination so protein was dissolved in a minimal volume of tris-HCl, pH 7.5, I=0.1M, and was passed down a G25 column equilibrated in the same buffer (see 7.3.4).

7.11.5 MEASUREMENT OF THE HAEM REDOX POTENTIAL

After calibration of the electrode had been achieved, the redox analysis mixture consisting of 15-20 μM b_2, 20 μM Fe^{3+}/EDTA and 14 μM in each mediator, was degassed for at least 30 minutes, with stirring, prior to potential determination. Degassing and stirring were continued throughout the experiment.

The protein was reduced by titrating in dithionite. Visible absorption spectra were recorded sequentially over the range 530 to 570nm and potentials were noted for the haem α-peak at 557nm. The protein was then oxidised by ferricyanide titration and the potentials were again recorded. All potentials were corrected for the Ag/AgCl reference electrode (E_m = +196mV).

Calculation of [ox]/[red] allowed the plotting of a Nernst plot ($\log_{10}$[ox]/[red] versus E_h) for both the reductive and oxidative sequences, both of which overlay with a slope equal, within experimental error, to that of

the calibration plot (59mV). The intercept of these plots with the E_h-axis gave the haem mid-point potential.

7.12 NUCLEAR MAGNETIC RESONANCE SPECTROSCOPY

7.12.1 GENERAL

All atoms have a magnetic moment (or spin) which orientates in a specific direction when the substance is under the influence of an external magnetic field. This phenomena constitutes the basis of NMR. The sample under test is placed in a strong uniform magnetic field which produces "splitting" of nuclear energy levels. The sample is then subjected to an additional weak oscillating magnetic field, the frequency of which is scanned over a specified range. At certain frequencies the "nuclear magnets" resonate with the field, undergoing transitions between the energy levels. These resonances are detected and recorded. The resulting NMR spectrum is further complicated by effects such as coupling between the nuclei.

Two-dimensional NMR experiments, such as correlation spectroscopy (COSY), can facilitate the assignment of resonances. In COSY, a second radiofrequency pulse is applied at an interval after the first pulse (see Figure 7.4 for basic 1D pulse sequence). The resonances of the individual protons are dependent upon this interval and, thus, a 2D spectrum can be built up by repeating the experiment whilst varying the pulse interval. The

FIGURE 7.4

PULSE SEQUENCE USED IN 1D NMR EXPERIMENTS

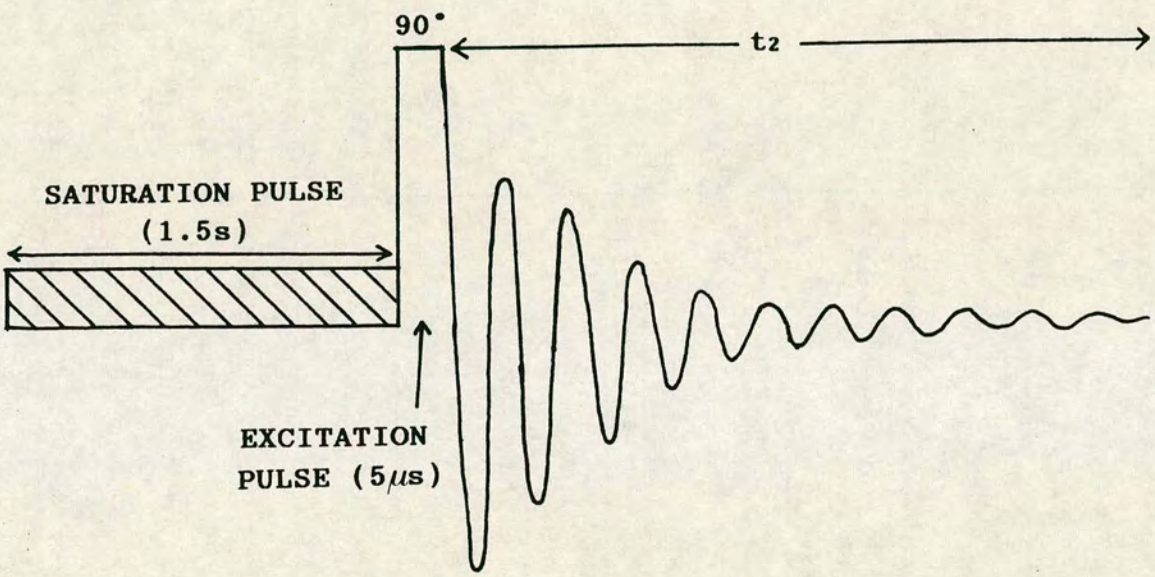

t_2 = DATA AQUISITION TIME (1.8s)

overlapping resonances of the 1D spectra are plotted along orthogonal axes producing a contour map, the "cross-peaks" of which are indicative of spin-spin coupling between the specific protons.

Proton NMR on the cytochrome *b*$_2$ core of flavocytochrome *b*$_2$ (10) has led to assignment of haem group resonances as described in Chapters 1 and 6. This has enabled further structural studies on the holoenzyme, as discussed in Chapters 5 and 6.

7.12.2 EXPERIMENTAL

All NMR studies were carried out at 25°C in D_2O using a Varian VXR 600S spectrometer operating at 600MHz. High quality quartz 7" NMR tubes (Wilmad) were used. Spectra were referenced to an internal standard as described in 6.2.4. In-tube measurement of pH was accomplished by use of a long stem glass probe electrode (Aldrich) which was calibrated as described in 7.2.1.

All 1D spectra were collected using the pulse sequence shown in Figure 7.4, and 512 scans were collected for each before Fourier Transformation was performed.

7.12.3 SAMPLE PREPARATION

Protein was fully purified and stored as an ammonium sulphate precipitate as described in 7.4.4. The required amount was dissolved in a minimal amount of 20mM phosphate buffer, pH 7.0, made up in D_2O (Sigma). The

solvent was exchanged several times by use of a Centricon-10 microconcentrator (Amicon). This was centrifuged at 4,500g for 60 minutes after each addition of fresh phosphate/D_2O buffer. Protein recovery from the membrane was achieved by inversion of the device and centrifugation at 300g for 2 minutes. Cytochrome *c* solution for titration was prepared in the same way using freeze-dried horse heart cytochrome *c* (type VI - Sigma).

7.13 REFERENCES

(1) Maniatis, T., Fritsch, E.F. & Sambrook, J., in *"Molecular Cloning: A Laboratory Manual"*, Cold Spring Harbour Press, Cold Spring Harbour, New York (1989).

(2) Black,M.T., White,S.A., Reid,G.A. & Chapman,S.K., *Biochem.J.*, **258**, 255 (1988).

(3) Freifelder, D., in *"Physical Biochemistry : Applications to Biochemistry and Molecular Biology"*, pg.526, W.H.Freeman and Co. (1976).

(4) Weber,K. & Osborn,M., *J.Biol.Chem.*, **244**, 4406 (1969).

(5) Shapiro,S.S. & Dennis,D., *Biochemistry*, **4**, 2283 (1965).

(6) Michaelis,M. & Menten,M.L., *Biochem.Z.*, **49**, 333 (1913).

(7) Lineweaver,H. & Burk,D., *J.Am.Chem.Soc.*, **56**, 658 (1934).

(8) Labeyrie,F., Baudras,A. & Lederer,F., *Methods Enzymol.*, **53**, 238 (1978).

(9) Dutton,P.L., *Methods. Enzymol.*, **54**, 411 (1978).

(10) Brunt,C.E., Cox,M.C., Thurgood,A.G.P., Moore,G.R., Reid,G.A. & Chapman, S.K., *Biochem.J.*, **283**, 87 (1992).

APPENDIX I

DERIVATION OF KINETIC EQUATIONS

(a) THE MICHAELIS-MENTEN EQUATION (1)

In 1913, Michaelis and Menten proposed the following scheme for single substrate reactions:-

$$E + S \underset{}{\overset{Ks}{\rightleftharpoons}} ES \xrightarrow{k_{cat}} E + P \qquad (i)$$

where E, S, ES and P are the enzyme, substrate, enzyme-substrate complex and product respectively. The catalytic reaction is divided into two processes. Firstly, enzyme and substrate combine to give an enzyme-substrate complex. This step is assumed to be rapid and reversible with no chemical changes occurring; the components are held together by physical forces. The chemical processes occur in the second step, with a first order rate constant, k_{cat} (the turnover number).

The equations are solved in the following manner:-

From (i): $$Ks = \frac{[E][S]}{[ES]} \qquad (ii)$$

The initial rate, v, can be represented as equation (iii)

$$v = k_{cat}[ES] \qquad (iii)$$

The total enzyme concentration, $[E_o]$, and that of the free enzyme, [E], are related by equation (iv):-

$$[E] = [E]_o - [ES] \qquad (iv)$$

Substituting into equation (ii):-

$$[ES] = \frac{[E]_o[S]}{K_s + [S]} \qquad (v)$$

and into (iii):-

$$v = \frac{[E]_o[S]k_{cat}}{K_s + [S]} \qquad (vi)$$

K_s, the dissociation constant of the enzyme-substrate complex, is equal to K_M, resulting in the familiar Michaelis-Menten equation:-

$$v = \frac{[E]_o[S]k_{cat}}{K_M + [S]} \qquad (vii)$$

where $k_{cat}[E]_o = V_{max}$ (viii)

(b) <u>THE LINEWEAVER-BURK PLOT</u> (2)

The Michaelis-Menten equation is often converted into linear form in order to analyse data graphically. One of the more common methods is the double-reciprocal or Lineweaver-Burk plot. Inversion of both sides of equation (vii) and substitution in equation (viii) gives:-

$$\frac{1}{v} = \frac{1}{V_{max}} + \frac{K_M}{V_{max}[S]} \qquad (ix)$$

A disadvantage of plotting 1/v versus 1/[S] is that data points at high substrate concentrations are compressed into a small region whereas those at low substrate concentrations are emphasised.

(c) COMPETITIVE INHIBITION (3)

A competitive inhibitor competes with the substrate for the active site. In the case of the Michaelis-Menten equation, a further equilibrium must be considered:-

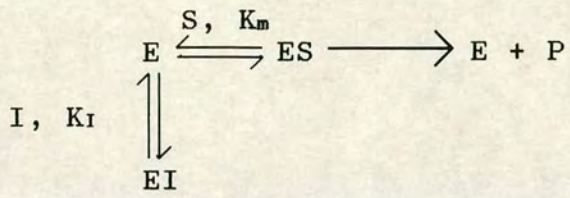

where I is the inhibitor and K_I is the dissociation constant of EI, the enzyme-inhibitor complex.
In this case, the enzyme concentration is given by the following equation:-

$$[E]_o = [ES] + [EI] + [E] \qquad (x)$$

Solving the equilibrium and rate equations given above gives equation (xi):-

$$v = \frac{[E]_o[S]k_{cat}}{[S] + K_M(1 + [I]/K_I)} \qquad (xi)$$

From equation (xi), it can be seen that competitive inhibition only affects K_M, increasing it by a factor of $(1 + [I]/K_I)$.

(d) NONCOMPETITIVE INHIBITION (3)

In this type of inhibition, substrate and inhibitor bind simultaneously to the enzyme, instead of competing for the same binding site. The following pattern occurs:-

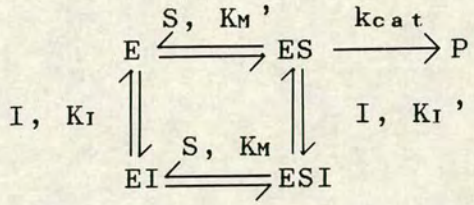

Assuming that the dissociation constant of S from ESI is the same as that from ES (*i.e.* $K_M = K_M'$) and that ESI does not react, it can be shown that:-

$$v = \frac{[E]_o[S]k_{cat}/(1 + [I]/K_I)}{[S] + K_M} \qquad \text{(xii)}$$

Thus, in noncompetitive inhibition, K_M is unaffected, but k_{cat} is lowered by a factor of $(1 + [I]/K_I)$. More commonly K_m is not equal to K_M' and both K_M and k_{cat} are altered. This is termed mixed inhibition. Another type of inhibition, uncompetitive, occurs when I binds to ES but not to E.

(e) SUBSTRATE INHIBITION

In some cases, inhibition occurs as a result of excess substrate binding to a second site. If this ternary complex is inactive, the rate equation is as follows:-

$$v = \frac{V_{max}}{1 + K_M/[S] + [S]/K_I} \qquad \text{(xiii)}$$

A plot of v versus $\log_{10}[S]$ gives a symmetrical bell-shaped curve with inflexion points equal to K_M and K_I. By differentiating equation (xiii) and setting it to

zero, the substrate concentration at which the maximal rate occurs (S_{opt}) can be calculated (equation (xiv)):-

$$S_{opt} = \sqrt{K_M . K_I} \qquad \text{(xiv)}$$

REFERENCES

(1) Michaelis, L. & Menten, M.L., *Biochem.Z.*, **49**, 333 (1913).

(2) Lineweaver, H. & Burk, D., *J.Am.Chem.Soc.*, **56**, 658 (1934).

(3) Fersht, A., in *"Enzyme Structure and Mechanism"* (2nd edition), Freeman, W.H. & Co., New York, pp.107 (1985).

APPENDIX II

LECTURE COURSES AND MEETINGS ATTENDED

LECTURE COURSES

(1) "Pesticides" - Dr.H.McNab (1990).

(2) "Inorganic Medicinal Chemistry" - Drs. S.K. Chapman and A.J.Welch (1991).

(3) "German Introductory Reading Course" - W.T. Webster (1990 - 1991).

(4) "Chemistry of Metals in Biological Systems" - Federation of European Biochemical Societies Advanced Course, Louvain-la-Neuve, Belgium (1992).

(5) "Departmental Research Seminars and Colloquia" (1990 - 1993).

(6) "Departmental Postgraduate Lectures" (1990 - 1993).

MEETINGS ATTENDED

(1) Meetings of the Scottish Protein Structure Group (SPSG), University of Stirling (November 1990 and 1992).

(2) Inorganic Biochemistry Discussion Group (IBDG), Christmas Meeting, King's College, London (1990).

(3) Fifth International Conference on Inorganic Biochemistry, University of Oxford (August 1991).

(4) Symposium on Protein Engineering, Royal Society of Edinburgh, Edinburgh (January 1992).

(5) "Metalloproteins - Genetic, Biochemical and Structural Approaches", IBDG and SPSG Meeting, University of Edinburgh (April 1992) (Speaker).

(6) University of Strathclyde Inorganic Club (USIC) Meetings (June 1991 and 1992).

(7) Symposium on Metal Complexes and Metalloenzymes, Royal Society of Chemistry, Dalton Division, University of Glasgow (September 1992).

(8) SERC/CRAC Graduate School, University of Stirling (June 1993).

(9) Sixth International Conference on Bioinorganic Chemistry, University of California, San Diego (August 1993).

APPENDIX III

PUBLICATIONS

PAPERS

(1) "The importance of the hinge in intramolecular electron transfer in flavocytochrome *b*$_2$."
White,P., Manson,F.D.C., Brunt,C.E., Chapman,S.K. & Reid,G.A., *Biochem.J.*, **291**, 89-94 (1993).

(2) "Probing the structure and function of flavocytochrome *b*$_2$ using protein engineering methods."
Chapman, S.K., White, P., Daff, S., Reid, G.A., Sharp,R.E. & Manson,F.D.C., in *"Flavins and Flavoproteins"* (1993) (in press).

(3) "The role of the interdomain hinge of flavocytochrome *b*$_2$ in intra- and inter-protein electron transfer."
Sharp,R.E., White,P., Chapman,S.K. & Reid,G.A., *Biochemistry* (in preparation).

ABSTRACTS

(1) "Electron transfer in flavocytochrome *b*$_2$ - effects of pH."
White,P., Reid,G.A. & Chapman,S.K., *J.Bioinorg.Chem.*, **43**, No.2-3, 166 (1991).

(2) "Investigation of interdomain communication in flavocytochrome *b*2 by generation of a domain-swap interspecies hybrid enzyme."
White,P., Short,D.M., Chapman,S.K. & Reid,G.A., *J.Bioinorg.Chem.*, **51**, No.1-2, 185 (1993).

(3) "The use of deletion mutants in the hinge region as functional probes of flavocytochrome *b*2."
Sharp,R.E., White,P., Chapman,S.K. & Reid,G.A., *J.Bioinorg.Chem.*, **51**, No.1-2, 184 (1993).

(4) "Cytochrome *c* binding and electron transfer properties of wild-type and mutant forms of flavocytochrome *b*2."
Sharp,R.E., White,P., Chapman,S.K. & Reid,G.A., *J.Bioinorg.Chem.*, **51**, No.1-2, 199 (1993).

The importance of the interdomain hinge in intramolecular electron transfer in flavocytochrome b_2

Patricia WHITE,* Forbes D. C. MANSON,† Claire E. BRUNT,* Stephen K. CHAPMAN* and Graeme A. REID†‡

*Department of Chemistry, Edinburgh Centre for Molecular Recognition, University of Edinburgh, West Mains Road, Edinburgh EH9 3JJ, and †Institute of Cell and Molecular Biology, Edinburgh Centre for Molecular Recognition, University of Edinburgh, Edinburgh EH9 3JR, Scotland, U.K.

The two distinct domains of flavocytochrome b_2 (L-lactate:cytochrome *c* oxidoreductase) are connected by a typical hinge peptide. The amino acid sequence of this interdomain hinge is dramatically different in flavocytochromes b_2 from *Saccharomyces cerevisiae* and *Hansenula anomala*. This difference in the hinge is believed to contribute to the difference in kinetic properties between the two enzymes. To probe the importance of the hinge, an interspecies hybrid enzyme has been constructed comprising the bulk of the *S. cerevisiae* enzyme but containing the *H. anomala* flavocytochrome b_2 hinge. The kinetic properties of this 'hinge-swap' enzyme have been investigated by steady-state and stopped-flow methods. The hinge-swap enzyme remains a good lactate dehydrogenase as is evident from steady-state experiments with ferricyanide as acceptor (only 3-fold less active than wild-type enzyme) and stopped-flow experiments monitoring flavin reduction (2.5-fold slower than in wild-type enzyme). The major effect of the hinge-swap mutation is to lower dramatically the enzyme's effectiveness as a cytochrome *c* reductase; $k_{cat.}$ for cytochrome *c* reduction falls by more than 100-fold, from 207 ± 10 s^{-1} (25 °C, pH 7.5) in the wild-type enzyme to 1.62 ± 0.41 s^{-1} in the mutant enzyme. This fall in cytochrome *c* reductase activity results from poor interdomain electron transfer between the FMN and haem groups. This can be demonstrated by the fact that the $k_{cat.}$ for haem reduction in the hinge-swap enzyme (measured by the stopped-flow method) has a value of 1.61 ± 0.42 s^{-1}, identical with the value for cytochrome *c* reduction and some 300-fold lower than the value for the wild-type enzyme. From these and other kinetic parameters, including kinetic isotope effects with [2-^{2}H]lactate, we conclude that the hinge plays a crucial role in allowing efficient electron transfer between the two domains of flavocytochrome b_2.

INTRODUCTION

Flavocytochrome b_2 (L-lactate:cytochrome *c* oxidoreductase, EC 1.1.2.3) from baker's yeast (*Saccharomyces cerevisiae*) is a tetramer of identical subunits each with M_r 57500 [1]. The enzyme is a soluble component of the mitochondrial intermembrane space [2], where it catalyses the oxidation of L-lactate to pyruvate and transfers electrons to cytochrome *c* [3]. The crystal structure of *Saccharomyces* flavocytochrome b_2 has been solved to 0.24 nm resolution [4] and reveals that each subunit consists of two distinct domains: an N-terminal haem-containing, or cytochrome, domain and a C-terminal FMN-containing domain. The two domains are connected by a single segment of polypeptide chain which constitutes the interdomain hinge (Figure 1a). That this segment of polypeptide functions as a hinge is supported by crystallographic [4] and n.m.r. data [5], all of which indicate that the cytochrome domain is relatively mobile. The primary structure of flavocytochrome b_2 from another yeast, *Hansenula anomala*, has been determined [6]. Although there is an overall 60% identity between the amino acid sequences of the *Hansenula* and *Saccharomyces* enzymes, there are striking differences in the primary structure and net charge of the hinge segment. We have suggested that these marked differences may account, at least in part, for the known kinetic differences between the flavocytochromes b_2 from the two yeasts [6]. To test this idea, and to probe the role of the hinge more broadly, we have constructed an interspecies hybrid enzyme consisting of the bulk of the *Saccharomyces* enzyme but containing the hinge section from the *Hansenula* enzyme (Figure 1b). This hybrid enzyme is referred to as the 'hinge-swap' flavocytochrome b_2.

MATERIALS AND METHODS

DNA manipulation, strains, media and growth

Standard methods for growth of *Escherichia coli*, plasmid purification, DNA manipulation and transformation were performed as described in Sambrook et al. [7].

Modification of the flavocytochrome b_2 genes

The plasmid pGR401 contains the entire *S. cerevisiae* flavocytochrome b_2-coding sequence on a 1.8 kb *Eco*RI–*Hin*dIII fragment [8]. The *H. anomala* flavocytochrome b_2 gene was subcloned from λFG1 [6] as a 5.7 kb *Bam*HI fragment into plasmid pTZ19r [9]. The resulting recombinant plasmid, pMB3, was used for site-directed mutagenesis by the method of Kunkel [10] (using oligonucleotides synthesized by the OSWEL DNA service, University of Edinburgh) to introduce cleavage sites for *Eco*RI and *Hin*dIII at the start and end respectively of the *H. anomala* flavocytochrome b_2 sequence encoding the mature protein. The oligonucleotide used to introduce the *Eco*RI site was also designed to introduce an ATG initiation codon immediately between the *Eco*RI site and the codon for Asp-1 of the mature protein. To facilitate transfer of coding sequence between plasmids, we also removed the *Hin*dIII site within the coding sequence of *H. anomala* flavocytochrome b_2 by introducing a silent mutation (using oligonucleotide 982D, gtcttgaaggctttgtg).

Abbreviation used: KIE, kinetic isotope effect.

‡ To whom correspondence should be addressed.

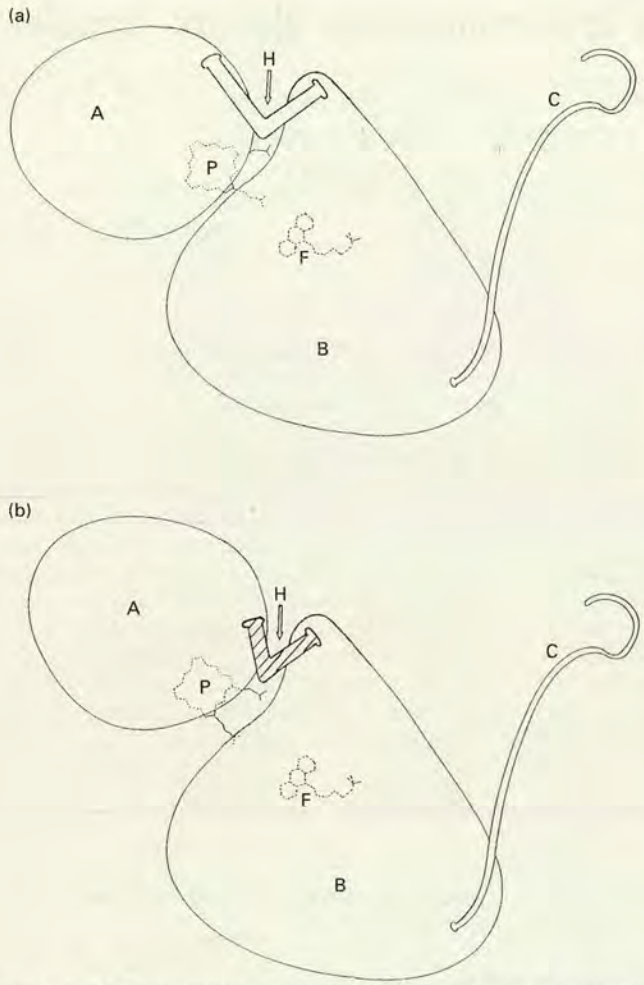

Figure 1 (a) Schematic representation of a wild-type flavocytochrome b_2 subunit based on the known three-dimensional structure and (b) schematic representation of a hinge-swap mutant flavocytochrome b_2 subunit

The mutant enzyme is shown with a shorter interdomain hinge (hatched) and it is postulated that this results in restriction of mobility and, possibly, an altered position of the haem domain. A, Haem domain; B, flavin domain; C, C-terminal tail; F, FMN; P, protohaem IX; H, interdomain hinge.

For construction of hybrid proteins, restriction-enzyme-cleavage sites were introduced at equivalent positions flanking the interdomain-hinge-coding region in both sequences (Figure 2a). An *Xba*I site occurs naturally in the *S. cerevisiae* sequence but the *Apa*I sites and the *Xba*I site in the *H. anomala* sequence were introduced by site-directed mutagenesis (Figure 2b) using the following oligonucleotides: 661G, catcttgggcccttagttgg (to insert an *Apa*I site in the *H. anomala* coding sequence); 662G, gaaaaccacctctagaccaaatgat (to insert an *Xba*I site in the *H. anomala* coding sequence); 660G, aaattggggccccttcaa (to insert an *Apa*I site in the *S. cerevisiae* coding sequence). Introduction of the *Apa*I sites did not alter the amino acid sequences, but introduction of the *Xba*I site into the *H. anomala* sequence necessitated replacement of Ser-112 by Asp, the amino acid residue found at the equivalent position in the *S. cerevisiae* enzyme. DNA sequences of the mutated flavocytochrome b_2 sequences were determined using a series of suitably designed primers in conjunction with the Sequenase kit (US Biochemicals). Two secondary mutations were found in the *H. anomala* coding sequence but in each case the encoded amino acid sequence was unaltered. The plasmids containing the modified *S. cerevisiae* and *H. anomala* coding sequences were named pFM200 and pFM102 respectively.

Construction and expression of the hinge-swap flavocytochrome b_2

Plasmid pFM200 was cleaved with *Apa*I and *Xba*I and the large fragment was isolated. The small *Apa*I–*Xba*I fragment, encoding the hinge region, was isolated from plasmid pFM102 and ligated to the large fragment from pFM200. The structure of recombinants was verified by restriction enzyme analysis and the hybrid coding sequence from one recombinant was subcloned on a 1.8 kb *Eco*RI–*Hin*dIII fragment into the expression vector pDS6 as previously described [11].

Enzymes

Wild-type and hinge-swap flavocytochromes b_2 expressed in *E. coli* were isolated from cells, which had been stored at −20 °C, using a previously reported purification procedure [11]. Purified enzyme preparations were stored under nitrogen at 4 °C as precipitates in 70 % $(NH_4)_2SO_4$.

Kinetic analysis

All kinetic experiments were carried out at 25±0.1 °C in Tris/HCl at pH 7.5, I 0.10 mol/l. The buffer concentration was 10 mM in HCl with I adjusted to 0.10 mol/l by addition of NaCl.

Steady-state kinetic measurements involving the enzymic oxidation of L-lactate were performed using a Beckman DU62 spectrophotometer with either cytochrome *c* (type VI, Sigma) or ferricyanide (potassium salt, BDH Chemicals) as electron acceptor as previously described [12].

Stopped-flow measurements were carried out with an Applied Photophysics SF.17MV stopped-flow spectrofluorimeter. Flavin reduction was monitored at 438.3 nm (a haem isosbestic point) and haem reduction at either 557 or 423 nm (results were identical at both wavelengths). Collection and analysis of data were as previously described [12].

K_m and $k_{cat.}$ parameters were determined using non-linear regression analysis.

Kinetic isotope effects (KIEs) were measured using L-[2-^{2}H]-lactate as previously described [12].

Measurement of redox potential

The midpoint potential of the haem groups in the wild-type and hinge-swap enzymes were determined spectrophotometrically using a previously published redox potentiometry method [13]. The mediators, *N*-ethylphenazonium sulphate, *N*-methylphenazonium sulphate, 2,3,5,6-tetramethylphenylenediamine and 2-hydroxy-1,4-naphthoquinone, were used as previously described [13]. Enzyme was reduced by titrating with sodium dithionite under anaerobic conditions and oxidized by titrating with potassium ferricyanide as reported elsewhere [14].

RESULTS

Steady-state kinetic analysis

Results from steady-state kinetic measurements on the hinge-swap enzyme using L-[2-^{1}H]lactate and L-[2-^{2}H]lactate as substrates and with ferricyanide and cytochrome *c* as electron acceptors are presented in Table 1, where they are compared with

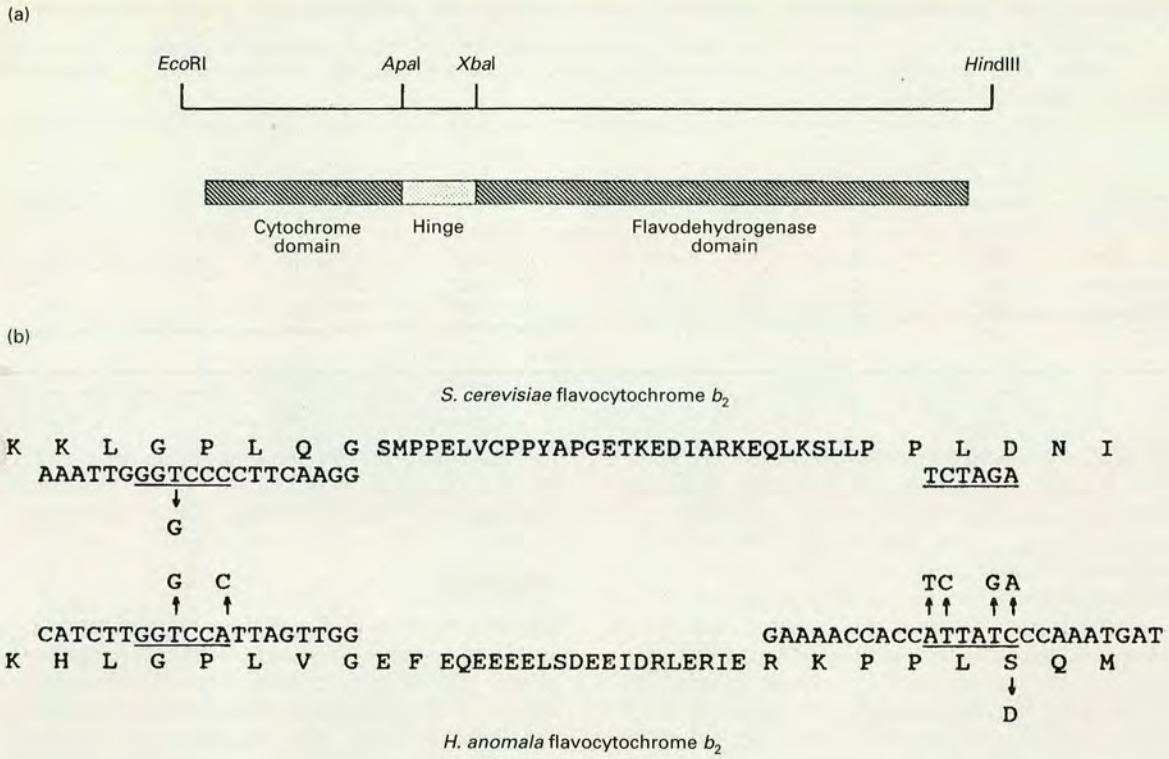

Figure 2 Construction of the hinge-swap flavocytochrome b_2

(**a**) DNA sequences encoding flavocytochrome b_2 from *S. cerevisiae* and *H. anomala* were modified to have the same general structure as represented by the restriction map above and the corresponding structure below (N-terminus at the left). (**b**) Sequence modifications introduced by site-directed mutagenesis at either end of the hinge-coding sequence are shown along with the DNA sequences around the introduced restriction sites and the amino acid sequence of the entire hinge regions. Site-directed modifications are indicated by arrows and the restriction sites used for construction of the hinge-swap enzyme are underlined.

Table 1 Steady-state kinetic parameters and ^{2}H KIEs for wild-type and hinge-swap flavocytochromes b_2

All experiments were carried out at 25 °C in Tris/HCl buffer, pH 7.5 (I 0.10). Concentrations of acceptors used with the hinge-swap enzyme were as follows: [cytochrome *c*], 15 μM; [ferricyanide], 8 mM. $k_{cat.}$ is expressed as mol of electrons transferred/s per mol of enzyme (as L-lactate is a two-electron donor these values can be halved to express them in terms of mol of substrate reduced/s). Abbreviations are as follows: [^{1}H]Lac, L-[2-^{1}H]lactate; [^{2}H]Lac, L-[2-^{2}H]lactate; Ferri, ferricyanide; Cyt. *c*, cytochrome *c*.

Enzyme	Electron acceptor	$k_{cat.}$ (s^{-1})		K_m (mM)		$10^{-5}\,k_{cat.}/K_m$ ($M^{-1}\cdot s^{-1}$)		KIE	Reference
		[^{1}H]Lac	[^{2}H]Lac	[^{1}H]Lac	[^{2}H]Lac	[^{1}H]Lac	[^{2}H]Lac		
Wild-type	Ferri	400 ± 10	86 ± 5	0.49 ± 0.05	0.76 ± 0.06	8.2	1.1	4.7 ± 0.4	[11]
Hinge-swap	Ferri	126 ± 6	61 ± 3	0.16 ± 0.02	0.60 ± 0.10	7.9	1.0	2.1 ± 0.2	This work
Wild-type	Cyt. *c*	207 ± 10	70 ± 10	0.24 ± 0.04	0.48 ± 0.10	8.6	1.5	3.0 ± 0.6	[11]
Hinge-swap	Cyt. *c*	1.62 ± 0.41	0.97 ± 0.29	0.002 ± 0.001	0.005 ± 0.003	8.1	1.9	1.7 ± 1.3	This work

previously reported values for the wild-type enzyme. It should be noted first that the hinge-swap enzyme is still a good lactate dehydrogenase as judged by the results with ferricyanide as electron acceptor (only a 3-fold decrease in the $k_{cat.}$ value in this case). However, it is apparent that there are a number of more significant differences between the kinetic properties of the wild-type and hinge-swap enzymes. The most striking of these differences is the very large (over 100-fold) decrease in the $k_{cat.}$ value for the hinge-swap enzyme when cytochrome *c* is used as the electron acceptor. The fact that $k_{cat.}$ values differ depending on whether ferricyanide or cytochrome *c* is used as electron acceptor indicates that electron flow to these acceptors has been affected in different ways by the hinge-swap mutation, with electron flow to cytochrome *c* being severely impaired. Thus the hinge-swap enzyme, although it remains a good lactate dehydrogenase, is a very poor cytochrome *c* reductase.

It has been previously shown that proton abstraction at C-2 of lactate is the major rate-limiting step in the wild-type enzyme [12,15]. From Table 1 it can be seen that the deuterium KIE values for the hinge-swap enzyme are lower than those for the wild-type enzyme with both electron acceptors. This suggests that electron-transfer reactions subsequent to C-2 proton abstraction contribute to overall rate limitation in the hinge-swap enzyme.

Table 2 Stopped-flow kinetic parameters and ^2H KIEs for reduction of FMN and haem in the wild-type and hinge-swap flavocytochromes b_2

All experiments were carried out at 25 °C in Tris/HCl buffer, *I* 0.10. Stopped-flow data were analysed as described in the Materials and methods section. Values of $k_{cat.}$ are expressed as number of prosthetic groups reduced/s. Where biphasic kinetics were observed, the values reported correspond to those of the rapid phase as previously described [12]. Abbreviations are as follows: [^{1}H]Lac, L-[2-^{1}H]lactate; [^{2}H]Lac, L-[2-^{2}H]lactate.

Enzyme	Prosthetic group reduction	$k_{cat.}$ (s^{-1})		K_m (mM)		KIE	Reference
		[^{1}H]Lac	[^{2}H]Lac	[^{1}H]Lac	[^{2}H]Lac		
Wild-type	FMN	604±60	75±5	0.84±0.20	1.33±0.28	8.1±1.4	[11]
Hinge-swap	FMN	240±12	38±2	0.37±0.02	0.56±0.01	6.3±0.7	This work
Wild-type	Haem	445±50	71±5	0.53±0.05	0.68±0.05	6.3±1.2	[11]
Hinge-swap	Haem	1.61±0.42	1.00±0.11	0.003±0.001	0.003±0.001	1.6±0.7	This work

The value of K_m for L-lactate seen with the hinge-swap enzyme is similar to that seen for the wild-type enzyme when ferricyanide is used as electron acceptor. However, with cytochrome *c* as electron acceptor the apparent K_m for L-lactate in the hinge-swap enzyme is dramatically decreased (Table 1). Clearly this K_m value is not a reflection of the K_d for L-lactate since its value is affected by steps after L-lactate binding, e.g. electron transfer to cytochrome *c*. It is interesting to note that, with cytochrome *c* as electron acceptor, the decrease in the K_m value for L-lactate seen with the hinge-swap enzyme is similar in magnitude to the decrease in $k_{cat.}$ (both decreased by around 100-fold with respect to the wild-type enzyme) so that the value of $k_{cat.}/K_m$ is in fact not greatly altered.

Stopped-flow kinetic analysis

Reduction of the FMN and haem groups of hinge-swap flavocytochrome b_2 by L-[2-^{1}H]lactate and L-[2-^{2}H]lactate was monitored directly using stopped-flow spectrophotometry. Kinetic parameters are summarized in Table 2. FMN reduction was monophasic at all lactate concentrations, whereas haem reduction was biphasic. This is in marked contrast with the results of previous work on wild-type enzyme in which biphasic kinetics were observed for FMN reduction, at least at high lactate concentrations [12,15–17]. For wild-type enzyme, it is known that the rapid phase corresponds to initial reduction of FMN and haem (with the slow phase being kinetically irrelevant in catalytic turnover of the enzyme) [12,15–17]. The effect of the hinge-swap mutation on the rate of FMN reduction is small, with $k_{cat.}$ for the mutant enzyme being only 2- to 3-fold lower than that for the wild-type enzyme. However, there are dramatic effects on the rate of haem reduction, with $k_{cat.}$ for the hinge-swap enzyme being over 300-fold less than that for the wild-type enzyme (Table 2). These results indicate that introducing the hinge-swap mutation has only a slight effect on electron transfer from L-lactate to FMN but must have a major effect on electron transfer from FMN to haem. This conclusion is supported by the KIE values reported in Table 2.

Redox potentials

There was the possibility that the hinge-swap mutation might have affected the redox potentials of the prosthetic groups. Clearly there can have been little effect on the flavin potential since the $k_{cat.}$ values for flavin reduction are not greatly altered by the mutation. However, it was possible that a large change in haem potential could have contributed to the dramatic lowering of the $k_{cat.}$ value for haem reduction in the hinge-swap enzyme. To check this, we measured the haem redox potentials for the wild-type and hinge-swap enzymes and found that these values are the same within experimental error: wild-type = -20 ± 2 mV; hinge-swap = -23 ± 3 mV.

DISCUSSION

The two domains of *S. cerevisiae* flavocytochrome b_2 are connected by a typical hinge sequence that contains several proline, glycine and charged residues. The most likely function of this hinge is to allow the cytochrome domain to move with respect to the flavin domain. This suggestion is supported by both crystallographic and n.m.r. experiments. In the three-dimensional structure of *S. cerevisiae* flavocytochrome b_2, two crystallographically distinct types of subunit are seen in the asymmetric unit. In one case, substrate is absent from the active site and the cytochrome domain is resolved. In the other, where pyruvate is found at the active site, no electron density is observed for the cytochrome domain, suggesting that it is positionally disordered [4]. In solution, n.m.r. spectroscopy shows that the cytochrome domain is substantially more mobile than would be expected for a protein as large as the flavocytochrome b_2 tetramer; the observed linewidths indicate considerable flexibility of this domain [5, and our unpublished work]. There is thus a significant body of evidence to indicate that the hinge is important in interdomain interactions. It is interesting therefore that the hinge sequence is dramatically different in flavocytochromes b_2 from *S. cerevisiae* and *H. anomala*; the hinge in the *H. anomala* enzyme is six residues shorter and considerably more acidic than in the *S. cerevisiae* enzyme [6]. We believe that these differences contribute to the well-known differences in the kinetic properties of the flavocytochromes b_2 from these two yeasts [18]. To test this idea and to probe the importance of the hinge more broadly, site-directed mutagenesis has been used to generate an interspecies hybrid which retains the cytochrome and flavin domains of *S. cerevisiae* flavocytochrome b_2 but has the hinge segment replaced by the equivalent segment from the *H. anomala* enzyme. The resulting hinge-swap flavocytochrome b_2 has some very interesting differences in its electron-transfer properties when compared with the original enzyme.

The catalytic cycle for flavocytochrome b_2 is shown in Scheme 1. The first step, electron transfer from lactate to flavin, is only slightly affected by the hinge-swap mutation. K_m and $k_{cat.}$ values for FMN reduction are only a little over 2-fold lower in the mutant enzyme than in the wild-type enzyme (Table 2). This indicates that the hinge is not of great importance in FMN reduction by lactate and thus the hinge-swap enzyme remains a good lactate dehydrogenase. This conclusion is supported by the steady-state measurements with ferricyanide as electron acceptor (Table 1). Steps after FMN reduction are very different

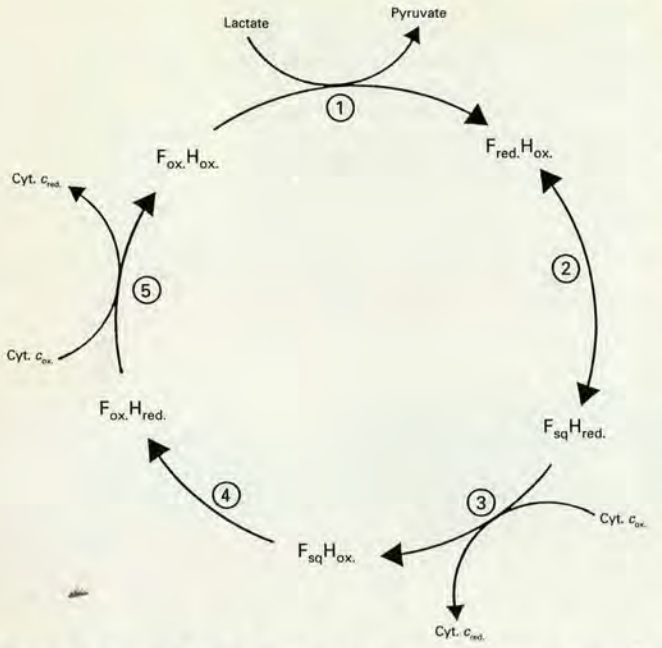

Scheme 1 Catalytic cycle of lactate oxidation and cytochrome *c* reduction by flavocytochrome b_2

① Oxidation of lactate to pyruvate and reduction of FMN. This is the slowest step in the case of the wild-type enzyme. ② Electron transfer from fully reduced FMN to haem resulting in the semiquinone form of FMN and reduced haem. This is the slowest step in the case of the hinge-swap enzyme. ③ The first cytochrome *c* molecule is reduced by electron transfer from the haem group of flavocytochrome b_2. ④ Electron transfer from the semiquinone form of FMN to haem resulting in fully oxidized FMN and reduced haem. ⑤ The second cytochrome *c* molecule is reduced by electron transfer from the haem group which regenerates the fully oxidized enzyme. The enzyme is now ready to repeat the cycle. Abbreviations: $F_{ox.}$, oxidized FMN; F_{red}, reduced FMN; F_{sq}, the semiquinone form of FMN; $H_{ox.}$, oxidized haem; H_{red}, reduced haem; Cyt. $c_{ox.}$, oxidized cytochrome *c*; Cyt. $c_{red.}$, reduced cytochrome *c*.

in the mutant and wild-type enzymes. The $k_{cat.}$ for haem reduction in the hinge-swap enzyme is some 300-fold lower than in the wild-type enzyme. This dramatic result indicates that there has been a major impairment of electron transfer from FMN to haem (step ② in Scheme 1). Clearly the hinge-swap mutation has disrupted interdomain communication. A possible explanation for this is that the hinge in the mutant enzyme, which is six residues shorter than in the wild-type enzyme, might be restricting hinge bending and thus preventing efficient recognition between the two domains, as indicated schematically in Figure 1(b).

The final steps in the catalytic cycle involve reduction of the physiological electron acceptor, cytochrome *c* (Scheme 1). Electrons can be transferred to cytochrome *c* only from the flavocytochrome b_2 haem [19,20]. It is therefore not surprising that the rate of cytochrome *c* reduction is greatly affected by the hinge-swap mutation (over 100-fold slower than in the wild-type enzyme). In fact, in the hinge-swap enzyme the $k_{cat.}$ value for reduction of cytochrome *c* is identical, within experimental error, to the $k_{cat.}$ for b_2-haem reduction. This means that, in the mutant enzyme, cytochrome *c* reduction does not contribute to rate limitation in the catalytic cycle. Considered together, these results indicate that FMN → haem electron transfer is the slowest step in the catalytic cycle of the hinge-swap flavocytochrome b_2. This conclusion is supported by the deuterium KIE values reported in Table 2. For FMN reduction there is only a slight erosion of the KIE; 8.1 for the wild-type and 6.3 for the mutant enzyme. This confirms that proton abstraction at C-2 of lactate is still rate-limiting for FMN reduction. However, for haem reduction there is a more significant lowering of the KIE value from 6.3 in the wild-type to 1.6 in the mutant enzyme. This indicates that, in contrast with the wild-type enzyme, there is little or no rate limitation to haem reduction arising from proton abstraction at C-2 of lactate in the hinge-swap flavocytochrome b_2. Also, since cytochrome *c* can only accept electrons from the haem group, it is not surprising that the KIE for cytochrome *c* reduction measured in the steady state is identical with the value for b_2-haem reduction measured by stopped-flow spectrophotometry.

The fact that FMN → haem electron transfer is the slowest step in the catalytic cycle of the hinge-swap enzyme allows us to explain another difference between this mutant enzyme and the wild-type flavocytochrome b_2. In the wild-type enzyme, flavin reduction monitored by stopped-flow spectrophotometry is biphasic. A number of workers have previously described the origin of this biphasic behaviour which arises because each flavocytochrome b_2 protomer requires three electrons for full reduction (i.e. each tetramer requires 12 electrons from six lactate molecules for full reduction) [12,15–17]. These workers have shown that the rapid phase corresponds to the initial reduction of flavin and haem groups and the slow phase (which is kinetically irrelevant during catalytic turnover of the enzyme) corresponds to the entry of the third electron which is permitted because of interprotomer electron transfer [12,15–17]. For interprotomer electron transfer to occur from one flavin group to another within the tetramer, the flavin must be in the semiquinone state, i.e. one of the electrons must have been passed on to the haem group and FMN → haem electron transfer must be faster than interprotomer electron transfer. In the hinge-swap enzyme, the reduction of the flavin is monophasic. This is because FMN → haem electron transfer is now slower than interprotomer electron transfer would be. Thus on the time scale for FMN reduction, only one phase is observed.

As already mentioned, the most likely reason for the effect of the hinge-swap mutation on the rate of FMN → haem electron transfer is that the shorter hinge has reduced flexibility and impaired recognition between the cytochrome and flavin domains. There is also the possibility that the mutation might have affected the redox potential of the haem groups. We have excluded this possibility by showing that the measured values of the haem redox potentials for the wild-type and hinge-swap enzymes are identical within experimental error.

Conclusions

From our studies on the hinge-swap flavocytochrome b_2, we draw the following conclusions: (i) the interdomain hinge has little influence on the lactate dehydrogenase function of the enzyme but is important for its role as a cytochrome *c* reductase; (ii) the hinge is crucial in mediating electron transfer between the flavin- and haem-containing domains of the enzyme; (iii) the hinge-swap mutation results in FMN → haem electron transfer becoming the slowest step in the catalytic cycle; (iv) the hinge-swap mutation has little or no effect on the redox potential of the haem group.

We thank Dr. G. W. Pettigrew for help in determining redox potentials. We are indebted to Professor F. S. Mathews, Dr. F. Lederer and Dr. M. Tegoni for helpful discussions. This work was supported by the Molecular Recognition Initiative of the Science and Engineering Research Council (SERC) through research grants and funding for the Edinburgh Centre for Molecular Recognition. We are grateful to the SERC for postgraduate support for P.W.

REFERENCES

1 Jacq, C. and Lederer, F. (1974) Eur. J. Biochem. **41**, 311–320
2 Daum, G., Böhni, P. C. and Schatz, G. (1982) J. Biol. Chem. **257**, 13028–13033
3 Appleby, C. A. and Morton, R. K. (1954) Nature (London) **173**, 749–752

4 Xia, Z.-X. and Mathews, F. S. (1990) J. Mol. Biol. **212**, 837–863
5 Labeyrie, F., Beloeil, J. C. and Thomas, M. A. (1988) Biochim. Biophys. Acta **953**, 134–141
6 Black, M. T., Gunn, F. J., Chapman, S. K. and Reid, G. A. (1989) Biochem. J. **263**, 973–976
7 Sambrook, J., Fritsch, E. F. and Maniatis, T. (1989) Molecular Cloning: A Laboratory Manual, 2nd edn., Cold Spring Harbor Laboratory Press, Cold Spring Harbor, NY
8 Reid, G. A., White, S., Black, M. T., Lederer, F., Mathews, F. S. and Chapman, S. K. (1988) Eur. J. Biochem. **178**, 329–333
9 Mead, D. A., Szczesna-Skorupa, E. and Kemper, B. (1986) Protein Eng. **1**, 67–74
10 Kunkel, T. A. (1985) Proc. Natl. Acad. Sci. U.S.A. **82**, 488–492
11 Black, M. T., White, S. A., Reid, G. A. and Chapman, S. K. (1989) Biochem. J. **258**, 255–259
12 Miles, C. S., Rouvière-Fourmy, N., Lederer, F., Mathews, F. S., Reid, G. A., Black, M. T. and Chapman, S. K. (1992) Biochem. J. **285**, 187–192
13 Dutton, P. L. (1978) Methods. Enzymol. **54**, 411–435
14 Brunt, C. E., Cox, M. C., Thurgood, A. G. P., Moore, G. R., Reid, G. A. and Chapman, S. K. (1992) Biochem. J. **283**, 87–90
15 Pompon, D., Iwatsubo, M. & Lederer, F. (1980) Eur. J. Biochem. **104**, 479–488
16 Pompon, D. (1980) Eur. J. Biochem. **106**, 151–159
17 Capeillère-Blandin, C. (1991) Biochem. J. **274**, 207–217
18 Labeyrie, F., Baudras, A. and Lederer, F. (1978) Methods Enzymol. **53**, 238–256
19 Ogura, Y. and Nakamura, T. (1966) J. Biochem. (Tokyo) **60**, 77–86
20 Capeillère-Blandin, C., Iwatsubo, M., Testylier, G. and Labeyrie, F. (1980) in Flavins and Flavoproteins (Yagi, K. and Yamamoto, T., eds.), pp. 617–630, Japan Scientific Societies Press, Tokyo

Received 27 July 1992/25 September 1992; accepted 2 October 1992